T.C.
REPUBLIC OF TURKEY
HACETTEPE UNIVERSITY
INSTITUTE OF HEALTH SCIENCES

HOX AND TALE TRANSCRIPTION FACTORS IN FANCONI ANEMIA BONE-MARROW MESENCHYMAL STEM CELLS: GENE EXPRESSION AND PROTEIN INTERACTIONS

MSc. Ilgın ÇAĞNAN

Program of Stem Cell
DOCTOR OF PHILOSOPHY THESIS

ANKARA
2018

T.C.
REPUBLIC OF TURKEY
HACETTEPE UNIVERSITY
INSTITUTE OF HEALTH SCIENCES

HOX AND TALE TRANSCRIPTION FACTORS IN FANCONI ANEMIA BONE-MARROW MESENCHYMAL STEM CELLS: GENE EXPRESSION AND PROTEIN INTERACTIONS

Ilgın ÇAĞNAN (MSc.)

Program of Stem Cell
DOCTOR OF PHILOSOPHY THESIS

ADVISOR OF THE THESIS
Assoc. Prof. Dr. Ayşen (GÜNEL) ÖZCAN

ANKARA
2018

HOX and TALE Transcription Factors in Fanconi Anemia Bone-Marrow Mesenchymal Stem Cells: Gene Expression and Protein Interactions

Ilgın Çağnan

This study has been approved and accepted as a PhD dissertation in the program of "Stem Cell" by the examining committee, whose members are listed below, on *10/01/2018*.

Chairman of the Committee :	Prof. Dr. A. Lale DOĞAN Hacettepe University
Advisor of the Dissertation :	Assoc. Prof. Dr. Ayşen (GÜNEL) ÖZCAN Hacettepe University
Member :	Assoc. Prof. Dr. Özlen KONU KARAKAYALI Bilkent University
Member :	Assoc. Prof. Dr. Bala GÜR DEDEOĞLU Ankara University
Member :	Assist. Prof. Dr. Fatima AERTS KAYA Hacettepe University

This dissertation has been approved by the committee above in conformity to the regulations and by laws of Hacettepe University Graduate Programs.

18 Ocak 2018

Prof. Dr. Dicle han ORHAN
Institute Director

YAYIMLAMA VE FİKRİ MÜLKİYET HAKLARI BEYANI

Enstitü tarafından onaylanan lisansüstü tezimin/raporumun tamamını veya herhangi bir kısmını, basılı (kağıt) ve elektronik formatta arşivleme ve aşağıda verilen koşullarla kullanıma açma iznini Hacettepe Üniversitesine verdiğimi bildiririm. Bu izinle Üniversiteye verilen kullanım hakları dışındaki tüm fikri mülkiyet haklarım bende kalacak, tezimin tamamının ya da bir bölümünün gelecekteki çalışmalarda (makale, kitap, lisans ve patent vb.) kullanım hakları bana ait olacaktır.

Tezin kendi orijinal çalışmam olduğunu, başkalarının haklarını ihlal etmediğimi ve tezimin tek yetkili sahibi olduğumu beyan ve taahhüt ederim. Tezimde yer alan telif hakkı bulunan ve sahiplerinden yazılı izin alınarak kullanılması zorunlu metinlerin yazılı izin alınarak kullandığımı ve istenildiğinde suretlerini Üniversiteye teslim etmeyi taahhüt ederim.

- **Tezimin/Raporumun 10/01/2025 tarihine kadar erişime açılmasını ve fotokopi alınmasını (İç Kapak, Özet, İçindekiler ve Kaynakça hariç) istemiyorum.**
  (Bu sürenin sonunda uzatma için başvuruda bulunmadığım takdirde, tezimin/raporumun tamamı her yerden erişime açılabilir, kaynak gösterilmek şartıyla bir kısmı veya tamamının fotokopisi alınabilir)

10/01/2018

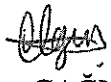

Ilgın ÇAĞNAN

ETHICAL DECLARATION

In this thesis study, I declare that all the information and documents have been obtained in the base of the academic rules and all audio-visual and written information and results have been presented according to the rules of scientific ethics. I did not do any distortion in data set. In case of using other works, related studies have been fully cited in accordance with the scientific standards. I also declare that my thesis study is original except cited references. It was produced by myself in consultation with supervisor Assoc. Prof. Dr. Ayşen (GÜNEL) ÖZCAN and written according to the rules of thesis writing of Hacettepe University Institute of Health Sciences.

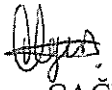

Ilgın ÇAĞNAN

ACKNOWLEDGEMENTS

I would like to express my special appreciation and thanks to my supervisor Assoc. Prof. Dr. Ayşen (Günel) Özcan for mentoring and encouraging my research as well as nurturing me to grow as a research scientist. I am thankful for her contributions of time, ideas and funding towards my Ph.D. studies.

I am grateful to Prof. Dr. Duygu Uçkan-Çetinkaya for always supporting me and allowing me to use all resources available at the Center for Stem Cell Research and Development.

I thank to Assist. Prof. Dr. Fatima Aerts-Kaya for her support and appreciate her guidance on flow cytometry analyses and co-culture experiments. I am thankful to Assoc. Prof. Özlen Konu for her valuable advice. I thank to Assoc. Prof. Dr. Güneş Esendağlı for opening his laboratory, whenever I was in need. I acknowledge the support received through collaborative work with Prof. Dr. Johan de Winter (deceased) and Dr. Najim Ameziane for mutational analysis, as well as, with Dr. Erdal Coşgun for statistical analysis.

I gratefully acknowledge the funding received towards my Ph.D. from The Scientific and Technological Research Council of Turkey (TÜBİTAK) 1001 (Grant numbers: 110S021 and 214Z033).

I thank to Emine Kılıç and Özlem Küçükbayrak for their help. A special thanks to my friends, Özge Burcu Şahan, Emre Gedik, Neşe Ünver, Çağla Defteralı and Gizem Vural for their help and moral support. I also would like to thank all my friends (especially Yağız Anasız, Beyza Gökçınar Yağcı, İrem Akar, Gülen Esken, İnci Cevher Zeytin, Burcu Şirin, Tülay Karaağaç Akyol, Beren Karaosmanoğlu) at Hacettepe University for sharing my joys and sorrows during my PhD.

I also thank to my family members, Duygu Kalfaoğlu and Duygu Güven for their moral support. Last but by no means least, I am very grateful to my parents, Halil Çağnan and İdil Çağnan, for all the things they sacrificed for me and who guided me all through my life with moral and emotional support.

ABSTRACT

Çağnan, I., HOX and TALE Transcription Factors in Fanconi Anemia Bone-Marrow Mesenchymal Stem Cells: Gene Expression and Protein Interactions, Hacettepe University Institute of Health Sciences Program of Stem Cell Doctor of Philosophy Thesis, Ankara, 2018. HOX/TALE proteins maintain tissue identity and their altered expression is seen in many cancers. The main aim of this thesis is to evaluate whether HOX/TALE gene expression changes due to genomic instability. To answer this question, Fanconi anemia (FA) bone marrow mesenchymal stem/stromal cells (BM-MSCs) were investigated. FA is an inherited bone marrow (BM) failure disease, which shows cancer predisposition due to genomic instability. FA BM-MSCs were characterized at molecular and cellular level compared to donors. The gene expression profile was evaluated by RT-qPCR. Differentially expressed gene was further analyzed to define its function related to BM-MSCs biology, as well as, to assess its interactions with the members of FA/BRCA pathway using co-immunoprecipitation (Co-IP). *PKNOX2* expression significantly decreased in FA cells compared to donors, and its expression was stimulated by rTGF-β1 treatment. When BM-MSCs, transfected with PKNOX2 expression plasmid (PKNOX2:MSC) were characterized, decrease in CD105 level and lateral motility were observed. Co-culture assays of cryopreserved $CD34^+$HSCs on PKNOX2:MSCs displayed increase in $CD34^+CD38^+$ percentage and clonogenic capacity. Proteome analysis following Co-IP revealed that a total of 219 proteins directly interacted with PKNOX2, but FA/BRCA pathway members were not among these proteins. However, interactors of PKNOX2 interactome may regulate double-strand break repair via NHEJ, HSC differentiation and G2/M transition. In conclusion, decrease in *PKNOX2* expression of FA BM-MSCs may cause cell cycle arrest, increase in NHEJ-related gene expression and trigger the formation of genomic unstable microenvironment that can promote hematopoietic defects seen in patients.

Key Words: FA, BM-MSC, TGF-β, FANCD2, *PKNOX2* expression

This study was funded by two TÜBİTAK 1001 projects (#110S021 and #214Z033).

ÖZET

Çağnan I., Fankoni Anemisi Kemik İliği Mezankimal Kök Hücrelerinde HOX ve TALE Transkripsiyon Faktörleri: Gen İfadeleri ve Protein Etkileşimleri, Hacettepe Üniversitesi Sağlık Bilimleri Enstitüsü Kök Hücre Programı Doktora Tezi, Ankara, 2018. HOX/TALE proteinleri doku kimliğinin korunmasında rol oynamaktadır ve bir çok kanserde ifadelerinin değiştiği gözlemlenmiştir. Bu tezin esas amacı, genomik kararsızlıkta HOX/TALE gen ifadelerinin değişip değişmediğinin araştırılmasıdır. Bu sorunun cevaplanması için Fankoni anemisi (FA) kemik iliği mezankimal kök/stromal hücreleri (Ki-MKH) incelemeye alındı. Kalıtsal bir kemik iliği yetmezliği olan FA hastalığı, genomik kararsızlığa bağlı olarak yüksek kanser riski taşımaktadır. Öncelikle, FA ve donör Ki-MKH'leri moleküler ve hücresel düzeyde karakterize edildi. Gen ifadeleri RT-qPCR ile ölçüldü. Farklı ifade olan genin kodladığı proteinin Ki-MKH biyolojisi üzerine etkisi ve FA/BRCA yolağı proteinleri ile etkileşiminin olup olmadığı ko-immünopresipitasyon (Ko-IP) yöntemiyle değerlendirildi. FA hücrelerinin *PKNOX2* ifadesinin donörlere oranla anlamlı düzeyde düştüğü ve rTGF-β1 indüksiyonunun *PKNOX2* ifadesinde arttışa yol açtığı saptandı. PKNOX2 ekspresyon plazmidi aktarılan BM-MKH'ler karakterize edildiğinde, CD105 seviyesinin ve lateral motilitesinin düştüğü gözlendi. Ko-kültür deneyleri, PKNOX2:MKH ile birlikte kültüre edilen donmuş $CD34^+$HKH'lerin $CD34^+CD38^+$ yüzdesinde ve klonojenitisinde artış olduğunu gösterdi. Ko-IP sonrası proteom analizleri, PKNOX2'nin 219 protein ile direk etkileştiğini ve bunlar arasında FA/BRCA yolağı üyelerinin olmadığını gösterdi. Ancak, PKNOX2 interaktomu ile etkileşen proteinlerin *NHEJ* aracılı DNA çift zincir kırıklarının tamirinde, HKH farklılaşmasında ve G2/M geçişinde rol oynadığı belirlendi. Sonuç olarak, FA Ki-MKH'lerinin *PKNOX2* ifadesindeki düşme, hücre siklusunun tutuklanmasına, *NHEJ* ilişkili gen ifadelerinin artışına ve genomik kararsız bir mikroçevrenin oluşumundan sorumlu olabilir ve hastalarda gözlemlenen hematopoetik bozulmanın altında yatan sebep olabilir.

Anahtar Kelimeler: FA, Ki-MKH, TGF-β, FANCD2, *PKNOX2* ifadesi

Bu tez, TÜBİTAK 1001 projeleri ile desteklenmiştir ***(****#110S021 ve #214Z033).*

TABLE OF CONTENTS

SYMBOLS and ABBREVIATIONS

Abd-A	Abdominal A
Abd-B	Abdominal B
Ang1	Angiopoietin-1
Akt	Serine/Threonine Kinase
ALPL	Alkaline Phosphatase, Tissue Non-Specific
AML	Acute Myeloid Leukemia
ANTP	Antennapedia
ARS	Alizarin Red S
ASC	Adult Stem Cell
BCA	Bicinchoninic Acid
BFU-E	Burst Forming Unit of Erythroid Cells
BM	Bone Marrow
BM-MSC	Bone Marrow Mesenchymal Stem/Stromal Cell
BME	2-mercaptoethanol
BMF	Bone Marrow Failure
BMP4	Bone Morphogenetic Protein 4
BMT	Bone Marrow Transplantation
BRIP1	BRCA1 Interacting Protein C-Terminal Helicase 1
BSA	Bovine Serum Albumin
Ca^{2+}	Calcium
CARC	CXCL12-Abundant Reticular Cell
CD	Cluster of Differentiation
cDNA	Complementary DNA
CERS	Ceramide Synthase
Dfd	Deformed
CFU-F	Colony Forming Unit Fibroblasts
CFU-GM	Colony Forming Unit Precursor of Granulocyte/Macrophage
CFU-GEMM	Colony Forming Unit Precursor of Granulocyte/Erythrocyte/Macrophage/Megakaryocyte
c-KIT	Proto-Oncogene Tyrosine-Protein Kinase Kit
CMV	Cytomegalovirus

CO_2	Carbon Dioxide
Co-IP	Co-Immunoprecipitation
ColE1	Colicin E1
Cp	Crossing Point
cPD	Cumulative Population Doubling
Ct	Threshold Cycle
C-terminus	Carboxyl-Terminus
CtIP	Retinoblastoma-Interacting Protein and Myosin-Like
CXCL12	C-X-C Motif Ligand 12
CXCR4	C-X-C Chemokine Receptor 4
ddH_2O	Distilled Water
DEB	Diepoxybutane
DEPC	Diethyl Procarbonate
DMEM-LG	Dulbecco's Modified Eagle's Medium-Low Glucose
DMSO	Dimethyl Sulfoxide
DNA-PK	DNA-Dependent Protein Kinase
Dnmt	DNA (Cytosine-5)-Methyltransferases
DTT	Dithiothreitol
E2	Ubiquitin-Conjugating Enzyme
E3	Ubiquitin-Protein Ligase
EDTA	Ethylenediaminetetraacetic Acid
EGFR	Epidermal Growth Factor Receptor
ERCC4	ERCC Excision Repair 4, Endonuclease Catalytic
ESC	Embryonic Stem Cell
FA	Fanconi Anemia
FAAP	FA Associated Protein
FAN1	FANCD2 and FANCI Associated Nuclease 1
FANCD2-L	Monoubiquitinated FANCD2
FANCD2-S	Unubiquitinated FANCD2
fc	Fold Change
FE	Fold Enrichment
FGF	Fibroblast Growth Factor

FI	Fluorescence Intensity
fi ori	Phage-Derived Origin of Replication
FOXO3a	Forkhead Box O3A Protein
GATA2	GATA-binding Protein 2
GLB1	Galactosidase Beta 1
GO	Gene Ontology
H3K4me3	Histone 3 Lysine 4
H3K27me3	Histone 3 Lysine 27
Hb	Hemoglobin Count
HD	Homeodomain
HDAC	Histone Deacetylase
HI-FBS	Heat-Inactivated Fetal Bovine Serum
HLA	Human Leukocyte Antigen
HNF	Hepatocyte Nuclear Factor
HOM-C	Homeotic Complex
HOXL	Homeobox-Like
HR	Homologous Recombination
HR1	Homology Region 1
HR2	Homology Region 2
HRP	Horseradish Peroxidase
HSC	Hematopoietic Stem Cell
HSPC	Hematopoietic Stem and Progenitor Cells
HUSCS-D	Hacettepe University Stem Cell Sciences-Donor
HUSCS-FA	Hacettepe University Stem Cell Sciences-Fanconi Anemia
ICAM-1	Intracellular Adhesion Molecule 1
ICL	Interstrand Crosslinks
ICM	Inner Cell Mass
IFN-γ	Interferon Gamma
IL-6	Interleukin-6
IL-10	Interleukin-10
IMDM	Iscove’ Modified Dulbecco’s Medium
Irx	Iroquois

Kan^r/Neo^r	Resistance to Kanamycin and Neomycin Analogs
Lab	Labial
LB	Luria Bertani
LepR	Leptin receptor
LPL	Lipoprotein Lipase
MDS	Myelodysplastic Syndrome
MEIS	Myeloid Ecotropic Viral Integration Site
MHC	Major Histocompatibility Complex
MI	Motility Index
MICE	Multivariate Imputation by Chained Equations
Mkx	Mohawk
MLPA	Multiplex Ligation-Dependent Probe Amplification
MMC	Mitomycin C
MOPS	3-(N-morpholino)propanesulfonic Acid
MSC	Mesenchymal Stem Cell
MWU	Mann Whitney U
NA	Information Not Available
NaCl	Sodium Chloride
NaOH	Sodium Hydroxide
NG2	Neural/Glial Antigen 2
NHEJ	Non-Homologous End Joining
NKL	NK-Like Homeobox
n-LC MS/MS	Mass Spectrometer with Nano Liquid Chromatography
N-terminus	Amino-terminus
NUP98	Nucleoporin 98
OCN	Osteocalcin
OCT-4	Octamer-binding Transcription Factor 4
OD	Optical Density
ORO	Oil Red O
PARP	Poly(ADP-ribose) Polymerase 1
PAX	Paired Box
PAX-L	Paired Box-Like

pb	Proboscipedia
PBS	Phosphate-Buffered Saline
Pbx	Pre-B cell Leukemia Factor Family
Pen/Strep	Penicillin and Streptomycin
PLT	Platelet Count
PKNOX	PBX/knotted Homeobox
PolyA	Polyadenylation Site
POU	Pit-Oct-Unc Family of Proteins
PPARG	Peroxisome Proliferator Activated Receptor Gamma
PRC1	Polycomb Repressive Complex 1
PRC2	Polycomb Repressive Complex 2
PRD	Paired Homeobox
PRE	Polycomb Response Element
PREP	Pbx-regulating Protein
PVDF	Polyvinylidene Difluoride
RT-qPCR	Reverse Transcriptase Quantitative Polymerase Chain Reaction
RA	Retinoic Acid
RAD51	BRCA1/BRCA2-Containing Complex, Subunit 5
RAR	Retinoic Acid Receptor
RFWD3	Ring Finger and WD Repeat Domain 3
RMI1	RecQ Mediated Genome Instability 1
RMI2	RecQ Mediated Genome Instability 2
ROS	Reactive Oxygen Species
RPA	Replication Protein A
rbap46	Retinoblastoma-Binding Protein p46
rbap48	Retinoblastoma-Binding Protein p48
rTGFβ1	Recombinant TGFβ1
RUNX2	Runt-Related Transcription Factor 2
RXR	Retinoid X Receptor
SA-β-gal	Senescence Associated β-galactosidase
SC	Stem Cell

SCF	Stem Cell Factor
Scr	Sex Combs Reduced
SD	Standard Deviation
SDS	Sodium Dodecyl Sulfate
SDS-PAGE	Sodium Dodecyl Sulfate Polyacrylamide Gel Electrophoresis
SLX4	Fanconi Anemia, Complementation Group P
SP7	Osterix
SUZ12	Suppressor of Zeste 12 Protein Homolog
SV40 ori	Mammalian Origin of Replication
TALE	Three-Amino-Acid Loop Extension
TBS	Tris Buffered Saline
TGF-β	Transforming Growth Factor Beta
TGFβR1	Transforming Growth Factor Beta Receptor 1
TGFβR2	Transforming Growth Factor Beta Receptor 2
Tie-2	Tunica Internal Endothelial Cell Kinase
Tgif	Transforming Growth-Interacting Factor
TMZ	Temozolomide
TNF-α	Tumor Necrosis Factor Alpha
Tris.Cl	(Hydroxymethyl)aminomethane Hydrochloride
UBE2T	Ubiquitin Conjugating Enzyme E2 T
Ubx	Ultrabithorax
UV	Ultraviolet
VCAM-1	Vascular Cell Adhesion Molecule 1
VEGF	Vascular Endothelial Growth Factor
WBC	White Blood Cell Count
XRCC2	X-Ray Repair Cross Complementing 2
ZF	Zinc Finger

FIGURES

TABLES

1. INTRODUCTION

Mesenchymal stem/stromal cells (MSCs) are important components of the bone marrow (BM) stroma, which is known as the 'niche' and regulate hematopoietic stem cell (HSC) maintenance (1, 2). MSCs are multipotent adult stem cells (ASCs) that have the ability to self-renew and also differentiate along mesenchymal and non-mesodermal lineages (3-7). MSCs contribute to tissue homeostasis through secretion of numerous growth factors and cytokines, as well as, via direct contact with target cells (8, 9). Dysregulation of the crosstalk between HSCs and the BM stromal cells can lead progressive bone marrow failure (BMF) and hematopoietic malignancies (10). Inherited or acquired syndromes that cause BMF are very rare and present with cytopenia. After BMF, the BM becomes hypocellular and BM transplantation (BMT) is the most commonly used treatment method at this stage (11, 12).

HOX genes are expressed in early stage hematopoietic cells and play a role in lineage commitment, as well as, in tissue remodeling processes (13). HOX genes are highly conserved homeobox genes that encode 'master regulator' homeodomain transcription factors and play a vital role in specifying anterior-posterior identity during embryonic development (14). In mammals, HOX genes are found in four clusters designated as A, B, C and D, which are located on different chromosomes and contain up to 13 genes (15). During adulthood, these genes are organ-specifically expressed and the HOX code provides a "biological fingerprint" for different cell types. Similar cell types, such as MSCs derived from different body sites exhibit distinct *HOX* expression (16-18). Three-amino-acid loop extension (TALE) proteins are co-factors of the HOX proteins and play important roles in HOX specificity (19, 20). Members of the TALE class have been shown to act as oncogenes (e.g. MEIS1) and tumor suppressors (e.g. PKNOX1) and have a function in DNA repair and maintenance of genomic stability (e.g. PKNOX1) (21-23). To date, no study has evaluated the HOX and TALE gene expression of MSCs in a genome unstable disease, prone to cancer, such as Fanconi anemia.

Fanconi anemia (FA) is a genetic disorder, which is characterized by the presence of hematopoietic defects such as BMF, myelodysplasia (MDS) and acute

myeloid leukemia (AML), as well as, developmental dysmorphisms (24, 25). At least 22 distinct FA complementation groups exist, due to mutations in *FANC* genes (26, 27). FANC proteins function in the FA/BRCA pathway, which mediates the repair of interstrand crosslinks through homologous recombination (28). Cells from patients are hypersensitive to DNA interstrand crosslinking (ICL) agents, such as mitomycin C (MMC) and diepoxybutane (DEB), that result in DNA damage by inducing high levels of chromosome breaks and genomic instability (28). Mutations in FANC genes affect quiescent HSCs and their progenitors in terms of the population size and differentiation abilities (29, 30). Aberrant hematopoietic microenvironment may also play an active role in inducing or sustaining BMF in FA. Studies investigating the role of FA MSCs for supporting HSCs showed contradictory results: Fancg$^{-/-}$ mouse MSCs exhibited impaired support of HSC proliferation, whereas human FancA$^{-/-}$ MSCs were able to support long-term HSC culture (31, 32). BM derived MSCs (BM-MSCs) from FA patients or murine models have similar immunophenotypes and differentiation capacity, but displayed a reduced capacity to form colony forming unit fibroblasts (CFU-Fs), a decreased proliferative potential, an increased senescence, hypersensitivity to MMC and an extended G2 phase transition compared to controls (31-33). Additionally, MSCs with non-functional FA pathway have increased spontaneous chromosome breaks compared to healthy donors (33). This evidence supports hypothesis that the presence of a genomic instability in MSCs, due to impaired FA pathway may trigger BMF. FA MSCs secrete higher stem cell factor (SCF) and interleukin-6 (IL-6) factors compared to controls (32). Further studies are necessary to evaluate the differences in cytokines and growth factors produced by FA-BM-MSCs. Hyperactive transforming growth factor beta (TGF-β) signaling in FA HSCs may cause BMF in patients (34). Neither the level of TGF-β production by FA BM-MSCs nor its possible role in progressive BMF through juxtacrine or paracrine signaling has been elucidated yet.

Manifestation of early hematopoietic dysfunction, coinciding with developmental malformations in FA patients suggests the possible involvement of developmental genes in the disease pathogenesis. As mentioned above, MSCs are known to be involved in the regulation of BM hematopoietic niches and *HOX* or TALE expression might be dysregulated in BM-MSCs obtained from FA patients,

resulting in the progression of bone marrow failure. Also, HOX and TALE protein(s) might interact with FA/BRCA pathway or associated proteins which might help to explain the bone marrow failure in FA patients. Therefore, the goals of this thesis were;

- to characterize BM-MSCs from FA patients and healthy donors in terms of their immunophenotype, differentiation potential, proliferation capacity, senescence and reactive oxygen species (ROS) production,
- to characterize cell cycle phases of BM-MSCs following DEB treatment,
- to evaluate expression and secretion levels of TGF-β in FA cells compared to donors,
- to investigate whether HOX and TALE gene expression levels differ in FA BM-MSCs compared to donors,
- to evaluate protein level of the differentially expressed HOX or TALE gene(s),
- to investigate whether differentially expressed HOX or TALE gene(s) is affected from DEB treatment,
- to transfect BM-MSCs with an expression plasmid to investigate biological characterization of the differentially expressed HOX or TALE gene(s), as well as, to obtain its protein interactions.

2. LITERATURE REVIEW

2.1. Stem Cells and Mesenchymal Stem/Stromal Cells

Stem cells (SCs) are clonogenic cells that form a small percentage of the total cell number within the body (35, 36). They are defined by their ability to maintain their undifferentiated state during numerous cell divisions, also referred to as the "self-renewal capacity", and also to differentiate into specialized (i.e. non-stem) cells forming the body of an adult, known as the differentiation potency (37).

According to their potency, SCs are classified into four groups (38, 39);

1) Totipotent SCs, also known as morula cells, have the ability to form the three germ layers of the developing embryo, as well as, extraembryonic cells (e.g. placenta).
2) Pluripotent SCs, also known as embryonic stem cells (ESCs), are obtained from the inner cell mass (ICM) of the blastocyst prior to implantation, and can differentiate into any type of cells except extraembryonic cells.
3) Multipotent SCs (e.g. ASCs) can produce cells of their tissue of origin only, unlike pluripotent ESCs.
4) Unipotent SCs (i.e. progenitor cells) with unlimited self-renewal capacity, can only differentiate into one type of cell.

ASCs reside throughout the adult body and are responsible for maintaining tissue homeostasis (40). Apart from having organ-specific markers, ASCs are generally characterized by expression of generic SC markers, such as OCT-4, nestin and ABC transporters, that regulate stemness properties such as quiescence, cell survival, self-renewal via asymmetric cell division and adhesion to the niche (41). ASCs can be subdivided into parenchymal SCs and MSCs. Parenchymal SCs give rise to non-connective tissues while MSCs differentiate into cells of connective tissue like fat, bone, smooth muscle and cartilage (1, 42-44). MSCs will be further discussed in this thesis.

MSCs are non-hematopoietic but stromal multipotent ASCs, that are defined as CFU-Fs (45). They are located within various tissues, such as BM, dental pulp,

umbilical cord blood, adipose tissue and brain and liver (46-50). MSCs have the ability to differentiate along various mesenchymal lineages, like adipocytes, osteoblasts and chondrocytes *in vitro* (3, 4). Additionally, they are shown to give rise to other cells with mesodermal or non-mesodermal origin, such as neuronal cells, endothelial cells, cardiomyocytes and hepatocytes (5-7, 51).

MSCs are rare (i.e. 0.001-0.01% of nucleated cells in BM) and heterogeneous cell populations due to existence of clones with distinct proliferation rates, differentiation capacities and morphologies *in vitro* (44, 52-54). For instance, single cells obtained from human umbilical cord blood derived MSCs are shown to have high or low *in vitro* differentiation potential, which is lost over time (55). Relating to this, MSCs from different source of origin cultured under same conditions, varied in their potencies, morphological appearances and mRNA expression (56-58).

The main disadvantage of studying MSCs is the lack of specific markers that can be used during their isolation. MSCs are defined to express cluster of differentiation (CD) 105, CD73 and CD90, while they do not express CD45, CD34, CD14 or CD11b, CD79alpha or CD19 and HLA-DR surface markers (59). However, the level of these surface molecules alters depending on passages, isolation method and tissues from which the cells are isolated. Overall, *in vitro* expansion and differentiation of these cells remains challenging.

MSCs are an attractive source for SC-based therapies. Currently, there are 281 active (case status: enrolling by invitation; recruiting; not yet recruited; active, not recruiting) and 154 completed MSC-based clinical trials (60). Although controversial, one of the most important features of MSCs as therapeutic agents, is their ability to escape the immune system due to the low expression levels of major histocompatibility complex (MHC) class I and absence of MHC class II (61, 62). They are also able to secrete numerous growth factors and cytokines, that can contribute to tissue regeneration by increasing angiogenesis and inhibiting apoptosis via immune modulation, such as inhibition of T-cell and B- cell proliferation, as well as, dendritic cell differentiation (9, 63-66). MSCs modulate immune system by secreting soluble molecules, like TGF-β, VEGF, interleukin-10 (IL-10), IL-6, tumor necrosis factor stimulated gene 6 protein, nitric oxide, indoleamine 2,3-dioxygenase

and prostaglandin E2 (67-72). Additionally, MSCs can also exert their immunomodulatory role through direct contact with target cells. MSCs directly interacting with T-cells are able to inhibit T-cell proliferation via Notch signaling (8). Through these interactions, MSCs are able to regulate BM microenvironment, also known as the 'niche'.

2.2. Bone Marrow as Hematopoietic Stem Cell Niche

During mammalian embryonic development, HSC production initially starts as blood islands within the yolk sac. Later during development, their production occurs in waves that starts in aorta-gonad-mesonephros, continues in placenta, fetal liver, spleen and then permanently shifts to the BM (73). During adulthood, BM is the HSC niche, which is designed in a way that provides a microenvironment responsible for keeping its resident SCs in a quiescence state thus supporting maintenance of self-renewal. Occasionally, HSCs divide, giving rise to short-term progenitors. These cells are able to regenerate sufficient numbers of mature blood cells to compensate for the cells that are lost over time (74, 75).

In 1978, the HSC niche was first described by Schofield (76). Self-renewing HSCs are thought to be localized near the trabecular endosteum of long bones, while progenitors with restricted potency are found towards more centralized areas (75, 77-80). Therefore, the presence of functionally distinct microenvironments (i.e. osteoblastic/endosteal and vascular niches) within BM has been suggested (Figure 2.1.) to be composed of different cell types, soluble molecules and extracellular matrix orchestrating intrinsic and extrinsic cues, responsible for regulating resident HSC numbers and function (79, 81-83). Niche components are as follows;

1) Cellular components such as osteoblastic cells, adipocytes, endothelial cells of sinusoidal vasculature, perivascular mesenchymal stem/progenitor cells as well as non-myelinating Schwann cells of the symphatic nervous system (84),
2) Molecular components,
    a. The interaction between factors and their receptors, such as C-X-C motif ligand 12 (CXCL12) and C-X-C chemokine receptor 4 (CXCR4) axis (85),
    b. Signaling cascades, such as the TGF-β pathway (86),

c. Extracellular matrix molecules, such as glycans and osteopontin (87-89),
d. Adhesion molecules, such as β1-integrins and vascular cell adhesion molecule 1 (VCAM-1 or CD106) (87, 90-92),
e. A chemical gradient, such as oxygen and calcium (Ca^{2+}) gradient (93-95).

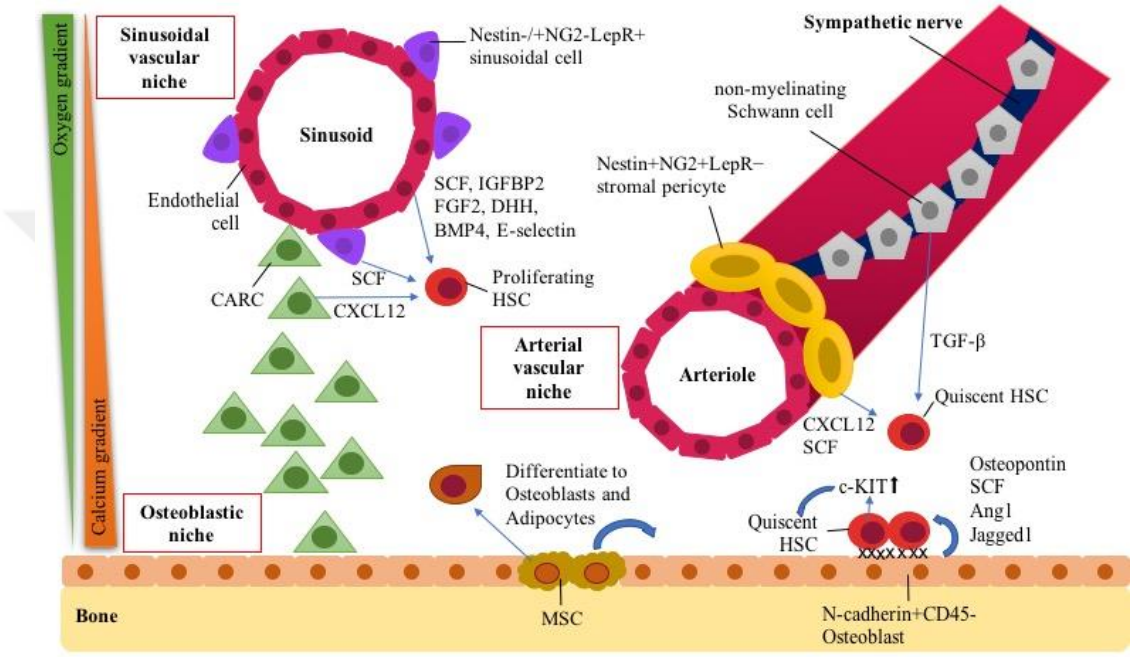

Figure 2.1. Schematic representation of bone marrow stem cell niches. (Adapted from Crane *et al*, (96).)

During embryogenesis, MSCs are present before HSCs at the sites of hematopoietic development, which is an indication that they are one of the factors responsible for organizing the HSC niches (97, 98). One of the mechanisms with which MSCs contribute to HSC fate is via their ability to differentiate into osteoblasts, adipocytes and reticular cells (43). Adipocytes within the BM have a negative impact on hematopoietic niches (99). HSCs and their progenitors derived from adipose or yellow BM, are less in number compared to cells derived from brown BM (99).

Slow-cycling HSCs are suggested to be stored within the osteoblastic niche and can be mobilized in response to a stress, such as tissue injury. Using live imaging or cell-tracing techniques, HSCs are reported to reside near the endosteum

(84, 100, 101). Long-term repopulating HSCs are also found to adhere directly to the N-cadherin^{+}CD45^{-} osteoblastic cell lining of the endosteum (79). Similarly, HSCs home to endosteum following 15 hours post-transplantation (78). One of the mechanisms controlling HSC engraftment is the high Ca^{2+} gradient through which HSCs travel to the endosteum (93). *In vivo* loss of osteoblasts causes downregulation of HSC numbers, as well as, mature monocytes and granulocytes in mice BM, showing that the size of the niche also affects the number of HSCs (102). In contrast, an increased osteoblast frequency resulted in upregulated HSC numbers (79, 82). Osteoblastic cells also regulate HSC quiescence by producing factors like SCF, osteopontin, angiopoietin-1 (Ang1), bone morphogenic protein 4 (BMP4) and Jagged-1 (82, 87, 103-105). β1-integrin and N-cadherin molecules activated by binding of Ang1 to Tie-2 receptor on HSCs, play a crucial role in the adhesion of HSCs to osteoblastic niche (104). SCF produced by osteoblasts also increase HSC adhesion to the niche, and use expression of c-KIT (CD117) to maintain HSC dormancy (103, 106). Osteopontin expressed by osteoblastic cells of the niche decreases HSC proliferation, and indirectly sustains adhesion to BM (87). *In vitro* and *in vivo* activation of parathyroid hormone/ parathyroid hormone-related protein receptors on osteoblasts resulted in increased levels of Jagged-1 production, that in turn contribute to an increased HSC frequency via Notch1 activation (82). HSCs also exert regulatory signals on their own niche. Hematopoietic progenitors induce differentiation of BM mesenchymal stromal cells into osteoblastic cells (107).

The second BM microenvironment responsible for HSC maintenance in terms of proliferation, differentiation and mobilization is called the vascular niche (80, 108). Short term repopulating cells reside in this vascular niche, where they differentiate to progenitors and enter the blood stream following maturation (109, 110). The oxygen concentration of the vascular niche is higher than in the osteoblastic niche, which enables HSCs to exit their dormant phase and start proliferation (94). Vascular endothelial cells are key components of this vascular niche (109). Primary human endothelial cells with constitutive *Akt* expression, support *in vitro,* as well as, *in vivo* HSC expansion through secretion of angiocrine factors, such as fibroblast growth factor 2, BMP4, insulin like growth factor binding protein 2 and desert hedgehog (111, 112). Lack of glycoprotein 130 cytokine

receptor on endothelial cells, an important factor for hematopoiesis, results in BM dysfunction through downregulation of HSC frequency and formation of hypocellular BM (113, 114). Additionally, E-selectin exclusively expressed by vascular niche cells triggers HSC proliferation and endothelial cells lacking *E-selectin* expression promote HSC dormancy, as well as, self-renewal capacity (115). The vascular niche is also important during HSC homing. Regeneration of endothelial cells lining sinusoids is halted upon VEGF2 deletion which inhibits HSC engraftment in irradiated mice (116). Following transplantation, endothelial cells within vascular niche also express molecules like VCAM-1, ICAM-1 and E-/P-selectin, that interact with HSC adhesion molecules, very late antigen 4, lymphocyte function-associated antigen 1 and CD44, respectively, that are essential for HSC rolling (117).

Perivascular stromal and endothelial cells are also responsible for HSC maintenance via membrane-bound *Scf* expression (118-120). Targeted depletion of *Scf* expression from osteoblasts neither affect HSC number nor function while its deletion from endothelial or Leptin receptor (LepR) positive perivascular stromal cells depleted HSCs (120). Additionally, Kunisaki and co-authors (121) report that non-cycling HSCs reside close to the arterial niche containing dormant $Nestin^{+}NG2^{+}LepR^{-}$ stromal pericytes instead of $Nestin^{-/+}NG2^{-}LepR^{+}$ sinusoidal cells. Upon specific ablation of neural/glial antigen 2 positive ($NG2^{+}$) mesenchymal cells, long-term repopulating HSC numbers decrease, while proliferating HSC frequency increases (121). Therefore, it is possible that the vascular niche has subclasses with different functions in HSC maintenance and quiescence (121, 122). These data challenge the classic niche concept.

Cxcl12 expression is also important for supporting HSC in the perivascular area of mice BM (123). Long term repopulating potential of HSCs is lost when *Cxcl12* is deleted from endothelial cells. In addition to long term repopulating potential, HSC dormancy and number are also affected, when *Cxcl12* is deleted from paired related homeobox 1 positive mesenchymal progenitors (123). Inhibition of Cxcl12 receptor, Cxcr4, also downregulates HSC number (85). HSCs expressing Cxcr4 are located at the same location as perivascular Cxcl12 expressing reticular

cells, also called CXCL12-abundant reticular cells (CARCs). CARCs are suggested to be same as, or progenitors derived from MSCs, due to their ability to differentiate towards adipogenic and osteogenic lineages (85, 124). HSCs interacting with CARCs are also in close proximity with endosteum indicating CARCs can be a common component of both niches (85, 123). Human $CD45^{-}CD146^{+}$ cells, equivalent of CARCs, transplanted to mice also form a bone-like structure containing hematopoietic cells and sinusoids (125).

Non-myelinating Schwann cells located near blood vessels in the BM, promote HSC quiescence through TGF-β activation (86). TGF-β signaling is one of the crucial factors that modulate HSC fate (126, 127). The TGF-β pathway is activated upon binding of ligands (e.g. TGF-βs) to the transmembrane kinase receptors, TGFβR1 and TGFβR2 (128, 129). Prior to binding, latent TGF-β complexes are cleaved by proteolytic degradation and activated TGF-β binds to a tetrameric receptor complex, followed by phosphorylation of TGFβR1 by TGFβR2 and activation of Smad dependent and independent intracellular signaling (130). Smad1/5/8 targeted by BMP signaling or Smad2/3 activated by TGF-β/activin/nodal signaling binds to Smad4 in order to be translocated to nucleus and to regulate target gene expression involved in stem cell pluripotency and differentiation (128, 129, 131-134). The effect of MSC produced TGF-β on HSCs remains to be elucidated. To date, TGF-β secreted by MSCs is known to regulate bone remodeling and deregulation of the pathway results in bone disorders (135).

Within the niche, there is no single cell, but rather a group of cells that regulate HSCs. This tight regulation also involves soluble factors, signaling pathways, adhesion molecules and extracellular matrix proteins. Impairment of the crosstalk between HSCs and niche components like BM stromal cells can lead to progressive BMF and hematopoietic malignancies (10).

2.3. Bone Marrow Failure Syndromes

BMF syndromes are a heterogeneous group of rare diseases that present with cytopenia (reduction in the number of blood cells) affecting at least one hematopoietic cell lineage (i.e. myeloid, megakaryocyte or erythroid). BM becomes

hypocellular following BMF and BMT is the only curative method (11, 12). BMF emerges due to inherited (Table 2.1.) or acquired (e.g. autoimmune disease, ionizing radiation, chemotherapy, toxins, viral/bacterial infections, antineoplastic agents) damages (136-138). Maturation defects seen in vitamin B12 deficiency, differentiation anomalies (e.g. myelodysplasia) of hematopoietic cells and marrow infiltration (e.g. multiple myeloma) are other causes of BMF (139, 140).

Patients with acquired or inherited BMF syndromes have a high susceptibility of developing cancer (141, 142). Acquired disorders (acquired aplastic anemia, acquired amegakaryocytic thrombocytopenia, paroxysmal nocturnal hemoglobinuria and myelodysplastic syndrome) are more common among adults and distinct syndromes share overlapping characteristics, thus making diagnosis harder (143, 144).

Besides reduction in the frequency of at least one hematopoietic cell line, inherited BMF disorders are also characterized by developmental anomalies. Depending on the disorder, hematological manifestations appear before birth (e.g. Diamond Blackfan anemia and severe congenital neutropenia), during childhood (e.g. FA) or even later in life (e.g. dyskeratosis congenita) (145, 146). Summary of clinical and genetic features of FA (25-27, 147), Congenital amegakaryocytic thrombocytopenia (148, 149), Dyskeratosis congenita (150-152), Diamond-Blackfan anemia (153, 154), Pearson syndrome (155), Severe congenital neutropenia (156), Shwachman Diamond anemia (156), Thrombocytopenia absent radius syndrome (156) and GATA2 deficiency (157) are given in Table 2.1.

Table 2.1. Summary of clinical and genetic characteristic of inherited bone marrow failure syndromes.

Disorder	Genetic Background	Impairment of Molecular Mechanisms	Hematological Manifestations	Other Clinical Manifestations	Associated Cancers
Fanconi anemia	Autosomal recessive or autosomal dominant or X-linked inheritance; Mutation in at least 22 *FANC* genes	FA/BRCA pathway involved in DNA repair	Anemia; neutropenia; and/or thrombocytopenia; or pancytopenia	Café au lait spots; abnormal radii and thumbs; short stature; microcephaly; ophthalmic malformations, failure in urogenital organ development; kidney failure	MDS; acute myeloid leukemia (AML); solid organ tumors of head and neck, female genitals, esophagus, liver
Congenital amegakaryocytic thrombocytopenia	Autosomal recessive inheritance; Mutation in *MPL* gene	HSC and megakaryocyte maintenance	Thrombocytopenia may progress to pancytopenia	-	MDS; acute lymphoblastic leukemia (ALL)
Dyskeratosis congenita	Autosomal recessive, autosomal dominant or X-linked inheritance; Mutation in *ACD, CTC1, PARN, DKC1, TERC, TERT, TINF2, NOP10, NHP2, WRAP53, RTEL1* or *TPP1* gene	Telomerase function and protein synthesis	Anemia; neutropenia; and/or thrombocytopenia; or pancytopenia; increased fetal hemoglobin (HbF) level	Nail dystrophy; mucosal leucoplakia; reticulated skin hyper-pigmentation; liver failure; pulmonary fibrosis; narrowing of esophagus	MDS; AML; solid organ tumors of head and neck, esophagus, stomach, colon, rectum

Table 2.1. (continued) Summary of clinical and genetic characteristic of inherited bone marrow failure syndromes.

Disorder	Genetic Background	Impairment of Molecular Mechanisms	Hematological Manifestations	Other Clinical Manifestations	Associated Cancers
Diamond-Blackfan anemia	Autosomal dominant or X-linked inheritance; Mutation in 16 genes encoding ribosomal proteins as well as in *GATA1*, *TSR2* or *FLVCR1* gene	Ribosome development	Anemia; increased HbF and red blood cell adenosine deaminase levels	Craniofacial defects; Short stature; abnormal thumbs; defects of heart and urogenital organs	MDS; AML; ALL; osteogenic sarcoma
Pearson syndrome	Deletion in mitochondrial DNA	Mitochondrial biogenesis	Sideroblastic anemia	Short stature	-
Severe congenital neutropenia	Autosomal recessive or autosomal dominant or X-linked inheritance; Mutation in *ELANE*, *HAX1*, *GFI1*, *G6PC3* or *THC1/WASP* gene	Myeloid lineage	Neutropenia	Severe infections	MDS, AML
Shwachman Diamond anemia	Autosomal recessive inheritance; Mutation in *SBDS* gene	Ribosome development	Neutropenia, anemia, and/or thrombocytopenia; or pancytopenia	Short stature; metaphyseal dysostosis; exocrine pancreatic dysfunction; malformations in neuron development	MDS; AML; ALL
Thrombocytopenia absent radius syndrome	Deletion of a part of chromosome 1 or mutation in *RMB8A* gene	mRNA localization, processing and transport	Thrombocytopenia	Bilateral absent radii; defects of thumbs; cardiac defects	MDS; AML; ALL
GATA2 deficiency	Autosomal dominant inheritance; Mutation in *GATA2* gene	Immune system	Neutropenia; or pancytopenia	Pulmonary disease; defects of vascular or lymphatic system	MDS, AML

2.4. Fanconi anemia

2.4.1. FA/BRCA Pathway

FA proteins are involved in the FA/BRCA pathway (Figure 2.2.) that plays a role in DNA ICL repair (146, 158). Upon ICL formation, DNA damage is recognized by the FANCM anchor complex (FANCM, FA associated protein (FAAP) 24/MHF1 and FAAP10/MHF2), which then reorganizes the fork and triggers the translocation of the FA core complex (i.e. FANCA, FANCB, FANCC, FANCE, FANCF, FANCG, FANCL, FAAP20 and FAAP100) to chromatin (159-163). These proteins are either found in the cytoplasm and/or nucleus (Table 2.2.). The FA core complex is divided into three sub-classes; FANCB-FANCL-FAAP100 (i.e. responsible for catalyzing monoubiquitination), FANCA-FANCG-FAAP20 and FANCC-FANCE-FANCF modules (164-166). Apart from these sub-modules, FANCA-FANCC, FANCA-FANCC-FANCF-FANCG, FANCA-FANCG, FANCB-FANCL, FANCC-FANCE protein interactions (Figure 2.2.) have been shown in cytoplasm and/or nucleus (167-179). Once assembled in the nucleus, the FA core complex binds to FANCT/UBE2T and forms an active enzyme containing ubiquitin-conjugating E2 (i.e. FANCT) and ubiquitin ligase E3 subunits (i.e. RING domain containing FANCL) (180-183). The E2/E3 enzyme promotes the monoubiquitination of FANCD2 at K561 and FANCI at K523 that then forms the ID2 complex (173, 184-186). The ID2 complex is then recruited to chromatin, where it binds to FANCD1/BRCA2, FANCR/RAD51 and FANCS/BRCA1 or triggers the translocation of FANCP/SLX4, FANCQ/ERCC4, CtIP and FAN1 to the sites of lesion (173, 187-193). FANCP and FANCQ act as endonucleases, that enable the continuation of translesion synthesis by pol zeta complex bound to REV1, REV3 and FANCV/REV7 (191, 194-196). FAAP20 has been reported to bind to REV1 protein to form an association between FA pathway and translesion DNA synthesis complex (197). Finally, the members of homologous recombination (HR) pathway (i.e. FANCD1, FANCJ/BRIP1, FANCN/PALB2, FANCO/RAD51C, FANCS, FANCR and FANCU/XRCC2) act to repair double strand breaks. Among proteins involved in HR, FANCR plays the key role by initiating homology search and strand pairing, while others act as helpers (198-200). Recently, FANCW/RFWD3 is identified as E3

ligase, that facilitates polyubiquitination of RPA and RAD51, followed by their removal and degradation required for completion of HR (201).

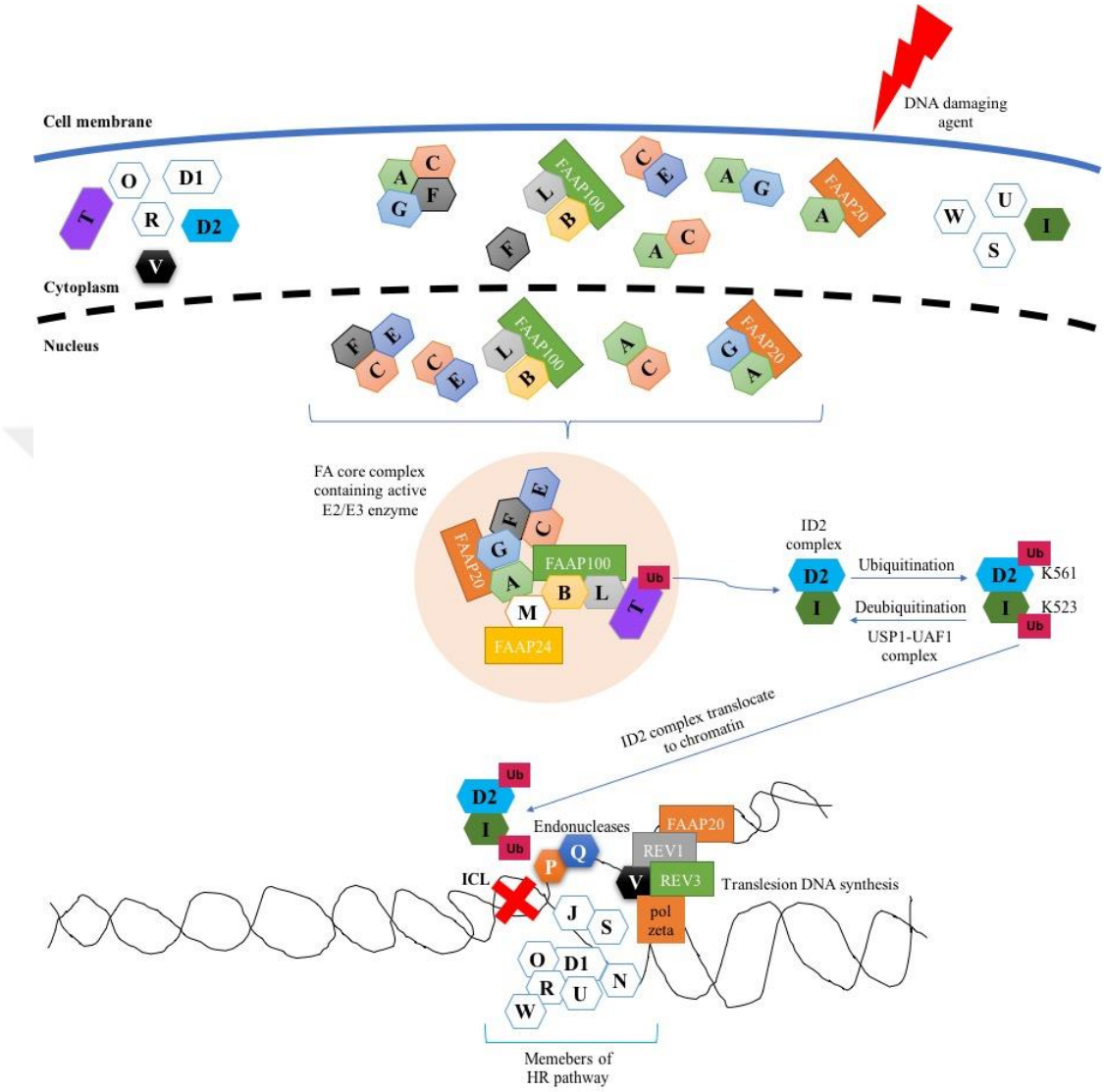

Figure 2.2. Schematic representation of the FA/BRCA pathway. (Adapted from Gueiderikh *et al*, (202).)

Table 2.2. Subcellular localization of FANC and associated proteins.

Protein	Subcellular Localization	Reference
FANCA	Nucleus and cytoplasm	(168, 170, 203)
FANCB	Nucleus and cytoplasm	(164)
FANCC	Nucleus and cytoplasm	(168, 170, 203)
FANCD1	Nucleus and cytoplasm	(204, 205)
FANCD2	Nucleus and cytoplasm	(206)
FANCE	Nucleus and cytoplasm	(174, 175, 178)
FANCF	Nucleus and cytoplasm	(207)
FANCG	Nucleus and cytoplasm	(171)
FANCI	Nucleus and cytoplasm	(208)
FANCJ	Nucleus	(209)
FANCL	Nucleus and cytoplasm	(164)
FANCM	Nucleus	(164)
FANCN	Nucleus	(210)
FANCO	Nucleus and cytoplasm	(211)
FANCP	Nucleus	(212)
FANCQ	Nucleus	(212)
FANCR	Nucleus and cytoplasm	(211)

Table 2.2. (Continued) Subcellular localization of FANC and associated proteins.

Protein	Subcellular Localization	Reference
FANCS	Nucleus and cytoplasm	(213)
FANCT	Nucleus and cytoplasm	(214)
FANCU	Nucleus and cytoplasm	(215)
FANCV	Nucleus and cytoplasm	(216, 217)
FANCW	Nucleus and cytoplasm	(218)
FAAP20	Nucleus and cytoplasm	(219)
FAAP24	Nucleus	(220)
FAAP100	Nuclear and cytoplasm	(164)

2.4.2. Genetic and Phenotypic Characteristics of Patients

Fanconi anemia (FA; MIM 227650) is named after the Swiss pediatrician, Dr. Guido Fanconi (221). It is a rare hereditary disorder (incidence 1:200,000-1:400,000; carrier frequency 1:156-1:209) characterized by hematological defects, a predisposition to leukemia and solid organ tumors (e.g. head, neck, female genitals, esophagus and liver), as well as, by several congenital anomalies (222, 223). At least 22 distinct FA complementation groups exist because of mutations in *FANC* genes. FA can be inherited in an autosomal recessive (FA-A, -C, -D1, -D2, -E, -F, -G, -I, -J, -L, -M, -N, -O, -P, -Q, -S, -T, -U, -V, -W), X-linked (FA-B), or autosomal dominant manner (FA-R) (26, 27).

Congenital anomalies include short stature, skin hypo-/hyper-pigmentation, microcephaly, extremity defects, eye defects and urogenital anomalies (27, 147). After birth, FA patients show signs of hematological defects, including a decrease in one or more hematopoietic cell lines (i.e. neutropenia, thrombocytopenia, anemia or pancytopenia; Figure 2.3. A-B), early-onset of aplastic anemia, MDS as well as AML (24, 25).

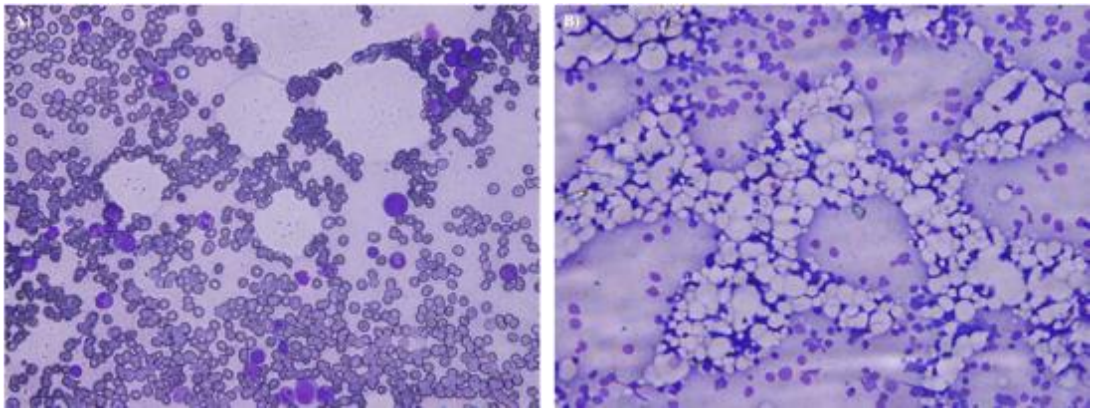

Figure 2.3. Bone marrow sections taken from Fanconi anemia patients showing; A) increased hypocellularity and B) elevated frequency of adipocytes (400x magnification) (Taken from Hacettepe University Pediatric Hematology Bone Marrow Transplantation Unit archives).

ICL formation in FA patients is followed by cellular toxicity, chromosomal anomalies and an increased rate of somatic mutations due to halted DNA replication and transcription (224, 225). Cells with a non-functional FA pathway show

hypersensitivity towards endogenous agents like reactive aldehyde or nitrogen mustard, as well as, exogenous agents, such as DEB and MMC, which are gold standard for diagnosis of FA (226-231). Treating mice lacking both FANCD2 and aldehyde dehydrogenase 2 enzyme with ethanol (i.e. break into aldehydes when oxidized) results in BMF (231). Exposure of cells with a defective FA signaling pathway to DEB and MMC results in chromosomal anomalies like breakage and/or radial formations (227, 228). Agents that damage DNA, such as alkylating agent Temozolomide (TMZ) without forming ICLs also activate the FA pathway. *FANCG*- and *FANCD1*-deficient cells are shown to be very sensitive to TMZ treatment, which promotes apoptosis (230, 232). Treatment of FA cells with MMC, DEB, nitrogen mustard or melphalan promotes delay in G2 phase transition and consequently cell cycle arrest at the G2/M phase (33, 233-235).

Impaired ICL repair results in genomic instability, but it is not the only mechanism responsible for FA pathophysiology (224). FANCD2 protein also acts to protects chromosomal integrity following replication-dependent one ended double strand breaks due to UV radiation, as well as, to stop lesion formation in chromosomes during mitosis and DNA at stalled replication forks (236-239). During the M-phase, FANCD2 and FANCM proteins cooperate with Bloom's complex (i.e. containing Bloom's Syndrome Helicase, DNA Topoisomerase IIIα, RecQ mediated genome instability 1 -RMI1- and RMI2) to stop the formation of chromosomal break points and ultrafine DNA bridges following replicative stress (236, 237). The frequency of ultrafine DNA bridges increases in BM hematopoietic cells with a non-functional FA pathway compared to controls, and results in incomplete cell-cycle and consequent apoptosis or genetic instability (240). This is a mechanism through which aplastic anemia may occur. However reverse mosaicism (i.e. somatic reversion of constitutional mutation) due to genetic instability is beneficial in some FA patients, in terms of partially restoring BM function. Somatic reversions in FA cells happen due to recombination of two compound heterozygote mutations or to spontaneously occurring point or frame shift mutations, that give rise to single functional allele or gene with an inactive function, respectively (241-243). A single revertant hematopoietic clone is able to improve BMF (241, 242).

2.4.3. Bone Marrow Failure in Fanconi anemia Patients

BMF in FA patients is treated by BMT. However, as a result of BMT, the frequency of secondary solid organ tumors or metabolic disturbances increases (244, 245). Mutations in FANC genes also affect quiescent HSCs and their progenitors. BM and umbilical cord blood of FA patients have lower HSC and progenitor frequencies compared to healthy counterparts (30, 246). The *in vitro* differentiation ability of BM hematopoietic progenitors derived from FA patients to CFU-GEMM (colony-forming unit precursor of granulocyte/erythrocyte/macrophage/megakaryocyte; multilineage hematopoietic progenitors), CFU-GM (colony-forming unit precursor of granulocyte/macrophage) and BFU-E (burst-forming unit of erythroid cells; the immature progenitors of erythroid lineage) is also lower than control cells (29, 247).

FA cells are sensitive towards cytokines, such as tumor necrosis factor α (TNF-α), interferon-γ (IFN-γ), macrophage inflammatory protein-1-α and TGF-β (34, 248-250). Intriguingly, TNF-α and IFN-γ levels are also very high in serum and BM collected from the patients (251, 252). ROS levels of *Fancc*$^{-/-}$ mice cells are shown to increase after TNF-α treatment, and may then initiate ICL formation and consequently cause unresolved DNA damage (253). Increased ROS and/or oxygen levels increase chromosomal aberrations or induce apoptosis and also FA cells are shown to expand better under hypoxic conditions (254-259). BM of mice lacking both FANCC and ROS detoxifying enzyme Cu/Zn superoxide dismutase had less cells than expected (260). Moreover, the FANCD2 protein directly interacts with FOXO3a following hydrogen peroxidase treatment and this interaction protects cells against oxidative stress by increasing the expression of FOXO3a targets that function as antioxidants (261). The ROS concentration is also known to affect HSC genetic stability and maintenance (262-267). Elevated levels of ROS in HSCs can be one of the reasons of BMF seen in patients.

Moreover, *in vivo* studies shed light upon the role of aberrant TGF-β signaling in FA BMF (34, 250). Autocrine TGF-β signaling is important for HSC fate (268). *Fancd2*$^{-/-}$ mice hematopoietic stem and progenitor cells (HSPCs) have elevated *Tgf-β1* gene expression and hyperactive TGF-β signaling in HSCs is

thought to be a novel therapeutic target for BMF (34). Additionally, TGF-β secretion from FA cells increase following treatment with ionizing irradiation and chemotherapy agents, which are essential for successful engraftment (250, 269). Therefore, suppression of TGF-β signaling in FA cells may help to reduce the cytotoxic effects of irradiation or chemotherapeutic drugs and increase engraftment efficiency (250). HSC niches may also play a pivotal role during the development of hematopoiesis under pathological circumstances (270). HSCs in disease state may also imprint the function of niche cells (271).

2.5. Possible Role of Mesenchymal Stromal/Stem Cells in Bone Marrow Failure Syndromes

Comparative studies of BM MSCs in healthy and disease conditions may help to understand the role of niche cells in HSC dynamics and provide insight into the disease pathogenesis. The Immunomodulatory role of MSCs may be impaired and initiate or furnish immune-mediated BMF syndromes, such as MDS and acquired aplastic anemia (272, 273). Many studies reveal a normal immunophenotype and multipotency for MSCs derived from MDS patients (274-279). However, few studies show alterations in CD105, CD90 and CD104 levels, as well as, defective differentiation potential (279-283). As part of HSC niches, MSCs contribute to HSC maintenance by differentiating into osteoblasts. and cells derived from MDS patients have reduced differentiation capacity along osteogenic lineages (279). In contrast to few studies indicating normal growth characteristics (278, 284), MDS MSCs also have decreased proliferative capacity, population doublings and CFU-F forming capacity as well as elevated senescence activity compared to controls (276, 279, 280, 283, 285). Intriguingly, MSCs from MDS patients carry genetic abnormalities and have alterations in their methylation profile compared to controls (274-276, 279, 283, 286, 287). This indicates a genetically unstable BM microenvironment with functional defects that may play a role in the progression of BMF. This is supported by misexpression of factors such as osteopontin, SCF, Ang1 and Jagged1 that are important for HSC maintenance (279). Furthermore, MSCs obtained from patients within low-risk stage have reduced TGF-β secretion, while cells derived from high-risk MDS patients have increased hepatocyte growth factor production compared to

controls (284). İmportant evidence that deregulation of MSCs affect HSC maintenance comes from a study where the MSC population within the BM of MDS patients is abnormally propagated and have elevated CXCL12 levels. Therefore, HSCs in close contact with a microenvironment bearing CXCL12 overexpression, may have deficits in certain cellular processes (288).

MSCs derived from aplastic anemia patients display decreased proliferation rates and clonogenic capacity, increased apoptosis as well as having alterations in genes expression related to vital cellular processes like TGF-β signaling and cell-cycle control (289-291). These findings support the fact that MSCs in disease-state have defective cellular functions which may affect HSC fate. There is an increase in the amount of fatty marrow in aplastic anemia patients which can be explained by elevated levels of PPARγ (peroxisome proliferator-activated receptor gamma) in patient-derived MSCs (292). Adipocytes are negative regulators of HSCs and increase in their number may contribute to HSC depletion (99).

In inherited pathological settings, such as FA, BM MSCs may also play a role in the establishment or progression of BMF. Mice MSCs lacking *Fancg* expression exhibit impaired support of *in vitro* HSC proliferation and differentiation to CFU-GM colonies, as well as *in vivo* HSC engraftment (31). However, *FancA*$^{-/-}$ human MSCs are able to support long-term HSC propagation (32). These two studies used distinct FA complementation groups to evaluate the HSC proliferation following their co-culture with FA BM MSCs which may explain the difference in results. Also, murine models of the disease may exhibit differences in terms of biological outcomes, compared to FA patients (293). BM derived MSCs from FA patients or murine models have similar immunophenotypes and differentiation capacity, but displayed reduced capacity to form CFU-Fs (colony forming unit fibroblasts), decreased proliferative potential, increased senescence activity, hypersensitivity to MMC and longer G2 phase transition compared to controls (31-33). Additionally, MSCs with a non-functional FA pathway have increased spontaneous chromosome breaks compared to healthy donors, but DEB treatment has no additive effect on the number of chromosomal breaks (33). This evidence supports hypothesis that the presence of genomic instability in MSCs is due to an impaired FA pathway. FA

MSCs secrete similar VEGF, but produce higher SCF and IL-6 cytokines compared to controls (32). IL-6 is reported to augment a niche beneficial for growth and survival of neuroblastoma cells and IL-6 levels are elevated in serum or BM of patients with neuroblastoma bone metastasis (294). Further studies are necessary to evaluate cytokines and growth factors produced by MSCs derived from BM of FA patients to clarify the role of cytokines for cancer predisposition in FA. As previously mentioned, hyperactive TGF-β signaling in HSCs may cause BMF in patients (34). Neither the level of TGF-β production by FA BM MSCs nor its possible role in progressive BMF through juxtacrine or paracrine signaling has been elucidated yet.

2.6. Regulators of Tissue Specification During Development

The most important question of developmental biology is how cell fate is determined. Cells are initially committed to a fate, that is a reversible state, thus enabling them to transform into other cell types. The next step is the determination stage during which pluripotent cells differentiate into a certain lineage through an irreversible process. In mammals, there are vast number of cell types each with a unique transcriptional program (295). During development, tissue specific gene expression together with epigenetic mechanisms (i.e. posttranslational modification of histones, DNA modifications, changes in nucleosome positioning, histone variants and non-coding RNAs) control the fate of stem/progenitor cells via precise spatio-temporal mechanisms (296-298). Studies involving pluripotent ESCs revealed the presence of genetic regulators of pluripotency, such as OCT4, POU class 5 homeobox 1, NANOG, Sex determining region Y-box 2, Sal-like protein 4, Caudal type homeobox 2 and Eomesodermin (299-303). Epigenetic processes like DNA methylation control the expression of such genes, thus preventing pluripotent stem cells to differentiate into specific cell lineages (304, 305). It has been reported that ESCs with no DNA (cytosine-5)-methyltransferases (*Dnmt1*, *Dnmt3a*, *Dnmt3b*) expression, can stay in undifferentiated state for longer periods of time (306). In ESCs, methylation mark on histone 3 lysine 4 (H3K4me3) chromatin domain as the transcription initiating histone modification is found at the promoter regions of the genes essential for pluripotency (307-309). Additionally, the promoter regions of

developmental transcription factors, like homeodomain transcription factors (e.g. Hox, Pax or Irx gene family) in ESCs contain opposing histone marks (H3K4me3 as active and histone 3 lysine 27 –H3K27me3- as repressive marks), called bivalent chromatin domains, that exist cooperatively to suspend the transcription until needed (308, 310-312). Upon receiving differentiation signals, the H3K27me3 mark of the developmental genes is removed to allow transcription, and commitment of the cell to a certain lineage (313).

Retinoic acid (RA) is one of the key elements maintaining cellular differentiation, proliferation and apoptosis via binding to its nuclear receptors called RA receptors (RAR) (314-316). Transcriptional activation of RA target genes, such as Hox genes in ESCs, can be achieved by binding of RA to the heterodimer of RAR-Retinoid X Receptor (RXR) already associated with a RA response element (RAREs) of the target (317-319). In the absence of RA ligand, the RAR-RXR heterodimer is in a close contact with corepressor proteins that form complexes with histone deacetylase (HDAC) 3 (320-322). HDAC3 reduces lysine residues on histones, thus causing a conformational change of nucleosomal structures followed by heterochromatin formation and transcriptional repression (323, 324). During RA treatment of human ESCs, lysine-specific demethylase 6B enzyme function to separate H3K27me3 histone modification from the promoter regions of genes within HOXA and HOXB clusters, thus allowing transcriptional activation and differentiation (325). Gillespie and Gudas (326) also report that *Hoxa1* expression in F9 embryonal carcinoma cells is halted by its interaction with RARγ-RXRα heterodimer and suppressor of zeste 12 protein homolog (SUZ12) repressor protein (polycomb group –PcG- protein) in the absence of RA.

PcG proteins act as transcriptional repressors, that are required to keep mammalian stem cells in a pluripotent state (327, 328). In mammals, there are two different PcG protein complexes, PRC1 (polycomb group RING finger protein 4, ring finger protein 1, polyhomeotic protein and chromobox family) and PRC2 (SUZ12, embryonic ectoderm development protein, enhancer of zeste homolog 2 and rbap48/46) (329). In *Drosophila*, PcG proteins repress target gene expression, such as Homeotic Complex (HOM-C; made of Antennapedia and Bithorax complexes) via

binding to Polycomb response elements (PREs) located away from the promoters (330). Within the human genome, Woo and co-workers (331) discover a conserved PRE region between *HOXD11* and *HOXD12* genes, which is a possible candidate for regulation of transcription. The *Hox* gene family, a member of homeodomain (HD) containing transcription factors, is a regulator of tissue specification.

2.7. Homeodomain Transcription Factors

In 1984, HD was first discovered in *Drosophila* (332, 333). The term 'homeo' comes from 'homeosis' defined as the alteration of an organ with another body part due to mutations in developmental genes. HD is a 60 amino acid long helix-turn-helix DNA binding motif encoded by an evolutionarily conserved 180 bp DNA sequence referred as the homeobox locus. The DNA binding motif is composed of three alpha helical structures together with an N-terminal arm. It has been reported that the third helix (referred as the recognition helix) and N-terminal region specifically binds to DNA, whereas a conserved region between the first and second alpha helix binds to the phosphate backbone (334, 335). Seven points (Leu 16, Phe 20 within the first helix and Trp 48, Phe 49, Asn 51, Arg 53, Lys/Arg 55 within the third helix) have been shown to be the most conserved regions across different species (336).

HD containing proteins are the master regulatory transcription factors that regulate axial patterning and establish regional identity during embryogenesis as well as act in regulating important cellular functions, such as differentiation and proliferation (337). An estimated number of 235 functional and 65 pseudo-homeobox genes exist within the human genome, which are classified into 11 superfamilies, known as ANTP (subdivided into HOXL and NKL), PRD (subdivided into PAX and PAXL), LIM, POU, HNF, SINE, TALE, CUT, PROS, ZF and CERS (338). In this thesis, I will only discuss the HOX genes and TALE homeobox class. HOX genes encode highly conserved proteins, that are the master regulators of positional identity during both pre- and post-natal life. Studying these genes can be vital in genome instability syndromes, such as in FA to gain a deeper understanding of tissue identity.

2.7.1. HOX Genes

HOX genes are evolutionarily conserved among animals with bilateral symmetry (339). HOX genes, members of HOXL subclass of ANTP homeobox class, are orthologous of the HOM-C (i.e. *lab, pb, Dfd, Scr, Antp, Ubx, Abd-A* and *Abd-B*) in *Drosophila* (336). They are classified into seven different gene families (Figure 2.4.) in mammals; Hox1 and Hox2, as the anterior (3' end) gene families, Hox3 gene family, Hox4, Hox5, Hox6-8, as the central gene families, and Hox9-13, as the posterior (5' end) gene families (338).

In humans, total of 39 HOX genes are found in four clusters (designated as A, B, C and D) located on different chromosomes (Figure 2.4.) (338). During development, their position on the chromosome is associated with their order of expression, which is known as the collinearity of HOX genes (340). The gene expression is controlled both spatially and temporarily. Within each cluster, the earliest activation of HOX gene transcription first occurs at the 3' end (i.e. Hox1 and Hox2) during early stages of embryogenesis (i.e. formation of primitive streak). At the later stages of development, transcriptional initiation is sequentially directed towards the 5', which corresponds to the posterior end of the embryo (341-348).

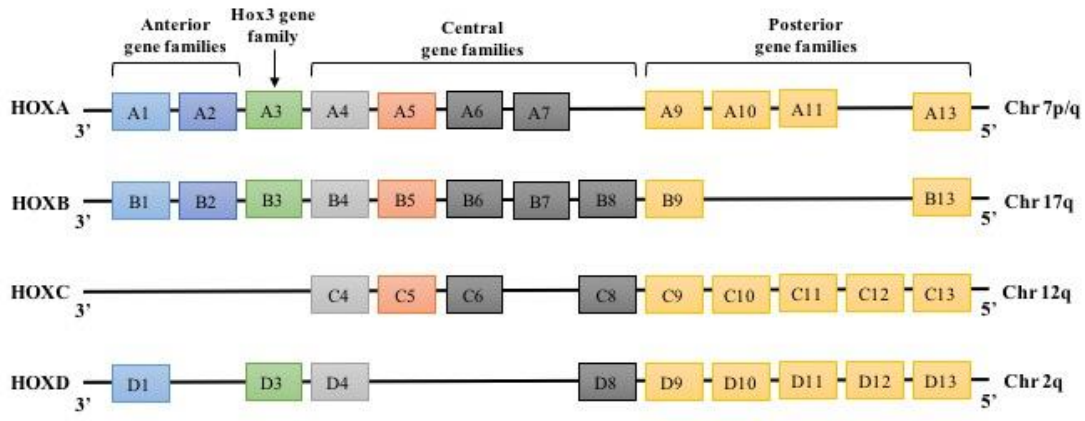

Figure 2.4. In humans, total of 39 HOX genes are found in four clusters, which are located on four different chromosomes.

The role of HOX genes in establishing the anterior-posterior body axis during embryonic development has long been known (14, 349). Members of each gene family (i.e. paralogous) are functionally redundant. Therefore, loss-of-function

mutation of a Hox gene has smaller effects compared to mutations in more than one member of a gene family that causes homeotic transformation in the axial skeleton (350-357). Additionally, HOX proteins also regulate hematopoiesis, lineage specification of cells, programmed cell death, migration, formation of new blood vessels, development of proximal-distal (i.e. dorsal-ventral) axis of limb-bud and organogenesis (349, 358, 359). Members of the Hox9-13 gene family function in limb development. *Hox9/10*, *Hox11* and *Hox13* gene expression are important for distinct segments of the limb, which are stylopod (humerus and femur), zeugopod (radius/ulna and tibia/fibula) and autopod (wrist/forepaw and ankle/hind paw), respectively (353, 356, 360, 361). As transcription factors, HOX proteins regulate the transcription of their target genes by interacting with a specific DNA sequence through their HD (362). An increase in the DNA binding affinity and specificity of HOX proteins has been reported once they assemble with their co-factors, known as TALE proteins (19, 20).

2.7.2. TALE Homeobox Class

In animals, a total of 20 functional genes has been attributed to this class and is grouped into six gene families; Pknox (*PKNOX1/PREP1* and *PKNOX2/PREP2*), Meis (*MEIS1, MEIS2* and *MEIS3*), Pbx (*PBX1, PBX2, PBX3* and *PBX4*), Irx (*IRX1, IRX2, IRX3, IRX4, IRX5* and *IRX6*), Mkx (*MKX*), or Tgif (*TGIF1, TGIF2, TGIFLX* and *TGIFLY*) gene family (338). In contrast, another study classified TALE proteins into five subclasses by combining Meis and Pknox under Meis class genes (363). Members of the TALE superfamily have a conserved atypical HD, containing three extra amino acids located between the first and second alpha helices. In addition to atypical HD, TALE proteins contain IRX domain, MKX domain, MEIS domain, PBC domain or TGIF domain (363-366). Pknox (Pbx/Knotted 1 homeobox), Meis (Myeloid Ecotropic Integration Site) and Pbx (Pre-B-cell leukemia homeobox) gene families have been extensively studies for their role in regulating DNA binding of HOX proteins. *PKNOX1, PKNOX2, MEIS1, MEIS2, PBX1, PBX2, PBX3* and *PBX4* genes will be further discussed in this thesis.

The HD of Pknox, Meis and Pbx proteins is located at the C-terminus, while two domains responsible for protein interactions are found near the N-terminus. The

MEINOX domain exists in MEIS gene family and a related one lies in the PBC domain of PBC class (364). Within PKNOX and MEIS proteins, the MEINOX domain can be broken down into two sub-classes called Homology Region 1 (HR1/MEIS A) and HR2/MEIS B that are collectively referred as the MEIS domain. In addition to the MEINOX domain, the Meis gene family also bear three more domains (MEIS-C, MEIS-D and MEIS-N) with unknown functions (363). The PBC domain of PBX proteins contains two conserved motifs, known as PBC-A and PBC-B (363). Although both MEIS-A and MEIS-B are suggested to be involved in binding to PBC domain, the MEIS-A domain is essentially needed to participate during PKNOX1 and PBX1 interaction (367, 368). Meis and Pknox proteins have a dissimilar C-terminus. Through their C-termini, Meis proteins (e.g. MEIS1) can directly interact with HOX proteins (e.g. HOX11-13) (369). Additionally, the PBC-A domain of PBX proteins is required to form a heterodimer with PKNOX proteins, like PKNOX2 (370). PKNOX-PBX heterodimers can also bind to HOX proteins and this ternary complex has increased transcriptional activity compared to PBX-HOX complexes (370). HOX genes belonging to anterior and central gene families recognize a TAAT motif, whereas members of posterior gene families bind to a TTAT motif (371). It has been shown that Pknox1 alone or in combination with Pbx1 binds to TGAXTGACAG sequence, but the Meis1-Pbx1 dimer recognizes TGATTGXX and TGACAG sequences (372, 373). The TGATTGXX sequence recognized by the Meis1-Pbx1 complex contains a consensus motif (TGATTXXT), previously identified as a PBX-HOX DNA binding sequence (334, 374).

2.8. Role of HOX and TALE Genes in Specification of Mesenchymal Stromal/Stem Cells

During adulthood, the tightly regulated Hox gene expression pattern continues to provide a “biological fingerprint” for different cell types, such as fibroblasts, muscle cells, HSCs and MSCs (15, 16, 375). MSCs of different sources (i.e. anatomical regions) have distinct HOX and TALE gene expression patterns, confirming the presence of positional memory (16-18, 376, 377). In mice, expression of *Hoxa9, Hoxb2/7/8, Hoxc6/8/9/10/11/12/13* and *Hoxd4/8* is altered in adult femoral bone marrow or adipose tissue derived MSCs, as well as in cells obtained from

juvenile spleen, aorta or thymus (377). A study carried out using *in vitro* cultured human MSCs derived from bone marrow, colon and dental pulp also show changes in HOX and TALE gene expression (18). MSCs from dental pulp had only slight *HOXA10, HOXB2, HOXC8/C9* and *HOXD1* expression, whereas MSCs from bone marrow (iliac crest, vertebrae or sternum) expressed most of HOX genes except *HOXB1, HOXC12, HOXD11/C12* (18). Like MSCs from bone marrow, colon derived cells expressed most of the HOX genes preferentially *HOXA11/A13, HOXD9/D13* but have no *HOXB1, HOXB13, HOXC6/C8/C9/C10/C11/C12/C13* or *HOXD11* expression (18). Compared to iliac crest MSCs, vertebrae and sternum cells had different levels of transcription. There was an increase in *HOXA3/A5, HOXB6/B7/B8/B9, HOXC4/C8, HOXD9* and decrease in *HOXC10/C11, HOXD3* expression of sternum derived MSCs (18). On the other hand, *HOXB8/B9* expression level increased and *HOXA1/A6/A7/A11, HOXC10/C11* expression levels decreased in MSCs from vertebrae (18). MSCs from different anatomical regions also express TALE genes at various levels. Intriguingly, *PBX1, PBX2, PBX3, PREP1, MEIS1* and *MEIS2* genes have the highest expression in colon-derived MSCs, whereas dental pulp has very low levels of *PBX3, MEIS1* and *MEIS2* (18). Another study regarding human tissues report that *HOXA9/A10, HOXB7, HOXC6/C8/C10, HOXD8* in the bone marrow, and *HOXA9/10, HOXC10, HOXD8* in the cord blood have significantly high expression levels (376). In concordance with this study, Liedtke *et al* (17) show that human cord blood and bone marrow derived MSCs had a similar HOX code especially *HOXA9, HOXB7, HOXC10* and *HOXD8* can be used as marker genes for these MSC populations.

Members of HOX and TALE classes may regulate the multilineage differentiation potential of MSCs. Osteogenic differentiation of BM-MSCs increases *HOXA10/A11, HOXC13* and *HOXD9/D13* expression (18, 378). Osteogenic induction also triggers *PBX1* and *PBX2* expression of iliac crest and sternum MSCs, while an increase in *MEIS1* expression is observed in cells from vertebrae (18). Furthermore, MSCs expressing *Hox11* are shown to have a higher differentiation potential, and play a role during bone reformation following fracture (379). During differentiation of MSCs into endothelial lineages, increase in *HOXA7, HOXB3* expression and decrease in *HOXA3, HOXB13* expression are observed (380).

2.9. HOX and TALE Gene Deregulation and Genome Instability

Genome instability either give rises to or result from alterations to DNA (i.e. increase in copy number, single-/double-strand breaks, conformational changes caused by DNA intercalators) and chromosomes (i.e. increase in number, translocations, inversions, deletions), thus causing deregulation of gene expression (e.g. HOX genes) and susceptibility to cancer. Deregulation of HD transcription factors in hematological malignancies (e.g. NUP98/HOXA9 translocation in acute myeloid leukemia) and solid tumors has long been known (381-384). Expression of various homeobox genes, known as tumor-suppressors, decreases, while expression of others, known as tumor-promoting genes, increases in tumors. In solid organ (e.g. lung and breast) tumors, abnormal epigenetic states (e.g. hypermethylation of CpG islands) are shown to be associated with *HOX* or other homeodomain containing gene misexpression (385). Various studies report that long non-coding RNAs (e.g. *HOTAIR*) or microRNAs (e.g. *miR-10b*) targeting HOXD cluster and *HOXD10,* respectively are deregulated in breast tumors causing increased metastasis (386, 387).

Deregulation of HOX gene expression may lead to increased proliferation (e.g. *FGF-2* expression increases via HOXB7 causing tumor growth), resistance to apoptosis (e.g. *EGFR* expression increases via HOXB7 causing resistance to tamoxifen), an increase in angiogenesis (e.g. HOXB7 induces VEGF-A and FGF-2 triggering formation of new veins), a decrease in mesenchymal-to-epithelial transition (e.g. inhibition of HOXA10), alterations in microenvironment (e.g. HOXA9 expressed by epithelial ovarian cancer cells activates TGF-β2 in BM-MSCs to adopt cancer-associated fibroblast properties), thus promoting cancer progression (388-394). Rubin *et al* (395) also suggest that HOXB7 is involved in DNA repair against ionizing irradiation by interacting with members of the non-homologous end-joining (NHEJ) pathway (i.e. ATP-dependent DNA helicase II 70kDa subunit, ATP-dependent DNA helicase II 80kDa subunit, DNA-PK and PARP). Additionally, TALE genes act as oncogenes (e.g. *MEIS1*) and tumor suppressors (e.g. *PREP1*), and function in DNA repair and maintaining genomic stability (e.g. *PREP1*) (21, 23).

Within the BM microenvironment, there is a tight interaction between HSCs and the niche components, such as BM-MSCs. BMF cannot solely depend on impaired HSC function, but rather to the combination of defects in the niche. FA HSCs have impaired TGF-β signaling, which is proposed as a mechanism of BMF (34). FA BM-MSCs may also bear defects in their differentiation potential, immunophenotype, proliferation capacity, senescence activity, ROS production as well as in their secretion of cytokines and growth factors, such as TGF-βs that may contribute to a defective BM. Genome instability of BM-MSCs due to FA disease state may also change their tissue identity and may trigger hematological defects. It is important to assess HOX and TALE gene expression levels and their functional role in FA BM-MSCs compared to control cells.

3. MATERIALS and METHODS

3.1. Cell Culture and Characterization of Bone Marrow Mesenchymal Stromal/Stem Cells

3.1.1. Patients and Controls

Cryopreserved BM-derived mononuclear cells (BM-MNCs) from FA patients (10.3 ±4.1 years old; Table 3.1.) obtained at Hacettepe University Pediatric Hematology Bone Marrow Transplantation unit were used for isolation of BM-derived MSCs (BM-MSCs). Patients (designated as HUSCS-FA01 - 12; n= 12) were diagnosed by clinical manifestations (Table 3.2. and 3.3.) and DEB treatment. Age-matched (FA family donors= 10.9 ±5.2; and unrelated donors= 12.8 ±8.9 years old; Table 3.1.) healthy donors (designated as HUSCS-D01 - 16; n= 16) served as controls. The study was approved by the Local Ethical Committee (Number 14, 24/08/2009) and Hacettepe University Non-interventional Clinical Research Ethics Board (GO 14/403-12, 23/07/2014; Appendix-1). Informed consent, where appropriate, was obtained from donors and FA patients enrolled in this study.

Table 3.1. Age and gender information of donors and Fanconi anemia patients.

Donor ID	Gender / Age (Years)ψ	FA Patient ID	Gender / Age (Years)ψ
HUSCS-D01*	F / 14	HUSCS-FA01	M / 9
HUSCS-D02*	M / 6	HUSCS-FA02	F / 6
HUSCS-D03*	F / 2	HUSCS-FA03	F / 12
HUSCS-D04*	M / 10	HUSCS-FA04	M / 14
HUSCS-D05*	F / 15	HUSCS-FA05	M / 14
HUSCS-D06*	M / 13	HUSCS-FA06	M / 9
HUSCS-D07*	M / 16	HUSCS-FA07	F / 5
HUSCS-D08	M / 2	HUSCS-FA08	M / 5
HUSCS-D09	M / 10	HUSCS-FA09.a	F / 13
HUSCS-D10	F / 18	HUSCS-FA09.b	M / 6
HUSCS-D11	M / 19	HUSCS-FA10	M / 17
HUSCS-D12	F / 3	HUSCS-FA11	F/ 13
HUSCS-D13	F / 25		
HUSCS-D14	F / 24		
HUSCS-D15	M / 7		
HUSCS-D16	M / 7		

* Indicates FA patient donors; ψ, Age of Donors and FA patients at the day of bone marrow transplantation.

Table 3.2. Characteristics of Fanconi anemia patients.

Sample ID	Anemia	DEB Test	Cytogenetic/ Peripheral Blood Dysplasia	Clinical Features
HUSCS-FA01	+	+	46, XY	Hypospadias, cryptorchidism, deviation to right at IVS and slight enlargement of left ventricle
HUSCS-FA02[#]	+	+	10p	Cafe au lait and hyperpigmentation
HUSCS-FA03	+	+	Out of 19 metaphases, 2 showed hypodiploidy and 1 showed 8+mar	Microphthalmia, hyperpigmentation, left kidney agenesis, hypothyroidism, bilateral hearing loss
HUSCS-FA04	+	+	Out of 10 metaphases, 7 showed non-clonal hypodiploidy and no structural anomalies	Cafe au lait, left kidney agenesis and osteopenia
HUSCS-FA05	+	+	17 metaphases were structurally normal. 3 metaphases showed non-clonal structural alterations indicating chromosomal instability	Microcephaly, microphthalmia, ptosis, cafe au lait and hyperpigmentation
HUSCS-FA06[*]	+	-	46, XY	Extremity anomalies, right ectopic kidney, right hydroureteronephrosis, right extra renal pelvis and patent ductus arteriosus

Table 3.2. (Continued) Characteristics of Fanconi anemia patients.

Sample ID	Anemia	DEB Test	Cytogenetic/ Peripheral Blood Dysplasia	Clinical Features
HUSCS-FA07*	+	-	17 metaphases were both structurally and quantitatively normal. 2 metaphases showed add(7)(q)	Microcephaly, microphthalmia, cafe au lait, hyperpigmentation, left ectopic kidney and growth retardation
HUSCS-FA08	+	+	46, XY	Extremity anomalies, unilateral kidney agenesis, atrial septal defect, ventricular septal defect, hypothyroidism and cryptorchidism
HUSCS-FA09.a**	+	+	46, XX	Microcephaly, hyperpigmentation, left kidney agenesis, growth retardation and hyperglycemia
HUSCS-FA09.b**	+	+	11q23 deletion at 1 metaphase and hypodiploidy at 2 metaphases.	Hydrocephaly, microphthalmia, ptosis, hyper/hypopigmentation, cafe au lait, cortical cyst and osteoporosis
HUSCS-FA10	-	+	out of 15 metaphases, 1 had del(1)(q11qter) and 5 had non-clonal hypodiploidy. +	Growth retardation, microcephaly, Cafe au lait and hyperpigmentation
HUSCS-FA11	+	+	out of 15 metaphases, 6 had der(4)t(1;4)(q11;p16); indication of partial trisomy 1q.	Microcephaly, microphthalmia, hyperpigmentation and mitral valve prolapse

DEB Test, Diepoxybutane Test; F, Female; M, Male; +, present; -, absent; * DEB Test results of FA-06 and FA-07 do not support International Fanconi Anemia Registry (IFAR) criteria (The Rockefeller University, 2013); # DEB test was positive for the sister of HUSCS-FA02 diagnosed as leukemia. ** HUSCS-FA09.a and HUSCS-FA09.b are siblings.

Table 3.3. Blood counts of Fanconi anemia patients.

Sample ID	Hb (g/dl)*	WBC (/μl)*	PLT (/μl)*
HUSCS-FA01	10.2	3600	32000
HUSCS-FA02	9.00	5100	69000
HUSCS-FA03	11.2	4300	122000
HUSCS-FA04	11.1	200	64000
HUSCS-FA05	8.20	2100	42000
HUSCS-FA06	7.70	1800	59000
HUSCS-FA07	10.4	2600	38000
HUSCS-FA08	10.0	5600	118000
HUSCS-FA09.a	10.4	4300	87000
HUSCS-FA09.b	9.80	3200	75000
HUSCS-FA10	15.0	8900	253000
HUSCS-FA11	10.0	3500	72000

Hb, Hemoglobin Count; WBC, White Blood Cell Count; PLT, Platelet Count; * Hb (g/dl), WBC (/μl) and PLT (/μl) counts of FA patients were obtained prior to the bone marrow transplantation.

3.1.2. Mutational Analysis of FA Patients

Mutation screening of the FA patients (n= 10; genomic DNA provided by Hacettepe University DNA biobank) was performed at Department of Clinical Genetics in VU University Medical Center, The Netherlands, according to the algorithm described earlier (396). Briefly, *FANCA* gene was investigated by complete sequencing by Sanger sequencing as well as for large deletions by Multiplex Ligation-Dependent Probe Amplification (MLPA) (397). For patients with no mutation in *FANCA* gene, coding regions and exon-intron boundaries of *FANC-A, -B, -C, -D2, -E, -F, -G, -I, -L, -M, BRCA1, BRCA2, BRIP1, ERCC4, PALB2, RAD51* and *SLX4* were sequenced using next generation sequencing with Miseq Illumina sequencer after enrichment with a custom HaloPlex Target Enrichment kit (Agilent, USA) as previously reported (398).

3.1.3. Culture of Bone Marrow Mesenchymal Stromal/Stem Cells

BM-MSCs were maintained in expansion (DMF10) medium in a 5% CO_2

incubator at 37°C. DMF10 medium consisting of 60% Dulbecco's modified Eagle's medium-low glucose (DMEM-LG; cat no: 31600-083, Gibco, UK) and 40% MCDB-201 medium (cat no: M6770-1L, Sigma-Aldrich, USA) supplemented with 10% heat-inactivated fetal bovine serum (HI-FBS; cat no: 102701106, Gibco), 1% penicillin and streptomycin (Pen/Strep; cat no: A2213, Biochrom AG, Germany) and 1% L-glutamine (cat no: K0282, Biochrom AG), was changed after 3 to 4 days. Once BM-MSCs reached confluency of 70–80%, they were washed with phosphate-buffered saline (PBS; cat no: A9162, Applichem, Germany) and trypsinized in 0.25% trypsin (cat no: 27250-018, Invitrogen, UK) containing 1mM ethylenediaminetetraacetic acid (EDTA; cat no: 15575020, Invitrogen) solution (Trypsin-EDTA). Passaged cells were then washed in DMF10 medium to stop the effect of trypsin enzyme, followed by centrifugation (Eppendorf, Germany) at 453 *x g* for 5 minutes at room temperature. BM-MSCs were then counted using Trypan Blue stain (cat no: 03-102-1B, Biological Industries, Israel) and replated. For later use, cells were frozen in DMEM-LG supplemented with 20% FBS-HI and 10% dimethyl sulfoxide (DMSO; cat no: D8418, Sigma-Aldrich) in a liquid nitrogen tank at 196°C. Passage 3 BM-MSCs were used for further experiments unless stated otherwise.

3.1.4. Gene Expression Analysis

RNA Isolation

Total RNA including small RNAs were isolated from MSCs using miRNeasy Mini Kit (cat no: 217004, Qiagen, USA) from passage 3 BM-MSCs obtained from donor and FA patients. Prior to RNA isolation, plasticware was treated with diethyl procarbonate (DEPC) to prevent RNase activity. Cultured cells were washed twice with PBS and then Qiazol Lysis Reagent (cat no: 79306, Qiagen) was directly added onto the cells. The cell lysates were collected with a rubber policeman and then transferred into a 1.5ml tube, followed by pipetting until no cell clumps were visible. Samples were stored at -80°C until RNA isolation. On the day of isolation, cell lysates were thawed completely, mixed with 140µl chloroform (cat no: A3633, Applichem) by shaking vigorously for 15 seconds and were then incubated for 2-3

minutes at room temperature, followed by centrifugation at 12,000 *x g* at 4°C for 15 minutes. Afterwards, RNA found at the most upper aqueous phase was transferred to a new collection tube (Qiagen) and was mixed with 1.5 volumes of 100% ethanol (cat no: A3678, Applichem). The mixture was then transferred into a RNeasy® Mini column (Qiagen), followed by centrifugation at 10,000 *x g* for 15 seconds at room temperature. The flow-through was discarded and the step was repeated for the remainder of the RNA sample. 350µl of Buffer RWT containing guanidinium thiocyanate (Qiagen) was added into RNeasy® Mini column, followed by centrifugation at 10,000 *x g* for 15 seconds at room temperature. The flow-through was discarded. At this step, on-column DNase digestion was performed using RNase-free DNase Set (cat no: 79254, Qiagen) in order to eliminate genomic DNA (gDNA) contamination. For each RNA sample, 10µl DNase I stock solution was mixed with 70µl Buffer RDD (ingredients not stated; Qiagen). The mixture was added directly onto the membrane of RNeasy® Mini column and incubated for 30 minutes at room temperature. 350µl of Buffer RWT was added into RNeasy® Mini column, followed by centrifugation as described before and the flow-through was discarded. 500µl of Buffer RPE (ingredients not stated; Qiagen) was added into RNeasy® Mini column, followed by centrifugation at 10,000 *x g* for 15 seconds at room temperature and the flow-through was discarded. This step was repeated but centrifugation was performed for 2 minutes. RNeasy® Mini column was placed onto a new tube and centrifuged at 10,000 *x g* for 1 minute at room temperature to further dry the membrane. RNeasy® Mini column was placed onto a 1.5ml collection tube (Qiagen) and RNA was eluted by adding 30-50µl RNase-free water (Qiagen), followed by centrifugation at 10,000 *x g* for 1 minute at room temperature. The tube containing eluted RNA samples were directly transferred onto ice. RNA concentration and quality was determined by NanoDrop ND-1000 (Thermo Fisher Scientific, USA) spectrometer. RNA samples were stored at -80°C until further use.

Synthesis of Complementary DNA

Complementary DNAs (cDNAs) were synthesized from RNA samples using Transcriptor High Fidelity cDNA Synthesis Kit (cat no: 05081963001, Roche, USA) according to the manufacturer's instructions. The reactions were set-up on ice unless

indicated otherwise. Briefly, RNA sample was mixed with 60µM Random Hexamer Primer and the final volume was brought up to 11.4µl by PCR grade water. The mixture was incubated at 65°C for 10 minutes using GeneAmp PCR System 9700 (Applied Biosystems, USA). Then, the tube containing template-primer mix were cooled on ice for 5 minutes and remaining components including 1X Transcriptor High Fidelity Reverse Transcriptase Reaction Buffer, 20U Protector RNase Inhibitor, Deoxynucleotide Mix (1mM each), 5mM dithiothreitol (DTT) and 10U Transcriptor High Fidelity Reverse Transcriptase were added into the tube, followed by brief centrifugation. The reverse transcription reaction conditions were 29°C for 10 minutes, 48°C for 60 minutes, followed by inactivation of reverse transcriptase enzyme at 85°C for 5 minutes. Then the tubes were placed on ice to stop the reaction. cDNA samples were stored at -20°C until further use.

Reverse Transcriptase Quantitative Polymerase Chain Reaction Analysis

Prior to reverse transcriptase quantitative polymerase chain (RT-qPCR), cDNAs were diluted 1:2 using PCR grade water. The final PCR reaction was carried out in 10µl in 96 or 384 well plates according to the manufacturer's instructions. Briefly, mix including 1X LightCycler® 480 Probes Master (cat no: 04707494001 or 04887301001, Roche) and 1X RealTime ready Assay (cat no: 05532957001 or 05583055001, Roche; details of primer-probe mix are outlined in Table 3.4.) was prepared and the final volume was adjusted to 8µl using PCR grade water for each reaction. Afterwards, 2µl of diluted cDNA was added onto the mix. Reactions were set-up on ice. RT-qPCR was performed using LightCycler® 480 II (Roche). PCR conditions were 95°C for 10 minutes, then 45 cycles of 95°C for 10 seconds, 60°C for 30 seconds and 72°C for 1 second, followed by a cooling step of 40°C for 30 seconds. Subsequently, the crossing point (Cp; also known as threshold cycle -Ct-) for target and reference genes for each sample was calculated according to Second Derivative Maximum Method using LightCycler® 480 Software (Roche). The Ct values equal to or greater than 40 were analyzed on gel electrophoresis and was accepted as a positive value if only the specific band was present on the gel. All target genes were normalized against the endogenous house-keeping gene, *ACTB*. To calculate relative gene expression, $2^{-\Delta Ct}$ (Equation 2.1.) method by applying log

transformation was used. For each individual sample, mean ΔCt of the technical replicates was calculated. Additionally, fold change was calculated by applying a log transformation to $2^{-\Delta\Delta Ct}$ method (399).

$$\Delta Ct = Ct_{Target\ gene} - Ct_{Reference\ gene} \quad (2.1.)$$

3.1.5. Immunophenotyping Bone Marrow Mesenchymal Stromal/Stem Cells

Immunophenotyping of BM-MSCs obtained from donor (n=16) and FA patients (n= 12) was done by flow cytometer (BD FACSAria, Becton Dickinson, USA) using FACS DIVA software. Passage 3 BM-MSCs were passaged using Trypsin-EDTA and were then washed in DMF10 medium, followed by centrifugation at 453 *x g* for 5 minutes at room temperature. Supernatant was discarded and the cell pellet was resuspended in PBS, followed by centrifugation at 453 *x g* for 5 minutes at room temperature. Washing step in PBS was repeated twice. Afterwards, single-cell suspensions were prepared in 100µl PBN buffer (containing PBS; bovine serum albumin -BSA-, cat no: 130-091-376, MACS, Miltenyi Biotec, Germany; and sodium azide) supplemented with 2% human AB serum, were stained by incubation with directly conjugated monoclonal antibodies for 15 minutes at room temperature according to the manufacturer's instructions. Cell surface antibodies against CD29, CD44, CD73, HLA-ABC, CD90, CD105, CD106, CD140b, CD144, CD146, CD166, CD200, CD271 were used to detect the cells from mesenchymal stromal cell origin. Endothelial cell marker anti-CD31 and hematopoietic cell markers anti-CD45 anti-CD14, anti-HLA-DR, anti-CD34 were used to exclude cells of hematopoietic origin. A general stem cell marker, anti-CD133 was also used. Details of antibodies were given in Table 3.5.

Table 3.4. Details of primers used in RT-qPCR.

Gene Name	Forward Primer	Reverse Primer	Amplicon Length (bps)
HOXA1	AGAAACCCTCCCAAAACAGG	GGTACTTGTTGAAGTGGAACTCCT	127
HOXA2	AATGGACACAATGGCGACTC	TTTTTCTCATTGCTGGTTAAAGG	52
HOXA3	AAGCAGAAAACCAGCAGCTC	GCGGTTGAAGTGGAACTCTT	144
HOXA4	CAGAAGAAGACAGACCCTTTCC	AGCTTGGATGAGCTGCCTTA	70
HOXA5	GCGCAAGCTGCACATAAG	CTGGTAGCGCGTGTAGGC	79
HOXA6	GGATGCAGCGGATGAACT	GGTAGCGGTTGAAGTGGAAC	123
HOXA7	GCTTGCCTGCTACCTAGTGC	AAAAGCTGCGGGCTGTAAG	67
HOXA9	AAAACAATGCTGAGAATGAGAGC	TATAGGGGCACCGCTTTTT	111
HOXA10	CCTTCCGAGAGCAGCAAA	TTGGCTGCGTTTTCACCT	71
HOXA11	CGGCAGCAGAGGAGAAAG	GTATAGGGGCAGCGCTTTT	133
HOXA13	ATGTACTGCCCCAAAGAGCA	GCTTCTTTCTCCCCCTCCTAT	112
HOXB1	CAGCTACGGGCCTTCTCA	CCGTAGCTCGAGGGATGA	78
HOXB2	TTAGCGTTTAATCCACTCCCTTT	AAAGATAACCGAGTGCCCAAT	60
HOXB3	CTGGGGCTCGATGTGAATA	CTGTTCCAAGCGGCTGAC	77
HOXB4	CTGGATGCGCAAAGTTCAC	GTGTAGGCGGTCCGAGAG	81
HOXB5	AAGCTTCACATCAGCCATGA	CGGTTGAAGTGGAACTCCTTT	107
HOXB6	CCCGCTGAGACATTACCC	AATAGGAGGAAGTGGCAAAGC	74

Table 3.4. (Continued) Details of primers used in RT-qPCR.

Gene Name	Forward Primer	Reverse Primer	Amplicon Length (bps)
HOXB7	GGATGCGAAGCTCAGGAA	CGTCAGGTAGCGATTGTAGTGA	104
HOXB8	CTTACTCTCTGCTTCCGTTCCT	TGGAACCAGATTTTGACCTGT	72
HOXB9	GACTCGTAAGCGGCGAATC	ACAAATTGAAGGGGACTGAGAA	60
HOXB13	CACCAGGTCCCTTTTGGAA	TGTACGGAATGCGTTTCTTG	102
HOXC4	ATCCCGCTGCCTCTACCT	CGAGCTCATGATCATTAATTTCC	90
HOXC5	CCCAGCAAGTGGTCCTAGAG	GGAGGGCACAGAAATTCG	66
HOXC6	AAAAGAGGAAAAGCGGGAAG	GGGACAGTCCTGGTCACTCT	62
HOXC8	GGACAAGGCCACTTAAATCAA	TGTAAGTTTGCCGTCCACTG	97
HOXC9	GCAGCAAGCACAAAGAGGA	CGTCTGGTACTTGGTGTAGGG	113
HOXC10	GACCTCCAATTTTAATTTCACCTG	AGAGGAAGGAGCGGGAAG	64
HOXC11	AAGTGGCACCATCGGAAC	CCGGTGCATAAGCTCGTC	63
HOXC12	AACTCTCAGACCGCTTGAATCT	ATTCTCCGGTTCTGAAACCA	64
HOXC13	CACTGGGCTCTCTCCAATG	CCGGTAGCTGCTCACCTC	129
HOXD1	TGGAACAACCCCCACTAAGTT	AAGTACCGGCCTCACGAA	78
HOXD3	AAGACAAAATTCAAGAAAACACACA	CCAATGTCTGCTGAATCCTG	93
HOXD4	GGGCGGGATTCTCTCTCTAA	CGCCAAGATTTTATGTTCTCAGT	64
HOXD8	GTTTCCGTGGATGAGACCAC	TGGAAGCGACTGTAGGTTTGT	69
HOXD9	GGGACGCCTCAAAATGTCT	TGGCCTATAAGCGAGTCCAC	66
HOXD10	CTGAGGTCTCCGTGTCCAGT	GCTGGTTGGTGTATCAGACTTG	77

Table 3.4. (Continued) Details of primers used in RT-qPCR.

Gene Name	Forward Primer	Reverse Primer	Amplicon Length (bps)
HOXD11	CACTCACCCACCCTCCTTC	AGAGACGTCATTAAACCCAAGG	71
HOXD12	TGGACAGAGGCCTTGTTTG	ACCGAAGGAAAAGCCTTAGC	61
HOXD13	GGGGTCACCGAGAAAGTCTA	TGGCCATTTTTAAAGCCATC	64
MEIS1	TTCACACTGGCCTTAAAGAGG	CCGTAATGGGGTAGATCGTC	97
MEIS2	CCAGTCAAATCGAGCAGGTT	GGGCTGACCCTCTGGACTAT	76
PBX1	GCTGTCACTGCTACCAATGTG	ACATGTTAAAAGAACTGGAAGAACC	94
PBX2	GACCAGAGCCTGGACGAG	ATGCTGAGGCCAGTTTTCTC	113
PBX3	AGCGTCCTGTGTGAGATCAA	GTCTCATTAGCTGGGGATCG	88
PBX4	TGCCTGTCAACACCTAGCTC	TGGAGAGAGGCCAGAGTCC	95
PKNOX1	GTTGAGTGGAGAGCCTGGAA	GCCTGTGATGGCACTTTGA	70
PKNOX2	TGCCACCAATATAATGCGTTC	CTCATCCTCCGTGGGGTAG	67
TGF-β1	ACTACTACGCCAAGGAGGTCAC	TGCTTGAACTTGTCATAGATTTCG	73
ACTB	GGCCAGGTCATCACCATT	GGATGCCACAGGACTCCAT	91
Adipsin	CATCGACCACGACCTCCT	GCCACGTCGCAGAGAGTT	123
PPARγ	GACAGGAAAGACAACAGACAAATC	GGGGTGATGTGTTTGAACTTG	96
LPL	TCGTTCTCAGATGCCCTACA	GCCTGATTGGTATGGGTTTC	87
RUNX2	GCCTAGGCGCATTTCAGAT	CTGAGAGTGGAAGGCCAGAG	66
ALPL	AGAACCCCAAAGGCTTCTTC	CTTGGCTTTTCCTTCATGGT	74
OCN	CCAGCCCTATGGATGTGG	TTTTCAGATTCCTCTTCTGGAGTT	72
SP7	GACTGCAGAGCAGGTTCCTC	TAACCTGATGGGGTCATGGT	60

Table 3.5. Details of antibodies used in flow cytometry analysis.

Antibody	Clone	Manufacturer
APC-/PE-anti-CD29	TS2/16; MAR4	Biolegend, USA; BD Pharmingen, USA
FITC-anti-CD44	BJ16; L178	Biolegend; BD OptiBuild
APC-/PE-/FITC-anti-CD73	AD2	Biolegend; BD Pharmingen
PE-/PECy7-anti-HLA-ABC	G46-2.6	BD Pharmingen
PE-/FITC-anti-CD90	5E10	BD Pharmingen; Biolegend
PE-anti-CD105	SN6	e-Bioscience, USA
APC-/FITC-anti-CD106	STA; 51-10C9	Biolegend; BD Pharmingen
PE-anti-CD140b	28D4	BD Pharmingen
APC-anti-CD144	BV9; 55-7H1	Biolegend; BD Pharmingen
PE-anti-CD146	SHM-57; P1H12	Biolegend; BD Pharmingen
PE-anti-CD166	3A6	Biolegend
PE-anti-CD200	MRC-OX104	BD Horizon
PE-/APC-anti-CD271	C40-1457; ME20.4-I.H4	BD Pharmingen; Miltenyi Biotec
FITC-anti-CD31	WM59	BD Pharmingen
FITC/PeCy7-anti-CD45	2D1; HI30; HI30	BD Pharmingen; BD Horizon; Biolegend
APC-anti-CD14	M5E2	BD Pharmingen
FITC-/APC-anti-HLA-DR	L243; G46-6	BD Biosciences; BD Pharmingen
PE-/FITC-/APC-anti-CD34	581	BD Pharmingen; Biolegend
PE-anti-CD133	AC133/Prominin-1	e-Bioscience

3.1.6. Differentiation Potential of Bone Marrow Mesenchymal Stromal/Stem Cells

Adipogenic Differentiation

90-100% confluent BM-MSCs obtained from donor (n= 16) and FA patients (n= 12) were maintained in the presence of adipogenic induction medium, consisting of DMEM-LG, 10% FBS-HI, 1% L-glutamine, 1% Pen/Strep, 1μM dexamethasone (cat no: D2915, Sigma), 60μM indomethacin (cat no: 17378, Sigma), 500μM 3-isobutyl-1-methylxanthine (cat no: I5879, Sigma) and 5μg/ml insulin (cat no: I6634, Sigma) in a 5% CO_2 incubator at 37°C for 21 days. The medium was changed every 3 to 4 days. Cultures were then washed with PBS, followed by fixation with 10% formaldehyde (cat no: A0877, Applichem) for 30 minutes. Cells were stained with Oil Red O (ORO; cat no: O0625, Sigma-Aldrich) for 10 minutes at room temperature, followed by followed by three washes with double distilled water (ddH_2O). Images were obtained with an inverted microscope (Olympus CKX41; Olympus, Japan). Uninduced cells were used as controls.

Osteogenic Differentiation

70-80% confluent BM-MSCs obtained from donor (n= 15) and FA patients (n= 11) were maintained in osteogenic differentiation medium consisting of DMEM-LG, 10% FBS-HI, 1% L-glutamine, 1% pen/strep, 100nM dexamethasone, 10mM ß-glycerophosphate (cat no: A2253, Applichem) and 0.2mM L-ascorbic acid (cat no: A4034, Sigma) in a 5% CO_2 incubator at 37°C for 21 days. The medium was changed every 3 to 4 days. BM-MSCs were then washed and fixed as described above, followed by staining with Alizarin Red S (ARS; cat no: A2306-0100, Sigma-Aldrich) at pH 4.2 for 10 minutes at room temperature. Cells were then washed three times with ddH_2O and images were obtained with an inverted microscope. Uninduced cells were used as controls.

Expression Levels of Adipogenic- or Osteogenic-Specific Genes

Details of RNA isolation, cDNA synthesis and RT-qPCR reactions were outlined above. cDNAs were synthesized from 260ng total RNAs. Adipogenic

differentiation was assessed by measuring the changes in *Adipsin*, *PPARγ* and Lipoprotein lipase (*LPL*) expression while osteogenic differentiation was determined by measuring the changes in Runt-related transcription factor 2 (*RUNX2*), Alkaline phosphatase (*ALPL*), Osteocalcin (*OCN*) and Osterix (*SP7*) (see Table 3.4.). Fold change in gene expression between adipogenic- or osteogenic- differentiated BM-MSCs (grown in differentiation medium) and untreated cells (grown in DMF10 medium) were determined. When no Ct value was obtained, ΔCt value was accepted as 25 in order to be able to calculate the fold change.

3.1.7. Effect of DEB Treatment on Cell Cycle of Bone Marrow Mesenchymal Stromal/Stem Cells

Hallmark of FA cells is the hypersensitivity to ICL agents such as DEB leading to cell cycle arrest, DNA damage and genomic instability. Therefore, cell cycle of BM-MSCs were characterized following DEB treatment. The protocol details were described previously (400, 401). In the published protocol, two different DEB concentrations (0.01 μg/ml and 0.1μg/ml) was used. Initially, a pilot study using both concentrations was performed to determine the effective dose on cell cycle analysis of FA and donor BM-MSCs. One day prior to DEB treatment, passage 2 BM-MSCs in DMF10 medium were seeded into tissue culture flasks. Afterwards, cells were treated with DEB (cat no: 202533, Sigma Aldrich) for 4 days. Untreated BM-MSCs were used as controls. Following DEB treatment, BM-MSCs were rinsed with PBS, followed by trypsinization by Trypsin-EDTA. Cells were then washed in DMF10 medium, followed by centrifugation at 453 *x g* for 5 minutes at room temperature. Supernatant was discarded and the cell pellet was resuspended in PBS, followed by centrifugation as described before. Supernatant was discarded and cells were stained with propidium iodide solution (PI). Flow cytometry analysis was performed using a FACSAria. Percentage of BM-MSCs in each cell cycle phase (i.e. dip G1, dip S-phase and dip G2) was analyzed (analysis type: manual, auto-linearity: no ploidy, mode: first cycle is diploid, all cycle events: > 3800, RCS: < 5) using ModFit LT 5.0 software (Verity Software House, Inc., USA).

Further analysis was performed using 0.1µg/ml DEB treatment because 0.01µg/ml had no effect on the cell cycle (Figure 3.1.). Percentage of BM-MSCs in each cell cycle phase was analyzed for donor (n= 3) and FA patient (n= 6) and where possible mean of technical replicates was calculated. Fold change in the percentage of positive cells in each cell cycle phase was calculated using Equation 2.2.

Fold change= % of DEB treated BM-MSCs - % of control BM-MSCs (2.2.)

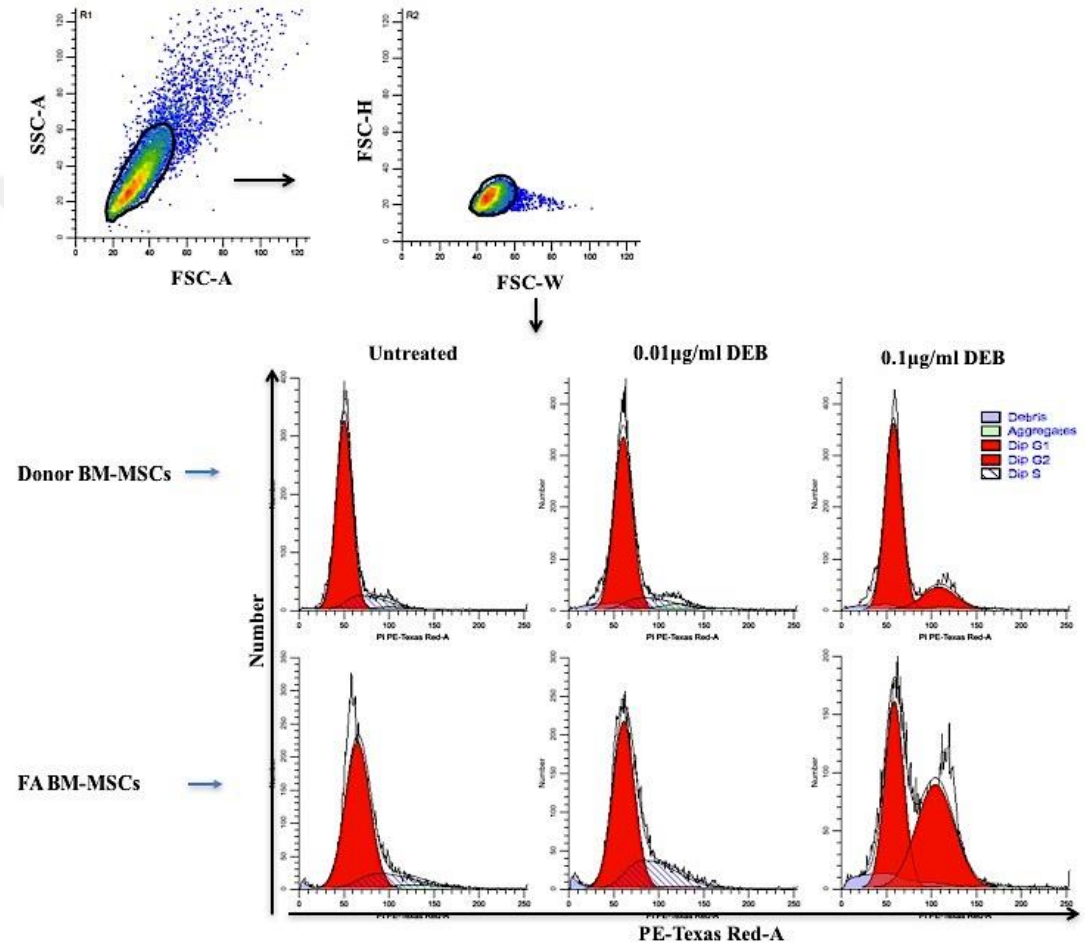

Figure 3.1. Representative flow cytometry analysis of cell cycle phases (i.e. dip G1, dip S-phase or dip G2, where dip means the peak) of BM-MSCs prior to and following 0.01µg/ml and 0.1µg/ml DEB treatment.

3.1.8. Population Doubling Analysis of Bone Marrow Mesenchymal Stromal/Stem Cells

Population doubling of passage 3-7 BM-MSCs derived from donor (n= 4) and FA patients (n= 5) were compared. Cells were expanded in DMF10 medium and

medium was changed every 3 to 4 days. Five technical replicates were performed for each independent sample. At the end of each passage, confluent BM-MSCs were washed with PBS, followed by trypsinization using Trypsin-EDTA. Cells were then washed in DMF10 medium, followed by centrifugation at 453 *x g* for 5 minutes at room temperature. Supernatant was discarded and the cell pellet was resuspended in PBS, followed by centrifugation at 453 *x g* for 5 minutes at room temperature. Cells from each technical replicate were counted using Trypan Blue stain. Cells from each replicate were centrifuged at 453 *x g* for 5 minutes at room temperature. Supernatant was discarded and pellet was resuspended in fresh DMF10 medium. Cells were recounted and seeded as 16,667 cells/well into a 6-well plate. At the end of each passage, population doubling (PD) was calculated for each technical replicate and the average was determined. When no cells were counted, PD was not determined for the technical replicate. PD was determined by using Equation 2.3. and Equation 2.4. Finally, cumulative (c) PD was calculated using mean PD values (402)

$$\text{Fold expansion} = \text{cells harvested} \div \text{cells seeded} \tag{2.3.}$$

$$\text{PD} = \log_{10}(\text{fold expansion} \div \log_{10} 2) \tag{2.4.}$$

3.1.9. Detection of Senescence Associated β-Galactosidase Activity of Bone Marrow Mesenchymal Stromal/Stem Cells

Cellular senescence of passage 3 and 6 BM-MSCs derived from donors (n=2) and FA patients (n= 3) were assessed using senescence associated β-galactosidase (SA-β-gal) Staining Kit (cat no: 9860, Cell Signaling Technology, USA) according to the manufacturer's instructions. Senescent cells but not presenescent, dormant or differentiated ones could be detected by β-galactosidase activity which was partly related to lysosomal β-D-galactosidase encoded by *GLB1* gene (403, 404). Briefly, BM-MSCs seeded into 6-well plate were washed with PBS, followed by fixation with 1X Fixative Solution (item no: 11674, Cell Signaling Technology) at room temperature for 10 minutes. Meanwhile, β-Galactosidase Staining Solution containing 1X Staining Solution (item no: 11675, Cell Signaling Technology), 1X Solution A (item no: 11676, Cell Signaling Technology), 1X Solution B (item no: 11677, Cell Signaling Technology) and 1mg/ml X-gal (item no: 11678, Cell

Signaling Technology) in dimethylformamide (cat no: D4551, Sigma-Aldrich) at pH 6.0 was prepared. Cells were rinsed two times with PBS and then stained using β-Galactosidase Staining Solution, followed by overnight incubation at 37°C in a dry incubator. Images were obtained with an inverted microscope. Senescent BM-MSCs were identified as blue-stained cells. For each sample, two different images were taken from different areas. The quantification of senescent cells was performed by counting the number positive and negative cells using 100X magnified images by Cell Counter plugin in ImageJ software (NIH, USA). Then, the percentage of positive cells was calculated using Equation 2.5. and Equation 2.6.

$$\text{Total cell count} = \text{positive cell count} + \text{negative cell count} \quad (2.5.)$$

$$\%\ \text{Positive cells} = (\text{positive cell count} \times 100) \div \text{total cell count} \quad (2.6.)$$

3.1.10. Reactive Oxygen Species Production by Bone Marrow Mesenchymal Stromal/Stem Cells

CM-H2DCFDA molecular probe (Invitrogen, USA) was used to detect ROS production in FA (n= 4) and donors (n= 3) BM-MSCs. Firstly, cells were trypsinized using Trypsin-EDTA and 5000 cells per well were incubated in 100µl PBS supplemented with/without 10µM CM-H2DCFDA in a 5% CO_2 incubator at 37°C for 30 minutes. Cells were then washed in PBS, followed by centrifugation at 453 *x g* for 5 minutes at room temperature. Pellets were then resuspended in PBS (100µl/well), transferred to a 96-well plate (cat no: 655086, Greiner Bio-One, Germany) and fluorescence was detected by FLUOstar Omega microplate reader (excitation= 485nm and emission= 520nm; BMG Labtech, Germany). PBS supplemented with/without CM-H2DCFDA was used as control. For each sample, total of five technical replicates were measured and their mean was calculated. Fluorescence intensity (FI) was determined by using Equation 2.7.-2.9.

$$\text{Normalized FI of cells} = \text{FI of stained cells} - \text{FI of cells in PBS} \quad (2.7.)$$

$$\text{Normalized FI of control} = \text{FI of PBS with 10µM probe} - \text{FI of PBS} \quad (2.8.)$$

$$\text{Normalized FI} = \text{normalized FI of cells} - \text{normalized FI of control} \quad (2.9.)$$

3.1.11. TGF-β Levels of Bone Marrow Mesenchymal Stromal/Stem Cells

TGF-β1 Gene Expression

Details of RNA isolation, cDNA synthesis and RT-qPCR reactions were outlined above. cDNAs were synthesized from 260ng total RNAs. Relative expression level of *TGF-β1* gene (see Table 3.4.) was compared between FA patients (n= 7) and donor (n= 10) cells. Following 0.1µg/ml DEB treatment for 4 days, fold change in *TGF-β1* gene expression between treated and untreated BM-MSCs of FA patients (n= 6) and donors (n= 3) were determined. When Ct value was not obtained, ΔCt value was accepted as 25 in order to be able to calculate the fold change.

Active TGF-β1, TGF-β2 and TGF-β3 Secretion

Active TGF-β1, TGF-β2 and TGF-β3 secretion levels by 70-80% confluent BM-MSCs obtained from donor (n= 8) and FA patients (n= 9) were determined using Bio-Plex Pro™ TGF-β 3-plex Assay (cat no: 171W4001M, Bio-Rad, USA) kit following manufacturer's instructions. Briefly, standard vial was reconstituted in 500µl DMF10 medium, followed by vortexing for 5 seconds and incubation on ice for 30 minutes. 4-fold serial dilution of standard was then performed to generate eight-point standard curve. Cell Culture supernatants (unknown samples) previously stored at -80°C, were thawed and were centrifuged at 1000 *x g* for 15 minutes at 4°C. 50µl of unknown sample was activated by adding 10µl of 1N hydrochloric acid, followed by incubation for 10 minutes at room temperature. Each sample was then neutralized by adding 10µl base solution containing 0.5M HEPES (cat no: HEP-B, Capricorn Scientific) and 1.2N sodium hydroxide, followed by 1:16 dilution using DMF10 medium. Empty DMF10 medium treated as unknown samples and diluted in 1:16 using medium, was included as a negative control. 50µl/well of coupled magnetic beads was added to the assay plate, followed by two washes with 100µl/well Bio-Plex® wash buffer. The wash buffer was discarded after plate was placed on the appropriate magnetic stand for at least 1 minute. 50µl/well of diluted standards, unknowns or negative control was then added to the plate and incubated on shaker at 900 rpm for 2 hours at room temperature, followed by three washes as described above. 25µl detection antibody was added to each well and incubated on

shaker at 900rpm for 1 hour at room temperature, followed by three washes as described above. Finally, 50µl/well of Streptavidin-PE was added to the plate and incubated on shaker at 900rpm for 30 minutes at room temperature, followed by three washes as described above. The beads were resuspended in 125µl/well assay buffer for detection of FI using Bioplex MAGPIX multiplex reader (Bio-Rad). Concentration vs. FI graph of known TGF-β1/2/3 standards was constructed by logistic-5PL regression analyses (Figure 3.2. A-C). FI of unknown samples or negative control was interpolated into the slope to find the corresponding concentration value (pg/ml). Concentration of the negative control was then subtracted from the concentration of each unknown sample in order to find the actual amount of TGF-β1/2/3 secreted by the cells.

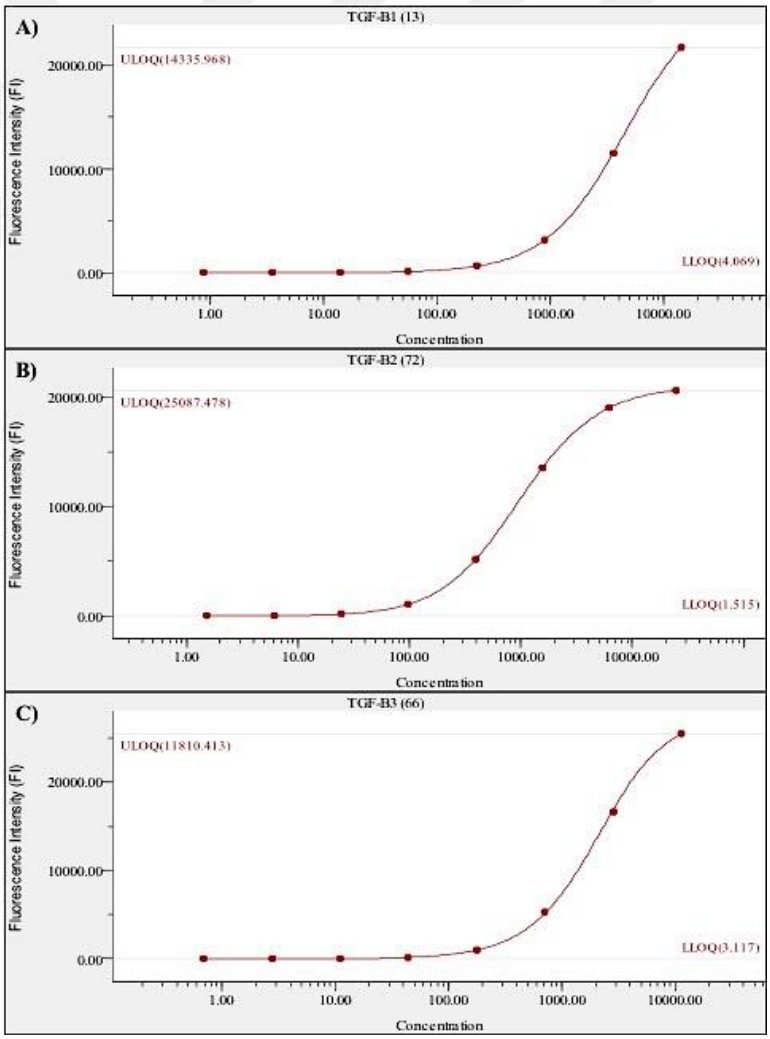

Figure 3.2. Concentration vs. FI graph of known A) TGF-β1, B) TGF-β2 and C) TGF-β3 standards was calculated by logistic-5PL regression analyses.

3.2. HOX and TALE Profile of Bone Marrow Mesenchymal Stromal/Stem Cells

3.2.1. HOX and TALE Gene Expression Pattern

Details of RNA isolation, cDNA synthesis and RT-qPCR reactions were outlined above. cDNAs were synthesized from 260ng total RNAs. Total of 39 HOX and 8 TALE gene expressions (see Table 3.4.) of cells obtained from FA patients (n= 12) and donors (n= 16) were assessed by calculating relative gene expression.

3.2.2. Effect of DEB Treatment on HOX and TALE Gene Expression

Effect of DEB treatment on gene expression was only determined on differentially expressed ones between FA and donor BM-MSCs. Details of RNA isolation, cDNA synthesis and RT-qPCR reactions were outlined above. cDNAs were synthesized from 260ng total RNAs. Following 0.1μg/ml DEB treatment for 4 days, fold change in gene expression between treated and untreated BM-MSCs of FA patients (n= 6) and donors (n= 3) were determined. When no Ct value was obtained, ΔCt value was accepted as 25 in order to be able to calculate the fold change.

3.2.3. Protein Level of Differentially Expressed Gene Between FA Patient and Donor Bone Marrow Mesenchymal Stromal/Stem Cells

Extraction of Total Protein Lysates

To obtain total protein lysates, BM-MSCs in DMF10 medium were washed twice with ice cold PBS and incubated on ice with Pierce® RIPA Buffer (cat no: 89900, Thermo Scientific) containing 1X protease inhibitor cocktail (cat no: P2714-1BTL, Sigma-Aldrich) for 5 minutes. Lysates were collected using cell scraper, centrifuged at 14,000 *x g*, 4°C for 15 minutes and supernatants were transferred to a new tube. Samples were stored at -80°C until further use.

Determining the Protein Concentration

Protein concentration was determined using Pierce™ BCA Protein Assay kit (cat no: 23225, Thermo Scientific™) following manufacturer's protocol. BSA

standards were prepared as described in Table 3.6. Each standard was diluted 1:20 in BCA working reagent (50:1, Reagent A:B), followed by incubation at 37°C for 30 minutes. The absorbance of each standard was measured at 562nm using NanoDrop ND-1000 spectrophotometer and standard curve was automatically constructed by the software (Figure 3.3.). The concentration of unknown samples was then determined using the above protocol. Lysing buffer solution containing protease inhibitor cocktail was used as blank.

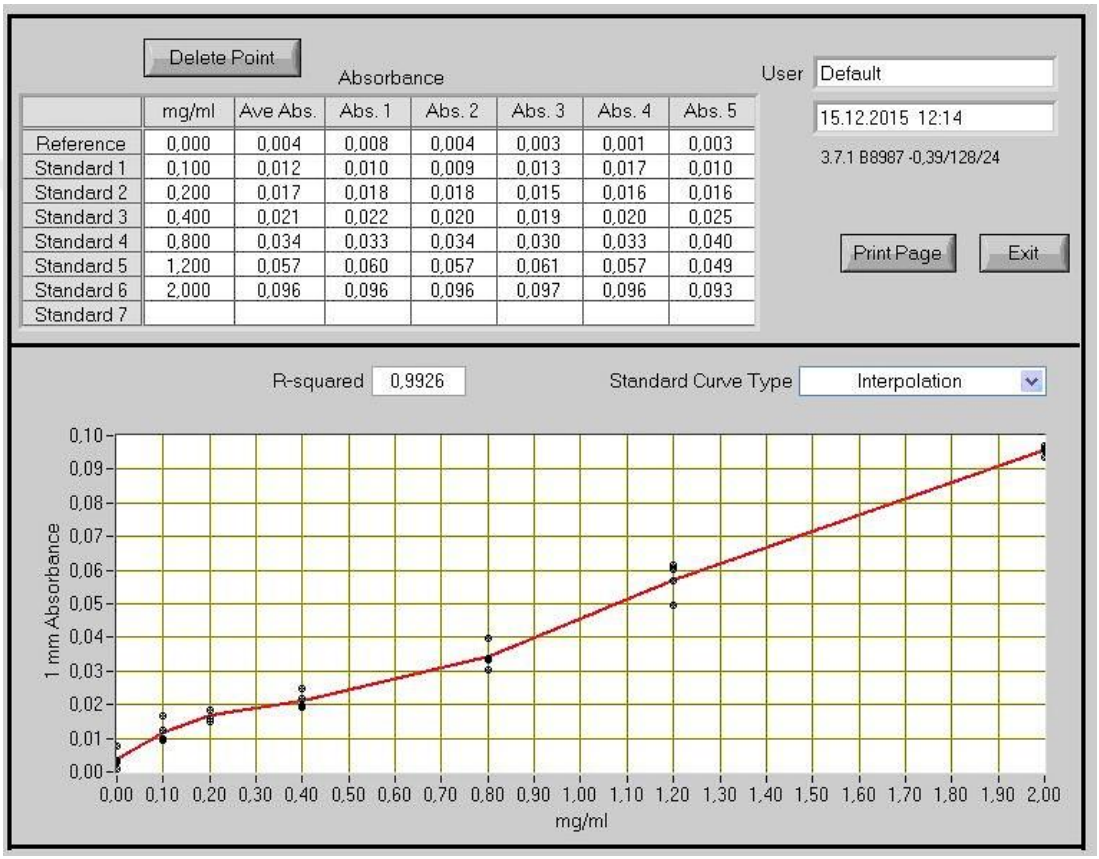

	mg/ml	Ave Abs.	Abs. 1	Abs. 2	Abs. 3	Abs. 4	Abs. 5
Reference	0,000	0,004	0,008	0,004	0,003	0,001	0,003
Standard 1	0,100	0,012	0,010	0,009	0,013	0,017	0,010
Standard 2	0,200	0,017	0,018	0,018	0,015	0,016	0,016
Standard 3	0,400	0,021	0,022	0,020	0,019	0,020	0,025
Standard 4	0,800	0,034	0,033	0,034	0,030	0,033	0,040
Standard 5	1,200	0,057	0,060	0,057	0,061	0,057	0,049
Standard 6	2,000	0,096	0,096	0,096	0,097	0,096	0,093
Standard 7							

Figure 3.3. Absorbance values corresponding to each standard obtained using NanoDrop ND-1000 spectrophotometer.

Table 3.6. Dilution and final concentration of BSA standards used for BCA assay.

Standard Number	BSA Standard Volume (µl)	Standard Initial Concentration (mg/ml)	Diluent* Volume (µl)	Standard Final Concentration (mg/ml)
1	-	-	50	0
2	2.5	2	47.5	0.1
3	5.0	2	45	0.2
4	10	2	40	0.4
5	20	2	30	0.8
6	30	2	20	1.2
7	50	2	-	2.0

* Lysing buffer solution containing 1X protease inhibitor cocktail was used as diluent.

Western Blot Analysis

Total protein lysates were used for sodium dodecyl sulphate polyacrylamide gel electrophoresis (SDS-PAGE) which was performed using 10% TGX Stain-Free FastCast Acrylamide kit (cat no: 161-0183, Bio-Rad) according to manufacturer's instructions. The maximum amount of protein lysate available was used for loading. The protein lysates were mixed with 4X Laemmli buffer (cat no: 161-0747, Bio-Rad) containing 355mM 2-mercaptoethanol (BME; cat no: 161-0710, Bio-Rad) and final volume was brought up to 60µl by ddH_2O. Samples were boiled for 5 minutes and along with Precision Plus Protein Dual Xtra standards (cat no: 161-0377, Bio-Rad) were loaded onto 1.5mm thick 10% gels for SDS-PAGE and run in 1X Tris/Glycine/SDS (cat no: 161-0772, Bio-Rad) running buffer at 100-120 V at room temperature. Proteins were then transferred (7 minutes, 2.5A and ≤ 25V) to a PVDF membrane (cat no: 170-4156 or 170-4272, Bio-Rad) using Trans-Blot Turbo Blotting system (cat no: 170-4155, Bio-Rad) and Trans-Blot Turbo Transfer System Transfer Pack (cat no: 170-4156, Bio-Rad).

Membranes were then blocked in 1X tris buffered saline (TBS; 20 mM Tris and 500 mM sodium chloride, pH 7.5) containing 0.1% Tween 20 (cat no: 161-0781, Bio-Rad) and 5% dry milk (cat no: 170-6404, Bio-Rad) for 1 hour at room temperature. Afterwards membranes were incubated with mouse-anti-PKNOX2 primary antibody (clone: 56.1, cat no: sc101857, Santa Cruz, USA; see Table 3.7.) diluted 1:100 in 1X TBS containing 0.1% Tween 20 and 5% dry milk overnight at 4°C. Membranes were washed three times with 1X TBS containing 0.1% Tween 20 (TBS-T) and were incubated with horseradish peroxidase conjugated (HRP-) goat-anti-mouse secondary antibody (cat no: AS003, Abclonal, USA; see Table 3.8.) diluted 1:2000 in 1X TBS containing 0.1% Tween 20 and 5% dry milk for 1 hour. Membranes were washed three times with TBS-T and peroxidase activity was determined using Clarity Western ECL Substrate kit (cat no: 170-5060, Bio-Rad) according to manufacturer's instructions. Briefly, Clarity western peroxidase reagent was mixed with Clarity western luminol/enhancer reagent in a 1:1 ratio. The mixture was then added onto the membrane, followed by incubation for 5 minutes at room temperature. Pictures were taken by Kodak Gel Logic 1500 Imaging System

(Thermo Fisher Scientific). Membranes were then washed in TBS-T, blocked in 5% dry milk TBS-T and reblotted with anti-β-ACTIN primary antibody (clone: D6A8, cat no: 8457S, Cell Signaling Technology; see Table 3.7.) in 5% dry milk TBS-T overnight at 4°C. Membranes were washed three times with TBS-T, incubated with HRP-goat-anti-rabbit secondary antibody (cat no: AS014, Abclonal, USA; see Table 3.8.) as mentioned above. Peroxidase activity was determined as outlined above. Densitometric analysis were carried out to evaluate mean grey value using ImageJ software (405). Then, PKNOX2 protein level of a sample was normalized to the corresponding β-ACTIN level which was used as an internal control.

3.3. Induction of Bone Marrow Mesenchymal Stromal/Stem Cells with Recombinant Human TGF-β1 Protein

3.3.1. Effect of Recombinant Human TGF-β1 Protein Induction on Cell Viability

$5x10^3$/well BM-MSCs from a donor were plated into 96 well plates and kept in a 5% CO_2 incubator at 37°C for 24 hours. Then, cells were treated with various concentration (0.01, 0.05, 0.1, 0.2, 1, 5 or 10ng/ml) of recombinant (r) TGFβ1 protein (cat no: 580702, BioLegend, USA) prepared in DMF10 medium for 12, 24 and 48 hours. Uninduced cells were also included as controls. Cell viability following rTGFβ1 induction was assessed using cell proliferation reagent WST-1 (cat no: 0501594401, Roche). At the end of the incubation period, 10µl/well WST-1 stain was added and incubated in a 5% CO_2 incubator at 37°C for 4 hours. Absorbance was measured at 450nm using Sunrise^{TM} Microplate Reader (Tecan, Switzerland) and analyzed with Magellan^{TM} data analysis software. A reference wavelength was set to 620nm. Five technical replicates were performed for each concentration at each incubation period. Mean absorbance value obtained from wells containing only medium (i.e. blank control) was subtracted from the absorbance value of each technical replicate. Then outlier analysis using IBM SPSS Statistics software (Version 24, IBM Corp., USA) was conducted on the normalized data in order to eliminate extreme values. Then, percentage of cell viability was calculated using Equation 2.10.

cell viability= (100 x mean of induced cells) ÷ mean of uninduced cells (2.10.)

3.3.2. Effect of Recombinant Human TGF-β1 Protein Induction on Cell Proliferation

Effect of rTGF-β1 treatment on the proliferation of BM-MSCs obtained from FA patients (n= 4) and donors (n= 2) was measured using the xCELLigence system and analyzed using RTCA software 1.2.1 (Roche Applied Sciences, Germany; ACEA Biosciences, USA). Firstly, cells were trypsinized by Trypsin-EDTA and counted by Trypan blue staining. 5000 cells per well were seeded into a 96-well E-Plate (ACEA Biosciences) and kept at 37°C for 30 minutes. The plate was then loaded onto the device kept in a 5% CO_2 incubator at 37°C and impedance value of each well, also known as a cell index value, was monitored every 15 minutes for about a day. The media of cells were replaced with DMF10 supplemented with 0.1 or 5ng/ml rTGF-β1. Untreated cells were used as controls. The cell index was automatically saved every 15 minutes and the media were replenished about every 48 hours. For each sample, four technical replicates were made and their mean was calculated. The cell index was normalized using the time point (26:41:34 hours) measured prior to addition of recombinant protein. Doubling time of BM-MSCs was also calculated between 37:46:27 and 68:17:04 hours after the first TGF-β1 treatment.

3.3.3. Effect of Recombinant Human TGF-β1 Protein Induction on Gene Expression

75000 donor BM-MSCs per well were plated into 6-well plates and were incubated in a 5% CO_2 incubator at 37°C. Afterwards cells were treated with 0.1 or 5 ng/ml rTGF-β1 protein for 24, 48 or 72 hours. Uninduced cells were used as controls. BM-MSCs were then trypsinized by Trypsin-EDTA, counted and were washed with PBS, followed by centrifugation at 453 *x g* for 5 minutes at room temperature. Washing step was repeated. Afterwards, RNA isolation, cDNA synthesis and RT-qPCR reaction were performed as outlined above. cDNAs were synthesized from 130ng total RNA. Fold change in gene expression levels between treated and untreated BM-MSCs were determined. Additionally, gene expression

levels were also compared between FA patients (n= 5) and donors (n= 5) treated with 0.1 or 5 ng/ml rTGF-β1 for 24 hours.

3.3.4. Effect of Recombinant Human TGF-β1 Protein Induction on PKNOX2 Protein Level

75000/well BM-MSCs of FA patient (n= 3) or donor (n= 3) were plated into 6-well plates followed by incubation in a 5% CO_2 incubator at 37°C. Afterwards cells were treated with 0.1 or 5 ng/ml rTGF-β1 protein for 24 hours. Uninduced cells were used as controls. For each experimental condition, cells from each independent individual were plated into two wells which were then pooled together during protein isolation. Protein lysates was run on 10% SDS-PAGE and PKNOX2 protein level was determined using western blotting as described above.

3.4. The Plasmid Used for PKNOX2 Overexpression: PKNOX2-pCMV6

Empty- (PCMV6-Entry; cat no: PS100001, OriGene Technologies Inc., USA; Figure 3.4. A) and PKNOX2 carrying-vectors (PKNOX2-pCMV6; cat no: RC206921, OriGene Technologies Inc.; Figure 3.4. B) were used. Both vectors contained fi ori (phage-derived ORI required for the replication and packaging of single stranded DNA into phage particles), SV40 ori (origin of replication within mammalian cells), Kan^r/Neo^r (antibiotic selection cassette conferred resistance to kanamycin -Kan- in *E. coli* and neomycin -Neo- analogs in mammalian cells), PolyA (polyadenylation site), ColE1 (Colicin E1 required for inhibition of other *E. coli* strains), CMV (cytomegalovirus) promoter and a Kozak consensus sequence (drove protein expression in mammalian cells) and MYC/DDK tag (small dual tag that enabled detection and purification of the ORF product with anti-DDK antibody). Additionally, PKNOX2-pCMV6 plasmid also included PKNOX2 human cDNA ORF clone which was fused with a MYC/DDK tag at its c-terminus (Figure 3.4. A). The size of pCMV6-Entry and PKNOX2-pCMV6 were 4.9kb and 6.3kb, respectively.

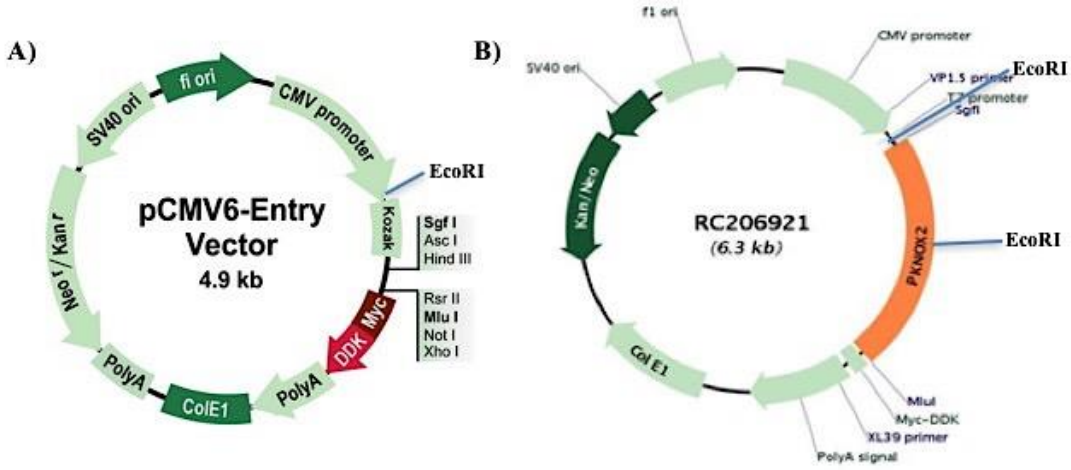

Figure 3.4. Vector maps of A) pCMV6-Entry (cat no: PS100001, OriGene Technologies Inc.), and B) PKNOX2-pCMV6 (cat no: RC206921, OriGene Technologies Inc.) plasmids.

3.4.1. Preparation of Chemically Competent JM109 *E. coli* Cells

A single colony of JM109 *E. coli* was inoculated into 3ml Luria Bertani (LB)-broth and kept at 37°C overnight with vigorous shaking. The overnight culture was then diluted 1:100 of the final volume in LB-broth and incubated at 37°C with vigorous shaking until optical density (OD) at 600nm is 0.45-0.55. Then bacterial culture was chilled on ice for 2 hours and poured into a 50ml tube, followed by centrifugation at 2500 *x g* for 10 minutes at 4°C. Following steps were performed on ice in the cold room. Supernatant was discarded, pellet was gently resuspended in 1ml ice cold fresh competent solution (40mM sodium acetate, 100mM calcium chloride, 70mM manganese(II) chloride tetrahydrate, pH 5.5) and then final volume was brought up to 2ml (1:2 of the starting volume) followed by incubation on ice for 45 minutes. The bacterial suspension was centrifuged at 1800 *x g* for 10 minutes at 4°C. The supernatant was discarded and the cell pellet was resuspended in ice cold competent solution (1:20 of the starting volume). Afterwards, 80% glycerol solution was added to bacterial suspension as 15% of the final volume and mixed well. Aliquots of 200µl were transferred to 1.5ml tubes and directly stored at -80°C until further use.

3.4.2. Heat-Shock Transformation of PKNOX2-pCMV6 and pCMV6-Entry Plasmids to Chemically Competent JM109 *E. coli* Cells

JM109 *E. coli* competent cells were then used for transformation. For each plasmid, 5µl of competent cell stock was thawed on ice. 100ng of plasmid DNA was directly added onto competent cells, followed by incubation on ice for 30 minutes. The mix was heat-shocked at 42°C for 1 minute, followed by incubation on ice for 5 minutes. Afterwards, 1.5ml non-selective LB-broth was directly inoculated with the mix and incubated in orbital shaker incubator at 37°C for 1 hour. Then the bacterial cultures were centrifuged at 6800 *x g* for 1 minute and most of the supernatant was removed. The pellet was then resuspended and was plated on LB-agar containing 25µg/ml Kanamycin (Sigma- Aldrich), followed by incubation overnight at 37°C. Overnight cultures were then used in plasmid DNA isolation described below.

3.4.3. Isolation of PKNOX2-pCMV6 and pCMV6-Entry plasmid DNAs

10ml LB-broth containing 25µg/ml Kanamycin was inoculated with a single colony from starter culture of either PKNOX2-pCMV6 or pCMV6-Entry plasmid, followed by incubation at 37°C for overnight with vigorous shaking. Then, 200µl from each overnight culture was transferred into 100ml LB-broth containing 25µg/ml Kanamycin (1:500 dilution), followed by incubation described above. Cultures were then harvested by centrifugation at 3000 *x g* for 40 minutes at 4°C and the supernatants were discarded. Plasmid DNAs were isolated using EndoFree Plasmid Maxi Kit (cat no: 12362, Qiagen) following manufacturer's instructions.

Briefly, each bacterial pellet was resuspended in 10ml Buffer P1 (50mM Tris.Cl, pH 8.0; 10mM EDTA) containing 1:1000 LyseBlue reagent and 100µg/ml RNase A, then lysed in 10ml Buffer P2 (200mM NaOH; 1% SDS w/v), followed by incubation for 5 minutes at room temperature. Afterwards, 10ml per sample pre-chilled Buffer P3 (3M potassium acetate, pH 5.5) was added to neutralize lysates. Each lysate was poured into a separate barrel of the QIAfilter Cartridge, followed by incubation for 10 minutes at room temperature and then filtered. 2.5ml/sample of Buffer ER was mixed with filtered lysates, followed by incubation on ice for 30 minutes. Afterwards, each filtered lysate was applied to a QIAGEN-tip 500,

previously equilibrated with Buffer QBT (750mM NaCl; 50mM MOPS, pH 7.0; 15% isopropanol v/v; 0.15% Triton® X-100 v/v). Each QIAGEN-tip 500 was then washed twice with 30ml Buffer QC (1M NaCl; 50mM MOPS, pH 7.0; 15% isopropanol v/v). Plasmid DNA was eluted in 15ml/sample Buffer QN (1.6M NaCl; 50mM MOPS, pH 7.0; 15% isopropanol v/v) (pre-heated to 65°C). DNA was precipitated by adding 10.5ml isopropanol (cat no: A3928, Applichem) per sample, followed by centrifugation at 3220 *x g* for 80 minutes at 4°C. Supernatant was gently discarded and pellet was washed with 5ml per sample endotoxin-free 70% ethanol by centrifugation at 3220 *x g* for 60 minutes at 4°C. The supernatant was gently discarded and each pellet was then air-dried for 10 minutes, followed by resuspension in 50µl endotoxin-free Buffer TE (10mM Tris.Cl, pH 8.0; 1mM EDTA). Concentration of DNAs was measured by NanoDrop ND-1000 spectrophotometer.

3.4.4. Restriction Digestion of PKNOX2-pCMV6 and pCMV6-Entry Plasmids

Plasmid sequences (OriGene Technologies Inc.) were submitted to NEBcutter V2.0 software and *EcoRI* restriction sites were identified (406). Thereafter, *EcoRI* enzyme (cat no: R0101S, NEB, UK) was used to digest pCMV6-Entry plasmid (restriction digestion product= 4.9 kb; Figure 3.5. and see Figure 3.4. A) and PKNOX2-pCMV6 plasmid (restriction digestion products= 5.6 and 0.65kb; Figure 3.5. and see Figure 3.4. B). The restriction digestion reaction was performed to cut 1µg DNA at 37°C for 2-4 hours. The products were run on 1% agarose gel along with 1kb DNA Ladder (cat no: N3232S, New England Biolabs Inc., USA).

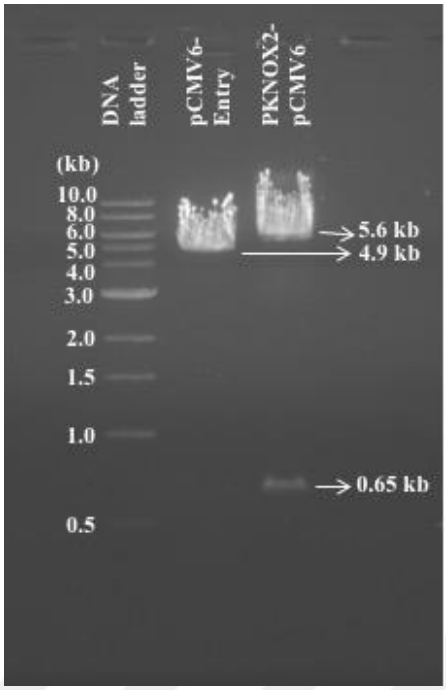

Figure 3.5. Restriction digestion products of PKNOX2-pCMV6 and pCMV6-Entry plasmids.

3.5. PKNOX2 Expression Plasmid Transfected to Bone Marrow Mesenchymal Stromal/Stem Cells

3.5.1. Transient Transfection of PKNOX2-pCMV6 and pCMV6-Entry Plasmids Using Electroporation

Passage 2 or 4 BM-MSCs were trypsinized using Trypsin-EDTA and washed twice with PBS, followed by centrifugation at 453 *x g* for 5 minutes. Neon transfection system (Invitrogen) was used for electroporation. For each transfection, total of $1x10^6$ cells were resuspended in Neon Resuspension buffer using 100µl Neon Tips (cat no: MPK10096, Invitrogen) and mixed with 12.5µg PKNOX2-pCMV6 or pCMV6-Entry plasmid DNA. The transfection condition was 990V, 40ms and 2 pulses. Following each electroporation, cells were immediately divided into two wells of a 6-well plate containing pre-heated DMEM-LG medium supplemented with 10% FBS-HI and 1% L-glutamine. Cells were incubated in a 5% CO_2 incubator at 37°C for a day. The medium was then replaced with fresh DMF10, followed by incubation in a 5% CO_2 incubator at 37°C. Along with the transfected cells, only pulsed and/or untransfected BM-MSCs were used as control.

3.5.2. Target Gene Expression Levels in PKNOX2 Overexpressing Bone Marrow Mesenchymal Stromal/Stem Cells

RNA was isolated from passage five 100% confluent PKNOX2:MSC and pCMV6:MSC as described before. cDNAs were synthesized from 260ng or 830ng total RNA and RT-qPCR was performed to determine *PKNOX2* and *HOXC13* as well as its paralog, *HOXA13* (see Table 3.4.) gene expression levels as outlined previously. Fold change in each normalized target gene expression of PKNOX2:MSCs versus pCMV6:MSCs was calculated by $2^{-\Delta\Delta Ct}$ method. When no Ct value was obtained, ΔCt value was accepted as 25 in order to be able to calculate the fold change.

3.5.3. Western Blot Analysis Following PKNOX2 Overexpression

Extraction and Quantification of Total Protein Lysates

To obtain total protein lysates, passage five 100% confluent cells were washed with ice cold PBS, followed by incubation with 1X lysing buffer solution (OriGene Technologies Inc.) containing 1X protease inhibitor cocktail on ice for 20 minutes. Plates were swirled occasionally. Lysates were collected using a cell scraper and transferred to a 1.5ml tube, followed by centrifugation at 14000 *x g* for 5 minutes at 4°C to pellet the cell debris. The supernatant was transferred to a new 1.5ml tube and stored at -80°C until further use. Protein concentration was determined using Pierce™ BCA Protein Assay kit as described before. Standard curve generated by the software was shown in Figure 3.6.

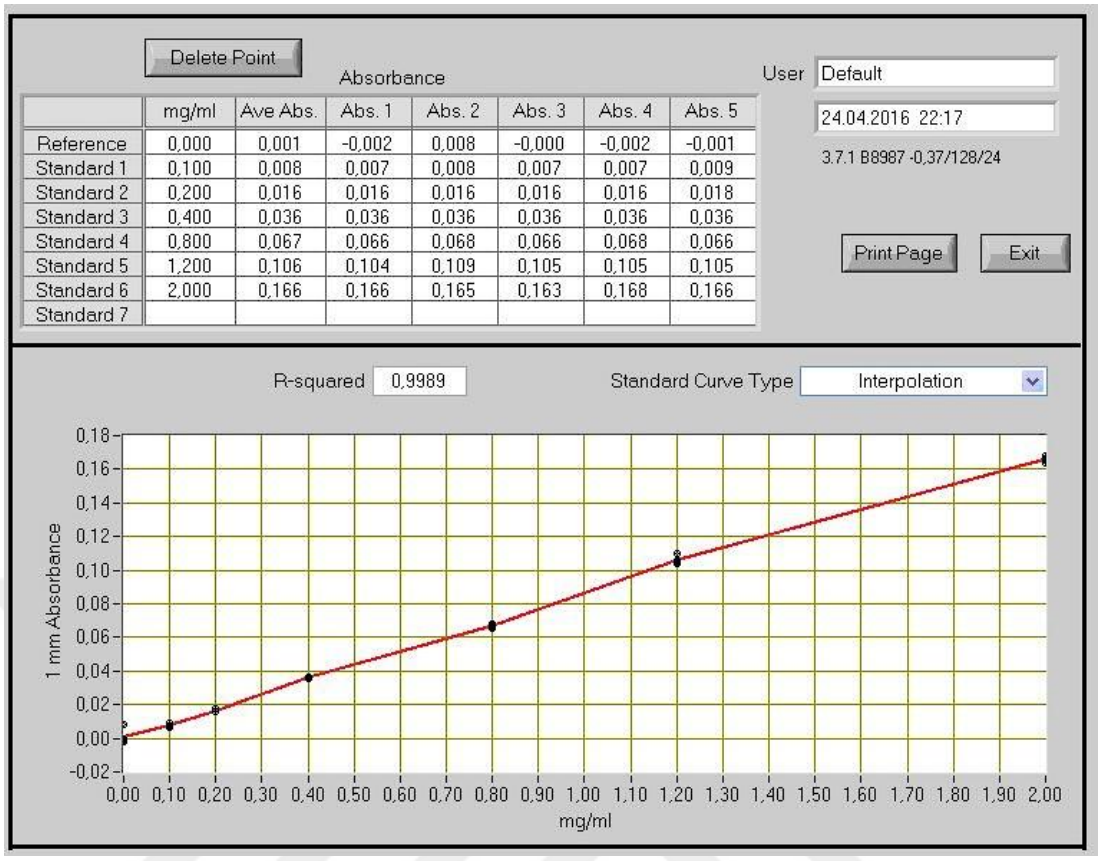

	mg/ml	Ave Abs.	Abs. 1	Abs. 2	Abs. 3	Abs. 4	Abs. 5
Reference	0,000	0,001	-0,002	0,008	-0,000	-0,002	-0,001
Standard 1	0,100	0,008	0,007	0,008	0,007	0,007	0,009
Standard 2	0,200	0,016	0,016	0,016	0,016	0,016	0,018
Standard 3	0,400	0,036	0,036	0,036	0,036	0,036	0,036
Standard 4	0,800	0,067	0,066	0,068	0,066	0,068	0,066
Standard 5	1,200	0,106	0,104	0,109	0,105	0,105	0,105
Standard 6	2,000	0,166	0,166	0,165	0,163	0,168	0,166
Standard 7							

Figure 3.6. Absorbance values corresponding to each standard obtained using NanoDrop ND-1000 spectrophotometer.

Western Blot Analysis

Total protein lysates from passage 5 PKNOX2:MSC, pCMV6:MSC, pulsed and untransfected cells were used for western blot analysis as described previously. 1-1.5mm thick 10% SDS-PAGE gels were used and the transfer conditions included transferring at 2.5A up to 25V for 7 or 10 minutes. Membranes were incubated with anti-PKNOX2, anti-HOXA13 or anti-FANCD2 primary antibody as described before. Afterwards, membrane initially blotted with anti-PKNOX2 or anti-HOXA13 were reblotted with anti-β-ACTIN antibody while membrane blotted with anti-FANCD2 was reblotted with anti-DDK primary antibody. Details of primary and secondary antibodies were given in Table 3.7. and Table 3.8., respectively.

Table 3.7. Primary antibody information.

	Clone	Host / Clonality	Final Dilution	Molecular weight (kDa)	Cat no.	Manufacturer
Anti-PKNOX2	56.1	Mouse Monoclonal	1:100	70	sc-101857	Santa Cruz, USA
Anti-DDK	4C5	Mouse Monoclonal	1:2000	-	TA50011-100	OriGene, USA
Anti-FANCD2	FI17	Mouse Monoclonal	1:100	150 and 162	sc-20022	Santa Cruz, USA
Anti-HOXA13	C-13	Rabbit Polyclonal	1:100	40	sc-46122	Santa Cruz, USA
Anti-β-ACTIN	D6A8	Rabbit Monoclonal	1:2500	45	8457S	Cell Signaling Technology, USA

Table 3.8. Secondary antibody information.

	Final Dilution	**Cat no.**	**Manufacturer**
Goat- anti-mouse	1/2000	AS003	Abclonal, USA
Goat- anti-mouse	1/1000	SA00001-1	Proteintech,
Goat-anti-rabbit	1/2000	AS014	Abclonal, USA
Goat-anti-rabbit	1/1000	SA00001-2	Proteintech,

3.5.4. Lateral Motility

One day post-electroporation, lateral motility of 100% confluent passage 5 PKNOX2:MSC was compared to pCMV6:MSC, pulsed or untransfected cell cultures using monolayer wound-healing assay. A wound was made per well of a 6-well plate using a sterile 200µl pipette tip. Total of three pictures of each wound were taken immediately at zero hour and then at various time points (2, 4, 6, 13, 20, 22, 24 and 36 hours) using an inverted microscope. Pictures of PKNOX2:MSCs were also taken at 42, 120 and 168 hours following wound formation. For each picture, the wound width was measured in pixels at three different points using ImageJ software and mean of these points was calculated. Then, overall mean of the three pictures taken for each condition at a particular time was calculated. Two technical replicates per condition were performed. Motility index (MI) was used to measure lateral motility using Equation 2.11. where W_t depicted the width of the wound at a particular time and W_0 depicted the width at 0 hour. MI value equaled to zero meant no cell movement whereas MI value equaled to 1 depicted complete wound closure (407).

$$MI = 1 - (Wt \div W0) \qquad (2.11.)$$

3.5.5. Adipogenic Differentiation Potential

Two days post-electroporation, DMF10 medium of 100% confluent passage 5 PKNOX2:MSC, pCMV6:MSC, pulsed or untransfected cell cultures was replaced with adipogenic differentiation medium. Uninduced cells were used as controls. Protocol details were outlined above. For quantitation of lipid accumulation, ORO content of each well was extracted by incubation in 1 ml 4% igepal CA-630 (cat no: I3021, Sigma-Aldrich) in 2-propanol (cat no: A3928, Applichem) for 1 hour at room temperature. Dye content was measured at 492nm with a Sunrise™ Microplate Reader and analyzed with Magellan™ data analysis software.

3.5.6. Osteogenic Differentiation Potential

Two days post-electroporation, DMF10 medium of 70-80% confluent passage 3 or 5 PKNOX2:MSC, pCMV6:MSC, pulsed or untransfected cell cultures was replaced with osteogenic differentiation medium. Uninduced cells were used as controls. Protocol details were outlined above. To quantify retention of ARS by calcium deposits, cells were incubated with 800µl/well 10% acetic acid at room temperature for 30 minutes, collected using a cell scraper, transferred to a 1.5ml tube and vortexed for 30 seconds. Samples were then heated to 85°C for 10 minutes, followed by incubation on ice for 5 minutes and centrifugation at 20000 *x g* for 15 minutes. 500µl supernatant per sample was transferred to a new 1.5ml tube, followed by neutralization using 200µl/tube 10% ammonium hydroxide. Absorbance was detected at 405nm using Sunrise™ Microplate Reader and analyzed with Magellan™ data analysis software (408).

3.5.7. Immunophenotypic Characterization

90% confluent passage 5 PKNOX2:MSC, pCMV6:MSC, pulsed and untransfected cell cultures were trypsinized using Trypsin-EDTA and washed with PBS as described above. The flow cytometry analyses were performed using FACS Aria instrument and BD FACSDiva™ software as described above. CD105, CD73, CD90, CD44, CD29, CD45, CD34, HLA-DR and CD31 levels were assessed (see Table 3.5.).

3.5.8. Active TGF-β1, TGF-β2 and TGF-β3 Secretion Levels

Following three days post-electroporation, active TGF-β1, TGF-β2 and TGF-β3 secretion levels by 100% confluent passage 5 PKNOX2:MSC and PCMV6:MSC cultures were determined using Bio-Plex Pro™ TGF-β 3-plex Assay kit following the protocol outlined above. Samples from at least two independent electroporations were studied and two technical repeats per sample were performed.

3.5.9. Co-Culturing $CD34^+$ Hematopoietic Stem Cells with Bone Marrow Mesenchymal Stromal/Stem Cells Overexpressing PKNOX2

Two or three days post-electroporation, 100% confluent passage 5 PKNOX2:MSC, pCMV6:MSC and untransfected cells were washed with PBS and used as feeder layer for cryopreserved or fresh cord blood derived $CD34^+$ hematopoietic stem cells ($CD34^+$HSCs). $CD34^+$HSCs were kindly provided by Assist. Prof. Dr. Fatima Aerts Kaya.

Expansion and Clonogenic Potential of Cryopreserved $CD34^+$ Hematopoietic Stem Cells

Prior to co-culture, cryopreserved $CD34^+$HSCs in 10% DMSO were thawed in PBS supplemented with 0.1% DNase 1, 2mM EDTA and 2% HI-FBS. Purity of $CD34^+$HSCs was determined using anti-CD34 (see Table 3.5.) and PE/FITC-anti-CD38 (HIT2, cat no: 555459, BD Pharmingen) antibodies by flow cytometry analysis as described above. To prevent low colony counts due to cryopreservation of cells, for clonogenic assays performed with previously cryopreserved cells, $2x10^4$ cells were added to 2ml Iscove' Modified Dulbecco's Medium (IMDM, cat no: 12440-061, Gibco) and 0.3ml (or 0.33ml) of these cells were then added onto 2.7ml (or 3ml) MethoCult™ H4434 Classic (methylcellulose medium; cat no: 04434 or 04444, StemCell Technologies, France). Afterwards, 1ml of cell suspension in methylcellulose medium was transferred to two 35mm dishes (cat no: 351008, BD Falcon), followed by incubation in a 5% CO_2 incubator at 37°C for 10-15 days. CFU-GEMM, BFU-E and CFU-GM were counted. The average of two replicate dishes was calculated and results were given per $1x10^3$ $CD34^+$HSCs.

$CD34^+$HSCs ($97.5x10^3$ /condition) in 2 ml StemMACS HSC expansion media (cat no: 130-100-463, MACS Miltenyi Biotec) supplemented with 1X StemMACS HSC expansion cocktail (cat no: 130-100-843, MACS Miltenyi Biotec) were seeded directly onto BM-MSCs, followed by incubation in a 5% CO_2 incubator at 37°C for 4 days. $CD34^+$HSCs or BM-MSCs cultured alone were used as controls. On day four, co-culture ($CD34^+$HSCs + BM-MSCs) or control cells were collected and total cell number was determined using Trypan blue stain. Clonogenic potential of HSCs after co-culture was determined according to protocol described above. Since the initial cell number was not known, equivalent of $2x10^4$ cells was used. Afterwards, immunophenotypes of cells were determined using CD73, CD34 (see Table 3.5.) and CD38 antibodies (Figure 3.7.) by flow cytometry analysis as described above. Total percentage of P1 and P2 gates (% Total; Figure 3.7.) was then used to determine the HSC number from the total cell number counted by Trypan blue after co-culture. In order to calculate HSC fold expansion after co-culture, the HSC number estimated after co-culture was divided by the total number of cells seeded. Fold expansion within only $CD34^+$, $CD38^+$ or $CD34^+CD38^+$ HSC population was determined by further multiplying the estimated HSC number with only CD34 (Q1; Figure 3.7.), only CD38 (Q4; Figure 3.7.) or double positive (Q2; Figure 3.7.) percentage, respectively and then normalized to total number of cells initially seeded.

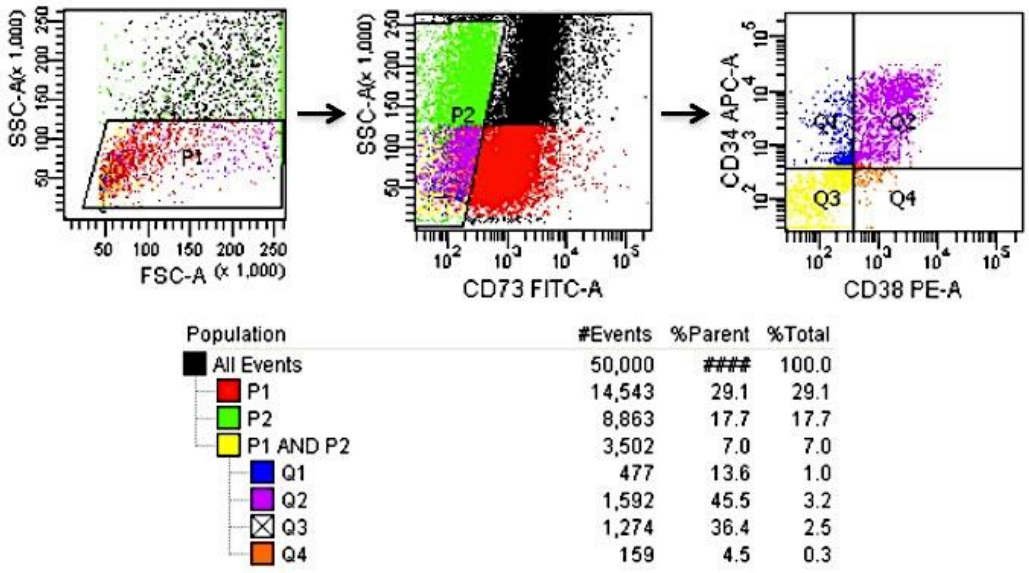

Figure 3.7. Representative images of how CD34 and CD38 levels of $CD34^+$ cells were determined from a mixed cell population of BM-MSCs and cryopreserved $CD34^+$HSCs following co-culture. Firstly, side-scattered light (SSC-A; depicts cell granulity) versus forward-scattered light (FSC-A; depicts cell size) graphic was constructed to gate (P1) cells with smaller granules (i.e. HSCs) out of all cells (i.e. all events). Then, SSC-A versus FITC-CD73 graphic was constructed to gate (P2) HSCs that were $CD73^-$ out of all cells. Lastly, APC-CD34 versus PE-CD38 graphic was used to determine only $CD34^+$ (Q1), $CD34^+CD38^+$ (Q2) or $CD38^+$ (Q4) HSCs within both P1 and P2 gates.

Expansion and Clonogenic Potential of Fresh $CD34^+$ Hematopoietic Stem Cells

One day prior to co-culture, $CD34^+$HSCs were enriched and total of $40x10^4$ cells were incubated overnight in 8 ml StemMACS HSC expansion media containing StemMACS HSC expansion cocktail in 5% CO_2 incubator at 37°C. $CD34^+$HSCs ($10x10^4$ per condition) in 2 ml media were then seeded directly onto BM-MSCs, followed by incubation as described above. Two technical replicates were made. Immunophenotyping using BD Accuri™ C6 flow cytometer along with BD CSamples™ Analysis software (BD Biosciences; Figure 3.8.) and clonogenic potential of $CD34^+$HSCs were determined according to above protocol. Total of $10x10^3$ $CD34^+$HSCs were used for determining clonogenic capacity.

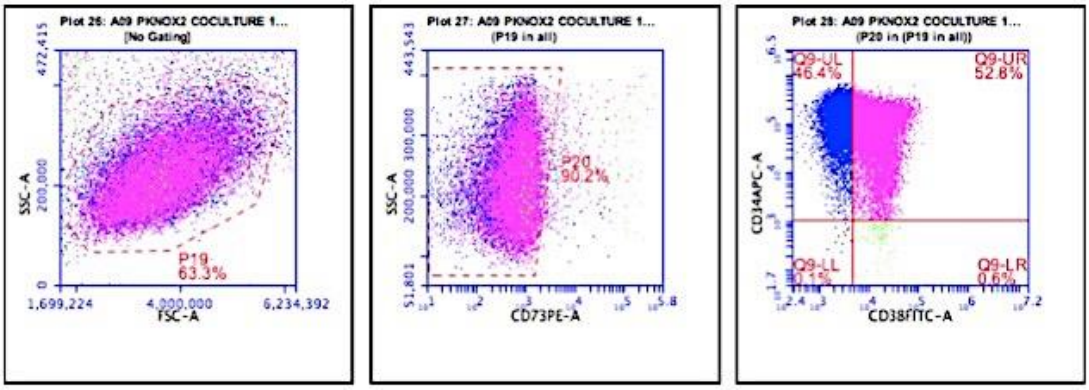

Figure 3.8. Representative images of how CD34 and CD38 levels of $CD34^+$ cells were determined from a mixed cell population of BM-MSCs and fresh $CD34^+$HSCs following co-culture. Firstly, SSC-A versus FSC-A was plotted to gate (P19) cells with smaller granules within all events. Then, SSC-A versus FITC-CD73 was plotted to gate (P20) HSCs that were $CD73^-$ in P19. Lastly, APC-CD34 versus PE-CD38 was plotted to determine only $CD34^+$ (QUL), $CD34^+CD38^+$ (QUR) or $CD38^+$ (QLR) HSCs within P20 in P19 in all events.

3.6. Identifying Proteins Interacting with PKNOX2

3.6.1. Optimizing Co-Immunoprecipitation Protocol

Anti-DDK magnetic immunoprecipitation kit (cat no: AR100024, OriGene Technologies Inc.) was used for co-immunoprecipitations (Co-IP). 25µl of magnetic bead, washed in 1ml lysing buffer solution containing protease inhibitor cocktail, was used per reaction. 50µl or same concentration (within in an experiment) of protein lysate from passage 4 or 5 PKNOX2:MSC, pCMV6:MSC, pulsed or untransfected cells was diluted in 450µl lysing buffer solution containing protease inhibitor cocktail, followed by pre-cleaning with control magnetic beads (Mouse IgG) by gently rotating for 1, 2, 4 or 16 hour(s) at room temperature. Tubes were placed in a magnetic separator and supernatant was transferred to a new tube containing anti-DDK magnetic beads for Co-IP reaction. Additionally, PKNOX2:MSCs protein lysates incubated with control magnetic beads overnight instead of anti-DDK beads were used as control. Samples were gently rotated overnight at 4°C, followed by three washes with 1X washing buffer. Flow-through following first wash was collected and used as negative control for downstream analysis. Protein samples were then eluted by boiling in 25µl/tube 2X SDS-PAGE

sample buffer (with 5% BME added either prior to or after elution) for 5 minutes. BSA-DDK protein was used as positive control for immunoprecipitation reaction. Co-IP elutes along with total protein lysates (at same concentration within an experiment) were then loaded to SDS-PAGE (protocol details are given above) either in the presence or absence of magnetic beads. Prior to developing, PVDF membranes were washed three times for 15 minutes or four times for 10 minutes with TBS-T. Membranes were further either washed or not with washing solution containing 500mM NaCl for 5 minutes. For detection of immunoprecipitated PKNOX2-DDK fusion protein either anti-DDK or anti-PKNOX2 primary antibody was used. Anti-FANCD2 primary antibody was used to determine whether FANCD2 directly co-immunoprecipitated with PKNOX2 protein.

3.6.2. Co-immunoprecipitation Followed by Mass Spectrometry Analysis to Identify PKNOX2 Interactome

Anti-DDK magnetic immunoprecipitation kit was used for Co-IP. 44.5 μg of protein lysate from passage 5 PKNOX2:MSC and pCMV6:MSC obtained 3 days post-electroporation were used for this experiment. Briefly, samples were pre-cleaned with control magnetic beads for 2 hours at room temperature and were incubated with anti-DDK magnetic beads overnight at 4°C. Three technical replicates per sample were performed. Co-IP elutes prepared in 25μl/tube 3X SDS-PAGE sample buffer were sent to Koç University Cell Biology and Proteomics Laboratory where the mass spectrometry analysis was performed using Q Exactive Quadrupole-Orbitrap Mass Spectrometer with nano Liquid Chromatography (n-LC MS/MS; Thermo Scientific) and analysed using Thermo Discoverer 1.4 software (Thermo Fisher Scientific) by Dr. Nurhan Özlü. Technical replicates were pooled together prior to analyses and each sample was analysed twice (i.e. first run depicted as ‘Run 1’ and the second run depicted as ‘Rep 1’) in mass spectrometry.

3.7. Statistical Analysis

To increase the performance of the statistical analysis done using HOX and TALE gene expression levels, missing values were imputed using Multivariate Imputation by Chained Equations (MICE) in R Statistical software by Dr. Erdal

Coşgun (409). MICE method has been broadly used in the statistics literature since work by Donald Rubin in the 1970s. Firstly, it initialized the missing entries with a default value, followed by updating each column by using an appropriate regression or classification algorithm. These updates are repeated a number of times, as specified by the Number of Iterations parameter (410, 411). Heat-map was constructed using single linkage (i.e. groups two clusters based on minimum distance between a case in group 1 and a case in group 2) as the clustering method and Euclidean (i.e. compares the association between actual measures) as the distance measure of genes and samples by Exiqon GeneEx software (USA). Spearman correlation test was conducted using GraphPad Prism 7 (GraphPad Software, Inc., USA).

Statistical analysis was performed using IBM SPSS Statistics software and the graphs showing mean with or without standard deviation (SD) were constructed using GraphPad Prism 7 unless indicated otherwise. When making pairwise comparisons of independent groups, Student's T-Test or Mann Whitney U (MWU) test was applied**.** Statistical significance threshold was considered as $P< 0.05$ for Student's T-Test and *exact* $P< 0.05$ for MWU test. To compare more than two related groups, Friedman's 2-way ANOVA by ranks test was used and if the *asymptotic P*-value was less than 0.05, All pairwise test with Bonferroni correction was then performed to test the significance of pairwise differences (i.e. *adjusted* $P< 0.05$ depicted the statistically significant difference).

Coefficient of variation which represents the ratio of SD to the mean, was calculated and expressed as a percentage to determine the variation among raw Ct values of *ACTB.*

4. RESULTS

4.1. Characterization of Bone Marrow Mesenchymal Stromal/Stem Cells

4.1.1. Mutation Screening of Fanconi anemia Patients

Mutations in *FANCA, FANCD2* or *FANCG* genes were investigated for the patients (Table 4.1.). One patient had no pathogenic mutation in *FANC-A, -B, -C, -D2, -E, -F, -G, -I, -L, -M, BRCA1, BRCA2, BRIP1, ERCC4, PALB2, RAD51* or *SLX4* gene (Table 4.1.). Three of the detected mutations (FANCA c.2851C>T, FANCA, c.2738A>C, FANCG c.1182_1192delinsC) were identified previously. Six of them (FANCA del exon 3-5, FANCA c.427-3C>G, FANCA c.3586G>T, FANCA del exon 1-2, FANCA c.1229G>A, FANCD2 c.1766+40T>G) were not described previously (Table 4.1.).

4.1.2. Immunophenotyping of Bone Marrow Mesenchymal Stromal/Stem Cells

All BM-MSCs were positive for specific mesenchymal markers (CD29, CD44, CD73, CD90, CD105, CD140b, CD146, CD166, HLA-ABC), whereas they had low or no (depicted as negative; $^{-}$) expression of others ($CD106^{low/-}$, $CD200^{low}$, $CD271^{-}$) (Figure 4.1. and Figure 4.2.). Additionally, all BM-MSCs were negative for endothelial markers (CD31 and CD144), hematopoietic markers (CD34, CD14, CD45, and HLA-DR), as well as the general stem cell marker, CD133 (Figure 4.1. and Figure 4.2.). MWU test showed that FA and donor BM-MSCs had similar immunophenotypes, but the CD29 level of patient cells was significantly higher than donors ($P< 0.05$; Figure 4.2.). CD106 level of patient MSCs was higher than donors, but the difference was not significant ($P= 0.397$; Figure 4.2.). The CD200 level of patients was relatively lower than donors ($P= 0.064$; Figure 4.2.).

Table 4.1. Results from mutational screening of the Fanconi anemia patients for known FA genes.

		Mutation		
Patient ID	**Comp. Group**	**cDNA Level**[***]	**Expected Consequence**	**Reference**
HUSCS-FA01[^]	FA-A	del exon 3-5[#]	Truncation	Novel
HUSCS-FA02	FA-A	c.427-3C>G	Aberrant Splicing	Novel
HUSCS-FA03	FA-A	c.3586G>T	p.Glu1196X	Novel
HUSCS-FA04	FA-A	del exon 1-2*	Truncation	Novel
HUSCS-FA05	FA-A	c.1229G>A	p.Trp410X	Novel
HUSCS-FA06	FA-A	c.2851C>T	p.Arg951Trp	[33]
HUSCS-FA07	FA-A	c.2738A>C	p.His913Pro	[33]
HUSCS-FA08	FA-G	c.1182_1192delinsC	p.(Glu395Trpfs*5)	[34]
HUSCS-FA09.a[**,^]	FA-D2	c.1766+40T>G	Aberrant Splicing	Novel
HUSCS-FA09.b[**]	FA-D2	c.1766+40T>G	Aberrant Splicing	Novel
HUSCS-FA10	?	No mutation in known FA genes	NA	NA

[**] HUFA09.a and HUFA09.b are siblings; [***] Nomenclature of the variants is based on the cDNA sequence using the following transcripts: *FANCA*, NM_000135.2, *FANCG*, NM_004629.1, *FANCD2*, NM_033084.3; [^] Proper segregation for patients from which DNA from the parents was available, was confirmed; [#] Deletion detected by MLPA, break points not known; ? No mutation in known FA genes; NA, information Not Available; * Mutation knowledge of HUSCS-FA04 is based on the patient's file records

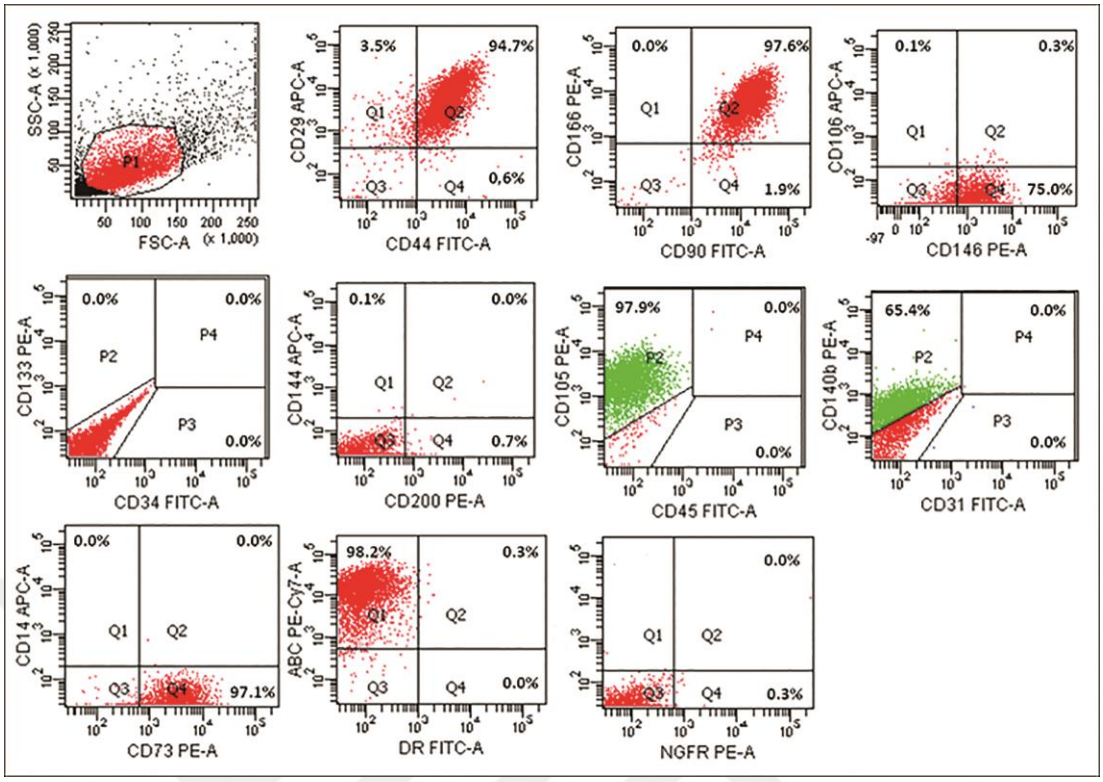

Figure 4.1. Representative flow cytometry analysis of CD29, CD44, CD166, CD90, CD106, CD146, CD133, CD34, CD144, CD200, CD105, CD45, CD140b, CD31, CD14, CD73, HLA-ABC, HLA-DR and CD271 (NGFR) surface markers.

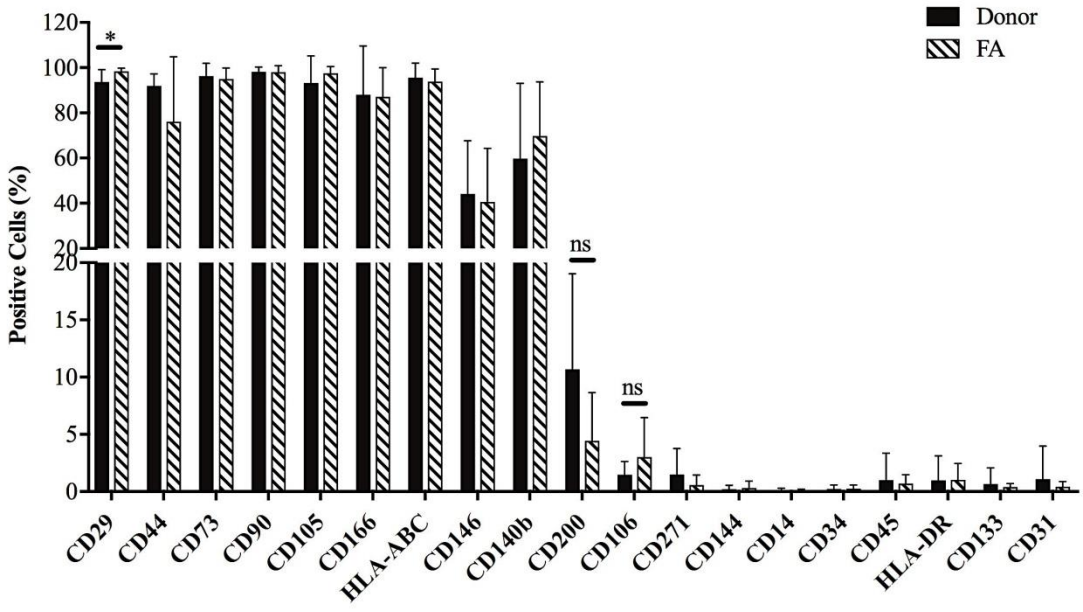

Figure 4.2. Immunophenotypes of donor and FA BM-MSCs. * depicts statistically significant difference ($P < 0.05$). ns depicts not significantly different.

4.1.3. Differentiation Potential of Bone Marrow Mesenchymal Stromal/Stem Cells

There were no differences in adipogenic and osteogenic potency between FA and donor BM-MSCs, as confirmed by ORO and ARS positivity, respectively (Figure 4.3.). Furthermore, FA patient and donor cells had similar expression levels of adipogenic-specific genes (*Adipsin, PPARγ and LPL*) (*P*> 0.05; Figure 4.4. A-C). Additionally, expression level of osteogenic-specific genes (*RUNX2, ALPL, OCN* and *SP7*) were not statistically different between groups (*P*> 0.05; Figure 4.5. A-D).

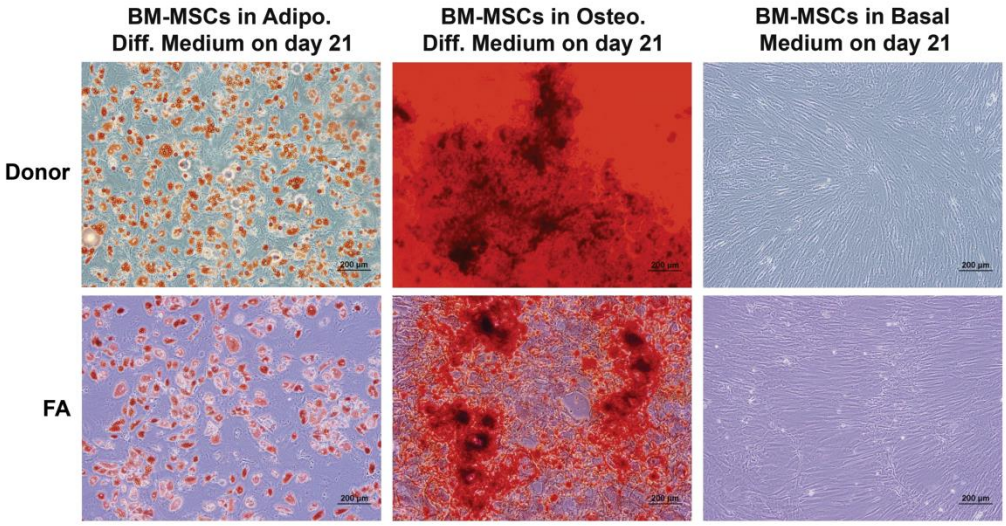

Figure 4.3. Representative images of donor and FA BM-MSCs differentiated to adipogenic and osteogenic lineages on day 21 following induction and compared with MSCs cultured in basal medium. BM-MSCs differentiated to adipogenic lineages were stained with ORO while cells differentiated to osteogenic lineages were stained with ARS (100x magnification).

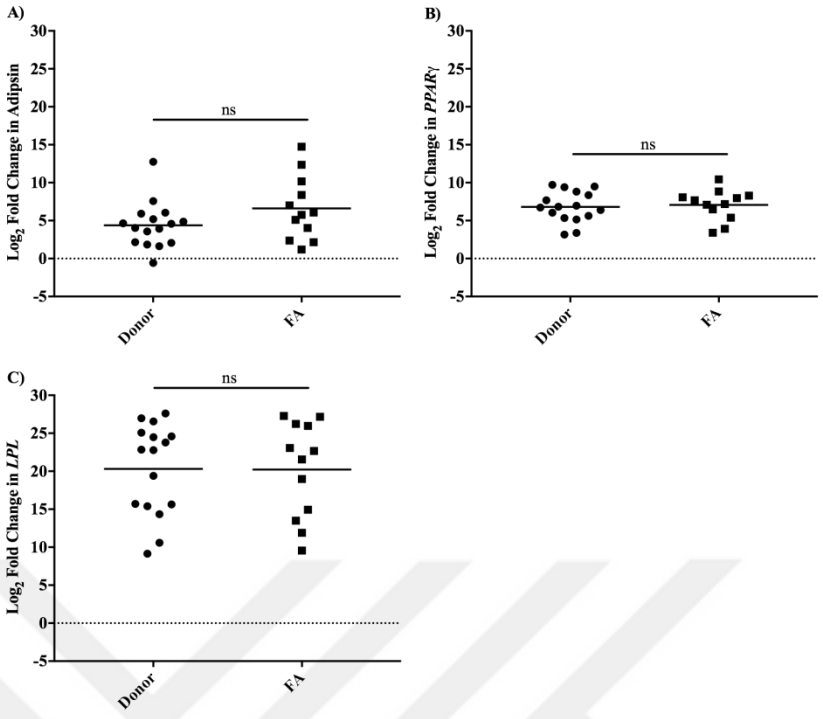

Figure 4.4. Fold change in the expression level of adipose-specific genes, A) *Adipsin*, B) *PPARγ* and C) *LPL* of BM-MSCs grown in adipogenic induction medium on day 21. ns depicts not significantly different.

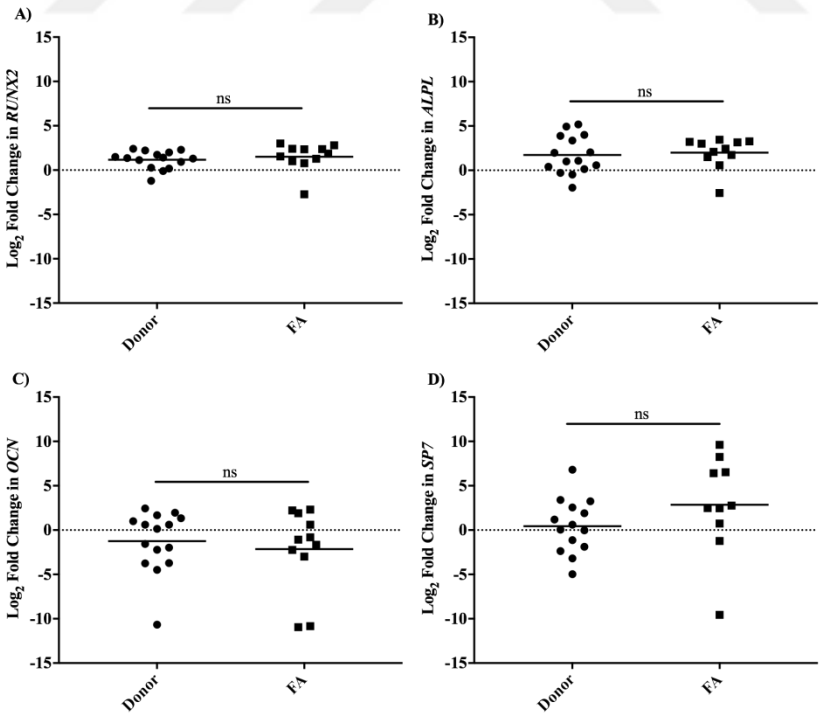

Figure 4.5. Fold change in the expression level of bone-specific genes, A) *RUNX*2, B) *ALPL*, C) *OCN* and D) *SP7* of BM-MSCs grown in osteogenic induction medium on day 21. ns depicts not significantly different.

4.1.4. Cell Cycle Analysis of Bone Marrow Mesenchymal Stromal/Stem Cells

Prior to DEB treatment, BM-MSCs were dominantly found in the dip G1 phase of the cell cycle (see Figure 3.1.). The fold change (fc) in each specific cell cycle phase between before and after DEB treatment of donor BM-MSCs was negligible (see Figure 3.1.). In contrast, FA derived cells shifted from dip G1 phase to dip G2 phase after treatment (see Figure 3.1.). Following DEB treatment, there was a significant decrease ($P< 0.05$) in FA BM-MSCs (fc= -29.83 ±11.67) in dip G1 phase compared to donor cells (fc= -5.13 ±5.69; Figure 4.6.). Within dip G2 phase, there was a significant increase ($P< 0.05$) in cells obtained from FA patients (fc= 36.18 ±13.40) compared to donors (fc= 0.29 ±0.24; Figure 4.6.). In the S-phase, there was no significant difference ($P> 0.05$) between patients (fc= -6.35 ±11.25) and donors (fc= 4.84 ±5.77; Figure 4.6.). Due to very few number (< 5000) of modelled events, one patient (HUSCS-FA06) with a mutation in *FANCA* gene was excluded from the analysis.

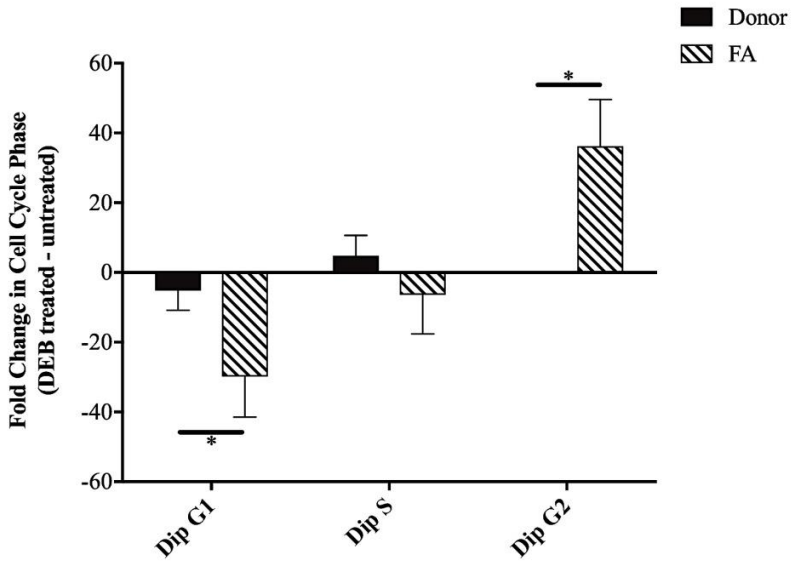

Figure 4.6. The effect of DEB treatment on cell cycle of FA patient and donor BM-MSCs. Following DEB treatment, there was a significant decrease in cells with non-functional FA pathway in dip G1 phase compared to donors. Within dip G2 phase, there was a significant increase in FA BM-MSCs compared to donors. The results are presented as fold change in the percentage of positive cells in each cell cycle phase (% of DEB treated BM-MSCs - % of control BM-MSCs). * depicts statistically significant difference ($P< 0.05$). Dip means the peak.

4.1.5. Population Doubling Analysis of Bone Marrow Mesenchymal Stromal/Stem Cells

At each passage, cPDs of donor and FA BM-MSCs were calculated to compare proliferative potency. Between passages 3 to 7, donor (cPD= 10.93 ±2.73) and *FANCA*-deficient cells (cPD= 10.30 ±0.16) had a similar proliferative potential (Figure 4.7.). Proliferation of *FANCG*-deficient BM-MSCs halted at P6 with a cPD of 8.86, thus had a similar proliferative capacity as donor cells (Figure 4.7.). BM-MSCs from one of the *FANCD2*-deficient patients stopped propagating at P4 (cPD= 1.33) and from another patient cPD was 7.90 at P7 (Figure 4.7.).

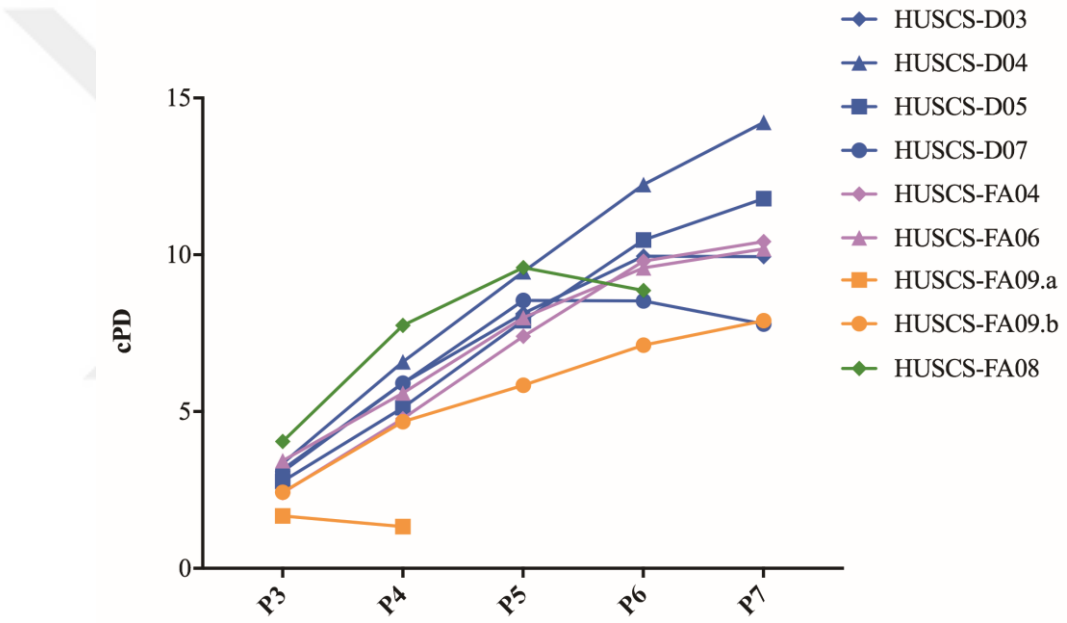

Figure 4.7. Proliferative potency of FA BM-MSCs was determined between passages 3 to 7 and compared with donors by calculating cumulative population doubling (cPD) at each passage.

4.1.6. Senescence Associated β-galactosidase Activity of Bone Marrow Mesenchymal Stromal/Stem Cells

SA-β-gal of passages 3 and 6 BM-MSCs derived from donor or FA patients was assessed (Figure 4.8. A). At passage 3, BM-MSCs obtained from patients with *FANCA* and unknown mutations exhibited similar SA-β-gal activity with each other but lower than donors (Figure 4.8. B). However, passage 6 cells from patients with *FANCA* and unknown mutation had higher SA-β-gal activity and enlarged cell

morphology compared to corresponding cells at passage 3 (Figure 4.8. B). Passage 6 donor cells had similar SA-β-gal activity as passage 3 donor cells (Figure 4.8. B). Intriguingly, passage 3 cells with *FANCD2* deficiency had elevated SA-β-gal and bigger cell morphology compared to other samples (Figure 4.8. B).

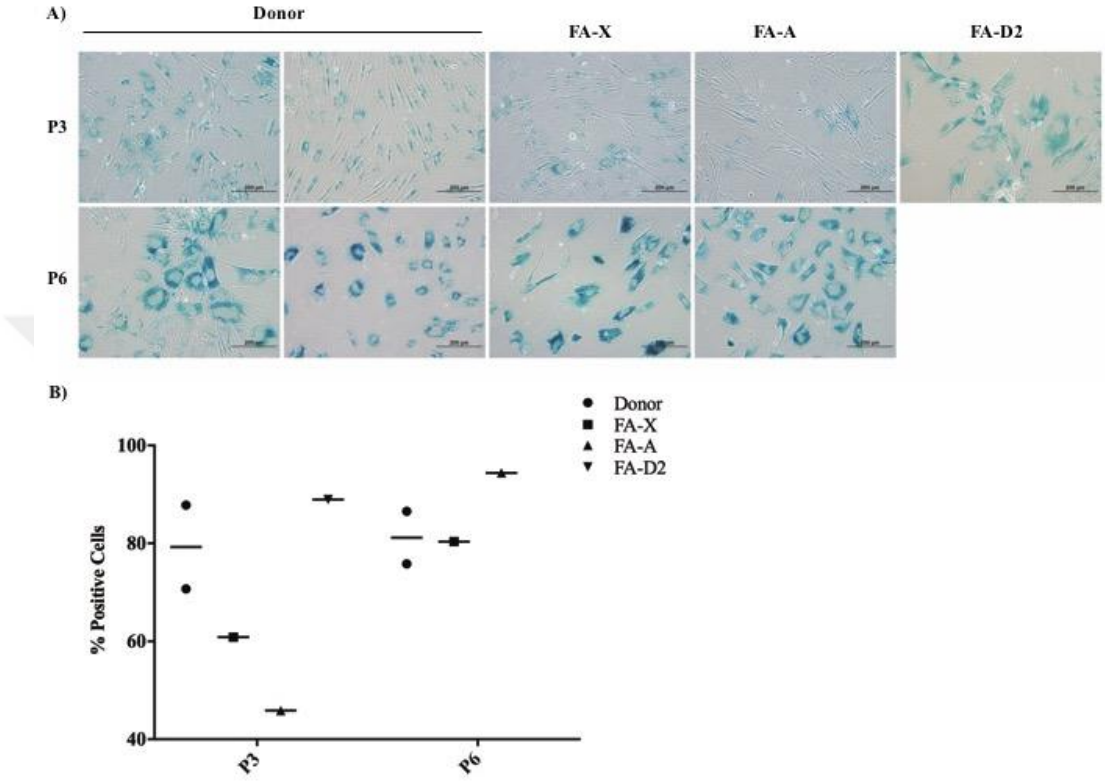

Figure 4.8. Senescence of FA patient BM-MSCs was evaluated at passage 3 (P3) and 6 (P6) by SA-β-gal activity and compared with donor cells. Patients with unknown FA mutations were depicted as FA-X. A) Representative images (200x magnification) and B) Percentage of senescent BM-MSCs.

4.1.7. Reactive Oxygen Species Production by Bone Marrow Mesenchymal Stromal/Stem Cells

FA Patient BM-MSCs produce slightly higher ROS compared to donor cells ($P > 0.05$; Figure 4.9.). Mean FI intensity of CM-H2DCFDA was 112002 ±15981 in controls, 150513 ±34648 in *FANCA*-deficient cells, 135111 ±12665 in *FANCD2*-deficient cells.

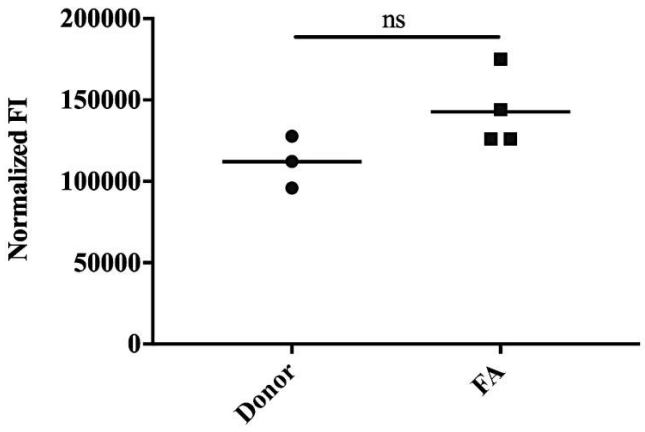

Figure 4.9. ROS production of FA patient (n= 4) and donor (n= 3) BM-MSCs was compared.

4.1.8. TGF-β Expression and Secretion Levels of Bone Marrow Mesenchymal Stromal/Stem Cells

All BM-MSCs expressed the *TGF-β1* gene (Fig. 4.10. A). The expression level of cells derived from FA patients was similar with donor BM-MSCs (*P*> 0.05; Figure 4.10. A). *TGF-β1* gene expression of the most BM-MSCs was not affected by the DEB treatment, except BM-MSCs from one donor (HUSCS-D11) and one FA patient (HUSCS-FA04), who had no expression following treatment (Figure 4.10. B). The level of *TGF-β1* gene expression did not differ between DEB treated BM-MSCs from donor and FA patients (*P*> 0.05; Figure 4.10. B). However, variation in TGF-β levels secreted by BM-MSCs was wide within groups. Mean TGF-β1 level was 808.32pg/mL ±953.30 for FA patient BM-MSCs and was not significantly different from donors (763.05pg/ml ±824.47; *P*> 0.05; Figure 4.10. C). TGF-β2 or TGF-β3 secretion of BM-MSCs was very low in comparision to TGF-β1 secretion (Figure 4.10. C). Mean TGF-β2 secretion was 99.58pg/ml ±123.20 by FA cells versus 112.70pg/ml ±97.42 by donors. Mean TGF-β3 production was 20.28pg/ml ±31.22 by patients and 17.44pg/ml ±23.48 by donors (*P*> 0.05; Figure 4.10. C). Intriguingly, cells obtained from either of the *FANCD2*-deficient patients did not secrete any of the TGF-β isoforms (Figure 4.10. D).

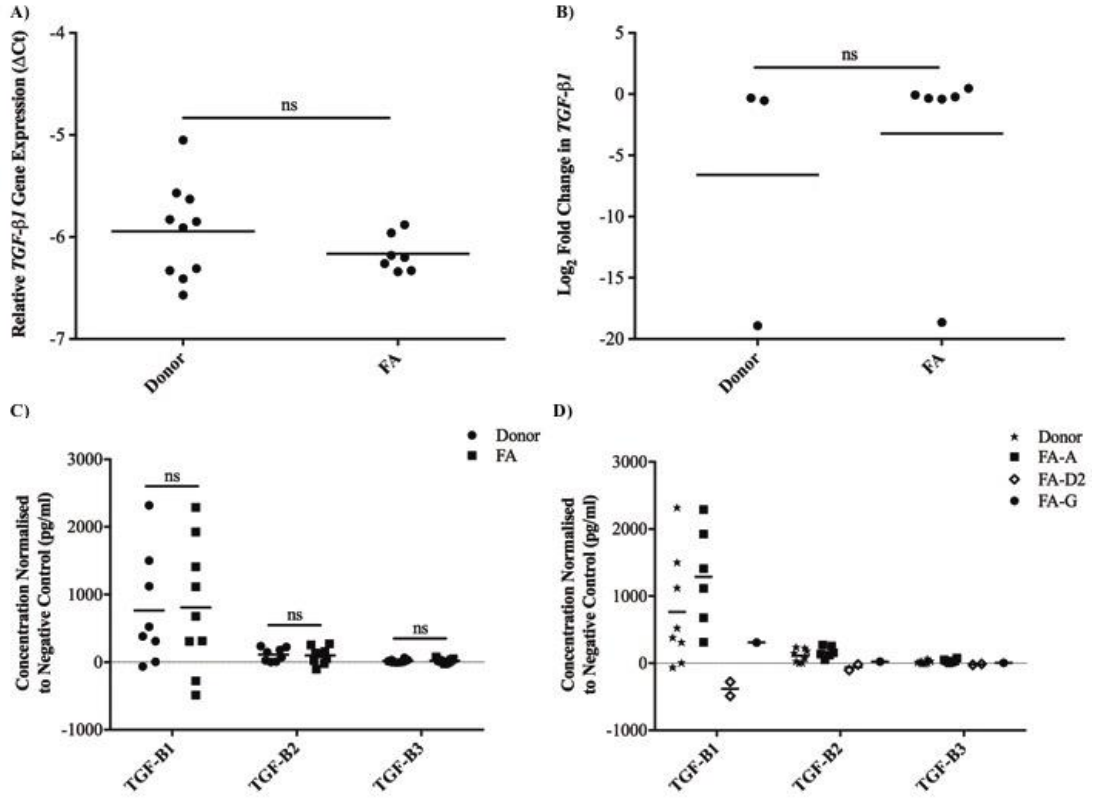

Figure 4.10. TGF-β gene expression and secretion levels of BM-MSCs derived from FA patients and donors. A) FA BM-MSCs had similar *TGF-β1* gene expression compared to donor cells (*P*> 0.05). B) DEB-treated FA and donor BM-MSCs had similar *TGF-β1* gene expression (*P*> 0.05). *TGF-β1* expression level was normalized to *ACTB.* C) Overall, there was a variation in the level of active TGF-β1, TGF-β2 or TGF-β3 secretion within each group. BM-MSCs produced very low amounts of TGF-β2 and TGF-β3. FA patients and donor cells produced similar amount of active TGF-β1, TGF-β2 or TGF-β3 (*P*> 0.05). D) FA-D2 BM-MSCs did not express TGF-β isoforms.

4.2. HOX and TALE Profile of Bone Marrow Mesenchymal Stromal/Stem Cells

4.2.1. HOX and TALE Gene Expression Pattern

Expression profile analysis of 39 HOX and 8 TALE genes in BM-MSCs derived from FA patients and healthy donors revealed a conserved expression pattern. Donor and FA patient BM-MSCs were highly associated in terms of HOX and TALE gene expression (r=0.9879, *P*< 0.0001). BM-MSCs did not express *HOXB1*, while *HOXB13, HOXC12, HOXD10, HOXD11*, *HOXD12* and *HOXD13* genes were transcribed at low levels and inconsistently (more than 40% of samples

had no expression as shown in Figure 4.11.). Due to low/inconsistent or absence of expression, *HOXB1, HOXB13, HOXC12, HOXD10, HOXD11, HOXD12* and *HOXD13* genes were excluded from imputation and further statistical analysis. There was no difference between imputed and non-imputed data sets ($P > 0.05$). Across donor and FA samples, coefficient of variation for Ct values of *ACTB* gene was 3.69%.

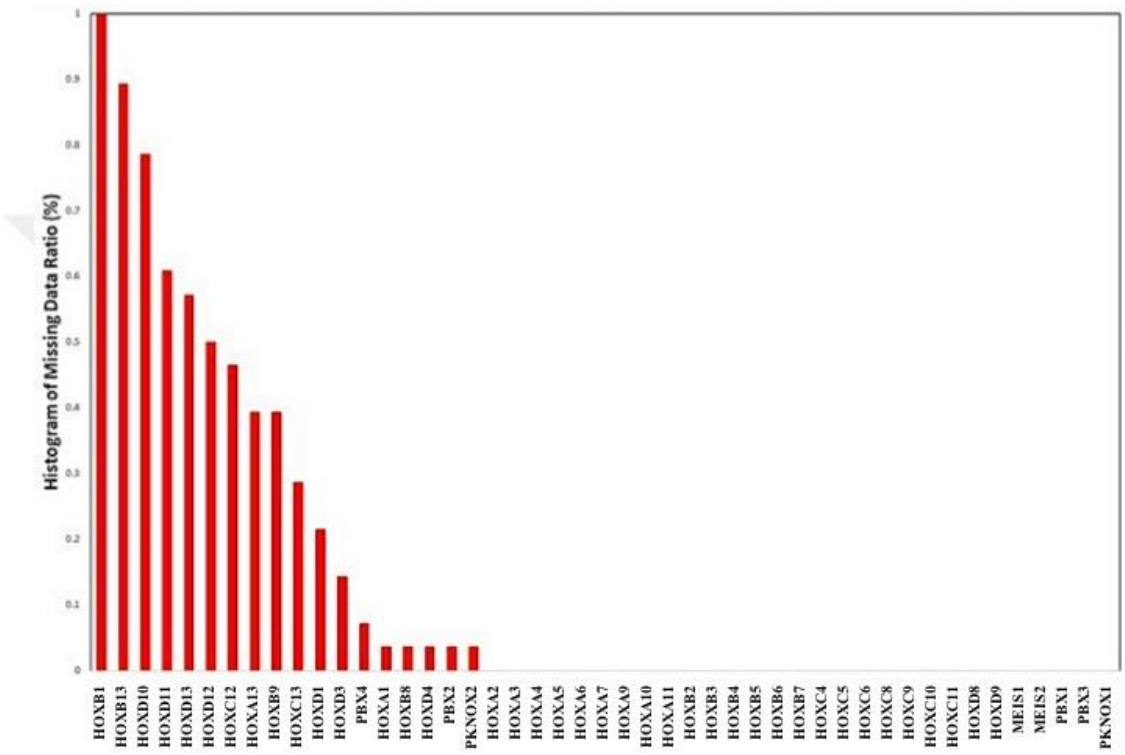

Figure 4.11. BM-MSCs had no or low expression of *HOXB1, HOXB13, HOXC12, HOXD10, HOXD11, HOXD12* and *HOXD13* genes. More than 40% of the analyzed samples had no expression of these genes, thus they were excluded from imputation and further statistical analysis.

Following imputation, gene expression of FA BM-MSCs was highly correlated with donor cells ($r = 0.9861$, $P < 0.0001$; Figure 4.12.). However, *PKNOX2* and *HOXC13* gene expression were differentially expressed between FA and donor cells (Figure 4.12.).

HOX and TALE gene expression was clustered using the single linkage method and the Euclidean distance between rows and columns (Figure 4.13.). Genes were clustered into six clusters, as outlined in Table 4.2. *HOXC10* gene had the highest expression level in all BM-MSCs (Figure 4.13. and Table 4.2.).

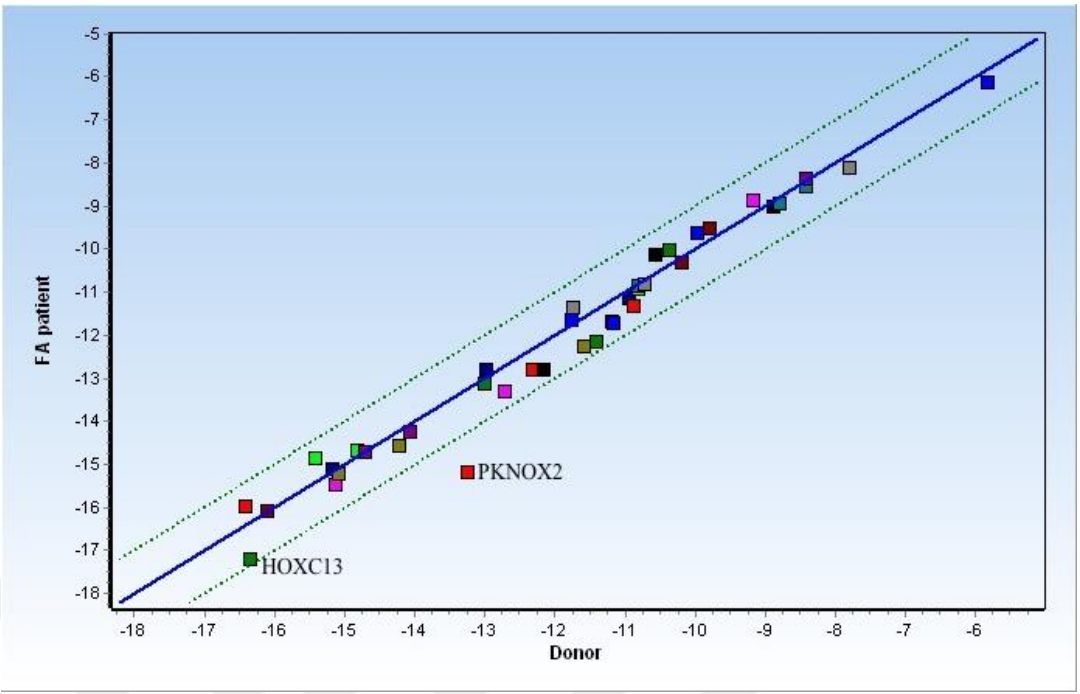

Figure 4.12. FA patient and Donor BM-MSCs were highly correlated in terms of HOX and TALE gene expression. The two outliers were *PKNOX2* and *HOXC13* genes.

Table 4.2. HOX and TALE genes were grouped into six clusters.

Cluster	Genes	Range of ΔCt
1	*HOXA13, HOXB4/B8, HOXD3/D4/D9, PBX4*	Min: -18.79 Max: -11.91
2	*HOXA1/A2/A3/A4/A5/A6/A7/A9/A10/A11, HOXB2/B3/B5/B6/B7, HOXC4/C5/C6/C8/C9/C11, HOXD8, MEIS1/2, PBX1/2/3, PKNOX1/2*	Min: - 17.59 Max: - 5.45
3	*HOXD1*	Min: -18.05 Max: -12.73
4	*HOXB9*	Min: -18.74 Max: -11.25
5	*HOXC13*	Min: -18.97 Max: -13.90
6	*HOXC10*	Min: -7.10 Max: -4.03

Min depicts minimum ΔCt value within the cluster. Max depicts maximum ΔCt value within the cluster.

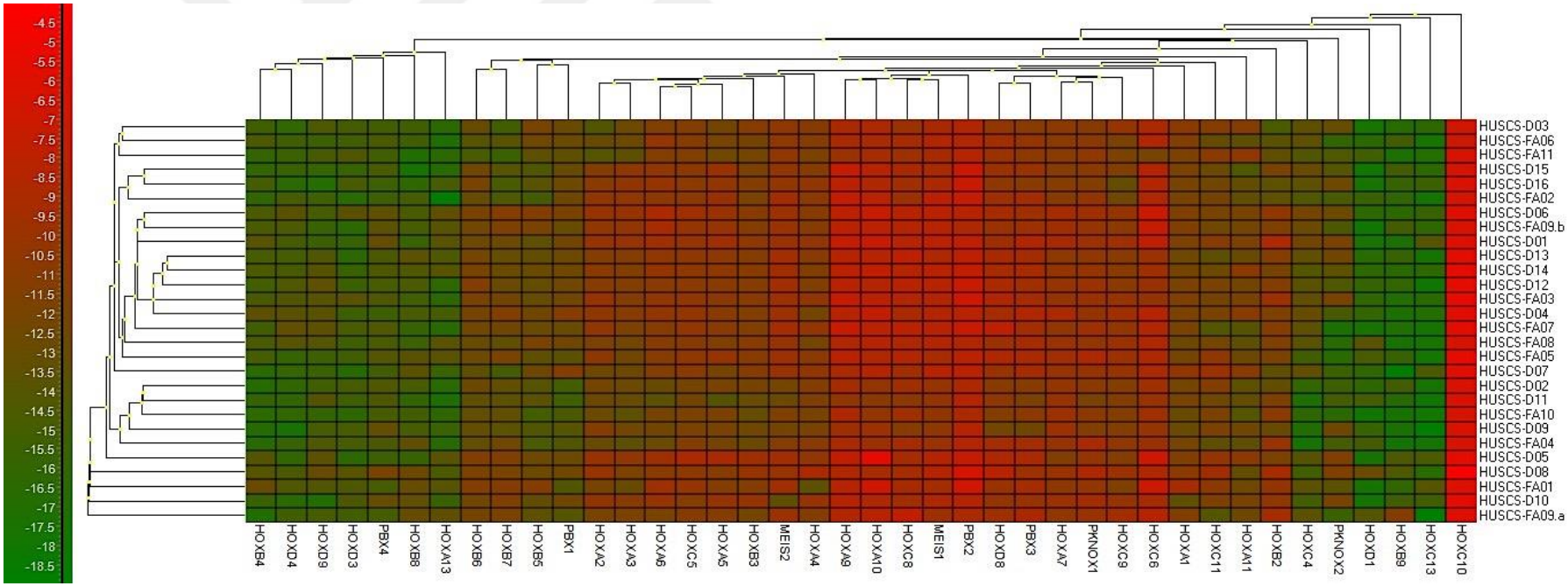

Figure 4.13. Heat map showing the HOX and TALE gene expression levels. Classification of genes as well as donor and FA patient samples visualized with dendrograms.

Expression of HOX genes in donor and FA BM-MSCs was not significantly different (*P*> 0.05; Figure 4.14.). Changes in *MEIS1, MEIS2, PBX1, PBX2, PBX3, PBX4* or *PKNOX1* gene expression between groups were not significant either (*P*> 0.05; Figure 4.14.). In contrast, *PKNOX2* expression in FA (-15.19 ± 1.49) was significantly lower than donors (-13.24 ± 1.37, *P*= 0.002; Figure 4.14.). In addition, FA-A (-15.00 ±1.80) and FA-D2 (-14.95 ±0.68) deficient cells had similar *PKNOX2* expression. *HOXC13* expression of FA cells (-17.21 ± 1.28) was relatively lower (*P*= 0.146) than that of donor BM-MSCs (-16.36 ± 1.47; Figure 4.14.). DEB treated FA and donor BM-MSCs did not show a significant fold change in *HOXC13* and *PKNOX2* gene expression (*P*> 0.05; Figure 4.15.). Across all DEB-treated/untreated samples, the coefficient of variation for the Ct value of the *ACTB* gene was 2.28%.

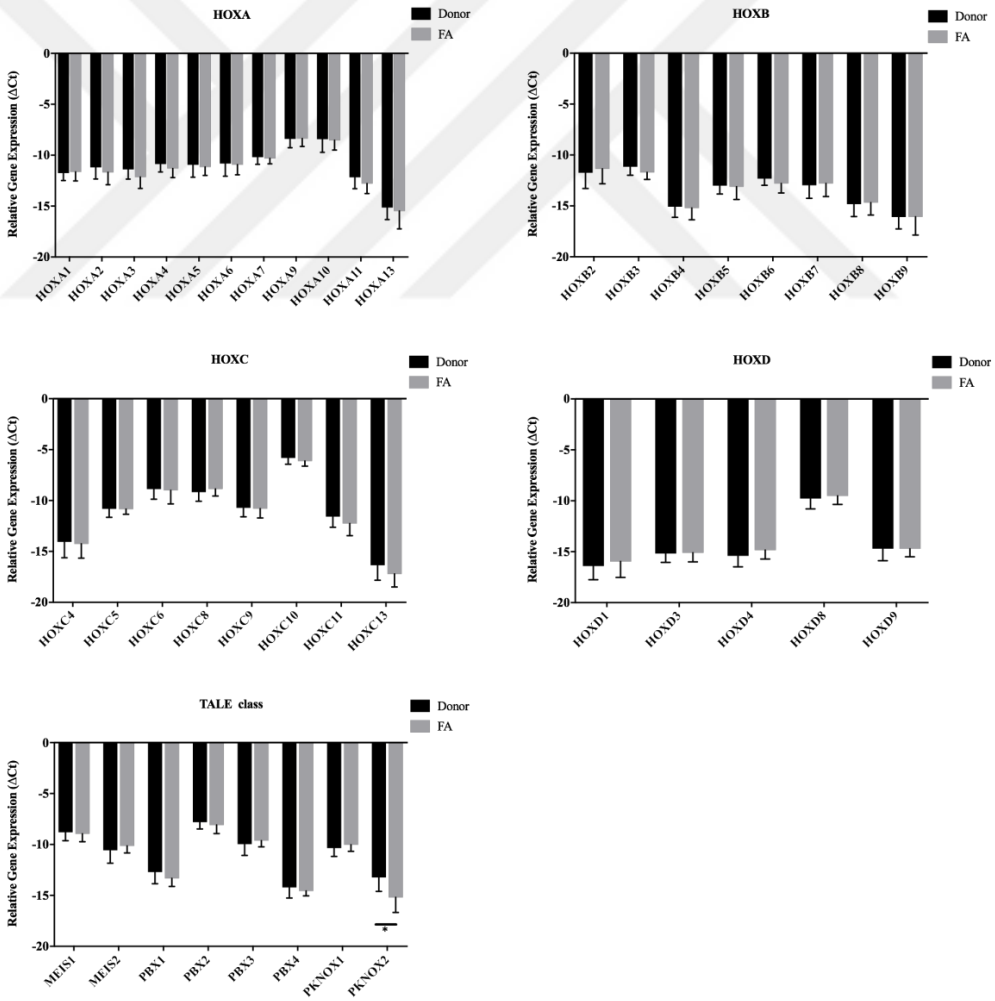

Figure 4.14. Relative HOX and TALE gene expression pattern of donor and FA patient BM-MSCs. * depicts statistically significant difference (*P*< 0.05).

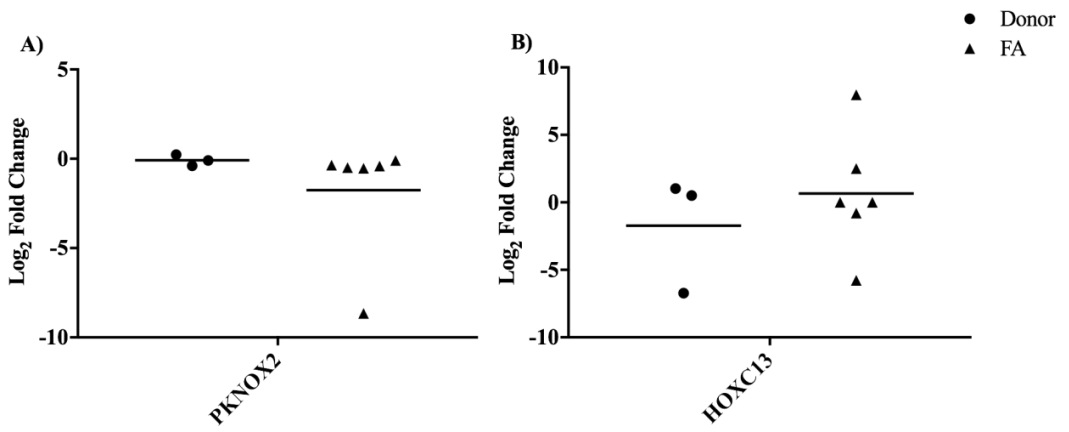

Figure 4.15. Effect of DEB treatment on A) *PKNOX2* and B) *HOXC13* gene expression of donor and FA patient BM-MSCs.

4.2.2. Protein Level of Differentially Expressed Gene

The PKNOX2 protein level was assessed in donor and FA patient BM-MSCs by western blotting. Three different protein bands were observed following immunoblotting with anti-PKNOX2 antibody of which two corresponded with 52 and 70kDa, respectively (Figure 4.16. A-B). All samples expressed higher levels of large isoform (70kDa) compared to smaller one (52kDa). Donors (1.19 ±0.33 or 0.24 ±0.06, respectively) and FA (1.21 ±0.28 or 0.30 ±0.07, respectively) had a similar level of large or small isoforms of PKNOX2 protein (P> 0.05; Figure 4.16. A-B). Additionally, *FANCA*- (1.27 ±0.28 or 0.31 ±0.08, respectively) and *FANCD2*- (1.08 ±0.30 or 0.29 ±0.06, respectively) deficient cells had no difference in expression of large or small variant.

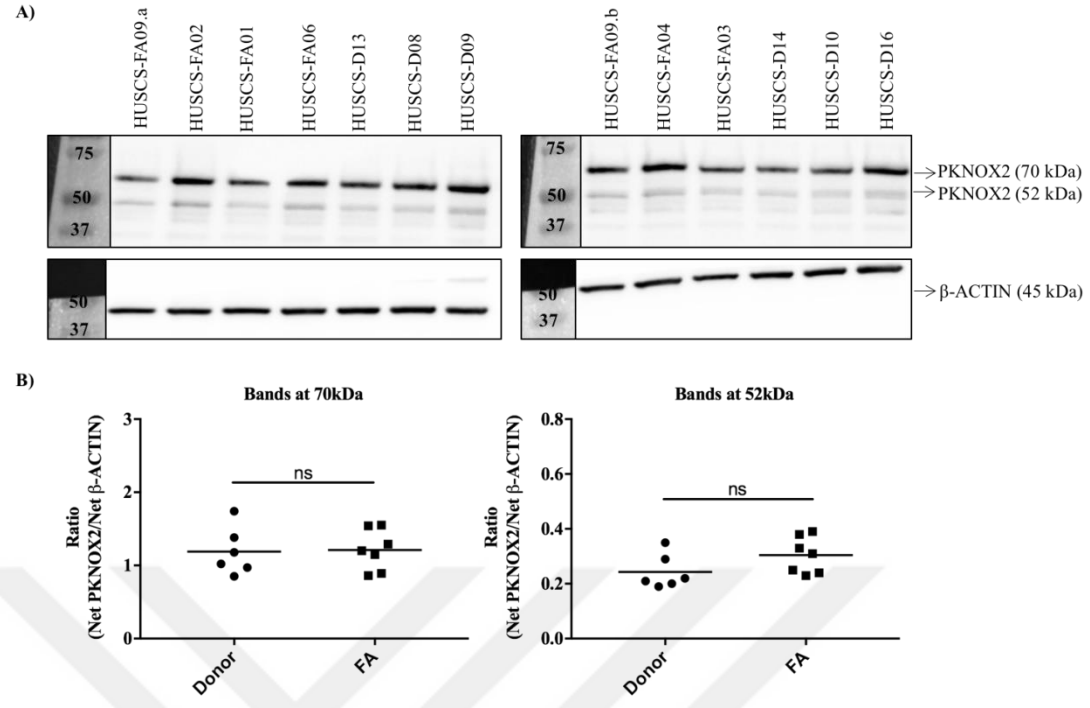

Figure 4.16. PKNOX2 protein level in FA patient and donor BM-MSCs was determined. A) 45µg protein was loaded on to each lane of 10% SDS-PAGE gel (exposure time= 5 minutes). B) Semi-quantitative analysis of PKNOX2 protein isoforms normalized to β-ACTIN are shown.

4.3. Induction of Bone Marrow Mesenchymal Stromal/Stem Cells with Recombinant Human TGF-β1 Protein

4.3.1. Effect of Recombinant Human TGF-β1 Protein Induction on Cell Viability

The effect of rTGF-β1 protein on BM-MSCs was determined following treatment with different concentrations (0.01, 0.05, 0.1, 0.2, 1, 5 and 10ng/ml) for 12, 24 and 48 hours. Following induction for 12 hours, cell viability decreased at concentrations above 1 ng/ml (i.e. cell viability= 58% at 10ng/ml), whereas longer incubation periods (i.e. 24 and 48 hours) showed an opposite effect, during which the cell viability increased as the concentration of rTGF-β1 protein increased (i.e. following induction for 24 and 48 hours cell viability at 10ng/ml was 118% and 104% of uninduced cells, respectively) (Figure 4.17.). Further experiments were performed only with 0.1 and 5ng/ml of rTGF-β1 protein.

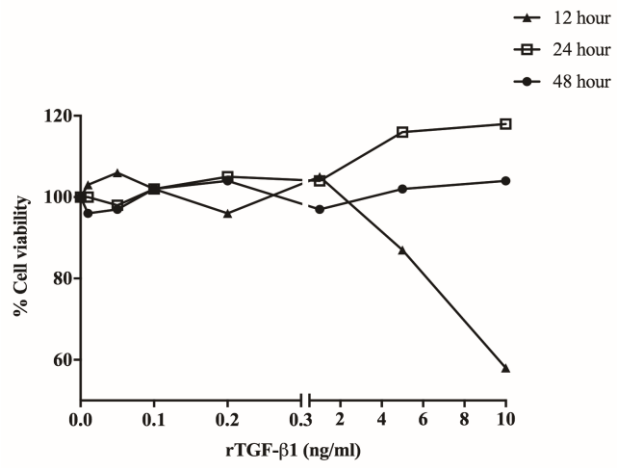

Figure 4.17. Effect of recombinant human TGF-β1 protein induction on the viability of BM-MSCs. Percentage of viable BM-MSCs obtained following rTGF-β1 induction was calculated as the ratio of mean absorbance of induced cells to mean absorbance of uninduced cells.

4.3.2. Effect of Recombinant Human TGF-β1 Protein Induction on Cell Proliferation

After rTGF-β1 treatment, BM-MSC proliferation increased in comparision to controls (Figure 4.18. A). Doubling time of cells was calculated after induction between 37:46:27 and 68:17:04 hours (Figure 4.18. A-B). For each condition (i.e. control, 0.1 or 5ng/ml), MWU test was used to investigate whether the doubling time between FA and donor BM-MSCs differed significantly. There was no difference between the doubling time of patient and donor cells ($P > 0.05$). The doubling time of donors (62.27 ±2.18 hours) and *FANCD2*-deficient (62.28 ±0.04 hours) cells cultured in DMF10 medium was similar but slightly higher than *FANCA*-deficient BM-MSCs (50.87 ±0.47 hours; Figure 4.18. B). Following 0.1 or 5ng/ml rTGF-β1 induction, a fold change in doubling time of donors (0.88 ±0.00 or 0.57 ±0.03, respectively), *FANCA*-deficient (0.83 ±0.02 or 0.66 ±0.06, respectively) and *FANCD2*-deficient (0.82 ±0.11 or 0.69 ±0.17, respectively) BM-MSCs was similar (Table 4.3.). At 219:13:38 hours, the cell index of donor (5.31 ±0.05), FA-A (4.11 ±1.55) and FA-D2 (5.61 ±0.95) cells in DMF10 medium was similar. Additionally, the cell index (at 219:13:38 hours) of 0.1 or 5ng/ml rTGF-β1 induced donor (5.21 ±0.10 and 5.14 ±0.79, respectively), FA-A (4.89 ±0.64 and 5.84 ±1.42, respectively) and FA-D2 (5.41 ±1.51 and 6.09 ±0.77, respectively) BM-MSCs did not change.

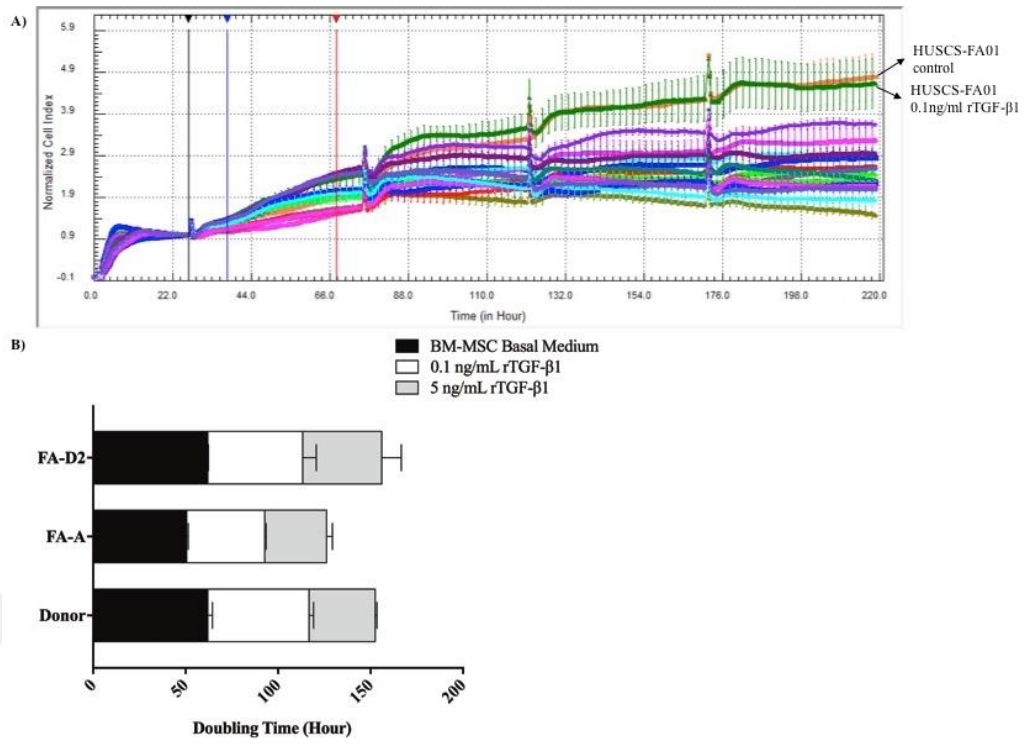

Figure 4.18. Proliferation of *FANCA*-deficient, *FANCD2*-deficient and donor BM-MSCs was assessed following 219:13:38 hours of rTGF-β1 induction. A) Line graph showing normalized cell index versus time measurements of real-time proliferation using xCELLigence RTCA systems. B) Doubling time of cells in DMF10 medium supplemented with or without 0.1 and 5ng/ml rTGF-β1 protein.

Table 4.3. Following the initial rTGF-β1 induction, fold change in doubling time of cells derived from FA patients and donors was determined.

	Fold Change in Doubling Time by rTGF-β1**		
	Control*	**0.1ng/ml rTGF-β1**	**5ng/ml rTGF-β1**
Donor	1.00 ±0.00	0.88 ±0.00	0.57 ±0.03
FA-A	1.00 ±0.00	0.83 ±0.02	0.66 ±0.06
FA-D2	1.00 ±0.00	0.82 ±0.11	0.69 ±0.17

* Depicts DMF10 medium; ** Fold change was the ration of doubling time of rTGF-β1 treated cells to the population doubling of corresponding BM-MSC cultured in DMF10 medium.

4.3.3. Effect of Recombinant Human TGF-β1 Protein on *PKNOX2, MEIS1, PBX1* and *TGF-β1* Expression Levels

Dose- and time-dependent effect of rTGF-β1 protein on *PKNOX2*, *TGF-β1*, *MEIS1* and *PBX1* expression of a donor BM-MSCs was determined by calculating

the fold change difference between induced and uninduced cells (Figure 4.19. A-D). Across all samples, the coefficient of variation for the Ct value of *ACTB* gene was 2.75%. The fold change in *TGF-β1* expression level increased as the dose of rTGF-β1 increased at 24, 48 or 72 hours (Figure 4.19. A-B). *TGF-β1* gene expression level of BM-MSCs induced with 0.1ng/ml rTGF-β1 decreased in time (Figure 4.19. A). Fold change in *PKNOX2* expression of BM-MSCs fluctuated for each dose of recombinant protein in time (Figure 4.19. B). Low doses of rTGF-β1 increased *PKNOX2* at 24 hours, but again dropped at 48 hours followed by a second increase at 72 hours (Figure 4.19. B). There was a slight change in *MEIS1* expressions following induction in time (Figure 4.19. C). Fold change in *PBX1* expression was -1.25 after 48 hours and decrease in the expression stayed stable after 72 hours (Figure 4.19. D).

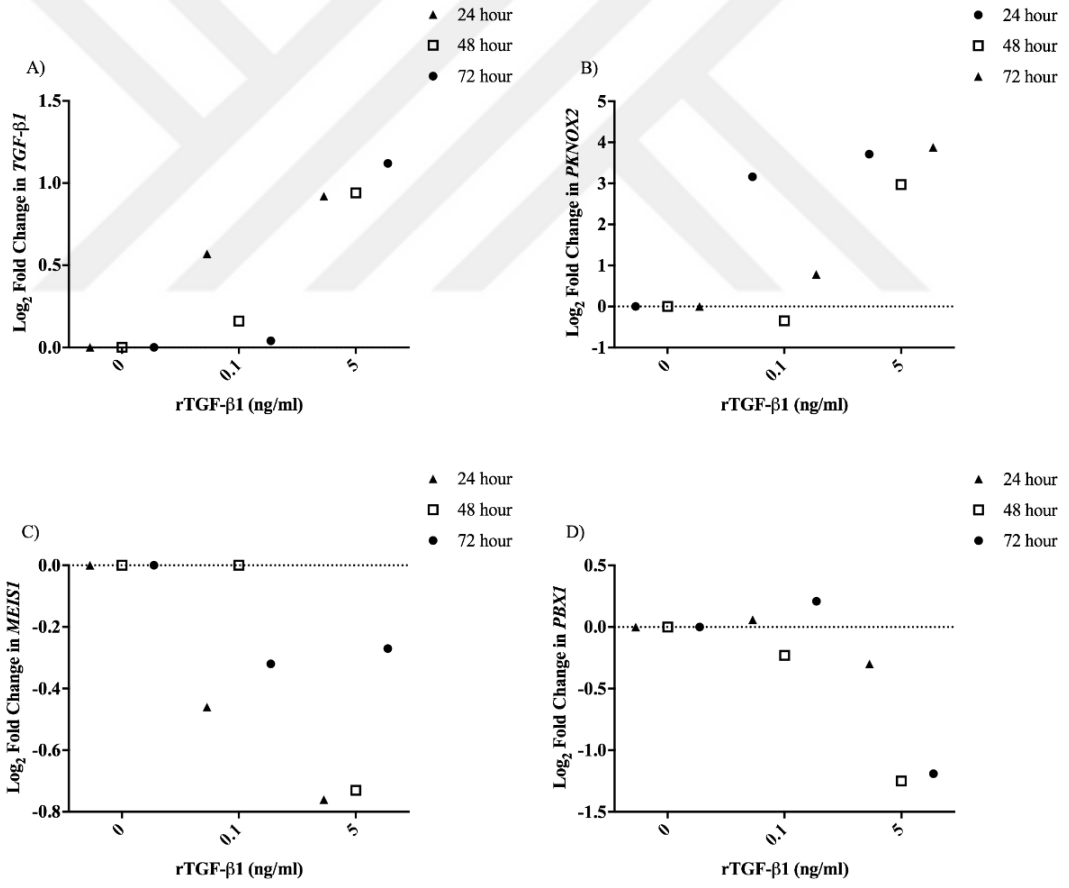

Figure 4.19. Fold change in A) *TGF-β1*, B) *PKNOX2*, C) *MEIS1* and D) *PBX1* gene expression level of BM-MSCs induced with 0.1 or 5ng/ml rTGF-β1 protein for 24, 48 and 72 hours.

Fold change in *TGF-β1*, *PKNOX2*, *MEIS1* and *PBX1* gene expression of FA patients (n= 5) and donor (n= 5) BM-MSCs induced with 0.1 or 5ng/ml rTGF-β1 for 24 hours were compared (Figure 4.20. A-D). For each experimental condition (i.e. control, 0.1 or 5ng/ml), the MWU test was used to investigate whether gene expression levels between FA and donor BM-MSCs differed significantly. There were no significant differences in *TGF-β1*, *PKNOX2*, *MEIS1* and *PBX1* gene expression levels between donor and FA cells at different concentrations of rTGF-β1 protein ($P > 0.05$; Figure 4.20. A-D).

Friedman's 2-way ANOVA by ranks test was used to determine whether fold change in gene expression altered as the rTGF-β1 protein concentration changed within the donor or FA BM-MSC group, and was followed by a Bonferroni corrected all pairwise test. As the dose of rTGF-β1 protein increased, *TGF-β1* gene expression increased in the donor or FA BM-MSC group (Figure 4.20. A). Donor BM-MSCs induced with 5ng/ml rTGF-β1 protein (fc= 1.10 ±0.16) had a significant increase (adjusted $P = 0.013$) in *TGF-β1* gene expression compared to control cells (fc= 0.00 ±0.00; Figure 4.20. A). *PKNOX2* gene expression changed in FA patient or donor BM-MSC groups treated with rTGF-β1 protein (Figure 4.20. B) and 5ng/ml rTGF-β1 upregulated *PKNOX2* gene expression in either donor (fc= 3.09 ±0.58) or FA patient (fc= 2.37 ±0.84) BM-MSCs significantly (adjusted $P < 0.05$). *MEIS1* or *PBX1* gene expression levels remained unchanged upon rTGF-β1 induction ($P > 0.05$; Figure 4.20. C-D).

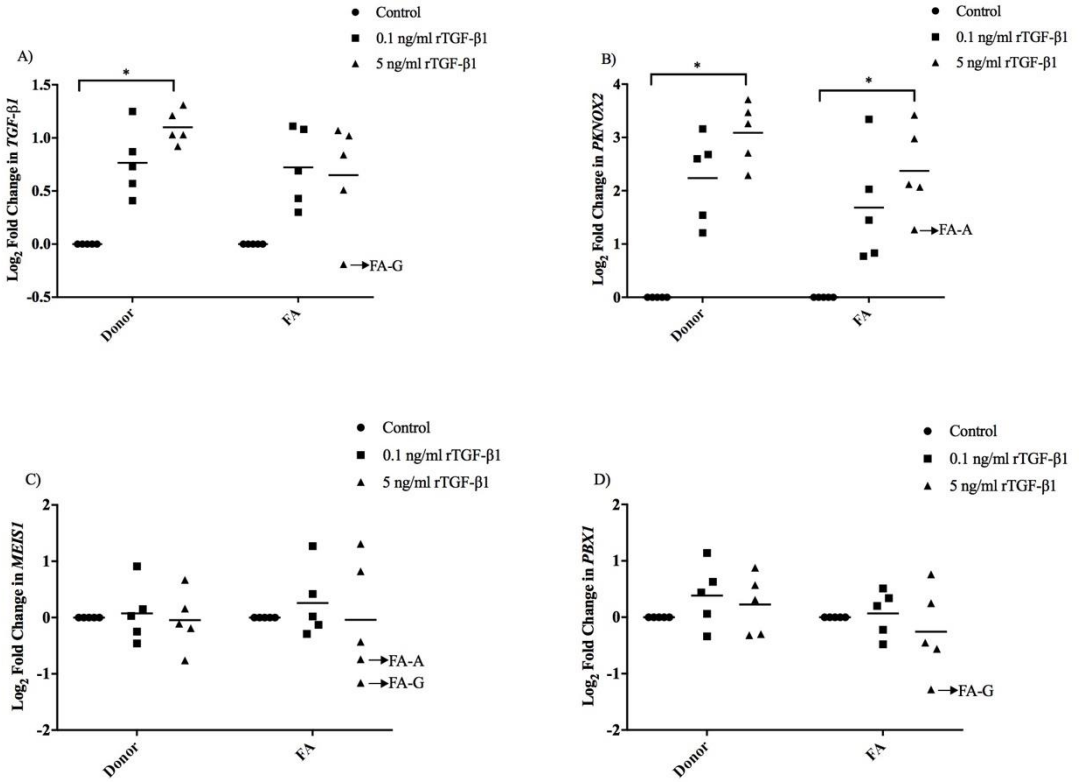

Figure 4.20. Fold change in A) *TGF-β1*, B) *PKNOX2*, C) *MEIS1* and D) *PBX1* gene expression of FA patients (n= 5) and donor (n= 5) BM-MSCs induced with 0.1 or 5ng/ml rTGF-β1 for 24 hours. * depicts statistically significant difference ($P< 0.05$).

4.3.4. Effect of Recombinant Human TGF-β1 Protein Induction on PKNOX2 Protein Level

PKNOX2 protein level was measured prior to and following treatment with 0.1 or 5ng/ml rTGF-β1 protein using western blotting. Two protein bands corresponding to 52 and 70kDa were quantified (Figure 4.21. A-B). All samples had higher level of the large variant (70kDa) compared to small isoform (52kDa). Both PKNOX2 and β-ACTIN levels of HUSCS-FA01 were lower than other samples, which might be due to technical problems, such as protein degradation. For each experimental condition (i.e. control, 0.1 or 5ng/ml), the MWU test was used to investigate whether the levels of PKNOX2 isoforms between FA and donor BM-MSCs differed significantly. There was no significant difference in PKNOX2 at a protein level between FA patients and donor BM-MSCs at any concentration of rTGF-β1 protein ($P> 0.05$; Figure 4.21. A-B). Friedman's 2-way ANOVA by ranks

test was used to determine whether levels of PKNOX2 variants varied as the rTGF-β1 protein concentration altered in donor or FA BM-MSC group, and was followed by the Bonferroni corrected all pairwise test. As the dose of rTGF-β1 protein increased, PKNOX2 protein level remained unchanged in both the donor or FA BM-MSC groups (*P*> 0.05; Figure 4.21. B).

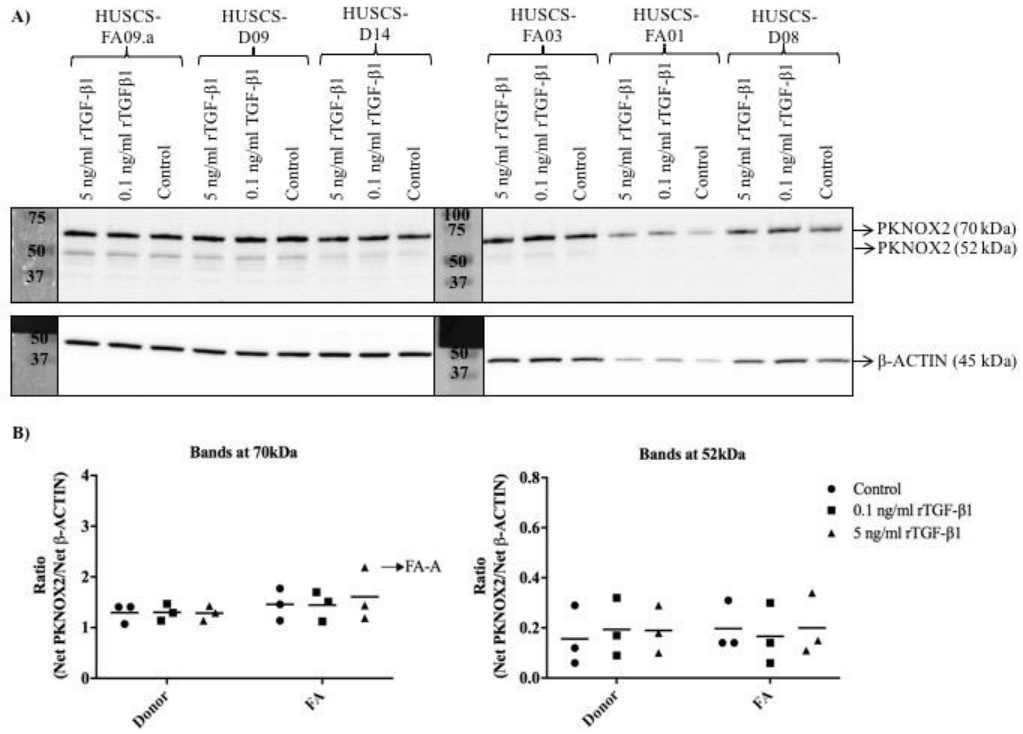

Figure 4.21. PKNOX2 protein level of FA patient and donor BM-MSCs was determined following rTGF-β1 protein induction. A) 20μg protein was loaded on to each lane of 10% SDS-PAGE gel (exposure time= 5 minutes). B) Semi-quantitative analysis of PKNOX2 protein variants normalized to β-ACTIN were shown.

4.4. Characterization of Bone Marrow Mesenchymal Stromal/Stem Cells Carrying PKNOX2 Expression Plasmid

Detailed characterization of the PKNOX2 expression plasmid transfected BM-MSCs could be performed by using more than one donor.

4.4.1. Gene Expression Levels Following PKNOX2 Overexpression

Following day 2 (D2) and 4 (D4) post-electroporation, PKNOX2 overexpression was confirmed at the mRNA level in BM-MSCs. *PKNOX2*

expression was 16.85 (±4.29) and 12.59-fold upregulated in BM-MSCs overexpressing PKNOX2 compared to pCMV6:MSCs at day +2 and +4 post-electroporation, respectively (Figure 4.22. A). Following PKNOX2 overexpression, fold change in expression of *HOXC13* gene as well as in its paralog gene *HOXA13* was assessed. *HOXA13* (fc= -0.05 ±1.98) expression remained unchanged but *HOXC13* expression (fc= -0.69 ±4.23) varied widely on day 2 of electroporation (Figure 4.22. B).

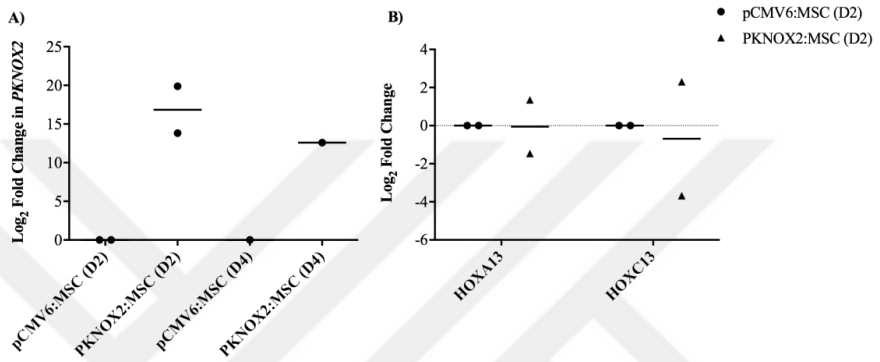

Figure 4.22. Fold change in A) *PKNOX2*, B) *HOXA13* and *HOXC13* gene expression levels in PKNOX2:MSC, compared to pCMV6:MSCs were determined. D2 and D4 depict day 2 and 4 following electroporation, respectively. HUSCS-D08 and HUSCS-D11 were used for the assay.

4.4.2. Western Blot Analysis Following PKNOX2 Overexpression

PKNOX2-DDK overexpression was confirmed in BM-MSCs using anti-DDK (Figure 4.23. A) and anti-PKNOX2 antibodies. (Figure 4.23. B). The PKNOX2-DDK fusion protein was heavier than the endogenous one and migrated slower the gel (Figure 4.23. B). Samples had higher levels of the large isoform (70kDa) compared to the small variant (52kDa) of endogenous PKNOX2 (Figure 4.23. B). The unubiquitinated (S; 150kDa) and monoubiquitinated (L; 162kDa) isoforms of the FANCD2 protein were assessed (Figure 4.24. A). FANCD2-L had a lower expression compared to FANCD2-S. Pulsed BM-MSCs had higher FANCD2 levels than other groups. The level of both isoforms decreased after plasmid transfection (Figure 4.24. A). The HOXA13 protein level was slightly decreased in PKNOX2:MSCs (Figure 4.24. B) However, electroporation, as well as, plasmid transfection also affected downregulation of the protein (Figure 4.24. B).

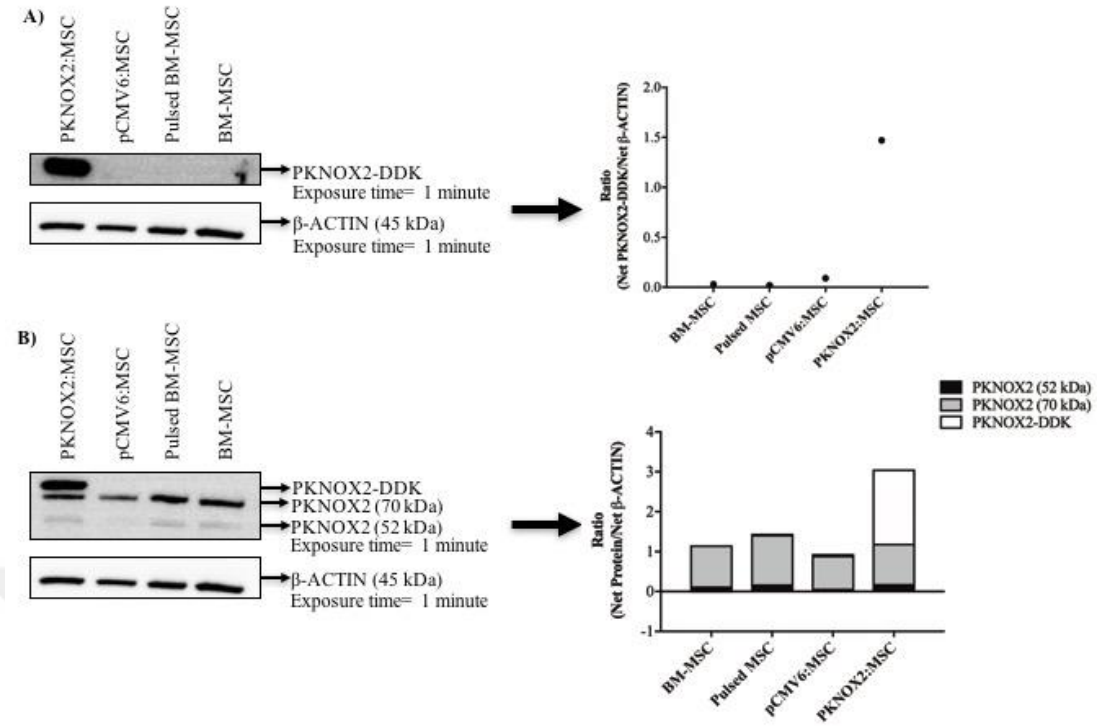

Figure 4.23. PKNOX2 protein level was confirmed using A) anti-DDK and B) anti-PKNOX2 antibodies following electroporation of PKNOX2-pCMV6 plasmid to BM-MSCs. 38µg protein was loaded on to each lane of 10% SDS-PAGE gel. Cells of HUSCS-D08 were used.

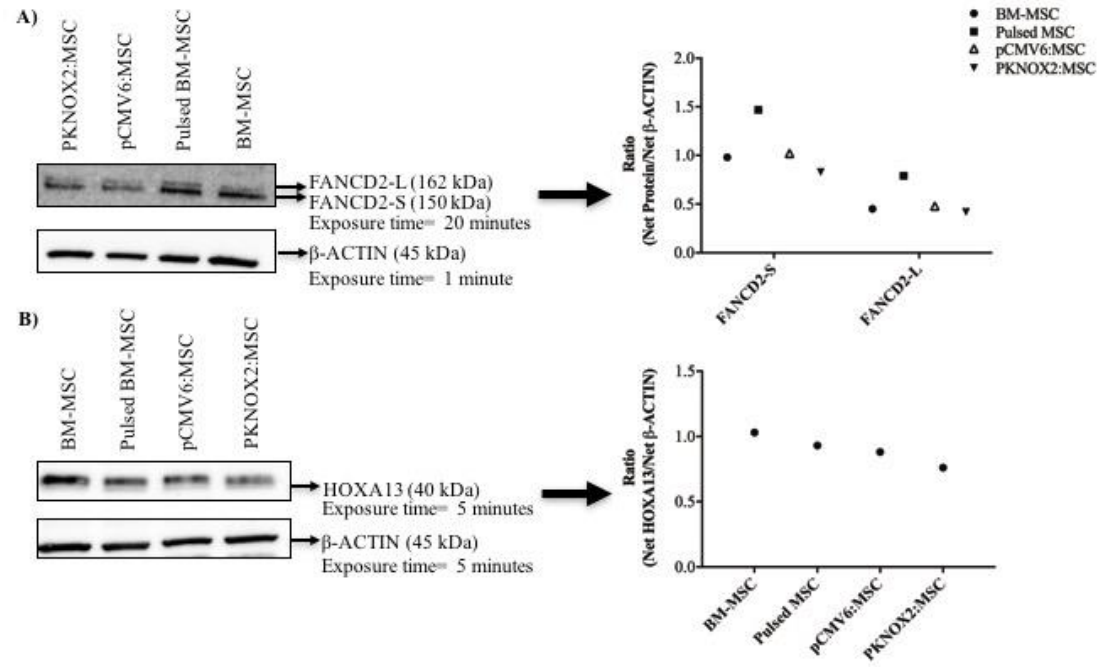

Figure 4.24. Levels of A) FANCD2 and B) HOXA13 proteins were determined following PKNOX2 overexpressing. 38µg protein was loaded on to each lane of 10% SDS-PAGE gel.

4.4.3. Lateral Motility

The wound-healing assay was used to measure lateral migration of PKNOX2:MSCs compared to pCMV6:MSCs, pulsed MSCs and untransfected cells (Figure 4.25. and Figure 4.26.). The motility index of all samples was similar after 2 hours (Figure 4.26.). 4 hours post-wounding, the lateral motility of pulsed cells was slightly higher than other conditions (Figure 4.26.). 6 hours post-wounding, there was a decrease in the motility index of PKNOX2 plasmid transfected cells compared to controls (Figure 4.26.). The wound closure of pulsed cells was nearly completed at 24 hours (Figure 4.25.) and their motility index was higher than BM-MSCs and pCMV6:MSCs at 20 hours post-wounding (Figure 4.26.). Wound closure in BM-MSC, pulsed cell and pCMV6:MSC cultures was completed at 36 hours, whereas the wound healing in PKNOX2:MSC cultures was nearly complete at 168 hours post-wounding (Figure 4.25. and Figure 4.26.).

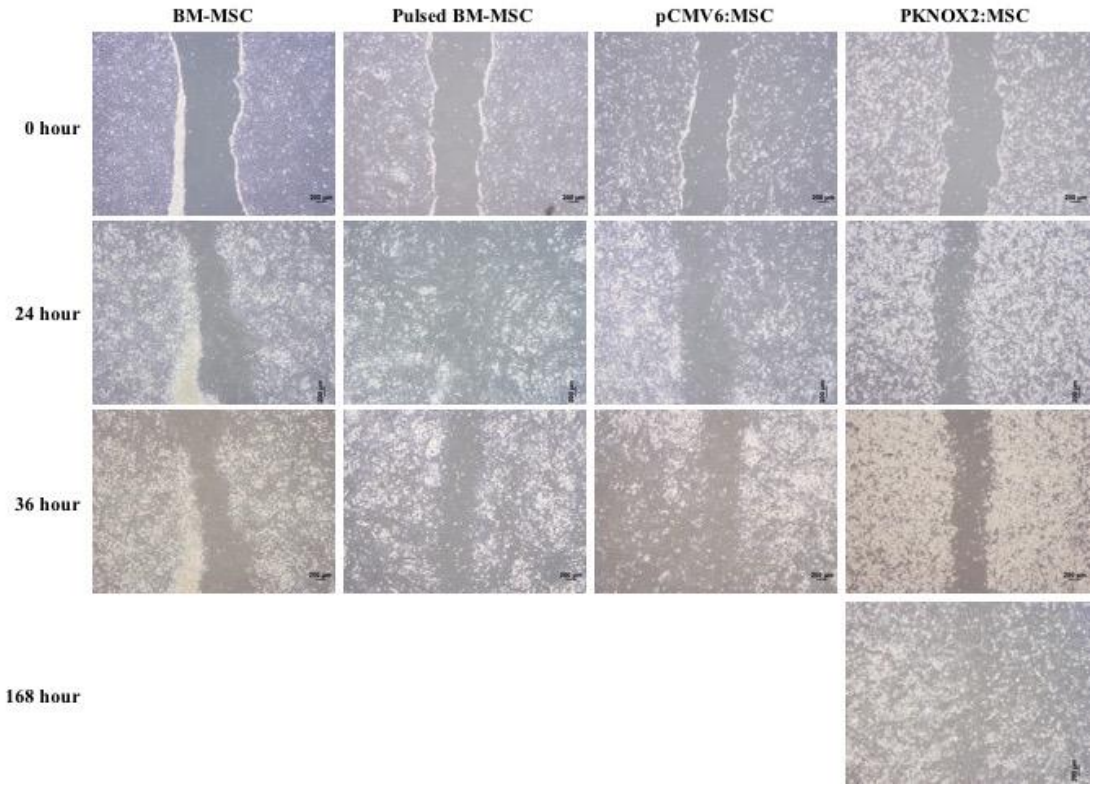

Figure 4.25. Representative images of wound-healing assay were taken at 0, 24, 36 and 168 hours post-wounding (40x magnification). The wound healing in BM-MSCs, pulsed cells and pCMV6:MSCs was complete at 36 hours. However, the wound healing in BM-MSCs overexpressing PKNOX2 was nearly complete at 168 hours.

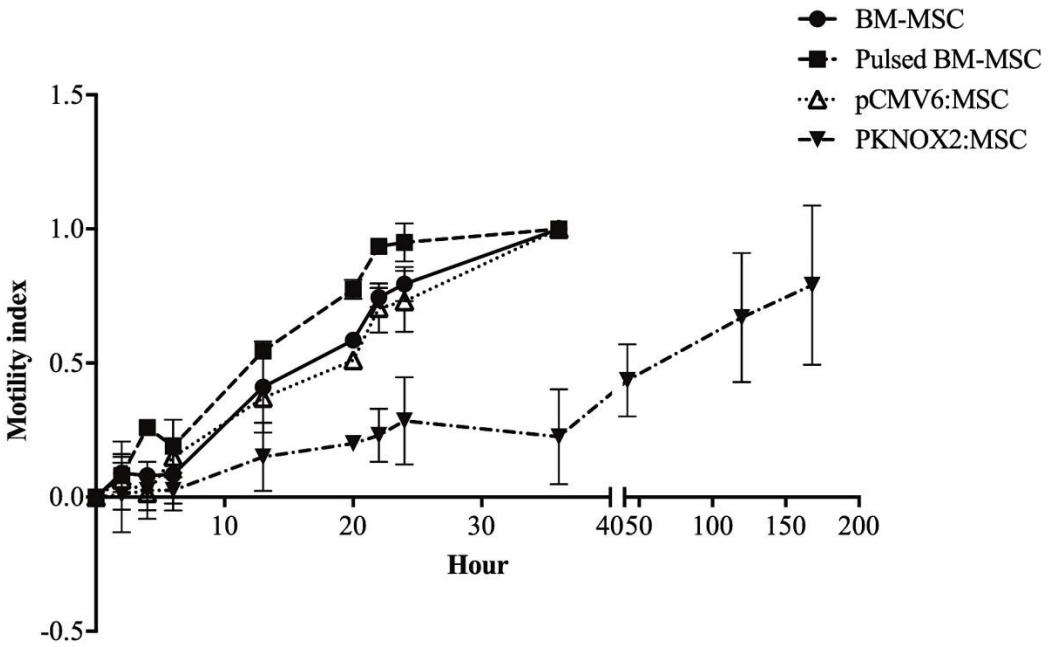

Figure 4.26. Motility index of PKNOX2 overexpressing BM-MSCs was lower than pCMV6:MSCs, pulsed and untransfected BM-MSCs. Cells of HUSCS-D11 were used.

4.4.4. Adipogenic and Osteogenic Differentiation Potential

PKNOX2:MSCs, pCMV6:MSCs, pulsed and control BM-MSCs were able to differentiate to adipogenic lineages as assessed by positive ORO staining of the lipid droplets (Figure 4.27. A-B). Additionally, cells cultured in DMF10 medium were used as control and stained negative with ORO (Figure 4.27. A). Following electroporation, adipogenic differentiation of BM-MSCs was slightly higher compared to untransfected cells (Figure 4.27. B).

Passage 3 BM-MSCs were able to differentiate into osteogenic lineage as shown by positive ARS staining (Figure 4.28. A-B). Cells cultured in DMF10 medium did not produce any calcium phosphate deposits, and stained negative for ARS. Following electroporation, passage 3 BM-MSCs had a lower capacity to differentiate to osteogenic lineages compared to untransfected cells (Figure 4.28. B). Passage 5 BM-MSCs were not able to differentiate to osteoblasts (Figure 4.28. A-B). When the experiment was repeated, most of the electroporated BM-MSCs lost their adherence once induced with osteogenic differentiation medium (Figure 4.28. B).

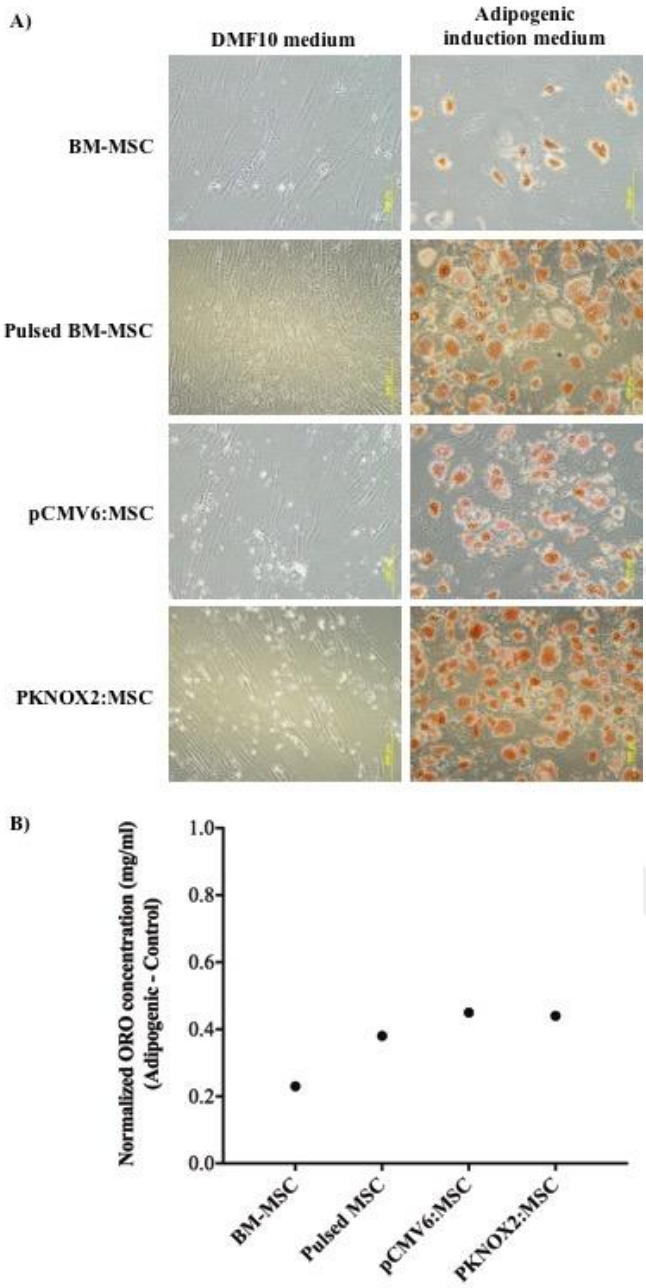

Figure 4.27. Adipogenic differentiation capacity of BM-MSCs transfected with PKNOX2 (n= 1) was compared with BM-MSCs (n= 1), pulsed cells (n= 1) and pCMV6:MSCs (n= 1). A) Representative images were taken following ORO staining (200x magnification). BM-MSCs induced in adipogenic differentiation medium stained positively with ORO while BM-MSCs cultured in DMF10 medium were not stained. B) For quantitation of lipid accumulation, ORO content was extracted and the absorbance was measured at 492nm, and then used to calculate concentration. Normalized ORO concentration was calculated by subtracting concentration of cells cultured in DMF10 medium from cells induced in adipogenic differentiation medium. Cells of HUSCS-D11 were used.

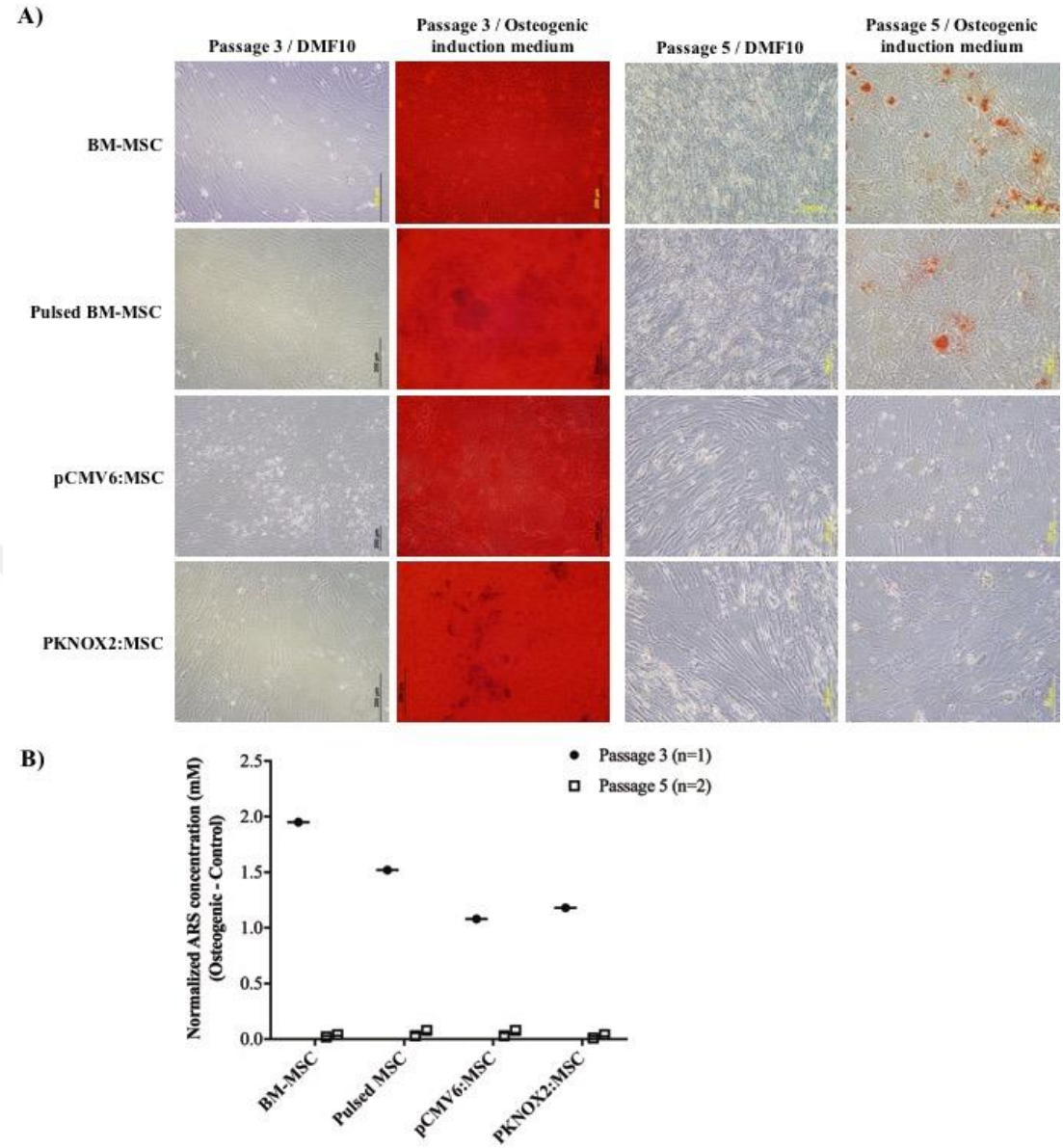

Figure 4.28. Osteogenic differentiation capacity of BM-MSCs transfected with PKNOX2 plasmid was compared with BM-MSCs, pulsed cells and pCMV6:MSCs. A) Representative images were taken following ARS staining (200x magnification). Passage 3 BM-MSCs (HUSCS-D09) induced in osteogenic differentiation medium stained positively while cells differentiated at passage 5 were negative for ARS. B) For quantification of calcium phosphate deposit formation, ARS content was extracted and the absorbance was measured at 405nm, which was then used to calculate concentration. Normalized concentration was calculated by subtracting ARS concentration of cells cultured in DMF10 medium from cells induced in osteogenic differentiation medium. Cells of HUSCS-D09 and HUSCS-D11 were used.

4.4.5. Immunophenotyping Analysis

CD105, CD73, CD44, CD29, CD90, CD31, HLA-DR, CD45 and CD34 levels were measured following PKNOX2 overexpression in BM-MSCs. CD105 level was downregulated by plasmid transfection, but downregulation in the PKNOX2 overexpressed cells was more prominent. CD73 level was downregulated in all transfected groups, that indicated electroporation effect. Following PKNOX2 plasmid transfection, CD29 level decreased in cells from HUSCS-D11, but was not altered in cells of HUSCS-D16. CD44 level did not change in PKNOX2:MSCs from HUSCS-D11, but was downregulated in PKNOX2:MSCs from HUSCS-D16. CD90 percentage did not change by PKNOX2 plasmid transfection. Cells were negative for endothelial (CD31) and hematopoietic markers (HLA-DR, CD45 and CD34) (Table 4.4.).

4.4.6. Active TGF-β1, TGF-β2 and TGF-β3 Secretion Levels

Following three days post-electroporation, cells secreted predominantly TGF-β1 and low amounts of other isoforms. Level of TGF-β1 secretion varied within each group (Figure 4.29.). BM-MSCs overexpressing PKNOX2 secreted similar amount of TGF-β1 (1905.92pg/ml ±1138.90; *P*= 0.800), TGF-β2 (210.51pg/ml ±90.64; *P*= 0.800) and TGF-β3 (62.04pg/ml ±35.53; *P*= 0.800) as pCMV6:MSCs (2443.66pg/ml ±1413.28, 241.97pg/ml ±105.11 and 72.96pg/ml ±39.78, respectively).

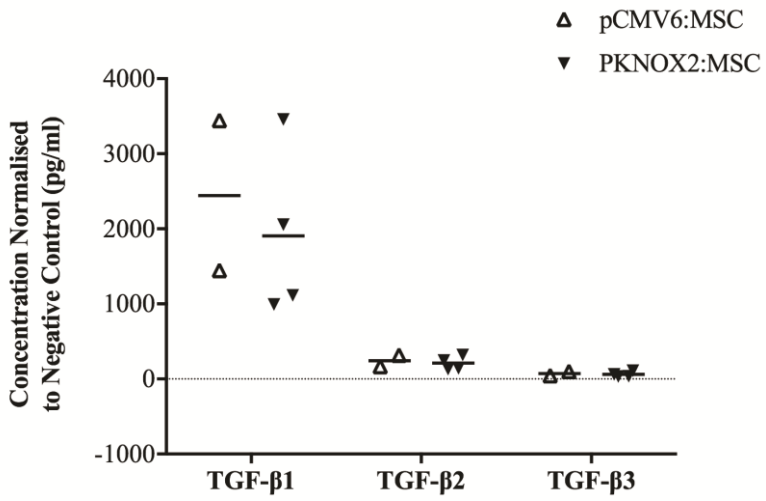

Figure 4.29. Levels of TGF-β1, TGF-β2 and TGF-β3 secretion by PKNOX2:MSCs and pCMV6:MSCs. Cells from HUSCS-D11 were used.

Table 4.4. Immunophenotyping BM-MSCs, pulsed BM-MSCs, pCMV6:MSCs and PKNOX2:MSCs from two donors.

	CD105	**CD73**	**CD44**	**CD29**	**CD90**	**CD31**	**HLA-DR**	**CD45**	**CD34**
BM-MSC (HUSCS-D11)	86.80	96.30	97.50	90.40	99.80	0.00	0.40	0.10	0.00
Pulsed BM-MSC (HUSCS-D11)	91.40	82.80	97.30	93.80	99.90	0.00	0.60	0.10	0.20
pCMV6:MSC (HUSCS-D11)	80.90	85.00	97.30	91.70	99.70	0.00	1.30	0.00	0.10
PKNOX2:MSC (HUSCS-D11)	73.50	86.00	96.80	76.10	99.60	0.00	2.10	0.10	0.10
BM-MSC (HUSCS-D16)	91.90	99.30	79.10	95.20	98.00	0.00	0.00	0.00	0.00
Pulsed BM-MSC (HUSCS-D16)	86.10	91.80	55.20	88.10	93.40	0.00	0.00	0.30	0.00
pCMV6:MSC (HUSCS-D16)	76.00	90.10	65.50	91.70	96.60	0.10	0.20	0.20	0.10
PKNOX2:MSC (HUSCS-D16)	59.80	88.10	47.50	89.50	92.40	0.00	0.00	0.00	0.00

4.4.7 Co-culturing Bone Marrow Mesenchymal Stromal/Stem Cells Overexpressing PKNOX2 with $CD34^+$ Hematopoietic Stem Cells

Co-culturing with Cryopreserved $CD34^+$ Hematopoietic Stem Cells

Prior to co-culture, the purity of cryopreserved $CD34^+$HSCs was determined by flow cytometry analysis and was found to be 44.50% $CD34^+CD38^-$, 3.90% $CD34^+CD38^+$ and 1.30% $CD34^-CD38^+$ (Figure 4.30.). On day 4 of culture, the percentage of early hematopoietic stem/progenitors ($CD34^+CD38^-$) of $CD34^+$HSCs from all conditions was decreased, whereas more mature hematopoietic phenotypes, including $CD34^+CD38^+$ and $CD34^-CD38^+$ levels were increased compared to cells on day zero (Figure 4.30.). $CD34^+$HSCs cultured for 4 days on PKNOX2:MSCs had a similar $CD34^+CD38^-$ percentage, but higher $CD34^+CD38^+$ and $CD34^-CD38^+$ levels compared to control $CD34^+$HSCs and cells co-cultured with BM-MSCs or pCMV6:MSCs (Figure 4.30.).

The effect of PKNOX2:MSCs on the expansion of $CD34^+$HSCs was assessed. A decrease in the fold expansion of total $CD34^+$HSCs was observed for all experimental conditions after four days of culture (Table 4.5.). However, fold expansion of total $CD34^+$HSCs co-cultured with PKNOX2:MSCs increased compared to $CD34^+$HSCs cultured on pCMV6:MSCs or BM-MSCs (Table 4.5.). However, on day 4 of co-culture, the fold expansion of HSCs was higher in control wells than of cells cultured on a feeder layer (Table 4.5.).

The clonogenic potential of $CD34^+$HSCs was determined by their ability to form CFU-GEMM, CFU-GM and BFU-E colonies (Figure 4.31. A-C). 4 days post-culturing, $CD34^+$HSCs cultured on PKNOX2:MSCs had a higher potential to form CFU-GEMM (fc= 7.00), CFU-GM (fc= 6.94) and BFU-E (fc= 6.67) compared with cells cultured alone. The differentiation capacity of $CD34^+$HSCs co-cultured with pCMV6:MSCs was similar to $CD34^+$HSCs cultured in the absence of feeder layers in terms of CFU-GEMM (fc= 0.85) and BFU-E (fc= 1.09). However, there was a slight increase in CFU-GM potential of cells cultured with pCMV6:MSCs (fc= 1.72). $CD34^+$HSCs cultured on BM-MSCs had a more restricted clonogenic potential and were only able to form CFU-GM colonies (Table 4.6.).

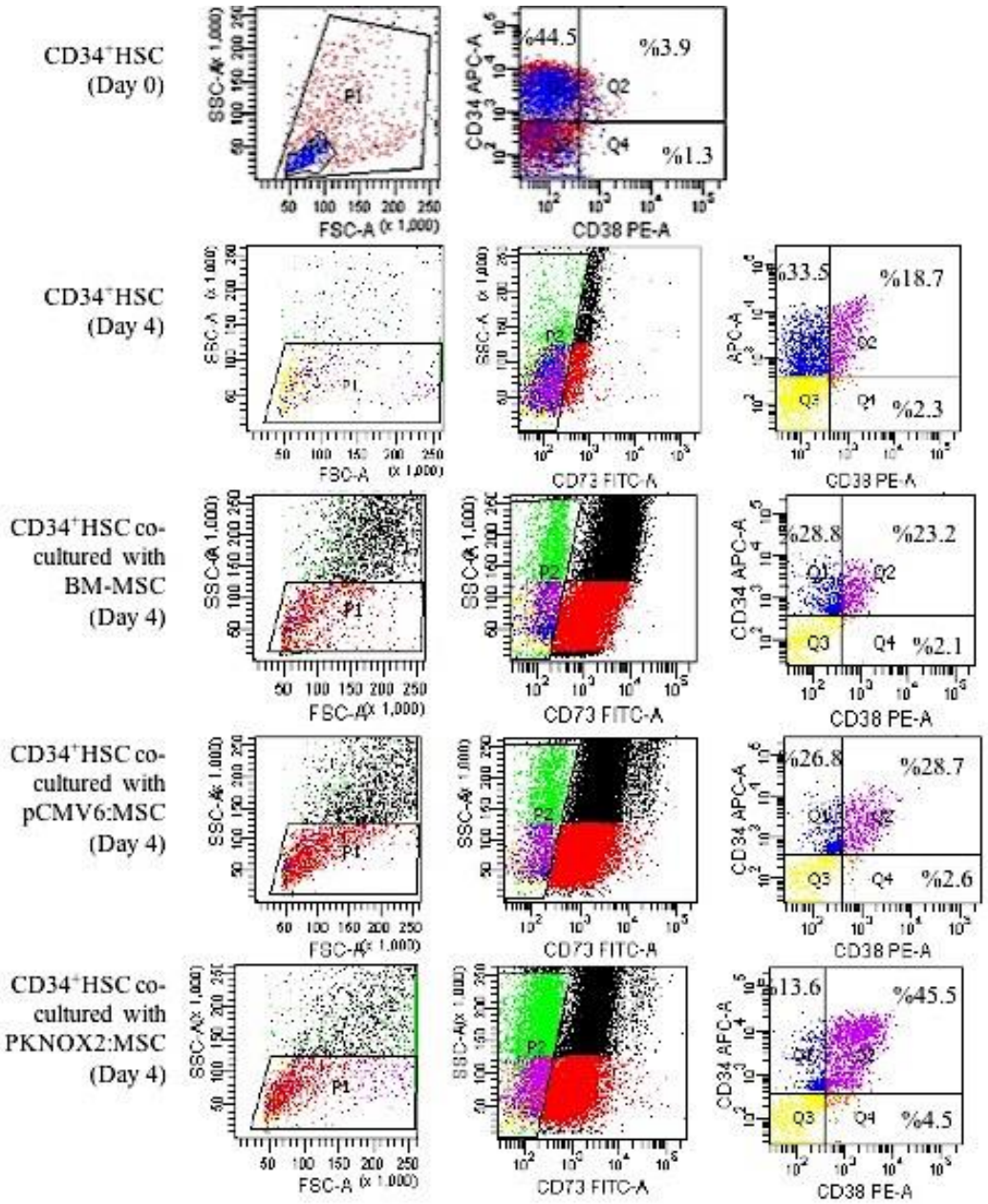

Figure 4.30. CD34 and CD38 levels of cryopreserved CD34^{+}HSCs prior to and on day four of co-culture. BM-MSCs of HUSCS-D11 were used.

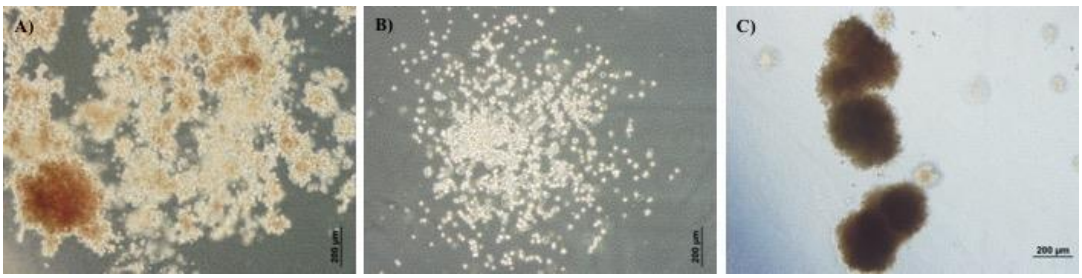

Figure 4.31. Representative images showing A) CFU-GEMM, B) CFU-GM and C) BFU-E colonies.

Table 4.5. Fold expansion of cryopreserved $CD34^+$HSCs on day four of co-culture.

	Fold Expansion			
	Total $CD34^+$HSC	**$CD34^+CD38^-$ HSC**	**$CD34^+CD38^+$ HSC**	**$CD34^-CD38^+$ HSC**
$CD34^+$HSCs (Day 4)	0.88	0.30	0.17	0.02
$CD34^+$HSCs co-cultured with BM-MSC (Day 4)	0.14	0.04	0.03	0.00
$CD34^+$HSCs co-cultured with pCMV6:MSC (Day 4)	0.11	0.03	0.03	0.00
$CD34^+$HSCs co-cultured with PKNOX2:MSC (Day 4)	0.23	0.03	0.10	0.01

Table 4.6. The clonogenic potential of cryopreserved $CD34^+$HSCs prior to and on day four of co-culture.

	Per 1000 $CD34^+$HSCs		
	CFU-GEMM number (fc)	**CFU-GM number (fc)**	**BFU-E number (fc)**
$CD34^+$HSCs (Day 0)	15	27	13
$CD34^+$HSCs (Day 4)	26 (1.0)	18 (1.0)	101 (1.0)
$CD34^+$HSCs co-cultured with BM-MSC (Day 4)	0 (-)	4 (0.22)	0 (-)
$CD34^+$HSCs co-cultured with pCMV6:MSC (Day 4)	22 (0.85)	31 (1.72)	110 (1.09)
$CD34^+$HSCs co-cultured with PKNOX2:MSC (Day 4)	182 (7.00)	125 (6.94)	674 (6.67)

(-) fold change (fc) was not calculated.

Co-culturing with Fresh $CD34^+$ Hematopoietic Stem Cells

Prior to co-culture, fresh $CD34^+$HSCs were 14.80% $CD34^+CD38^-$, 72.50% $CD34^+CD38^+$ and 7.30% $CD34^-CD38^+$ (Figure 4.32. A). On day four of culture, $CD34^+$HSCs from all experimental conditions had higher $CD34^+CD38^-$ percentage and lower $CD34^+CD38^+$ and $CD34^+CD38^-$ percentages compared to cells on day zero (Figure 4.32. A-B). $CD34^-CD38^+$ (49.25% ±4.03), $CD34^+CD38^+$ (49.85% ±4.17) and $CD34^-CD38^+$ (0.70% ±0.14) levels of $CD34^+$HSCs cultured on PKNOX2:MSCs were similar to cells cultured on pCMV6:MSCs (44.50% ±6.08, 54.60% ±5.66 and 0.85% ±0.35, respectively) or BM-MSCs (50.45% ±11.81, 48.90% ±11.60 and 0.50% ±0.14, respectively) (Figure 4.32. B). On day 4 of culture, $CD34^+CD38^+$ level of control $CD34^+$HSCs (19.00% ±2.40) was lower than cells co-cultured on a feeder layer (Figure 4.32. B).

Fold expansion of fresh $CD34^+$HSCs cultured on BM-MSCs overexpressing PKNOX2 was evaluated. Following co-culture, $CD34^+$HSC numbers increased in all experimental conditions (Figure 4.33.). Fold expansion of $CD34^+CD38^-$ HSCs cultured on PKNOX2:MSCs was slightly higher than for other groups (Figure 4.33.). Furthermore, fold expansion of $CD34^+CD38^+$ HSCs co-cultured with PKNOX2:MSCs or pCMV6:MSCs increased compared to cells cultured alone or on BM-MSCs. Expansion in the $CD34^-CD38^+$ HSCs population was not observed (Figure 4.33.).

The effect of PKNOX2:MSCs on the clonogenic potential of $CD34^+$HSCs was determined following co-culture (Figure 4.34.). $CD34^+$HSCs seeded prior to co-culture had a higher capacity to form CFU-GEMM and BFU-E colonies compared to cells cultured for four days, which formed few or no colonies (Figure 4.34.). $CD34^+$HSCs cultured for four days had more restricted differentiation potential and mostly formed CFU-GM colonies (Figure 4.34.). Cultured $CD34^+$HSCs had the highest capacity to differentiate to CFU-GM colonies, whereas other experimental conditions had comparable CFU-GM colony forming capacities with each other (Figure 4.34.).

A)

	% $CD34^+CD38^-$	% $CD34^+CD38^+$	% $CD34^-CD38^+$
$CD34^+$HSC (D0)	14.80	72.50	7.30

B)

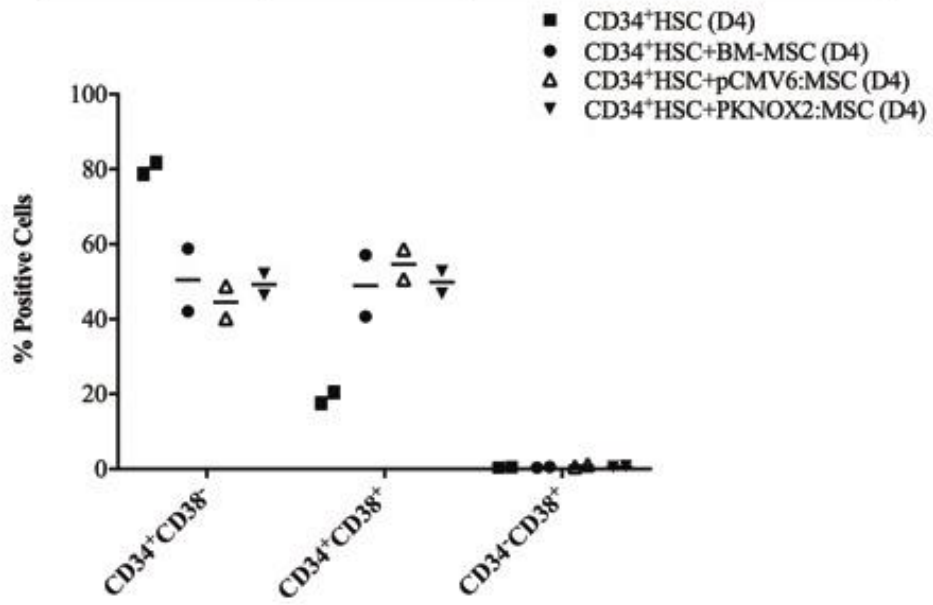

Figure 4.32. CD34 and CD38 levels of fresh $CD34^+$HSCs A) prior to (D0) and B) on day four (D4) of co-culture. BM-MSCs of HUSCS-D08 were used.

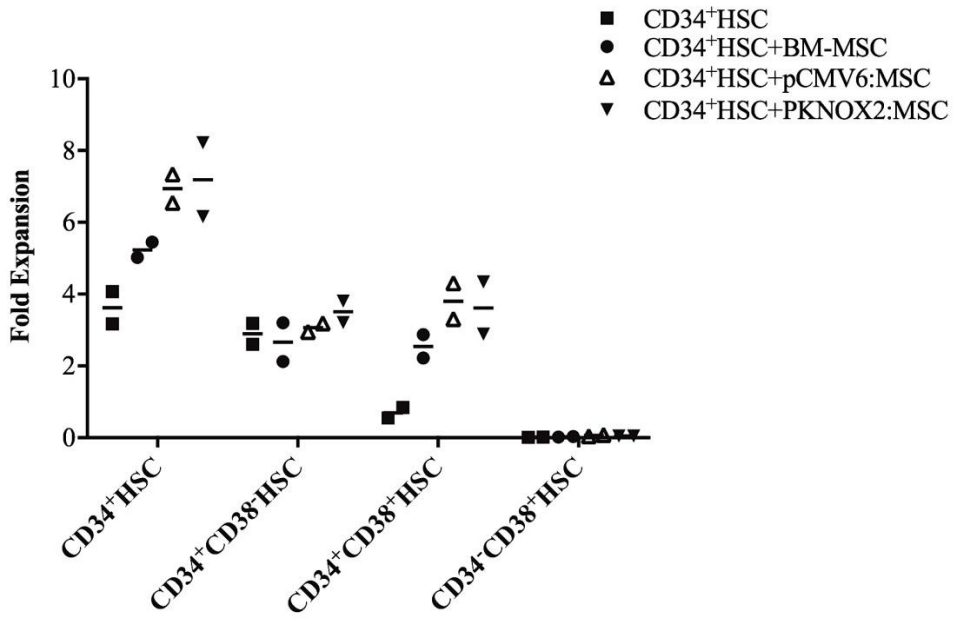

Figure 4.33. Fold expansion of fresh $CD34^+$HSCs prior to and on day four of co-culture. After co-culture, fold expansion of all HSCs ($CD34^+$HSC) were calculated. Additionally, fold expansion of $CD34^+CD38^-$, $CD34^+CD38^+$ and $CD34^-CD38^+$ cells following co-culture were calculated according to percentages obtained from flow cytometry analysis.

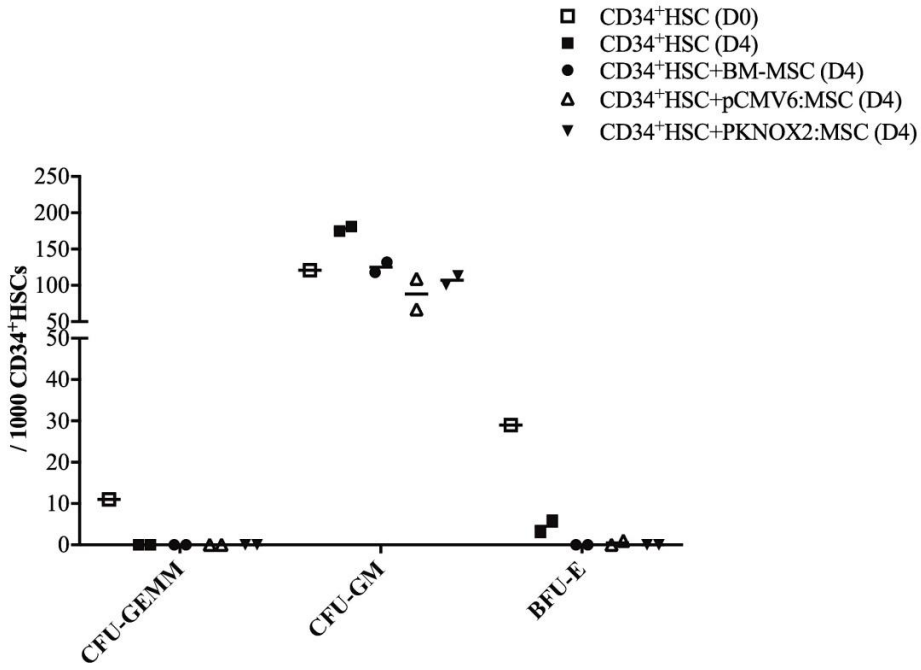

Figure 4.34. The clonogenic potential of fresh CD34$^+$HSCs prior to (D0) and on day four (D4) of co-culture.

4.5. Identifying Proteins Interacting with PKNOX2

4.5.1. Optimizing Co-Immunoprecipitation Protocol for Identifying Proteins Directly Interacting with PKNOX2

Firstly, the manufacturer's routine protocol was applied and pre-cleaning with magnetic beads at room temperature for one hour and incubation with anti-DDK magnetic beads overnight at 4°C were done and anti-DDK beads were loaded to gel together with proteins. Using anti-DDK primary antibody, PKNOX2-DDK protein was detected in PKNOX2:MSC Co-IP product (Figure 4.35. A). Traces of PKNOX2-DDK protein were also found in the flow-through of Co-IP reaction with PKNOX2:MSC protein and not with pCMV6:MSC lysates (Figure 4.35. A). Positive band for PKNOX2-DDK was only present in total protein from PKNOX2:MSCs and not from BM-MSCs or pCMV6:MSCs. BSA-DDK was used as positive control for Co-IP reaction. However, high levels of unspecific binding (i.e. near 25, 50, 100 and 150kDa) were obtained in all three Co-IP products (Figure 4.35. A).

Secondly, the manufacturer's routine protocol was re-applied but pre-cleaning with magnetic beads was performed at room temperature for two hours and

Co-IP products were separated from anti-DDK magnetic beads prior to SDS-PAGE. Using anti-PKNOX2 primary antibody, the PKNOX2-DDK protein was detected in PKNOX2:MSC Co-IP product (Figure 4.35. B). The PKNOX2-DDK protein band was not observed in the flow-through of Co-IP reactions. The PKNOX2-DDK was only present in total protein from PKNOX2:MSCs whereas endogenous PKNOX2 (70 kDa) was present in total proteins from all groups (Figure 4.35. B). Unspecific binding (i.e. near 25, 50, 100 and 150kDa) was also obtained in all three Co-IP products (Figure 4.35. B).

The above protocol (Figure 4.35. B) was re-applied but 5% BME was added to sample buffer after boiling and separating Co-IP products from the anti-DDK magnetic beads. 44.45 µg protein lysate was used per Co-IP reaction. Prior to the ECL reaction, membrane was additionally washed with 500nM NaCl containing wash buffer at room temperature for 5 minutes. Using anti-DDK primary antibody, PKNOX2-DDK protein was not detected in PKNOX2:MSC Co-IP products incubated with anti-DDK magnetic beads, but was observed in Co-IP products performed with control magnetic (pre-clean) beads (Figure 4.35. C). A low amount of PKNOX2-DDK protein was observed in the PKNOX2:MSC flow-through. A band for BSA-DDK was present, showing that the Co-IP reaction worked (Figure 4.35. C). A positive band for PKNOX2-DDK was only present in the total protein from PKNOX2:MSCs and not from control groups. Unspecific binding was mainly observed near 25, 50, 100 and 150kDa in all four Co-IP products (Figure 4.35. C).

Pre-cleaning of PKNOX2:MSC proteins with control magnetic beads was then extended to 4 or 16 hours at room temperature and Co-IP reaction was performed using anti-DDK magnetic beads or control beads as described above. 42.85 µg protein lysate was used per Co-IP reaction Using anti-DDK primary antibody, PKNOX2-DDK protein was detected in both PKNOX2:MSC Co-IP products (Figure 4.35. D). Traces of the protein were observed in Co-IP reactions with control magnetic beads and in the flow-through of Co-IP reactions (Figure 4.35. D). A positive band was detected for total protein from PKNOX2:MSCs, but not from pCMV6:MSCs. Background, as described above, was observed for all four Co-IP products (Figure 4.35. D).

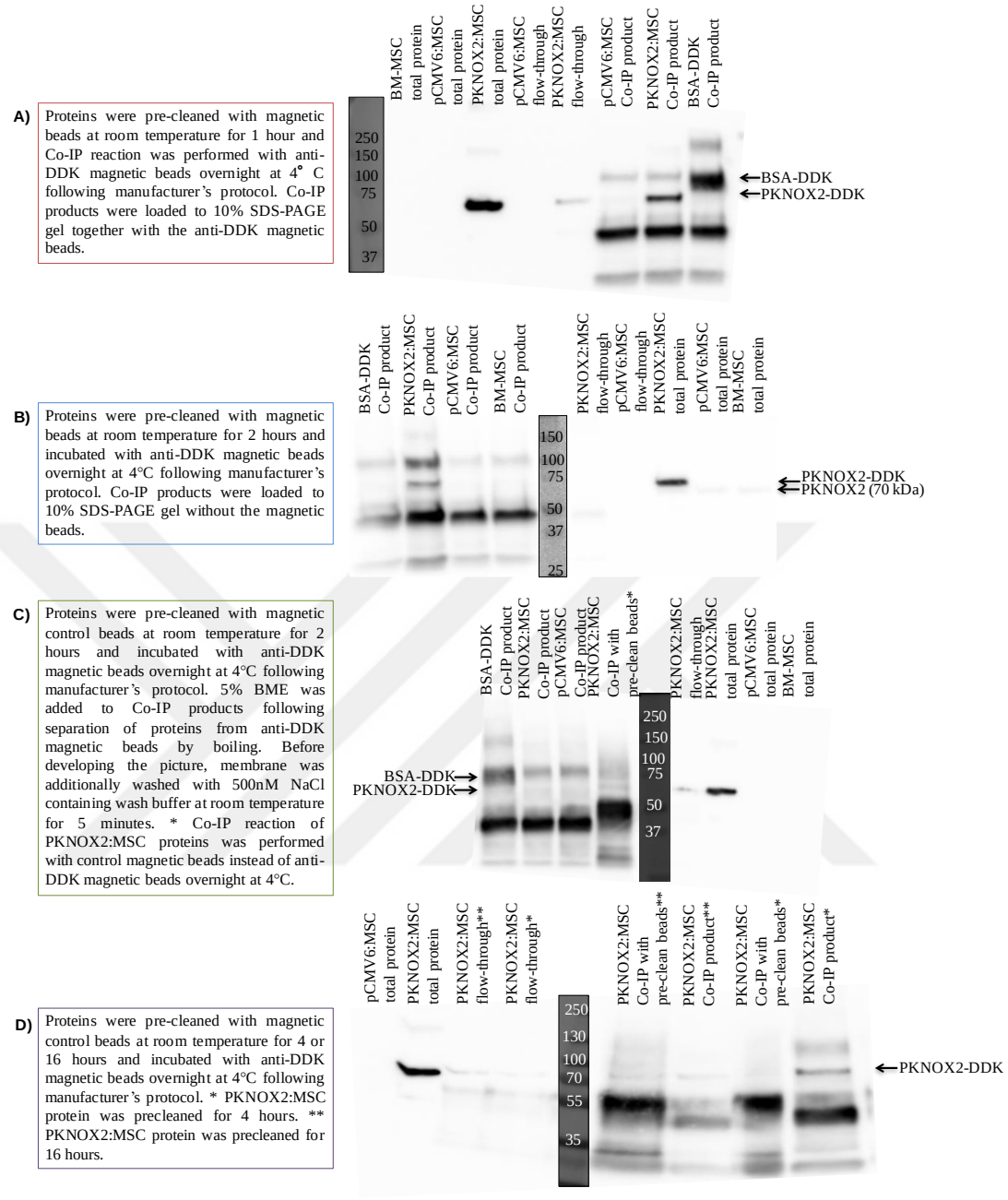

Figure 4.35. Optimization procedures applied to co-immunoprecipitation protocol (A-D).

Following Co-IP, interaction between FANCD2 and PKNOX2 proteins was assessed. The membrane shown in Figure 4.35. B was reblotted with anti-FANCD2 primary antibody (Figure 4.36. A). A positive band for FANCD2 was observed in total proteins from PKNOX2:MSC, pCMV6:MSC and BM-MSCs and no protein was detected in flow-through samples, as well as in BSA:DDK, pCMV6:MSC and BM-MSC Co-IP products. PKNOX2:MSC Co-IP product had a band corresponding

to FANCD2 molecular weight (150 kDa; Figure 4.36. A), which was also present as background signal after initial immunoblotting with anti-PKNOX2 primary antibody (Figure 4.36. B). Therefore, the experiment was repeated using a different set of lysates. 44.45 μg protein lysate was used per Co-IP reaction and immunoblotting was performed only with anti-FANCD2 antibody (Figure 4.36. B). FANCD2 protein was present in all total protein samples, but was not observed following Co-IP reaction of PKNOX2:DDK protein (Figure 4.36. B). Unspecific binding, which might be due to protein charges or interaction between hydrophobic surfaces, was still present (Figure 4.36. B). Therefore, mass-spectrometry analyses after Co-IP were performed to determine whether FANC proteins were among the PKNOX2 interactome.

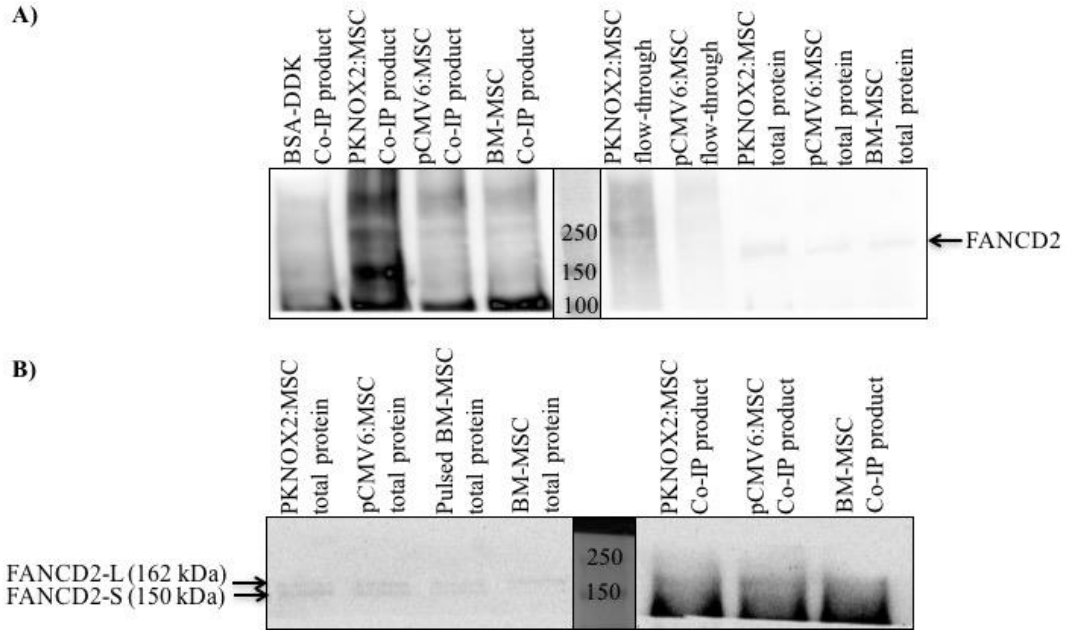

Figure 4.36. Following Co-IP, direct interaction between PKNOX2 and FANCD2 proteins was analysed. A) On 10% SDS-PAGE gel reblotted using anti-FANCD2 antibody, PKNOX2:MSC Co-IP product had a band corresponding to FANCD2 protein (150kDa) but was also previously present after first blotting with anti-PKNOX2 antibody (see Figure 4.35. B). B) SDS-PAGE gel blotted with only anti-FANCD2 antibody, showed no band for FANCD2 protein in neither of the Co-IP products.

4.5.2. Co-Immunoprecipitation Followed by Mass spectrometry Analysis to Identify PKNOX2 Interactome

Mass spectrometry analysis following co-immunoprecipitation of PKNOX2-DDK protein was used to identify proteins directly interacting with PKNOX2. Co-IP

products from pCMV6:MSC proteins were used as negative control. Three replicates of Co-IP products from either PKNOX2-DDK or pCMV6 carrying MSC (HUSCS-D11) protein extracts, were used for mass spectrometry. PKNOX2 protein was only detectable in mass spectrometry analysis of PKNOX2:MSCs Co-IP products (number of unique peptides= 4 and coverage= 17.58% in 'Run 1' and number of unique peptides= 7 and coverage= 13.56% in 'Rep 1'), but not in control (pCMV6:MSCs). 331 proteins in 'Run 1' and 317 proteins in 'Rep 1' were identified to interact with PKNOX2 while 227 in 'Run 1' and 272 in 'Rep 1' were detected to co-immunoprecipitate with control plasmid.

'Rep 1' and 'Run 1' lists were combined for both plasmids and analysed using Venny 2.1 software (412) to exclude proteins interacting with both plasmids or only with pCMV6-Entry plasmid (Figure 4.37. A). A total of 219 proteins was identified to be only interacting with PKNOX2-DDK. The coverage of mass spectrometry analyses for proteins only interacting with PKNOX2 ranged from 56.95% – 0.37%. FANCD2 protein and other FANC/BRCA pathway members were not identified as direct PKNOX2 interactors (data not shown).

Gene Ontology (GO) enrichment analyses (Analyses type: PANTHER Overrepresentation Test, released on 13/04/2017; Annotation version: GO Ontology database, released on 28/11/2017) were initially performed using a list of proteins only interacting with PKNOX2 (Figure 4.37. A) (413-415). Three of the 219 proteins were identified as uncharacterized protein or Ig kappa chain V regions, thus a total of 216 proteins were used. Parent GO terms for biological processes, molecular functions or PANTHER pathways involved by PKNOX2 interactors were listed in Table 4.7.-Table 4.9., respectively. PKNOX2 interacted with proteins that function mostly in binding to and processing ribosomal RNA and cytoskeletal proteins (i.e. vinculin) or polymers (i.e. actin filaments), as well as in forming structural integrity of the ribosome and cellular cytoskeleton (Table 4.7. and Table 4.8.). PKNOX2 associated proteins were also act in cadherin binding, GTP binding and nucleoside-triphosphatase activity (Table 4.8.). Additionally, they played a role in cytoskeletal regulation by Rho GTPase, integrin signaling pathway and inflammation mediated chemokine and cytokine signaling pathway (Table 4.9.).

Additionally, the analyses were repeated for unspecifically bound proteins (Figure 4.37. A and Table 4.10.-Table 4.12.). 344 out of 347 unspecifically bound proteins were used for these analyses among which three of them were determined as Ig kappa or heavy chain V regions. Like PKNOX2 interactors, unspecifically bound proteins were found to act in ribosomal large subunit biogenesis, SRP-dependent cotranslational protein targeting to membrane, viral transcription, translational initiation, rRNA processing and cytoskeleton organization (Table 4.10.). PKNOX2 interactors had a role in the ribosomal large unit assembly (Table 4.7.), which is a subclass of ribosomal large subunit biogenesis involved by unspecific proteins (Table 4.10.). Additionally, the fold enrichment (FE) of PKNOX2 interactors involved in ribosomal large unit assembly (FE= 20.43; Table 4.7.) was higher than unspecific proteins (FE= 9.58; Table 4.10.). Unspecifically bound proteins were also identified to play a role in molecular (Table 4.11.) and PANTHER pathways (Table 4.12.) similar to PKNOX2 interactors (Table 4.8. and Table 4.9., respectively).

28 proteins were identified to be shared between ‘Rep 1’ and ‘Run 1’ lists of PKNOX2 (Figure 4.37. B), and none of the FANC proteins were among them. These proteins were further analysed via HitPredict software (Figure 4. 37. C) to construct a more detailed interaction network (416-418). Specific accession numbers obtained from mass spectrometry analyses were used as identifiers and no interactions were found for 5 proteins. Proteins interacting with PKNOX2 interactors were identified to regulate hematopoietic stem cell differentiation, negatively regulate of G2/M transition of mitotic cell cycle as well as involved in double-strand break repair via NHEJ (Table 4.13.; cut-off value is $P \leq 0.001$ and FE ≥ 5).

Protein list obtained from proteomic profiling of undifferentiated human bone marrow stromal cells (419) was used as a reference to determine which of the proteins interacting with PKNOX2 interactors were expressed in these cells (Figure 4.37. D). 39.5% (n= 486) of the proteins identified using HitPredict software (n= 1230) were found in bone marrow stromal cells (Figure 4.37. D). Further enrichment of proteins increased the fold expansion (Table 4.14.; cut-off value is $P \leq 0.001$ and FE ≥ 5) of previously mentioned biological processes; regulation of hematopoietic stem cell differentiation (FE= 17.92) and negative regulation of G2/M transition of

mitotic cell cycle (FE= 12.11). The interactors of PKNOX2 interacting proteins, expressed by the bone marrow stromal cells, were also involved in double-strand break repair via NHEJ (FE= 8.14) but the P-value (5.74E-03) was slightly higher than the threshold ($P \leq 0.001$).

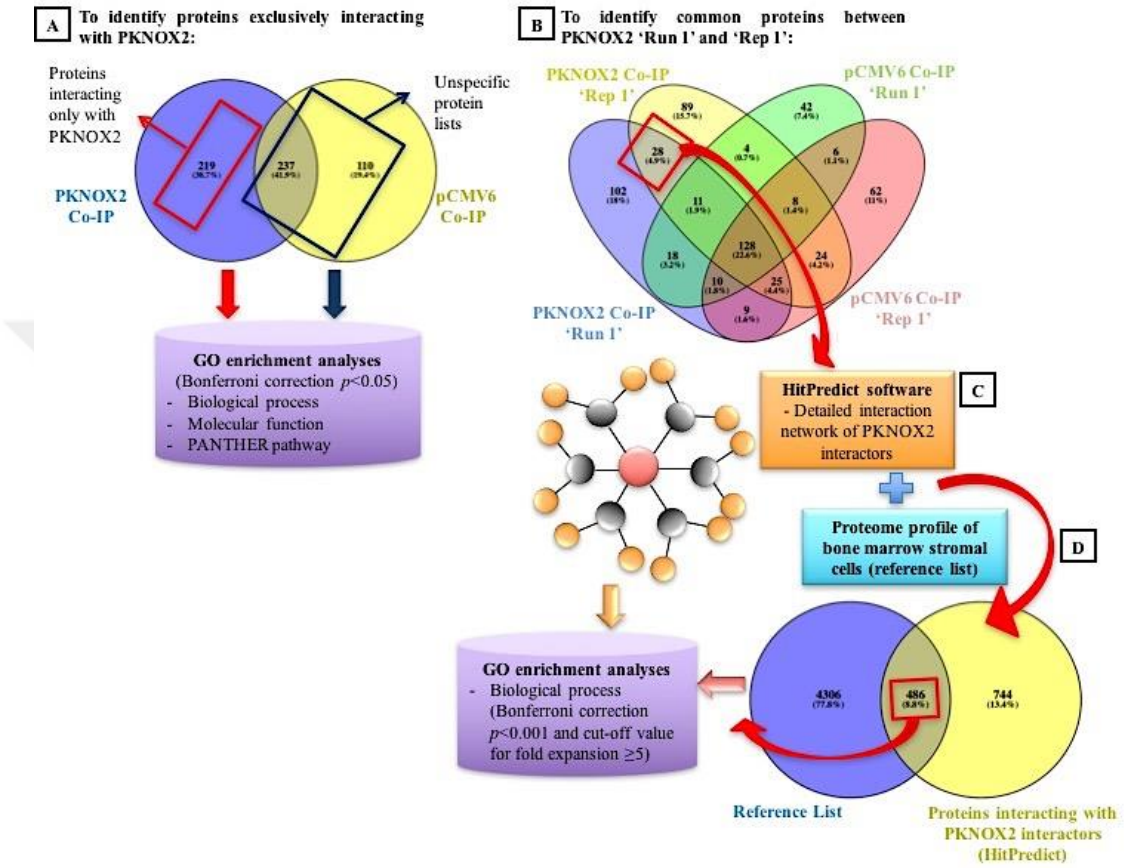

Figure 4.37. Overview of follow-up analyses of proteome data. A) Schematic workflow for identifying biological processes, molecular function and PANTHER pathways associated with only PKNOX2 interactors via GO enrichment analyses. A total of 219 were identified to interact exclusively with PKNOX2-DDK. B) 28 proteins were identified to be shared between PKNOX2 'Run 1' and 'Rep 1'. HitPredict software was used to identify proteins interacting with PKNOX2 interactors. A total of 1230 different proteins were identified and C) biological processes related to these proteins were determined. D) Proteins interacting with PKNOX2 interactors were further enriched to identify ones expressed in bone marrow stromal cells using a previously published data set (depicted as Reference list) (419). 486 out of 1230 proteins interacting with PKNOX2 interactors were determined to be expressed by bone marrow stromal cells. GO enrichment analyses was repeated to identify biological processes played by proteins interacting with PKNOX2 interactors and also expressed by bone marrow stromal cells.

Table 4.7. Proteins directly interacting with PKNOX2 were involved in variety of biological processes.

	Homo sapiens Reference List	**Uploaded List**				
GO Biological Process Complete	**#**	**#**	**Expected**	**Fold Enrichment**	**+/-**	**P-value**
ribosomal large subunit assembly	30	6	.29	20.43	+	5.61E-03
SRP-dependent cotranslational protein targeting to membrane	93	17	.91	18.67	+	1.14E-12
viral transcription	114	17	1.12	15.23	+	3.03E-11
nuclear-transcribed mRNA catabolic process, nonsense-mediated decay	119	17	1.17	14.59	+	6.02E-11
translational initiation	143	20	1.40	14.29	+	3.43E-13
Regulation of lamellipodium organization	43	6	0.42	14.16	+	4.53E-02
rRNA processing	259	18	2.54	7.10	+	1.31E-06
cytoskeleton organization	962	35	9.42	3.72	+	2.07E-07
actin filament-based process	503	18	4.92	3.66	+	2.53E-02

Table 4.7. (Continued) Proteins directly interacting with PKNOX2 were involved in variety of biological processes.

	Homo sapiens Reference List	**Uploaded List**				
GO Biological Process Complete	**#**	**#**	**Expected**	**Fold Enrichment**	**+/-**	**P-value**
regulation of biological quality	3622	62	35.46	1.75	+	3.35E-02
Unclassified	3676	9	35.99	.25	-	0.00E00

Homo sapiens reference list, are the genes known to play a role in a particular pathway and are used as reference list of GO; Uploaded list, are genes uploaded by the user; Uploaded list #, total number of genes known to play a role in a particular pathway; Expected, number of genes expected to be in a pathway over whole genome; Fold enrichment, ratio of number of observed genes over number of expected genes; +/-, Fold enrichment is depicted as '-' if the value is less than 1 whereas it is depicted as '+' if the value is bigger than >1; P-value, is the probability of uploaded gene list to be found within genes of a particular pathway and $P< 0.05$ is considered statistical significant (413-415).

Table 4.8. Molecular function of proteins directly interacting with PKNOX2.

	Homo sapiens Reference List	Uploaded List				
GO Molecular Function Complete	**#**	**#**	**Expected**	**Fold Enrichment**	**+/-**	**P-value**
vinculin binding	11	4	.11	37.14	+	1.57E-02
rRNA binding	60	7	.59	11.92	+	8.28E-03
structural constituent of ribosome	169	17	1.65	10.28	+	5.57E-09
actin filament binding	161	13	1.58	8.25	+	3.23E-05
structural constituent of cytoskeleton	108	8	1.06	7.57	+	4.32E-02
cadherin binding	295	15	2.89	5.19	+	9.37E-04
GTP binding	383	15	3.75	4.00	+	2.22E-02
nucleoside-triphosphatase activity	834	25	8.16	3.06	+	2.58E-03
Unclassified	3666	12	35.89	.33	-	0.00E00

Homo sapiens reference list, are the genes known to play a role in a particular pathway and are used as reference list of GO; Uploaded list, are genes uploaded by the user; Uploaded list #, total number of genes known to play a role in a particular pathway; Expected, number of genes expected to be in a pathway over whole genome; Fold enrichment, ratio of number of observed genes over number of expected genes; +/-, Fold enrichment is depicted as '-' if the value is less than 1 whereas it is depicted as '+' if the value is bigger than >1; P-value, is the probability of uploaded gene list to be found within genes of a particular pathway and $P < 0.05$ is considered statistical significant (413-415).

Table 4.9. Proteins interacting with PKNOX2 play roles in three of PANTHER pathways.

	Homo sapiens Reference List	**Uploaded List**				
PANTHER Pathways	**#**	**#**	**Expected**	**Fold Enrichment**	**+/-**	**P-value**
Cytoskeletal regulation by Rho GTPase	80	9	.78	11.49	+	2.05E-05
Huntington disease	135	8	1.32	6.05	+	1.03E-02
Integrin signaling pathway	162	9	1.59	5.67	+	5.91E-03
Inflammation mediated by chemokine and cytokine signaling pathway	230	10	2.25	4.44	+	1.67E-02

Homo sapiens reference list, are the genes known to play a role in a particular pathway and are used as reference list of GO; Uploaded list, are genes uploaded by the user; Uploaded list #, total number of genes known to play a role in a particular pathway; Expected, number of genes expected to be in a pathway over whole genome; Fold enrichment, ratio of number of observed genes over number of expected genes; +/-, Fold enrichment is depicted as '-' if the value is less than 1 whereas it is depicted as '+' if the value is bigger than >1; P-value, is the probability of uploaded gene list to be found within genes of a particular pathway and $P< 0.05$ is considered statistical significant (413-415).

Table 4.10. GO Biological processes enriched for unspecific protein lists.

	Homo sapiens Reference List	**Uploaded List**				
GO Biological Process Complete	**#**	**#**	**Expected**	**Fold Enrichment**	**+/-**	**P-value**
cytoskeletal anchoring at plasma membrane	10	5	.16	30.50	+	7.25E-03
SRP-dependent cotranslational protein targeting to membrane	93	40	1.52	26.23	+	5.75E-39
nuclear-transcribed mRNA catabolic process, nonsense-mediated decay	119	41	1.95	21.01	+	3.22E-36
viral transcription	114	39	1.87	20.87	+	3.53E-34
cytoplasmic translation	46	15	.75	19.89	+	3.59E-11
translational initiation	143	45	2.34	19.19	+	2.19E-38
collagen fibril organization	42	10	.69	14.52	+	2.73E-05
tRNA aminoacylation for protein translation	49	10	.80	12.45	+	1.15E-04
intermediate filament cytoskeleton organization	41	8	.67	11.90	+	4.60E-03
peptide cross-linking	59	10	.97	10.34	+	6.39E-04
rRNA processing	259	41	4.25	9.65	+	3.11E-23
ribosomal large subunit biogenesis	70	11	1.15	9.58	+	3.04E-04

Table 4.10. (Continued) GO Biological processes enriched for unspecific protein lists.

	Homo sapiens Reference List	**Uploaded List**				
GO Biological Process Complete	**#**	**#**	**Expected**	**Fold Enrichment**	**+/-**	**P-value**
collagen catabolic process	65	10	1.07	9.38	+	1.54E-03
homotypic cell-cell adhesion	53	8	.87	9.21	+	3.03E-02
Cornification	113	17	1.85	9.18	+	1.10E-07
osteoblast differentiation	121	16	1.98	8.06	+	2.82E-06
protein heterooligomerization	103	13	1.69	7.70	+	2.23E-04
cell junction assembly	139	16	2.28	7.02	+	1.99E-05
protein stabilization	159	15	2.61	5.75	+	8.21E-04
negative regulation of protein ubiquitination	140	12	2.30	5.23	+	4.15E-02
neutrophil degranulation	482	41	7.90	5.19	+	1.47E-13
platelet activation	142	12	2.33	5.15	+	4.78E-02
regulation of mRNA stability	154	13	2.52	5.15	+	1.97E-02
regulation of organelle assembly	157	13	2.57	5.05	+	2.43E-02

Table 4.10. (Continued) GO Biological processes enriched for unspecific protein lists.

	Homo sapiens Reference List	Uploaded List				
GO Biological Process Complete	**#**	**#**	**Expected**	**Fold Enrichment**	**+/-**	**P-value**
protein folding	234	18	3.84	4.69	+	8.90E-04
regulation of protein polymerization	187	14	3.07	4.57	+	3.19E-02
Phagocytosis	242	18	3.97	4.54	+	1.45E-03
regulation of supramolecular fiber organization	307	20	5.03	3.97	+	2.40E-03
actin cytoskeleton organization	430	27	7.05	3.83	+	4.09E-05
regulation of actin filament-based process	340	20	5.57	3.59	+	1.14E-02
cell division	488	26	8.00	3.25	+	1.92E-03
cellular response to growth factor stimulus	472	24	7.74	3.10	+	1.27E-0
response to toxic substance	499	25	8.18	3.06	+	9.91E-03
microtubule-based process	581	27	9.53	2.83	+	1.50E-02
cell morphogenesis	632	28	10.36	2.70	+	2.36E-02
positive regulation of organelle organization	620	27	10.17	2.66	+	4.87E-02
response to organonitrogen compound	881	38	14.44	2.63	+	7.01E-04

Table 4.10. (Continued) GO Biological processes enriched for unspecific protein lists.

	Homo sapiens Reference List	**Uploaded List**				
GO Biological Process Complete	**#**	**#**	**Expected**	**Fold Enrichment**	**+/-**	**P-value**
regulation of anatomical structure morphogenesis	968	40	15.87	2.52	+	9.53E-04
negative regulation of apoptotic process	851	33	13.95	2.37	+	5.00E-02
cellular response to endogenous stimulus	1105	42	18.12	2.32	+	4.09E-03
response to oxygen-containing compound	1444	54	23.68	2.28	+	1.29E-04
plasma membrane bounded cell projection organization	1039	38	17.04	2.23	+	3.65E-02
movement of cell or subcellular component	1424	51	23.35	2.18	+	1.30E-03
regulation of localization	2603	75	42.68	1.76	+	6.97E-03
Unclassified	3676	11	60.27	< 0.2	-	0.00E00

Homo sapiens reference list, are the genes known to play a role in a particular pathway and are used as reference list of GO; Uploaded list, are genes uploaded by the user; Uploaded list #, total number of genes known to play a role in a particular pathway; Expected, number of genes expected to be in a pathway over whole genome; Fold enrichment, ratio of number of observed genes over number of expected genes; +/-, Fold enrichment is depicted as '-' if the value is less than 1 whereas it is depicted as '+' if the value is bigger than >1; P-value, is the probability of uploaded gene list to be found within genes of a particular pathway and $P< 0.05$ is considered statistical significant (413-415).

Table 4.11. GO molecular function enriched for unspecific protein lists.

	Homo sapiens Reference List	**Uploaded List**				
GO Molecular Function Complete	**#**	**#**	**Expected**	**Fold Enrichment**	**+/-**	**P-value**
platelet-derived growth factor binding	11	5	.18	27.72	+	4.19E-03
disordered domain specific binding	31	9	.51	17.71	+	1.13E-05
structural constituent of ribosome	169	40	2.77	14.44	+	1.69E-29
aminoacyl-tRNA ligase activity	45	10	.74	13.55	+	1.90E-05
structural constituent of cytoskeleton	108	23	1.77	12.99	+	6.01E-15
cadherin binding	295	58	4.84	11.99	+	7.85E-40
cell-cell adhesion mediator activity	31	6	.51	11.80	+	4.71E-02
rRNA binding	60	11	.98	11.18	+	2.34E-05
double-stranded RNA binding	67	11	1.10	10.01	+	7.13E-05
actin filament binding	161	20	2.64	7.58	+	1.86E-08
extracellular matrix structural constituent	78	9	1.28	7.04	+	2.34E-02
mRNA binding	197	17	3.23	5.26	+	1.48E-04
GTPase activity	291	20	4.77	4.19	+	3.80E-04
GTP binding	383	25	6.28	3.98	+	2.67E-05

Table 4.11. (Continued) GO molecular function enriched for unspecific protein lists.

	Homo sapiens Reference List	**Uploaded List**				
GO Molecular Function Complete	**#**	**#**	**Expected**	**Fold Enrichment**	**+/-**	**P-value**
ATPase activity, coupled	364	19	5.97	3.18	+	4.05E-02
protein kinase binding	576	28	9.44	2.96	+	1.46E-03
identical protein binding	1683	64	27.59	2.32	+	8.42E-07
adenyl ribonucleotide binding	1534	48	25.15	1.91	+	4.47E-02
drug binding	1757	54	28.81	1.87	+	2.01E-02
transmembrane signaling receptor activity	1271	4	20.84	< 0.2	-	1.74E-02
Unclassified	3666	8	60.11	< 0.2	-	0.00E00

Homo sapiens reference list, are the genes known to play a role in a particular pathway and are used as reference list of GO; Uploaded list, are genes uploaded by the user; Uploaded list #, total number of genes known to play a role in a particular pathway; Expected, number of genes expected to be in a pathway over whole genome; Fold enrichment, ratio of number of observed genes over number of expected genes; +/-, Fold enrichment is depicted as '-' if the value is less than 1 whereas it is depicted as '+' if the value is bigger than >1; P-value, is the probability of uploaded gene list to be found within genes of a particular pathway and $P < 0.05$ is considered statistical significant (413-415).

Table 4.12. PANTHER pathways enriched for unspecific protein lists.

	Homo sapiens Reference List	**Uploaded List**				
PANTHER Pathways	**#**	**#**	**Expected**	**Fold Enrichment**	**+/-**	**P-value**
Glycolysis	20	5	.33	15.25	+	3.68E-03
Cytoskeletal regulation by Rho GTPase	80	11	1.31	8.39	+	2.07E-05
Integrin signaling pathway	162	13	2.66	4.89	+	6.16E-04
Huntington disease	135	10	2.21	4.52	+	1.54E-02
Unclassified	18605	277	305.04	.91	-	0.00E00
Glycolysis	20	5	.33	15.25	+	3.68E-03

Homo sapiens reference list, are the genes known to play a role in a particular pathway and are used as reference list of GO; Uploaded list, are genes uploaded by the user; Uploaded list #, total number of genes known to play a role in a particular pathway; Expected, number of genes expected to be in a pathway over whole genome; Fold enrichment, ratio of number of observed genes over number of expected genes; +/-, Fold enrichment is depicted as '-' if the value is less than 1 whereas it is depicted as '+' if the value is bigger than >1; P-value, is the probability of uploaded gene list to be found within genes of a particular pathway and $P< 0.05$ is considered statistical significant (413-415).

Table 4.13. GO Biological processes enriched for proteins interacting with PKNOX2 interactors.

	Homo sapiens Reference List	**Uploaded List**				
GO Biological Process Complete	**#**	**#**	**Expected**	**Fold Enrichment**	**+/-**	**P-value**
DNA replication-dependent nucleosome assembly	10	9	.58	15.60	+	9.79E-05
histone H3 deacetylation	21	14	1.21	11.56	+	4.43E-07
negative regulation of telomere maintenance via telomerase	21	11	1.21	9.08	+	5.71E-04
regulation of hematopoietic stem cell differentiation	77	39	4.44	8.78	+	6.24E-20
regulation of transcription from RNA polymerase II promoter in response to hypoxia	79	37	4.56	8.12	+	1.15E-17
regulation of cellular amino acid metabolic process	62	29	3.58	8.11	+	2.70E-13
NIK/NF-kappaB signaling	86	40	4.96	8.06	+	3.42E-19
negative regulation of ubiquitin-protein ligase activity involved in mitotic cell cycle	72	33	4.15	7.94	+	3.26E-15
anaphase-promoting complex-dependent catabolic process	81	37	4.67	7.92	+	2.61E-17
positive regulation of ubiquitin-protein ligase activity involved in regulation of mitotic cell cycle transition	77	35	4.44	7.88	+	3.57E-16

Table 4.13. (Continued) GO Biological processes enriched for proteins interacting with PKNOX2 interactors.

	Homo sapiens Reference List	**Uploaded List**				
GO Biological Process Complete	**#**	**#**	**Expected**	**Fold Enrichment**	**+/-**	**P-value**
SCF-dependent proteasomal ubiquitin-dependent protein catabolic process	73	32	4.21	7.60	+	3.92E-14
negative regulation of G2/M transition of mitotic cell cycle	89	36	5.13	7.01	+	4.09E-15
double-strand break repair via nonhomologous end joining	53	21	3.06	6.87	+	1.27E-07
stimulatory C-type lectin receptor signaling pathway	123	48	7.10	6.76	+	2.40E-20
DNA replication-independent nucleosome assembly	39	15	2.25	6.67	+	1.46E-04
antigen processing and presentation of exogenous peptide antigen via MHC class I, TAP-dependent	76	29	4.38	6.61	+	4.62E-11
positive regulation of gene expression, epigenetic	55	20	3.17	6.30	+	1.68E-06
Fc-epsilon receptor signaling pathway	135	49	7.79	6.29	+	1.67E-19

Table 4.13. (Continued) GO Biological processes enriched for proteins interacting with PKNOX2 interactors.

	Homo sapiens Reference List	Uploaded List				
GO Biological Process Complete	**#**	**#**	**Expected**	**Fold Enrichment**	**+/-**	**P-value**
regulation of megakaryocyte differentiation	51	18	2.94	6.12	+	2.10E-05
Wnt signaling pathway, planar cell polarity pathway	101	35	5.83	6.01	+	1.29E-12
tumor necrosis factor-mediated signaling pathway	129	44	7.44	5.91	+	2.99E-16
regulation of histone acetylation	53	18	3.06	5.89	+	3.78E-05
response to gamma radiation	56	19	3.23	5.88	+	1.44E-05
regulation of mRNA stability	154	49	8.88	5.51	+	3.76E-17
T cell receptor signaling pathway	155	49	8.94	5.48	+	4.89E-17
activation of MAPKK activity	54	17	3.12	5.46	+	2.96E-04
ATP-dependent chromatin remodeling	67	21	3.87	5.43	+	8.20E-06
histone lysine methylation	68	21	3.92	5.35	+	1.06E-05
positive regulation of canonical Wnt signaling pathway	124	37	7.15	5.17	+	1.75E-11

Table 4.13. (Continued) GO Biological processes enriched for proteins interacting with PKNOX2 interactors.

	Homo sapiens Reference List	**Uploaded List**				
GO Biological Process Complete	**#**	**#**	**Expected**	**Fold Enrichment**	**+/-**	**P-value**
regulation of intracellular steroid hormone receptor signaling pathway	75	22	4.33	5.08	+	1.09E-05

Homo sapiens reference list, are the genes known to play a role in a particular pathway and are used as reference list of GO; Uploaded list, are genes uploaded by the user; Uploaded list #, total number of genes known to play a role in a particular pathway; Expected, number of genes expected to be in a pathway over whole genome; Fold enrichment, ratio of number of observed genes over number of expected genes; +/-, Fold enrichment is depicted as '-' if the value is less than 1 whereas it is depicted as '+' if the value is bigger than >1; P-value, is the probability of uploaded gene list to be found within genes of a particular pathway and $P< 0.001$ is considered statistical significant (413-415).

Table 4.14. GO Biological processes enriched for proteins interacting with PKNOX2 interactors and expressed by bone marrow stromal cells.

	Homo sapiens Reference List	**Uploaded List**				
GO Biological Process Complete	**#**	**#**	**Expected**	**Fold Enrichment**	**+/-**	**P-value**
positive regulation of RNA polymerase II transcriptional preinitiation complex assembly	10	7	.23	30.18	+	4.85E-05
regulation of hematopoietic stem cell differentiation	77	32	1.79	17.92	+	2.63E-25
regulation of cellular amino acid metabolic process	62	24	1.44	16.69	+	1.29E-17
negative regulation of ubiquitin-protein ligase activity involved in mitotic cell cycle	72	25	1.67	14.97	+	2.39E-17
SCF-dependent proteasomal ubiquitin-dependent protein catabolic process	73	25	1.69	14.77	+	3.31E-17
positive regulation of ubiquitin-protein ligase activity involved in regulation of mitotic cell cycle transition	77	26	1.79	14.56	+	7.53E-18
NIK/NF-kappaB signaling	86	29	1.99	14.54	+	3.38E-20
anaphase-promoting complex-dependent catabolic process	81	27	1.88	14.37	+	1.70E-18

Table 4.14. (Continued) GO Biological processes enriched for proteins interacting with PKNOX2 interactors and expressed by bone marrow stromal cells.

	Homo sapiens Reference List	**Uploaded List**				
GO Biological Process Complete	**#**	**#**	**Expected**	**Fold Enrichment**	**+/-**	**P-value**
regulation of transcription from RNA polymerase II promoter in response to hypoxia	79	26	1.83	14.19	+	1.41E-17
antigen processing and presentation of exogenous peptide antigen via MHC class I, TAP-dependent	76	23	1.76	13.05	+	1.81E-14
negative regulation of G2/M transition of mitotic cell cycle	89	25	2.06	12.11	+	3.34E-15
regulation of mRNA stability	154	39	3.57	10.92	+	1.31E-23
Wnt signaling pathway, planar cell polarity pathway	101	25	2.34	10.67	+	6.13E-14
stimulatory C-type lectin receptor signaling pathway	123	30	2.85	10.52	+	4.45E-17
Fc-epsilon receptor signaling pathway	135	31	3.13	9.90	+	5.36E-17
positive regulation of canonical Wnt signaling pathway	124	28	2.88	9.74	+	6.56E-15
positive regulation of gene expression, epigenetic	55	12	1.28	9.41	+	9.29E-05
tumor necrosis factor-mediated signaling pathway	129	28	2.99	9.36	+	1.78E-14
regulation of megakaryocyte differentiation	51	11	1.18	9.30	+	4.26E-04

Table 4.14. (Continued) GO Biological processes enriched for proteins interacting with PKNOX2 interactors and expressed by bone marrow stromal cells.

	Homo sapiens Reference List	Uploaded List				
GO Biological Process Complete	**#**	**#**	**Expected**	**Fold Enrichment**	**+/-**	**P-value**
T cell receptor signaling pathway	155	32	3.59	8.90	+	2.69E-16
DNA duplex unwinding	75	14	1.74	8.05	+	3.95E-05
negative regulation of canonical Wnt signaling pathway	167	29	3.87	7.49	+	1.39E-12
regulation of mRNA splicing, via spliceosome	79	13	1.83	7.10	+	5.94E-04
Fc-gamma receptor signaling pathway involved in phagocytosis	86	14	1.99	7.02	+	2.13E-04
protein deubiquitination	286	43	6.63	6.48	+	1.20E-17
translational initiation	143	18	3.32	5.43	+	1.13E-04
MAPK cascade	374	45	8.67	5.19	+	6.33E-15
viral process	654	76	15.17	5.01	+	1.46E-26

Homo sapiens reference list, are the genes known to play a role in a particular pathway and are used as reference list of GO; Uploaded list, are genes uploaded by the user; Uploaded list #, total number of genes known to play a role in a particular pathway; Expected, number of genes expected to be in a pathway over whole genome; Fold enrichment, ratio of number of observed genes over number of expected genes; +/-, Fold enrichment is depicted as '-' if the value is less than 1 whereas it is depicted as '+' if the value is bigger than >1; P-value, is the probability of uploaded gene list to be found within genes of a particular pathway and $P< 0.001$ is considered statistical significant (413-415).

5. DISCUSSION

More than a decade on, the interaction between HSCs and their niche has been widely studied, but there are still unanswered questions about the stromal cell components of the BM microenvironment. Stroma is not only important for HSC maintenance, but also can trigger changes in cellular identity. Therefore, it is critical to study stromal cells such as BM-MSCs under genome instable conditions, which may help us to gain more understanding on their role of tissue support as well as progression of cancers like leukemia. The initial objective of this thesis was to characterize BM-MSCs obtained from FA patients in comparison to healthy donors.

5.1. Characterization of Bone Marrow Mesenchymal Stromal/Stem Cells from Fanconi Anemia Patients Compared to Donors

Herein, eleven of the FA patients were molecularly profiled to identify their mutations. Molecular classification of one subject showed no mutation in *FANC-A, -B, -C, -D2, -E, -F, -G, -I, -L, -M, BRCA1, BRCA2, BRIP1, ERCC4, PALB2, RAD51* or *SLX4* gene, which might result from technical difficulties, such as poor sequencing coverage or participation of other FA causing genes. Overall, six of the identified mutations of which five in *FANCA* and one in *FANCD2* were novel. Most of the classified cases had pathogenic variations in *FANCA* gene (n= 7), which is reported as the most frequently mutated FA gene (420). Two patients with negative DEB-test results had mutations in FANCA gene. This might be explained by reverse mosaicism seen in lymphocytes (241-243). Additionally, one individual had mutation in *FANCG* gene, while two siblings were identified to carry mutated *FANCD2* gene. Studies carried out in humans, as well as, in animal models report that mutations in *FANCD2* have severe phenotypes (421-423). In humans, mutations classified to FA-D2 complementation group are only hypomorphic suggesting biallelic null mutations are sufficient to cause death (423). Patients with mutated *FANCD2* have various congenital anomalies and hematological defects (423). In this study, FA-D2 patients possessed typical disease symptoms, including microcephaly, hyper/hypopigmentation, growth retardation and microphthalmia.

BM-MSCs from FA patients and donors were characterized according to their immunophenotypes, differentiation potentials, proliferative capacities, senescence activity, ROS production and TGF-β levels. Various cell surface markers indicating mesenchymal (CD29, CD44, CD73, CD90, CD105, CD140b, CD146, CD166, HLA-ABC, CD106, CD200, CD271), endothelial (CD31 and CD144) or hematopoietic (CD34, CD14, CD45, and HLA-DR) origin, as well as CD133, as general stem cell marker were used in this study. BM-MSCs were positive for CD29, CD44, CD73, CD90, CD105, CD166, CD140b and HLA-ABC surface markers, in line with previously published data (59, 424-426). Cells did not consistently express CD146, as previously shown (427). Additionally, cells had low or no CD106, CD200 and CD271 levels. Culturing MSCs triggers downregulation of CD106 level (428). Intriguingly, CD106 level of FA BM-MSCs was slightly higher than donors. CD106 is an adhesion molecule that plays an important role in HSC maintenance within the niche (429). Increase in CD106 expression may keep HSCs in dormancy and decrease the number of cycling HSCs. BM-MSCs had no CD31, CD144, CD34, CD14, CD45, HLA-DR and CD133 expression. This is in concordance with the previously published data (59, 424, 430-433). FA BM-MSCs had similar cell surface marker level, as donors, as previously described (32, 33). Notably, the mesenchymal marker CD29 (β1-integrin) level of patient cells was significantly higher than donors. CD29 is important to maintain migration of MSCs (434, 435). Additionally, β1-integrin expressed by osteoblastic niche is important for adhesion of HSCs to the niche, thus help to keep HSCs in quiescence (104). Elevated CD29 expression in FA BM may apply as a physical force that keeps HSCs to stay in dormancy and consequently decrease their ability to expand or differentiate. Further investigation is required to elucidate whether dysregulation of CD29 plays a role in FA pathogenesis. Besides CD200 (OX-2) expression by FA BM-MSCs was lower than donors. CD200 receptor (CD200R) is only expressed by myeloid-lineage cells and the interaction between CD200-CD200R inhibits TNF-α secretion by macrophage like cells (436). *Fancc*$^{-/-}$ mice cells are sensitive towards TNF-α and ROS levels are shown to increase due to TNF-α treatment, which may then initiate ICL formation and consequently may cause unresolved DNA damage (253). We also showed that ROS production was higher in FA BM-MSCs compared to donors. TNF-α increase in the

FA bone marrow environment may be a consequence of lower CD200 expression of FA BM-MSCs (252).

Adipogenic and osteogenic differentiation capacities of FA and donor BM-MSCs were obtained using histochemical staining, as well as, RT-qPCR analysis measuring the change in expression of differentiation-specific genes such as *Adipsin, PPARγ, LPL, RUNX2, ALPL, OCN* and *SP7*. Differentiation potential varied a lot and BM-MSCs had higher tendency to commit to adipogenic lineages compared to osteogenic lineages. An inverse relationship between osteogenic and adipogenic differentiation is reported and MSCs triggered via steady-state signaling pathways can be more potent towards differentiating into a certain lineage (437). Fold change in *Adipsin* and *PPARγ* gene expression increased following adipogenic stimulation, but were lower than the increased fold change measured for *LPL* expression. Graneli and co-authors (438) show that *LPL* and *PPARγ* gene expression levels are upregulated following 14 days post-adipogenic induction and also the increase in *LPL* expression was more prominent. Fold change in the expression of osteogenesis-related genes, *RUNX2, ALPL, OCN* and *SP7* was low. Increase in *RUNX2* or *ALPL* gene expression following induction was more promising compared to change in *OCN* and *SP7* genes. Our results in correlation with Gulliot and colleagues (439) show similar *RUNX2* and *ALPL* gene expression on day 21 of osteogenic induction. Unlike our findings, *OCN* and *SP7* gene expression are revealed to increase continuously following differentiation (439). Miron and Zhang (440) point out that OCN is a marker of mature osteoblasts and is not expressed by pre-osteoblasts. Based on these findings, we were most probably able to differentiate BM-MSCs to pre-osteoblasts. Low *OCN* and *SP7* expression obtained in this study may increase as a result of extended culture period in osteogenic medium. Additionally, BM-MSCs from FA patients and donors had comparable differentiation capacities as previously shown. However, a recent study report that FA MSCs lack osteogenic differentiation potential (33, 441). Impairment of osteoblastic function can trigger MDS and AML, thus defective BM (270).

ICL-inducing reagents, such as MMC and DEB cause chromosomal aberrations, genomic instability and consequently cellular toxicity in cells with non-

functional FA pathway (224, 225, 442). Additionally, MMC treatment is reported to cause a cell cycle arrest in dermal fibroblasts from FA patients, as well as, in Brca1$^{-/-}$ mouse embryonic fibroblasts (233, 442). BM-MSCs from FA patients are reported to be hypersensitive to MMC treatment (32). Mantelli and co-authors (33) characterized BM-MSCs with prolonged G2 transition as well as having spontaneous chromosomal breaks that were not upregulated after DEB treatment. Insensitivity of MSCs to DEB treatment can be explained by their resistance towards cytotoxic agents (443). Here, FA BM-MSCs treated with 0.1μg/ml DEB for four days were arrested in G2/M phase. The frequency of FA BM-MSCs in G1 phase was decreased, whereas there was no change in the number of cells within S-phase following DEB treatment. In the report by Mantelli *et al* (33), the incubation of BM-MSCs with DEB is 59 hours, which is shorter than the period used in this study. Therefore, exposure for longer periods of time may be required until the cellular failure due to DEB treatment occurs. Genomic instability in FA BM-MSCs may also make the arrest in G2/M phase apparent.

Proliferation of FA BM-MSCs was compared to donors between passage 3 to 7 using population doubling assay. BM-MSCs from both FA-A and FA-G patients had similar but from FA-D2 patients had lower proliferative capacity compared with donors. Proliferative capacity of FA and donor BM-MSCs were also compared in terms of doubling time and were found to be similar. In a previous report, *FANCA*-deficient and donor cells are shown to have comparable cPD between passages 1 to 5 (33). *FANCA*-deficient and donor BM-MSCs used in this study had similar senescence activity and were expanded until passages 8-10 and passages 7-11, respectively. However, Mantelli *et al* (33) show that *FANCA*-deficient cells (passages 4-17) undergo growth arrest earlier than donor BM-MSCs (passages 13-21). Furthermore, *FANCG*- (passage 6) and *FANCD2*- (passage 4 and 7) deficient BM-MSCs used in this study had relatively lower *in vitro* expansion capacity than donors. Concordantly, cell displaying *FANCD2* mutation had a slightly higher β-gal associated senescence activity at passage 3. These results correlate with senescence propensity of the FA cells, as a result of the genomic instability in MSCs, due to the impaired FA pathway.

TGF-β signaling has pleiotropic effects in the BM. On one hand, it suppresses HSC proliferation and supports HSC dormancy, but on the other hand, it promotes M to G1 progression in BM stromal cells (126, 444, 445). In this thesis, rTGF-β1 induction increased proliferation of BM-MSCs. Tgf-β1 is also shown to play a role in the progression of a BM disease called myelofibrosis in mice (446). Recently, overactive TGF-β signal transduction has been suggested to cause BMF (34). TGF-β expression or production by FA BM-MSCs and its possible role in BMF has not been studied before. The *TGF-β1* gene is a downstream target of TGF-β signaling (447). Therefore, *TGF-β1* expression of FA BM-MSCs was compared to donors, but there was no significant difference between groups. DEB treatment had no effect on the expression level. Additionally, TGF-β1, TGF-β2 and TGF-β3 secretion levels by BM-MSCs with a defective FA pathway were also similar to controls. However, BM-MSCs from individuals with *FANCD2* mutation did not secrete TGF-β1, TGF-β2 and TGF-β3 at all. TGF-β1-deficient mice develop an autoimmune reaction (448). Autoimmunity is a factor associated with inadequate blood production (449). Autocrine TGF-β signaling has been widely studied (450-452) and *FANCD2*-deficient BM-MSCs with impaired TGF-β production may lead to cellular defects and trigger BMF. Additionally, Zhang and co-authors (34) reveal overexpression of *Tgf-β1* in *Fancd2*$^{-/-}$ mice HSPCs, which may result in increased TGF-β secretion into BM. Downregulation of TGF-β production by BM-MSCs might be a response to such conditions. Accordingly, bone marrow stroma from aplastic anemia patients has significantly lower TGF-β1 production than controls (453). Inducing FA BM-MSCs with rTGF-β1 protein had no significant effect on the proliferation compared to donor cells. Lastly, TGF-β1 induced mice BM-MSCs have increased senescence activity compare to controls, which is partly associated with elevated levels of ROS production (454). In this study, FA BM-MSCs were found to have increased ROS production. Similarly, Kumari and co-authors (455) also report that FA cells are characterized with increased ROS levels, thus downregulation of TGF-β secretion in FA-D2 BM-MSCs can be a protective response. A report on oxidative stress showing a decrease in TGF-β signaling supports this conclusion (456).

5.2. HOX and TALE Profile of Fanconi Anemia Bone Marrow Stromal Cells in Comparison to Donors

The main objective of this thesis was to determine whether HOX and TALE profiles of BM-MSCs change in Fanconi anemia. During adult life, tightly regulated *HOX* expression pattern continues to provide a "biological fingerprint" for different cell types (16, 375). Expression of HOX and TALE genes may change gradually in the diseases with a predisposition to cancer. Loss of cellular identity via alterations in the HOX pathway is one of the driving mechanisms of cancer development, such as solid tumors and leukemia (457, 458). Regarding FA BM-MSCs, the HOX code did not show major changes except for *HOXC13* expression, which was expressed at slightly lower levels in patient cells compared to donors. BM-MSCs are reported to express most of the HOX genes except *HOXB1/B13*, *HOXC12* and *HOXD10-13* (17, 18). Additionally, *HOXA9-10*, *HOXC6*, *HOXC8*, *HOXC10* and *HOXD8* expression is relatively higher than other HOX genes in healthy BM-MSCs (17, 18), as observed in our study. On the other hand, Liedtke and colleagues (17) report that BM-MSCs do not express *HOXA3/A11/A13*, *HOXB2/B3/B8/B9*, *HOXC11/C13* and *HOXD1* genes, yet in our study, these genes had intermediate to low levels of expression in healthy donor samples. The difference might have resulted from higher sensitivity of TaqMan probes used in our study compared to SYBR Green used in the aforementioned study (17, 459).

Low DNA binding specificity of HOX proteins is increased through protein-protein interactions with the members of TALE gene class (19, 20). Expression analysis in this thesis also revealed that all the members of TALE gene class were actively expressed in BM-MSCs. Significant downregulation of *PKNOX2* gene expression with no change in the protein level was observed in FA patients' BM-MSC, as compared to healthy samples. It is known that mRNA level may not correlate with protein level due to post-transcriptional modifications or half-lives of proteins (460). On the other hand, a whole genome microarray study (GSE17233) shows an increase of *PKNOX2* expression in FA peripheral blood mononuclear cells compared to donors.

PKNOX2 is a transcription factor encoded by *PKNOX2* gene located on chromosome 11q24-q25 (370, 461). In humans, *PKNOX2* is expressed in many tissues (e.g. brain, skeletal muscle, heart, ovary, placenta, lung, pancreas, prostate, testis and small intestine), but has no or very low expression in colon, kidney, spleen, thymus, liver and peripheral blood leukocytes (370, 461). Additionally, *Pknox2* is expressed throughout development of mice embryos, and is exclusive to neuronal cells in the vomeronasal organ at postnatal stages (462, 463). NIH3T3 mouse embryo fibroblast cell line has five different isoforms of PKNOX2 protein (464). Three of these isoforms detected by C-terminal PKNOX2 antibody (two close to 62kDa and one at 47kDa), are mainly found in nucleus (464). Two of the isoforms (25 and 62kDa) detected by N-terminal specific antibody, are prominent in nucleus and cytoplasm, respectively (464). In this thesis, more than one variant of PKNOX2 protein (including 70 and 52kDa) were detected in human BM-MSCs. The PKNOX2 isoform, showing SDS-PAGE displayed molecular weight approximately 70kDa, corresponds to the previously *in vitro* synthesized protein by Fognani *et al* (370).

HD regions of PKNOX2 (Figure 5.1.) and PKNOX1 share an overall similarity of 52% and their HDs have almost identical sequence 94%, thus they are referred as paralog genes (370, 461). It has been reported that HDs of these two proteins differ in the first helix and the first loop (370). Due to their sequence similarity, PKNOX2 and PKNOX1 proteins may also have similar functions. PKNOX1 is known to function in the maintenance of genomic stability, thus PKNOX2 may also be a potential player in the DNA repair of FA stromal environment (23, 370). Concordancely, a whole genome RNA interference study shows an increase in cellular sensitivity to ionizing radiation by *PKNOX2* silencing (465). However, no change in *HOXC13* and *PKNOX2* expression of BM-MSCs was obtained by ICL-inducing agent, DEB, in this study. On the other hand, distinct tissue distribution of PKNOX2 and PKNOX1 give a hint of discrete PKNOX2 functions (370). Indeed, the linkage studies showing association of PKNOX2 with schizophrenia and alcohol dependence supports this assumption (466, 467). Additionally, it regulates transcription through sequence-specific DNA binding and actin filament/monomer binding (464).

Figure 5.1. Domains of PBX/knotted 1 Homeobox 2 protein (468).

5.3. Role of Recombinant Human TGF-β1 Protein on Fanconi Anemia Bone Marrow Stromal Cells in Comparison to Donors

Expression of *Pknox2* plays a vital role in limb development of mice (361, 469). *Pknox2* overexpression in mice limb bud mesenchyme results in a hypoplastic radius and ulna, which are common defects observed in FA patients (469). Furthermore, overexpressed *PKNOX2* is shown to perturbate ossification and chondrogenic differentiation as well as to lower *Hox10-11* and *Col2* gene expression, and Bmp/Smad signaling in the mice limb (469). These results implicate that PKNOX2 functions in development via BMP/SMAD pathway through Hox activity. A comparative expression microarray study (GSE46019) shows a significant increase of *PKNOX2* expression in BM-MSCs after TGF-β1 stimulation (470). These studies confirm the association between TGF-β signaling and PKNOX2. Here, stimulation of BM-MSCs with rTGF-β1 protein had both a dose and time-dependent effect on *PKNOX2* gene expression. Haley *et al*, (471) also report that TGF-β induction of epithelial NCI-H358 cells affected *PKNOX2* gene expression in a time-

dependent manner that peak at 18 hours, decreases by 24 hours and is then again upregulated by 72 hours. In this study, rTGF-β1 protein induction increased *TGF-β1* gene expression of BM-MSCs in a concentration dependent manner at 24, 48 or 72 hours, as previously described (447). In response to TGF-β1, there was either no change or a slight decrease in the expression of *MEIS1* and *PBX1* genes, known to encode transcription factors, that interact with PKNOX2. Lastly, it was investigated whether the misexpression of *PKNOX2* in FA BM-MSCs is further impaired by increased TGF-β1 stimulation. As the concentration of recombinant protein increased, PKNOX2 gene and protein expression of patients behaved like donors. Additionally, *TGF-β1* expression of donor and patients increased whereas *PBX1* and *MEIS1* mRNA levels did not change significantly upon induction. These results suggest that downregulation in *PKNOX2* expression is not due to aberrant TGF-β signaling in FA BM-MSCs. Additionally, TGF-β1, TGF-β2 and TGF-β3 secretion level by PKNOX2:MSCs was compared with controls and no statistically significant difference was obtained. Therefore, it is possible to conclude that PKNOX2 is a target of TGF-β signaling, but not vice versa.

5.4. Characterization of Bone Marrow Mesenchymal Stromal/Stem Cells Carrying PKNOX2 Expression Plasmid

PKNOX2 contains a HR 1 and HR2 within the N-terminal region (Figure 5.1.), which involves in protein-protein interactions (370, 461, 462). Due to its differential expression in FA BM-MSCs, PKNOX2 protein may interact with the members of FA/BRCA pathway. Therefore, PKNOX2 expression plasmid was transiently overexpressed in BM-MSCs, and expression was confirmed at both mRNA and protein level. PKNOX2 overexpressing BM-MSCs had similar differentiation capacity as controls, but immunophenotypic properties were slightly skewed. The CD105 (endoglin) level was downregulated following PKNOX2 plasmid transfection. Additionally, wound closure of PKNOX2:MSCs took longer to be completed than donors. CD105 is a member of the TGF-β receptor complex and is known to play a role during wound healing (472).

In order to assess the effect of PKNOX2 overexpression in the BM niche on HSC expansion and differentiation, PKNOX2:MSCs were co-cultured with either

cryopreserved or fresh $CD34^+$HSCs. The purity of $CD34^+$HSCs was established by determining their CD34 and CD38 positivity prior to and following co-culture. $CD34^+$HSCs are defined as a heterogeneous population consisting of multipotent cells and further defined according to their CD38 expression (473). $CD34^+CD38^-$ HSCs are the most primitive cells with self-renewal, as well as, myeloid and lymphoid differentiation capacities (474-478). However, it is also reported that $CD34^+CD38^{low}$HSCs are capable of long-term repopulation and CD38 positivity is related to G1 phase of the cell cycle (479). Following co-culture with PKNOX2:MSCs, pCMV6:MSCs or BM-MSCs, $CD34^+CD38^+$HSC percentage and fold expansion of fresh $CD34^+$HSCs remarkably increased compared to cells cultured alone. This suggests that co-culturing $CD34^+$HSCs with BM-MSCs increases the number of cycling HSCs and may be more advantageous for transplantation.

Cryopreserving HSCs in DMSO decreases their engraftment capacity and/or cell viability (480). Similarly, the frequency of $CD34^+$HSCs and $CD34^+CD38^-$HSCs, as well as the capacity to form total CFU and CFU-GM decrease after cryopreservation (481). Additionally, two studies comparing colony-forming capacity between HSCs frozen under controlled and uncontrolled conditions state that CFU-GM levels are downregulated in HSCs following uncontrolled rate freezing procedure (482, 483). Here, cryopreserved HSCs had lower $CD34^+CD38^-$ and $CD34^+CD38^+$ compared to fresh HSCs after culture. Following co-culture with PKNOX2:MSCs, CD34 and CD38 double positivity (45.5%) of cryopreserved cells was upregulated, and was comparable to fresh HSCs (49% ±4.17). Additionally, co-culturing cryopreserved HSCs with PKNOX2:MSCs also increased their CFU potential, while proliferative capacity was not affected. Cryopreservation is shown to cause cellular stress like hypothermia, increase solute concentration, free radical production, ionic imbalances, elevated protease activation, protein degradation and consequently increase programmed cell death due to altered proteomic and genomic profile of the cells (484-486). Upon DNA damage, HSCs have been shown to terminally differentiate which may be responsible to avoid self-renewal, thus progressive DNA damage in the niche (487). Therefore, PKNOX2:MSCs may induce differentiation of HSCs as a response to DNA damage.

5.5. Protein Interactions of PKNOX2 in Bone Marrow Mesenchymal Stromal/Stem Cells

Since *HOXC13* expression was also downregulated in FA cells, the effect of PKNOX2 overexpression on this gene and its paralog *HOXA13* expression was assessed. Following overexpression, *HOXC13* expression varied between individual experiments and *HOXA13* expression did not alter. A decrease in HOXA13 protein level was observed, which was also affected by the electroporation. PKNOX2 is probably not a transcriptional regulator of *HOXA13* and *HOXC13* genes. The effect of PKNOX2 overexpression was assessed on the key player of FA/BRCA pathway, FANCD2 but no specific changes were observed. However, the FANCD2 level increased following electroporation, which might be due to ROS production.

In order to identify proteins directly interacting with PKNOX2, Co-IP was performed followed by western blotting. Only the presence of PKNOX2-DDK protein was demonstrated in specific Co-IP products. Throughout the western blots, unspecific binding, which might be due to protein charges or interaction between hydrophobic surfaces, was present and made the interpretation of the results difficult. Prior to western blot analysis, heating up Co-IP products using a sample buffer consisting of denaturing reagents (e.g. DTT or BME) released both heavy (50kDa) and light (25kDa) chains of the primary antibody bound to magnetic beads. Consequently, using secondary antibodies that recognize both chains for western blot detection of the Co-IP sample results in unspecific binding. The easiest solution would be to add denaturing reagent following separation of Co-IP products from the beads. Here, no specific band for PKNOX2-DDK protein was obtained, when the samples were initially boiled in the absence of BME.

Mass-spectrometry analyses after Co-IP were performed to determine the PKNOX2 interactome. Initially, it was confirmed that PKNOX2 protein was only detectable in mass spectrometry analysis of PKNOX2:MSCs Co-IP products, but not in control. There was no direct interaction between PKNOX2 and FANC proteins. The sequence coverage of PKNOX2 protein within the sample was low, which might result in the loss of important information. Nevertheless, false discovery rate used for analyzing mass spectrometry results was stringent (0.01%). Therefore, it is highly

likely that the proteins identified as unique PKNOX2 interactor are true. GO enrichment analysis of proteins only interacting with PKNOX2 revealed roles in forming structural integrity of the ribosome and cellular cytoskeleton. It has been reported that PKNOX2 protein interacts with actin (i.e. F- and G-actin) and microtubule (i.e. β-tubulin) cytoskeletons following its export from nucleus via chromosome region maintenance 1 (CRM1)-mediated nuclear export (464). To create a more detailed interaction network, proteins interacting with PKNOX2 were analysed using HitPredict software. Intriguingly, proteins indirectly associated with PKNOX2 were identified to be involved in many biological processes, but most importantly to control differentiation of HSC, to negatively regulate G2/M transition of mitotic cell cycle and to affect double-strand break repair via NHEJ. This new list was then filtered using proteins obtained from proteomic profiling of undifferentiated human bone marrow stromal cells to determine, which of these proteins interacting with PKNOX2 interactors were expressed only in this specific cell population (419). Further enrichment of the proteins elicited the effect of biological pathways.

Proteins indirectly associated with PKNOX2 are suggested to maintain HSC differentiation. Herein, cryopreserved $CD34^{+}$HSCs co-cultured with PKNOX2 overexpressing BM-MSCs had increased CFU potential in comparison with controls. In the niche, PKNOX2 expressed by BM-MSCs may indirectly regulate HSC differentiation. Additionally, proteins indirectly associated with PKNOX2 were negative regulators of G2/M transition and were involved in G1/S transition of the mitotic cell cycle. In this study, FA BM-MSCs underwent cell cycle arrest at G2 phase and the number of cells in G1 phase decreased after DEB induction. Another study even shows that FA BM-MSCs have a prolonged G2 phase transition independent of an ICL agent (33). Therefore, downregulation of *PKNOX2* gene expression may play a role in cell cycle arrest. In this thesis, interactors of proteins, which have direct interaction with PKNOX2 were defined as members of NHEJ pathway. Recently, it is suggested that suppressing hyperactive TGF-β signaling in HSCs from Fancd2$^{-/-}$ mice, increases HR related gene expression such as *Brca2* and *Xrcc1* and HSC survival, but downregulates NHEJ gene expression like *Lig4* and *Prkdc* (34). MSCs are known to resolve IR-induced double strand breaks through NHEJ pathway and *PKNOX2* silencing has been suggested to upregulate cellular

sensitivity to IR (465, 488). In the light of these findings and the results of this thesis showing decreased *PKNOX2* expression in FA BM-MSCs, it is possible to conclude that PKNOX2 protein may be involved in the NHEJ pathway.

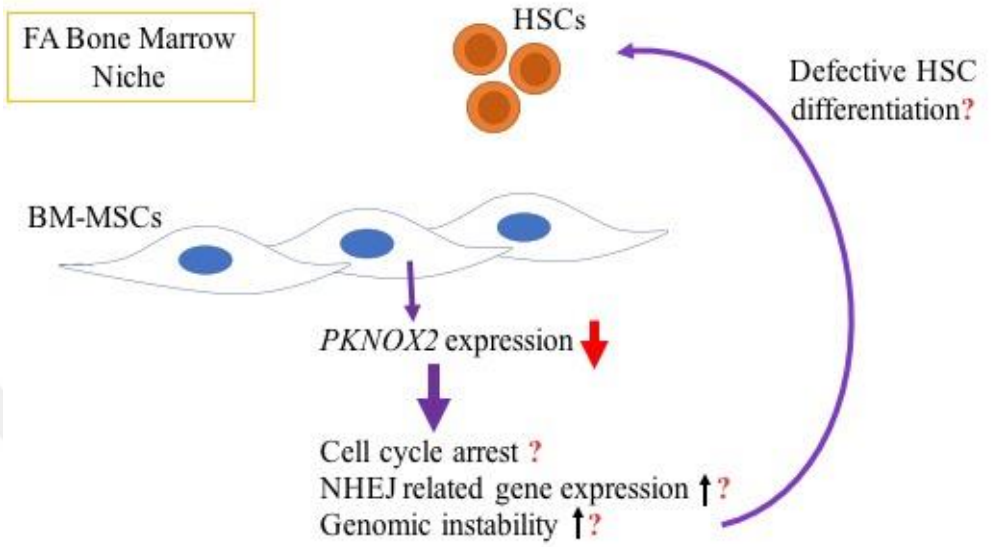

Figure 5.2. BM-MSCs derived from FA patients has lower *PKNOX2* expression compared to donor cells. In view of PKNOX2 protein-protein interaction analysis, disregulation of PKNOX2 in FA cells may cause activation of NHEJ-related gene expression, cell cycle arrest and differentiation of HSCs.

In conclusion, a comprehensive characterization of FA and donor BM-MSCs offered valuable insights into how BM microenvironment changes in disease state. *PKNOX2* expression of FA BM-MSCs was significantly lower than donors. HSCs or other cellular components of the bone marrow microenvironment may have a role in the misexpression of *PKNOX2* in BM-MSCs, which needs to be elucidated. Proteins indirectly interacting with PKNOX2 were involved in negative regulation of G2/M transition, DNA repair via NHEJ pathway and differentiation of HSC. It can be proposed that a genomic unstable BM niche may cause PKNOX2 disregulation and its misexpression may trigger activation of NHEJ-related gene expression, cell cycle arrest in FA BM-MSCs and consequently differentiation of HSCs, that may result in HSC exhaustion (Figure 5.2.). The outcomes of this thesis provide new insights in how the microenvironment changes due to genomic unstable conditions and provide more information with respect to FA pathophysiology.

6. CONCLUSIONS and FUTURE PERSPECTIVES

According to the results of the thesis, it is concluded that;

- Mutation analyses of FA patients revealed total of six new pathogenic variants (FANCA del exon 3-5, FANCA c.427-3C>G, FANCA c.3586G>T, FANCA del exon 1-2, FANCA c.1229G>A, FANCD2 c.1766+40T>G). It will be important to confirm these new pathogenic variants by functional assays.
- DEB treatment of FA BM-MSCs caused G2/M phase arrest as known to happen in HSCs. It will be intriguing to investigate the effect of other ICL-inducing agents such as MMC on cell cycle of BM-MSCs from FA patients carrying different pathogenic mutations.
- BM-MSCs from FA-D2 patients had a lower proliferative potential, higher senescence activity and no TGF-β1/β2/β3 secretion. We reported these results in our recent paper published in Stem Cell Reviews and Reports (489).
- Among 39 HOX genes and 8 TALE genes, only *PKNOX2* expression was disregulated in BM-MSCs from FA patients with a significant decrease compared to donors. *HOXC13* expression level of FA BM-MSCs was also slightly downregulated.
- DEB treatment had no effect on either *HOXC13* or *PKNOX2* expression. It may be important to see whether other ICL-inducing agents change HOX/TALE gene expression in BM-MSCs.
- rTGF-β1 induced *PKNOX2* expression, as well as *TGF-β1*.
- PKNOX2 overexpression in BM-MSCs from different donors caused a wide variation in *HOXC13* expression. It will be important to increase sample size to determine effect of PKNOX2 on HOXC13.
- PKNOX2 overexpression in BM-MSCs resulted in downregulation of CD105 and a decreased wound-healing capacity. The role of TGF-β/CD105 interaction on the BM niche needs to be further explored.
- Proteom analysis of Co-IP products did not show any interactions between PKNOX2 and FANC proteins.

- Co-culture aasays performed with cryopreserved $CD34^+$HSCs and PKNOX2 overexpressing BM-MSCs revealed increased $CD34^+CD38^+$ percentage and CFU potential of HSCs. However, increase in $CD34^+CD38^+$ percentage of fresh $CD34^+$HSCs was not specific to cells co-cultured with PKNOX2 overexpressing BM-MSCs. The effect of PKNOX2:MSC on cryopreserved HSCs needs to be elucidated further.
- Confirmation of PKNOX2-interacting proteins obtained in the proteome analysis will put more insight to the role of PKNOX2 on the cross-talk between stromal and hematopoietic stem cells in genome unstable conditions. In addition, proteins interacting with PKNOX2 interactome have functions in negative regulation of G2/M transition, HSC differentiation and NHEJ pathway which is worth to investigate further.

7. REFERENCES

1. Pittenger MF, Mackay AM, Beck SC, Jaiswal RK, Douglas R, Mosca JD, et al. Multilineage potential of adult human mesenchymal stem cells. Science. 1999;284(5411):143-7.

2. Mendez-Ferrer S, Michurina TV, Ferraro F, Mazloom AR, Macarthur BD, Lira SA, et al. Mesenchymal and haematopoietic stem cells form a unique bone marrow niche. Nature. 2010;466(7308):829-34.

3. Caplan AI. Mesenchymal stem cells. J Orthop Res. 1991;9(5):641-50.

4. Prockop DJ. Marrow stromal cells as stem cells for nonhematopoietic tissues. Science. 1997;276(5309):71-4.

5. Makino S, Fukuda K, Miyoshi S, Konishi F, Kodama H, Pan J, et al. Cardiomyocytes can be generated from marrow stromal cells in vitro. J Clin Invest. 1999;103(5):697-705.

6. Oswald J, Boxberger S, Jorgensen B, Feldmann S, Ehninger G, Bornhauser M, et al. Mesenchymal stem cells can be differentiated into endothelial cells in vitro. Stem Cells. 2004;22(3):377-84.

7. Snykers S, De Kock J, Rogiers V, Vanhaecke T. In vitro differentiation of embryonic and adult stem cells into hepatocytes: state of the art. Stem Cells. 2009;27(3):577-605.

8. Liotta F, Angeli R, Cosmi L, Fili L, Manuelli C, Frosali F, et al. Toll-like receptors 3 and 4 are expressed by human bone marrow-derived mesenchymal stem cells and can inhibit their T-cell modulatory activity by impairing Notch signaling. Stem Cells. 2008;26(1):279-89.

9. Caplan AI, Correa D. The MSC: an injury drugstore. Cell Stem Cell. 2011;9(1):11-5.

10. Schepers K, Pietras EM, Reynaud D, Flach J, Binnewies M, Garg T, et al. Myeloproliferative neoplasia remodels the endosteal bone marrow niche into a self-reinforcing leukemic niche. Cell Stem Cell. 2013;13(3):285-99.

11. Dalle JH, Peffault de Latour R. Allogeneic hematopoietic stem cell transplantation for inherited bone marrow failure syndromes. Int J Hematol. 2016;103(4):373-9.

12. Georges GE, Storb R. Hematopoietic stem cell transplantation for acquired aplastic anemia. Curr Opin Hematol. 2016;23(6):495-500.

13. Alharbi RA, Pettengell R, Pandha HS, Morgan R. The role of HOX genes in normal hematopoiesis and acute leukemia. Leukemia. 2013;27(5):1000-8.

14. McGinnis W, Krumlauf R. Homeobox genes and axial patterning. Cell. 1992;68(2):283-302.

15. Yamamoto M, Takai D, Yamamoto F, Yamamoto F. Comprehensive expression profiling of highly homologous 39 hox genes in 26 different human adult tissues by the modified systematic multiplex RT-pCR method reveals tissue-specific expression pattern that suggests an important role of chromosomal

structure in the regulation of hox gene expression in adult tissues. Gene Expr. 2003;11(3-4):199-210.

16. Ackema KB, Charite J. Mesenchymal stem cells from different organs are characterized by distinct topographic Hox codes. Stem Cells Dev. 2008;17(5):979-91.

17. Liedtke S, Buchheiser A, Bosch J, Bosse F, Kruse F, Zhao X, et al. The HOX Code as a "biological fingerprint" to distinguish functionally distinct stem cell populations derived from cord blood. Stem Cell Res. 2010;5(1):40-50.

18. Picchi J, Trombi L, Spugnesi L, Barachini S, Maroni G, Brodano GB, et al. HOX and TALE signatures specify human stromal stem cell populations from different sources. J Cell Physiol. 2013;228(4):879-89.

19. Rauskolb C, Peifer M, Wieschaus E. extradenticle, a regulator of homeotic gene activity, is a homolog of the homeobox-containing human proto-oncogene pbx1. Cell. 1993;74(6):1101-12.

20. Mann RS, Chan SK. Extra specificity from extradenticle: the partnership between HOX and PBX/EXD homeodomain proteins. Trends Genet. 1996;12(7):258-62.

21. Thorsteinsdottir U, Kroon E, Jerome L, Blasi F, Sauvageau G. Defining roles for HOX and MEIS1 genes in induction of acute myeloid leukemia. Mol Cell Biol. 2001;21(1):224-34.

22. Longobardi E, Iotti G, Di Rosa P, Mejetta S, Bianchi F, Fernandez-Diaz LC, et al. Prep1 (pKnox1)-deficiency leads to spontaneous tumor development in mice and accelerates EmuMyc lymphomagenesis: a tumor suppressor role for Prep1. Mol Oncol. 2010;4(2):126-34.

23. Iotti G, Longobardi E, Masella S, Dardaei L, De Santis F, Micali N, et al. Homeodomain transcription factor and tumor suppressor Prep1 is required to maintain genomic stability. Proc Natl Acad Sci U S A. 2011;108(29):E314-22.

24. Kutler DI, Singh B, Satagopan J, Batish SD, Berwick M, Giampietro PF, et al. A 20-year perspective on the International Fanconi Anemia Registry (IFAR). Blood. 2003;101(4):1249-56.

25. Kee Y, D'Andrea AD. Molecular pathogenesis and clinical management of Fanconi anemia. J Clin Invest. 2012;122(11):3799-806.

26. Knies K, Inano S, Ramirez MJ, Ishiai M, Surralles J, Takata M, et al. Biallelic mutations in the ubiquitin ligase RFWD3 cause Fanconi anemia. J Clin Invest. 2017;127(8):3013-27.

27. Mamrak NE, Shimamura A, Howlett NG. Recent discoveries in the molecular pathogenesis of the inherited bone marrow failure syndrome Fanconi anemia. Blood Rev. 2017;31(3):93-9.

28. D'Andrea AD, Grompe M. The Fanconi anaemia/BRCA pathway. Nat Rev Cancer. 2003;3(1):23-34.

29. Bagnara GP, Strippoli P, Bonsi L, Brizzi MF, Avanzi GC, Timeus F, et al. Effect of stem cell factor on colony growth from acquired and constitutional (Fanconi) aplastic anemia. Blood. 1992;80(2):382-7.

30. Kelly PF, Radtke S, von Kalle C, Balcik B, Bohn K, Mueller R, et al. Stem cell collection and gene transfer in Fanconi anemia. Mol Ther. 2007;15(1):211-9.

31. Li Y, Chen S, Yuan J, Yang Y, Li J, Ma J, et al. Mesenchymal stem/progenitor cells promote the reconstitution of exogenous hematopoietic stem cells in Fancg-/- mice in vivo. Blood. 2009;113(10):2342-51.

32. Lecourt S, Vanneaux V, Leblanc T, Leroux G, Ternaux B, Benbunan M, et al. Bone marrow microenvironment in fanconi anemia: a prospective functional study in a cohort of fanconi anemia patients. Stem Cells Dev. 2010;19(2):203-8.

33. Mantelli M, Avanzini MA, Rosti V, Ingo DM, Conforti A, Novara F, et al. Comprehensive characterization of mesenchymal stromal cells from patients with Fanconi anaemia. Br J Haematol. 2015;170(6):826-36.

34. Zhang H, Kozono DE, O'Connor KW, Vidal-Cardenas S, Rousseau A, Hamilton A, et al. TGF-beta Inhibition Rescues Hematopoietic Stem Cell Defects and Bone Marrow Failure in Fanconi Anemia. Cell Stem Cell. 2016;18(5):668-81.

35. Marshman E, Booth C, Potten CS. The intestinal epithelial stem cell. Bioessays. 2002;24(1):91-8.

36. Caplan AI. Adult mesenchymal stem cells for tissue engineering versus regenerative medicine. J Cell Physiol. 2007;213(2):341-7.

37. Weissman IL. Stem cells: units of development, units of regeneration, and units in evolution. Cell. 2000;100(1):157-68.

38. Avasthi S, Srivastava RN, Singh A, Srivastava M. Stem Cell: Past, Present and Future- A Review Article. Internet Journal of Medical Update. 2008;3(1):22-30.

39. Alvarez CV, Garcia-Lavandeira M, Garcia-Rendueles ME, Diaz-Rodriguez E, Garcia-Rendueles AR, Perez-Romero S, et al. Defining stem cell types: understanding the therapeutic potential of ESCs, ASCs, and iPS cells. J Mol Endocrinol. 2012;49(2):R89-111.

40. Biteau B, Hochmuth CE, Jasper H. Maintaining tissue homeostasis: dynamic control of somatic stem cell activity. Cell Stem Cell. 2011;9(5):402-11.

41. Alison MR, Brittan M, Lovell MJ, Wright NA. Markers of adult tissue-based stem cells. Handb Exp Pharmacol. 2006(174):185-227.

42. Tavassoli M, Crosby WH. Transplantation of marrow to extramedullary sites. Science. 1968;161(3836):54-6.

43. Friedenstein AJ, Piatetzky S, II, Petrakova KV. Osteogenesis in transplants of bone marrow cells. J Embryol Exp Morphol. 1966;16(3):381-90.

44. da Silva Meirelles L, Chagastelles PC, Nardi NB. Mesenchymal stem cells reside in virtually all post-natal organs and tissues. J Cell Sci. 2006;119(Pt 11):2204-13.

45. Friedenstein AJ, Chailakhjan RK, Lalykina KS. The development of fibroblast colonies in monolayer cultures of guinea-pig bone marrow and spleen cells. Cell Tissue Kinet. 1970;3(4):393-403.

46. Shi S, Gronthos S. Perivascular niche of postnatal mesenchymal stem cells in human bone marrow and dental pulp. J Bone Miner Res. 2003;18(4):696-704.

47. Kang SG, Shinojima N, Hossain A, Gumin J, Yong RL, Colman H, et al. Isolation and perivascular localization of mesenchymal stem cells from mouse brain. Neurosurgery. 2010;67(3):711-20.

48. Zebardast N, Lickorish D, Davies JE. Human umbilical cord perivascular cells (HUCPVC): A mesenchymal cell source for dermal wound healing. Organogenesis. 2010;6(4):197-203.

49. Gerlach JC, Over P, Turner ME, Thompson RL, Foka HG, Chen WC, et al. Perivascular mesenchymal progenitors in human fetal and adult liver. Stem Cells Dev. 2012;21(18):3258-69.

50. James AW, Zara JN, Zhang X, Askarinam A, Goyal R, Chiang M, et al. Perivascular stem cells: a prospectively purified mesenchymal stem cell population for bone tissue engineering. Stem Cells Transl Med. 2012;1(6):510-9.

51. Arthur A, Rychkov G, Shi S, Koblar SA, Gronthos S. Adult human dental pulp stem cells differentiate toward functionally active neurons under appropriate environmental cues. Stem Cells. 2008;26(7):1787-95.

52. Muraglia A, Cancedda R, Quarto R. Clonal mesenchymal progenitors from human bone marrow differentiate in vitro according to a hierarchical model. J Cell Sci. 2000;113 (Pt 7):1161-6.

53. Colter DC, Sekiya I, Prockop DJ. Identification of a subpopulation of rapidly self-renewing and multipotential adult stem cells in colonies of human marrow stromal cells. Proc Natl Acad Sci U S A. 2001;98(14):7841-5.

54. Pittenger MF, Martin BJ. Mesenchymal stem cells and their potential as cardiac therapeutics. Circ Res. 2004;95(1):9-20.

55. Sarugaser R, Hanoun L, Keating A, Stanford WL, Davies JE. Human mesenchymal stem cells self-renew and differentiate according to a deterministic hierarchy. PLoS One. 2009;4(8):e6498.

56. Lee RH, Kim B, Choi I, Kim H, Choi HS, Suh K, et al. Characterization and expression analysis of mesenchymal stem cells from human bone marrow and adipose tissue. Cell Physiol Biochem. 2004;14(4-6):311-24.

57. Panepucci RA, Siufi JL, Silva WA, Jr., Proto-Siquiera R, Neder L, Orellana M, et al. Comparison of gene expression of umbilical cord vein and bone marrow-derived mesenchymal stem cells. Stem Cells. 2004;22(7):1263-78.

58. Kaltz N, Ringe J, Holzwarth C, Charbord P, Niemeyer M, Jacobs VR, et al. Novel markers of mesenchymal stem cells defined by genome-wide gene expression analysis of stromal cells from different sources. Exp Cell Res. 2010;316(16):2609-17.

59. Dominici M, Le Blanc K, Mueller I, Slaper-Cortenbach I, Marini F, Krause D, et al. Minimal criteria for defining multipotent mesenchymal stromal cells. The International Society for Cellular Therapy position statement. Cytotherapy. 2006;8(4):315-7.

60. NIH, U.S. National Library of Medicine [Internet]. 2017 [Accessed on 01 August 2017]. Available from: www.clinicaltrials.gov

61. Le Blanc K, Tammik C, Rosendahl K, Zetterberg E, Ringden O. HLA expression and immunologic properties of differentiated and undifferentiated mesenchymal stem cells. Exp Hematol. 2003;31(10):890-6.

62. Griffin MD, Ryan AE, Alagesan S, Lohan P, Treacy O, Ritter T. Anti-donor immune responses elicited by allogeneic mesenchymal stem cells: what have we learned so far? Immunol Cell Biol. 2013;91(1):40-51.

63. Di Nicola M, Carlo-Stella C, Magni M, Milanesi M, Longoni PD, Matteucci P, et al. Human bone marrow stromal cells suppress T-lymphocyte proliferation induced by cellular or nonspecific mitogenic stimuli. Blood. 2002;99(10):3838-43.

64. Tse WT, Pendleton JD, Beyer WM, Egalka MC, Guinan EC. Suppression of allogeneic T-cell proliferation by human marrow stromal cells: implications in transplantation. Transplantation. 2003;75(3):389-97.

65. Ramasamy R, Fazekasova H, Lam EW, Soeiro I, Lombardi G, Dazzi F. Mesenchymal stem cells inhibit dendritic cell differentiation and function by preventing entry into the cell cycle. Transplantation. 2007;83(1):71-6.

66. Rosado MM, Bernardo ME, Scarsella M, Conforti A, Giorda E, Biagini S, et al. Inhibition of B-cell proliferation and antibody production by mesenchymal stromal cells is mediated by T cells. Stem Cells Dev. 2015;24(1):93-103.

67. Krampera M, Cosmi L, Angeli R, Pasini A, Liotta F, Andreini A, et al. Role for interferon-gamma in the immunomodulatory activity of human bone marrow mesenchymal stem cells. Stem Cells. 2006;24(2):386-98.

68. Ryan JM, Barry F, Murphy JM, Mahon BP. Interferon-gamma does not break, but promotes the immunosuppressive capacity of adult human mesenchymal stem cells. Clin Exp Immunol. 2007;149(2):353-63.

69. Ren G, Zhang L, Zhao X, Xu G, Zhang Y, Roberts AI, et al. Mesenchymal stem cell-mediated immunosuppression occurs via concerted action of chemokines and nitric oxide. Cell Stem Cell. 2008;2(2):141-50.

70. English K, Ryan JM, Tobin L, Murphy MJ, Barry FP, Mahon BP. Cell contact, prostaglandin E(2) and transforming growth factor beta 1 play non-redundant roles in human mesenchymal stem cell induction of CD4+CD25(High) forkhead box P3+ regulatory T cells. Clin Exp Immunol. 2009;156(1):149-60.

71. Meirelles Lda S, Fontes AM, Covas DT, Caplan AI. Mechanisms involved in the therapeutic properties of mesenchymal stem cells. Cytokine Growth Factor Rev. 2009;20(5-6):419-27.

72. Kyurkchiev D, Bochev I, Ivanova-Todorova E, Mourdjeva M, Oreshkova T, Belemezova K, et al. Secretion of immunoregulatory cytokines by mesenchymal stem cells. World J Stem Cells. 2014;6(5):552-70.

73. Mikkola HK, Orkin SH. The journey of developing hematopoietic stem cells. Development. 2006;133(19):3733-44.

74. Cheshier SH, Morrison SJ, Liao X, Weissman IL. In vivo proliferation and cell cycle kinetics of long-term self-renewing hematopoietic stem cells. Proc Natl Acad Sci U S A. 1999;96(6):3120-5.

75. Wilson A, Murphy MJ, Oskarsson T, Kaloulis K, Bettess MD, Oser GM, et al. c-Myc controls the balance between hematopoietic stem cell self-renewal and differentiation. Genes Dev. 2004;18(22):2747-63.

76. Schofield R. The relationship between the spleen colony-forming cell and the haemopoietic stem cell. Blood Cells. 1978;4(1-2):7-25.

77. Gong JK. Endosteal marrow: a rich source of hematopoietic stem cells. Science. 1978;199(4336):1443-5.

78. Nilsson SK, Johnston HM, Coverdale JA. Spatial localization of transplanted hemopoietic stem cells: inferences for the localization of stem cell niches. Blood. 2001;97(8):2293-9.

79. Zhang J, Niu C, Ye L, Huang H, He X, Tong WG, et al. Identification of the haematopoietic stem cell niche and control of the niche size. Nature. 2003;425(6960):836-41.

80. Kiel MJ, Yilmaz OH, Iwashita T, Yilmaz OH, Terhorst C, Morrison SJ. SLAM family receptors distinguish hematopoietic stem and progenitor cells and reveal endothelial niches for stem cells. Cell. 2005;121(7):1109-21.

81. Heissig B, Hattori K, Dias S, Friedrich M, Ferris B, Hackett NR, et al. Recruitment of stem and progenitor cells from the bone marrow niche requires MMP-9 mediated release of kit-ligand. Cell. 2002;109(5):625-37.

82. Calvi LM, Adams GB, Weibrecht KW, Weber JM, Olson DP, Knight MC, et al. Osteoblastic cells regulate the haematopoietic stem cell niche. Nature. 2003;425(6960):841-6.

83. Avecilla ST, Hattori K, Heissig B, Tejada R, Liao F, Shido K, et al. Chemokine-mediated interaction of hematopoietic progenitors with the bone marrow vascular niche is required for thrombopoiesis. Nat Med. 2004;10(1):64-71.

84. Lo Celso C, Scadden DT. The haematopoietic stem cell niche at a glance. J Cell Sci. 2011;124(Pt 21):3529-35.

85. Sugiyama T, Kohara H, Noda M, Nagasawa T. Maintenance of the hematopoietic stem cell pool by CXCL12-CXCR4 chemokine signaling in bone marrow stromal cell niches. Immunity. 2006;25(6):977-88.

86. Yamazaki S, Nakauchi H. Bone marrow Schwann cells induce hematopoietic stem cell hibernation. Int J Hematol. 2014;99(6):695-8.

87. Nilsson SK, Johnston HM, Whitty GA, Williams B, Webb RJ, Denhardt DT, et al. Osteopontin, a key component of the hematopoietic stem cell niche and regulator of primitive hematopoietic progenitor cells. Blood. 2005;106(4):1232-9.

88. Stier S, Ko Y, Forkert R, Lutz C, Neuhaus T, Grunewald E, et al. Osteopontin is a hematopoietic stem cell niche component that negatively regulates stem cell pool size. J Exp Med. 2005;201(11):1781-91.

89. Haylock DN, Nilsson SK. The role of hyaluronic acid in hemopoietic stem cell biology. Regen Med. 2006;1(4):437-45.

90. Priestley GV, Scott LM, Ulyanova T, Papayannopoulou T. Lack of alpha4 integrin expression in stem cells restricts competitive function and self-renewal activity. Blood. 2006;107(7):2959-67.

91. Priestley GV, Ulyanova T, Papayannopoulou T. Sustained alterations in biodistribution of stem/progenitor cells in Tie2Cre+ alpha4(f/f) mice are hematopoietic cell autonomous. Blood. 2007;109(1):109-11.

92. Lewandowski D, Barroca V, Duconge F, Bayer J, Van Nhieu JT, Pestourie C, et al. In vivo cellular imaging pinpoints the role of reactive oxygen species in the early steps of adult hematopoietic reconstitution. Blood. 2010;115(3):443-52.

93. Adams GB, Chabner KT, Alley IR, Olson DP, Szczepiorkowski ZM, Poznansky MC, et al. Stem cell engraftment at the endosteal niche is specified by the calcium-sensing receptor. Nature. 2006;439(7076):599-603.

94. Parmar K, Mauch P, Vergilio JA, Sackstein R, Down JD. Distribution of hematopoietic stem cells in the bone marrow according to regional hypoxia. Proc Natl Acad Sci U S A. 2007;104(13):5431-6.

95. Winkler IG, Barbier V, Wadley R, Zannettino AC, Williams S, Levesque JP. Positioning of bone marrow hematopoietic and stromal cells relative to blood flow in vivo: serially reconstituting hematopoietic stem cells reside in distinct nonperfused niches. Blood. 2010;116(3):375-85.

96. Crane GM, Jeffery E, Morrison SJ. Adult haematopoietic stem cell niches. Nat Rev Immunol. 2017;17(9):573-90.

97. Campagnoli C, Roberts IA, Kumar S, Bennett PR, Bellantuono I, Fisk NM. Identification of mesenchymal stem/progenitor cells in human first-trimester fetal blood, liver, and bone marrow. Blood. 2001;98(8):2396-402.

98. Mendes SC, Robin C, Dzierzak E. Mesenchymal progenitor cells localize within hematopoietic sites throughout ontogeny. Development. 2005;132(5):1127-36.

99. Naveiras O, Nardi V, Wenzel PL, Hauschka PV, Fahey F, Daley GQ. Bone-marrow adipocytes as negative regulators of the haematopoietic microenvironment. Nature. 2009;460(7252):259-63.

100. Lo Celso C, Fleming HE, Wu JW, Zhao CX, Miake-Lye S, Fujisaki J, et al. Live-animal tracking of individual haematopoietic stem/progenitor cells in their niche. Nature. 2009;457(7225):92-6.

101. Xie Y, Yin T, Wiegraebe W, He XC, Miller D, Stark D, et al. Detection of functional haematopoietic stem cell niche using real-time imaging. Nature. 2009;457(7225):97-101.

102. Zhu J, Garrett R, Jung Y, Zhang Y, Kim N, Wang J, et al. Osteoblasts support B-lymphocyte commitment and differentiation from hematopoietic stem cells. Blood. 2007;109(9):3706-12.

103. Kinashi T, Springer TA. Adhesion molecules in hematopoietic cells. Blood Cells. 1994;20(1):25-44.

104. Arai F, Hirao A, Ohmura M, Sato H, Matsuoka S, Takubo K, et al. Tie2/angiopoietin-1 signaling regulates hematopoietic stem cell quiescence in the bone marrow niche. Cell. 2004;118(2):149-61.

105. Taichman RS. Blood and bone: two tissues whose fates are intertwined to create the hematopoietic stem-cell niche. Blood. 2005;105(7):2631-9.

106. Lyman SD, Jacobsen SE. c-kit ligand and Flt3 ligand: stem/progenitor cell factors with overlapping yet distinct activities. Blood. 1998;91(4):1101-34.

107. Jung Y, Song J, Shiozawa Y, Wang J, Wang Z, Williams B, et al. Hematopoietic stem cells regulate mesenchymal stromal cell induction into osteoblasts thereby participating in the formation of the stem cell niche. Stem Cells. 2008;26(8):2042-51.

108. Yoon KA, Cho HS, Shin HI, Cho JY. Differential regulation of CXCL5 by FGF2 in osteoblastic and endothelial niche cells supports hematopoietic stem cell migration. Stem Cells Dev. 2012;21(18):3391-402.

109. Kopp HG, Avecilla ST, Hooper AT, Rafii S. The bone marrow vascular niche: home of HSC differentiation and mobilization. Physiology (Bethesda). 2005;20:349-56.

110. He N, Zhang L, Cui J, Li Z. Bone marrow vascular niche: home for hematopoietic stem cells. Bone Marrow Res. 2014;2014:128436.

111. Butler JM, Nolan DJ, Vertes EL, Varnum-Finney B, Kobayashi H, Hooper AT, et al. Endothelial cells are essential for the self-renewal and repopulation of Notch-dependent hematopoietic stem cells. Cell Stem Cell. 2010;6(3):251-64.

112. Kobayashi H, Butler JM, O'Donnell R, Kobayashi M, Ding BS, Bonner B, et al. Angiocrine factors from Akt-activated endothelial cells balance self-renewal and differentiation of haematopoietic stem cells. Nat Cell Biol. 2010;12(11):1046-56.

113. Yoshida K, Taga T, Saito M, Suematsu S, Kumanogoh A, Tanaka T, et al. Targeted disruption of gp130, a common signal transducer for the interleukin 6 family of cytokines, leads to myocardial and hematological disorders. Proc Natl Acad Sci U S A. 1996;93(1):407-11.

114. Yao L, Yokota T, Xia L, Kincade PW, McEver RP. Bone marrow dysfunction in mice lacking the cytokine receptor gp130 in endothelial cells. Blood. 2005;106(13):4093-101.

115. Winkler IG, Barbier V, Nowlan B, Jacobsen RN, Forristal CE, Patton JT, et al. Vascular niche E-selectin regulates hematopoietic stem cell dormancy, self renewal and chemoresistance. Nat Med. 2012;18(11):1651-7.

116. Hooper AT, Butler JM, Nolan DJ, Kranz A, Iida K, Kobayashi M, et al. Engraftment and reconstitution of hematopoiesis is dependent on VEGFR2-mediated regeneration of sinusoidal endothelial cells. Cell Stem Cell. 2009;4(3):263-74.

117. Mazo IB, Gutierrez-Ramos JC, Frenette PS, Hynes RO, Wagner DD, von Andrian UH. Hematopoietic progenitor cell rolling in bone marrow microvessels: parallel contributions by endothelial selectins and vascular cell adhesion molecule 1. J Exp Med. 1998;188(3):465-74.

118. Barker JE. Sl/Sld hematopoietic progenitors are deficient in situ. Exp Hematol. 1994;22(2):174-7.

119. Barker JE. Early transplantation to a normal microenvironment prevents the development of Steel hematopoietic stem cell defects. Exp Hematol. 1997;25(6):542-7.

120. Ding L, Saunders TL, Enikolopov G, Morrison SJ. Endothelial and perivascular cells maintain haematopoietic stem cells. Nature. 2012;481(7382):457-62.

121. Kunisaki Y, Bruns I, Scheiermann C, Ahmed J, Pinho S, Zhang D, et al. Arteriolar niches maintain haematopoietic stem cell quiescence. Nature. 2013;502(7473):637-43.

122. Nombela-Arrieta C, Pivarnik G, Winkel B, Canty KJ, Harley B, Mahoney JE, et al. Quantitative imaging of haematopoietic stem and progenitor cell localization and hypoxic status in the bone marrow microenvironment. Nat Cell Biol. 2013;15(5):533-43.

123. Greenbaum A, Hsu YM, Day RB, Schuettpelz LG, Christopher MJ, Borgerding JN, et al. CXCL12 in early mesenchymal progenitors is required for haematopoietic stem-cell maintenance. Nature. 2013;495(7440):227-30.

124. Omatsu Y, Sugiyama T, Kohara H, Kondoh G, Fujii N, Kohno K, et al. The essential functions of adipo-osteogenic progenitors as the hematopoietic stem and progenitor cell niche. Immunity. 2010;33(3):387-99.

125. Sacchetti B, Funari A, Michienzi S, Di Cesare S, Piersanti S, Saggio I, et al. Self-renewing osteoprogenitors in bone marrow sinusoids can organize a hematopoietic microenvironment. Cell. 2007;131(2):324-36.

126. Blank U, Karlsson S. TGF-beta signaling in the control of hematopoietic stem cells. Blood. 2015;125(23):3542-50.

127. Yahata T, Ibrahim AA, Muguruma Y, Eren M, Shaffer AM, Watanabe N, et al. TGF-beta-induced intracellular PAI-1 is responsible for retaining hematopoietic stem cells in the niche. Blood. 2017;130(21):2283-94.

128. Heldin CH, Miyazono K, ten Dijke P. TGF-beta signalling from cell membrane to nucleus through SMAD proteins. Nature. 1997;390(6659):465-71.

129. Shi Y, Massague J. Mechanisms of TGF-beta signaling from cell membrane to the nucleus. Cell. 2003;113(6):685-700.

130. Annes JP, Munger JS, Rifkin DB. Making sense of latent TGFbeta activation. J Cell Sci. 2003;116(Pt 2):217-24.

131. James D, Levine AJ, Besser D, Hemmati-Brivanlou A. TGFbeta/activin/nodal signaling is necessary for the maintenance of pluripotency in human embryonic stem cells. Development. 2005;132(6):1273-82.

132. Feng XH, Derynck R. Specificity and versatility in tgf-beta signaling through Smads. Annu Rev Cell Dev Biol. 2005;21:659-93.

133. Gadue P, Huber TL, Paddison PJ, Keller GM. Wnt and TGF-beta signaling are required for the induction of an in vitro model of primitive streak formation using embryonic stem cells. Proc Natl Acad Sci U S A. 2006;103(45):16806-11.

134. Sumi T, Tsuneyoshi N, Nakatsuji N, Suemori H. Defining early lineage specification of human embryonic stem cells by the orchestrated balance of canonical Wnt/beta-catenin, Activin/Nodal and BMP signaling. Development. 2008;135(17):2969-79.

135. Crane JL, Cao X. Bone marrow mesenchymal stem cells and TGF-beta signaling in bone remodeling. J Clin Invest. 2014;124(2):466-72.

136. Hoffman R, Bruno E, Elwell J, Mazur E, Gewirtz AM, Dekker P, et al. Acquired amegakaryocytic thrombocytopenic purpura: a syndrome of diverse etiologies. Blood. 1982;60(5):1173-8.

137. Gewirtz AM, Sacchetti MK, Bien R, Barry WE. Cell-mediated suppression of megakaryocytopoiesis in acquired amegakaryocytic thrombocytopenic purpura. Blood. 1986;68(3):619-26.

138. Parker CJ. Update on the diagnosis and management of paroxysmal nocturnal hemoglobinuria. Hematology Am Soc Hematol Educ Program. 2016;2016(1):208-16.

139. Bouchnita A, Eymard N, Moyo TK, Koury MJ, Volpert V. Bone marrow infiltration by multiple myeloma causes anemia by reversible disruption of erythropoiesis. Am J Hematol. 2016;91(4):371-8.

140. Green R. Vitamin B12 deficiency from the perspective of a practicing hematologist. Blood. 2017;129(19):2603-11.

141. Socie G, Henry-Amar M, Bacigalupo A, Hows J, Tichelli A, Ljungman P, et al. Malignant tumors occurring after treatment of aplastic anemia. European Bone Marrow Transplantation-Severe Aplastic Anaemia Working Party. N Engl J Med. 1993;329(16):1152-7.

142. Garcia-Manero G. Myelodysplastic syndromes: 2015 Update on diagnosis, risk-stratification and management. Am J Hematol. 2015;90(9):831-41.

143. Araten DJ, Swirsky D, Karadimitris A, Notaro R, Nafa K, Bessler M, et al. Cytogenetic and morphological abnormalities in paroxysmal nocturnal haemoglobinuria. Br J Haematol. 2001;115(2):360-8.

144. Zhang L. Inherited and Acquired Bone Marrow Failure Syndromes: In the Era of Deep Gene Sequencing. Leukemia. 2016;4(4).

145. Dokal I, Vulliamy T. Inherited bone marrow failure syndromes. Haematologica. 2010;95(8):1236-40.

146. Wegman-Ostrosky T, Savage SA. The genomics of inherited bone marrow failure: from mechanism to the clinic. Br J Haematol. 2017;177(4):526-42.

147. Mehta PA, Tolar J. Fanconi Anemia. In: Adam MP, Ardinger HH, Pagon RA, Wallace SE, Bean LJH, Mefford HC, et al., editors. GeneReviews(R). Seattle (WA)1993.

148. Ballmaier M, Germeshausen M. Congenital amegakaryocytic thrombocytopenia: clinical presentation, diagnosis, and treatment. Semin Thromb Hemost. 2011;37(6):673-81.

149. Geddis AE. Congenital amegakaryocytic thrombocytopenia. Pediatr Blood Cancer. 2011;57(2):199-203.

150. Savage SA, Alter BP. Dyskeratosis congenita. Hematol Oncol Clin North Am. 2009;23(2):215-31.

151. Dokal I. Dyskeratosis congenita. Hematology Am Soc Hematol Educ Program. 2011;2011:480-6.

152. Mason PJ, Bessler M. The genetics of dyskeratosis congenita. Cancer Genet. 2011;204(12):635-45.

153. Clinton C, Gazda HT. Diamond-Blackfan Anemia. In: Adam MP, Ardinger HH, Pagon RA, Wallace SE, Bean LJH, Mefford HC, et al., editors. GeneReviews(R). Seattle (WA)1993.

154. Rey MA, Duffy SP, Brown JK, Kennedy JA, Dick JE, Dror Y, et al. Enhanced alternative splicing of the FLVCR1 gene in Diamond Blackfan anemia disrupts FLVCR1 expression and function that are critical for erythropoiesis. Haematologica. 2008;93(11):1617-26.

155. DiMauro S, Hirano M. Mitochondrial DNA Deletion Syndromes. In: Adam MP, Ardinger HH, Pagon RA, Wallace SE, Bean LJH, Mefford HC, et al., editors. GeneReviews(R). Seattle (WA)1993.

156. Boztug K, Klein C. Genetic etiologies of severe congenital neutropenia. Curr Opin Pediatr. 2011;23(1):21-6.

157. Spinner MA, Sanchez LA, Hsu AP, Shaw PA, Zerbe CS, Calvo KR, et al. GATA2 deficiency: a protean disorder of hematopoiesis, lymphatics, and immunity. Blood. 2014;123(6):809-21.

158. Ceccaldi R, Sarangi P, D'Andrea AD. The Fanconi anaemia pathway: new players and new functions. Nat Rev Mol Cell Biol. 2016;17(6):337-49.

159. Gurtan AM, D'Andrea AD. Dedicated to the core: understanding the Fanconi anemia complex. DNA Repair (Amst). 2006;5(9-10):1119-25.

160. Coulthard R, Deans AJ, Swuec P, Bowles M, Costa A, West SC, et al. Architecture and DNA recognition elements of the Fanconi anemia FANCM-FAAP24 complex. Structure. 2013;21(9):1648-58.

161. Ciccia A, Ling C, Coulthard R, Yan Z, Xue Y, Meetei AR, et al. Identification of FAAP24, a Fanconi anemia core complex protein that interacts with FANCM. Mol Cell. 2007;25(3):331-43.

162. Kim JM, Kee Y, Gurtan A, D'Andrea AD. Cell cycle-dependent chromatin loading of the Fanconi anemia core complex by FANCM/FAAP24. Blood. 2008;111(10):5215-22.

163. Singh TR, Saro D, Ali AM, Zheng XF, Du CH, Killen MW, et al. MHF1-MHF2, a histone-fold-containing protein complex, participates in the Fanconi anemia pathway via FANCM. Mol Cell. 2010;37(6):879-86.

164. Ling C, Ishiai M, Ali AM, Medhurst AL, Neveling K, Kalb R, et al. FAAP100 is essential for activation of the Fanconi anemia-associated DNA damage response pathway. EMBO J. 2007;26(8):2104-14.

165. Huang Y, Leung JW, Lowery M, Matsushita N, Wang Y, Shen X, et al. Modularized functions of the Fanconi anemia core complex. Cell Rep. 2014;7(6):1849-57.

166. Rajendra E, Oestergaard VH, Langevin F, Wang M, Dornan GL, Patel KJ, et al. The genetic and biochemical basis of FANCD2 monoubiquitination. Mol Cell. 2014;54(5):858-69.

167. Kruyt FA, Waisfisz Q, Dijkmans LM, Hermsen MA, Youssoufian H, Arwert F, et al. Cytoplasmic localization of a functionally active Fanconi anemia group A-green fluorescent protein chimera in human 293 cells. Blood. 1997;90(9):3288-95.

168. Kupfer GM, Naf D, Suliman A, Pulsipher M, D'Andrea AD. The Fanconi anaemia proteins, FAA and FAC, interact to form a nuclear complex. Nat Genet. 1997;17(4):487-90.

169. Kruyt FA, Youssoufian H. The Fanconi anemia proteins FAA and FAC function in different cellular compartments to protect against cross-linking agent cytotoxicity. Blood. 1998;92(7):2229-36.

170. Naf D, Kupfer GM, Suliman A, Lambert K, D'Andrea AD. Functional activity of the fanconi anemia protein FAA requires FAC binding and nuclear localization. Mol Cell Biol. 1998;18(10):5952-60.

171. Waisfisz Q, de Winter JP, Kruyt FA, de Groot J, van der Weel L, Dijkmans LM, et al. A physical complex of the Fanconi anemia proteins FANCG/XRCC9 and FANCA. Proc Natl Acad Sci U S A. 1999;96(18):10320-5.

172. de Winter JP, Leveille F, van Berkel CG, Rooimans MA, van Der Weel L, Steltenpool J, et al. Isolation of a cDNA representing the Fanconi anemia complementation group E gene. Am J Hum Genet. 2000;67(5):1306-8.

173. Garcia-Higuera I, Taniguchi T, Ganesan S, Meyn MS, Timmers C, Hejna J, et al. Interaction of the Fanconi anemia proteins and BRCA1 in a common pathway. Mol Cell. 2001;7(2):249-62.

174. Pace P, Johnson M, Tan WM, Mosedale G, Sng C, Hoatlin M, et al. FANCE: the link between Fanconi anaemia complex assembly and activity. EMBO J. 2002;21(13):3414-23.

175. Taniguchi T, D'Andrea AD. The Fanconi anemia protein, FANCE, promotes the nuclear accumulation of FANCC. Blood. 2002;100(7):2457-62.

176. Meetei AR, Levitus M, Xue Y, Medhurst AL, Zwaan M, Ling C, et al. X-linked inheritance of Fanconi anemia complementation group B. Nat Genet. 2004;36(11):1219-24.

177. Thomashevski A, High AA, Drozd M, Shabanowitz J, Hunt DF, Grant PA, et al. The Fanconi anemia core complex forms four complexes of different sizes in different subcellular compartments. J Biol Chem. 2004;279(25):26201-9.

178. Leveille F, Ferrer M, Medhurst AL, Laghmani el H, Rooimans MA, Bier P, et al. The nuclear accumulation of the Fanconi anemia protein FANCE depends on FANCC. DNA Repair (Amst). 2006;5(5):556-65.

179. Mukhopadhyay SS, Leung KS, Hicks MJ, Hastings PJ, Youssoufian H, Plon SE. Defective mitochondrial peroxiredoxin-3 results in sensitivity to oxidative stress in Fanconi anemia. J Cell Biol. 2006;175(2):225-35.

180. Meetei AR, de Winter JP, Medhurst AL, Wallisch M, Waisfisz Q, van de Vrugt HJ, et al. A novel ubiquitin ligase is deficient in Fanconi anemia. Nat Genet. 2003;35(2):165-70.

181. Machida YJ, Machida Y, Chen Y, Gurtan AM, Kupfer GM, D'Andrea AD, et al. UBE2T is the E2 in the Fanconi anemia pathway and undergoes negative autoregulation. Mol Cell. 2006;23(4):589-96.

182. Alpi A, Langevin F, Mosedale G, Machida YJ, Dutta A, Patel KJ. UBE2T, the Fanconi anemia core complex, and FANCD2 are recruited independently to chromatin: a basis for the regulation of FANCD2 monoubiquitination. Mol Cell Biol. 2007;27(24):8421-30.

183. Alpi AF, Pace PE, Babu MM, Patel KJ. Mechanistic insight into site-restricted monoubiquitination of FANCD2 by Ube2t, FANCL, and FANCI. Mol Cell. 2008;32(6):767-77.

184. Sims AE, Spiteri E, Sims RJ, 3rd, Arita AG, Lach FP, Landers T, et al. FANCI is a second monoubiquitinated member of the Fanconi anemia pathway. Nat Struct Mol Biol. 2007;14(6):564-7.

185. Smogorzewska A, Matsuoka S, Vinciguerra P, McDonald ER, 3rd, Hurov KE, Luo J, et al. Identification of the FANCI protein, a monoubiquitinated FANCD2 paralog required for DNA repair. Cell. 2007;129(2):289-301.

186. Joo W, Xu G, Persky NS, Smogorzewska A, Rudge DG, Buzovetsky O, et al. Structure of the FANCI-FANCD2 complex: insights into the Fanconi anemia DNA repair pathway. Science. 2011;333(6040):312-6.

187. Wang X, Andreassen PR, D'Andrea AD. Functional interaction of monoubiquitinated FANCD2 and BRCA2/FANCD1 in chromatin. Mol Cell Biol. 2004;24(13):5850-62.

188. MacKay C, Declais AC, Lundin C, Agostinho A, Deans AJ, MacArtney TJ, et al. Identification of KIAA1018/FAN1, a DNA repair nuclease recruited to DNA damage by monoubiquitinated FANCD2. Cell. 2010;142(1):65-76.

189. Yamamoto KN, Kobayashi S, Tsuda M, Kurumizaka H, Takata M, Kono K, et al. Involvement of SLX4 in interstrand cross-link repair is regulated by the Fanconi anemia pathway. Proc Natl Acad Sci U S A. 2011;108(16):6492-6.

190. Kim Y, Spitz GS, Veturi U, Lach FP, Auerbach AD, Smogorzewska A. Regulation of multiple DNA repair pathways by the Fanconi anemia protein SLX4. Blood. 2013;121(1):54-63.

191. Klein Douwel D, Boonen RA, Long DT, Szypowska AA, Raschle M, Walter JC, et al. XPF-ERCC1 acts in Unhooking DNA interstrand crosslinks in cooperation with FANCD2 and FANCP/SLX4. Mol Cell. 2014;54(3):460-71.

192. Murina O, von Aesch C, Karakus U, Ferretti LP, Bolck HA, Hanggi K, et al. FANCD2 and CtIP cooperate to repair DNA interstrand crosslinks. Cell Rep. 2014;7(4):1030-8.

193. Unno J, Itaya A, Taoka M, Sato K, Tomida J, Sakai W, et al. FANCD2 binds CtIP and regulates DNA-end resection during DNA interstrand crosslink repair. Cell Rep. 2014;7(4):1039-47.

194. Zhang N, Liu X, Li L, Legerski R. Double-strand breaks induce homologous recombinational repair of interstrand cross-links via cooperation of MSH2, ERCC1-XPF, REV3, and the Fanconi anemia pathway. DNA Repair (Amst). 2007;6(11):1670-8.

195. Hara K, Hashimoto H, Murakumo Y, Kobayashi S, Kogame T, Unzai S, et al. Crystal structure of human REV7 in complex with a human REV3 fragment and structural implication of the interaction between DNA polymerase zeta and REV1. J Biol Chem. 2010;285(16):12299-307.

196. Budzowska M, Graham TG, Sobeck A, Waga S, Walter JC. Regulation of the Rev1-pol zeta complex during bypass of a DNA interstrand cross-link. EMBO J. 2015;34(14):1971-85.

197. Kim H, Yang K, Dejsuphong D, D'Andrea AD. Regulation of Rev1 by the Fanconi anemia core complex. Nat Struct Mol Biol. 2012;19(2):164-70.

198. Baumann P, West SC. Role of the human RAD51 protein in homologous recombination and double-stranded-break repair. Trends Biochem Sci. 1998;23(7):247-51.

199. Boulton SJ. Cellular functions of the BRCA tumour-suppressor proteins. Biochem Soc Trans. 2006;34(Pt 5):633-45.

200. Park JY, Singh TR, Nassar N, Zhang F, Freund M, Hanenberg H, et al. Breast cancer-associated missense mutants of the PALB2 WD40 domain, which directly binds RAD51C, RAD51 and BRCA2, disrupt DNA repair. Oncogene. 2014;33(40):4803-12.

201. Inano S, Sato K, Katsuki Y, Kobayashi W, Tanaka H, Nakajima K, et al. RFWD3-Mediated Ubiquitination Promotes Timely Removal of Both RPA and RAD51 from DNA Damage Sites to Facilitate Homologous Recombination. Mol Cell. 2017;66(5):622-34 e8.

202. Gueiderikh A, Rosselli F, Neto JBC. A never-ending story: the steadily growing family of the FA and FA-like genes. Genet Mol Biol. 2017;40(2):398-407.

203. Du W, Li J, Sipple J, Chen J, Pang Q. Cytoplasmic FANCA-FANCC complex interacts and stabilizes the cytoplasm-dislocalized leukemic nucleophosmin protein (NPMc). J Biol Chem. 2010;285(48):37436-44.

204. Yano K, Morotomi K, Saito H, Kato M, Matsuo F, Miki Y. Nuclear localization signals of the BRCA2 protein. Biochem Biophys Res Commun. 2000;270(1):171-5.

205. Han X, Saito H, Miki Y, Nakanishi A. A CRM1-mediated nuclear export signal governs cytoplasmic localization of BRCA2 and is essential for centrosomal localization of BRCA2. Oncogene. 2008;27(21):2969-77.

206. Zhang T, Du W, Wilson AF, Namekawa SH, Andreassen PR, Meetei AR, et al. Fancd2 in vivo interaction network reveals a non-canonical role in mitochondrial function. Sci Rep. 2017;7:45626.

207. Leveille F, Blom E, Medhurst AL, Bier P, Laghmani el H, Johnson M, et al. The Fanconi anemia gene product FANCF is a flexible adaptor protein. J Biol Chem. 2004;279(38):39421-30.

208. Boisvert RA, Rego MA, Azzinaro PA, Mauro M, Howlett NG. Coordinate nuclear targeting of the FANCD2 and FANCI proteins via a FANCD2 nuclear localization signal. PLoS One. 2013;8(11):e81387.

209. The Human Protein Atlas: BRIP1 [Internet]. [Accessed on 01 October 2017]. Available from: https://www.proteinatlas.org/ENSG00000136492-BRIP1/cell

210. Ma J, Cai H, Wu T, Sobhian B, Huo Y, Alcivar A, et al. PALB2 interacts with KEAP1 to promote NRF2 nuclear accumulation and function. Mol Cell Biol. 2012;32(8):1506-17.

211. Gildemeister OS, Sage JM, Knight KL. Cellular redistribution of Rad51 in response to DNA damage: novel role for Rad51C. J Biol Chem. 2009;284(46):31945-52.

212. Svendsen JM, Smogorzewska A, Sowa ME, O'Connell BC, Gygi SP, Elledge SJ, et al. Mammalian BTBD12/SLX4 assembles a Holliday junction resolvase and is required for DNA repair. Cell. 2009;138(1):63-77.

213. Ruffner H, Verma IM. BRCA1 is a cell cycle-regulated nuclear phosphoprotein. Proc Natl Acad Sci U S A. 1997;94(14):7138-43.

214. Gong YQ, Peng D, Ning XH, Yang XY, Li XS, Zhou LQ, et al. UBE2T silencing suppresses proliferation and induces cell cycle arrest and apoptosis in bladder cancer cells. Oncol Lett. 2016;12(6):4485-92.

215. Miller KA, Hinz JM, Yamada NA, Thompson LH, Albala JS. Nuclear localization of Rad51B is independent of Rad51C and BRCA2. Mutagenesis. 2005;20(1):57-63.

216. Zhang H, Chatterjee A, Singh KK. Saccharomyces cerevisiae polymerase zeta functions in mitochondria. Genetics. 2006;172(4):2683-8.

217. Xu G, Chapman JR, Brandsma I, Yuan J, Mistrik M, Bouwman P, et al. REV7 counteracts DNA double-strand break resection and affects PARP inhibition. Nature. 2015;521(7553):541-4.

218. Liu S, Chu J, Yucer N, Leng M, Wang SY, Chen BP, et al. RING finger and WD repeat domain 3 (RFWD3) associates with replication protein A (RPA) and facilitates RPA-mediated DNA damage response. J Biol Chem. 2011;286(25):22314-22.

219. Ali AM, Pradhan A, Singh TR, Du C, Li J, Wahengbam K, et al. FAAP20: a novel ubiquitin-binding FA nuclear core-complex protein required for functional integrity of the FA-BRCA DNA repair pathway. Blood. 2012;119(14):3285-94.

220. Collis SJ, Ciccia A, Deans AJ, Horejsi Z, Martin JS, Maslen SL, et al. FANCM and FAAP24 function in ATR-mediated checkpoint signaling independently of the Fanconi anemia core complex. Mol Cell. 2008;32(3):313-24.

221. Lobitz S, Velleuer E. Guido Fanconi (1892-1979): a jack of all trades. Nat Rev Cancer. 2006;6(11):893-8.

222. Rosenberg PS, Tamary H, Alter BP. How high are carrier frequencies of rare recessive syndromes? Contemporary estimates for Fanconi Anemia in the United States and Israel. Am J Med Genet A. 2011;155A(8):1877-83.

223. Lopez-Martinez D, Liang CC, Cohn MA. Cellular response to DNA interstrand crosslinks: the Fanconi anemia pathway. Cell Mol Life Sci. 2016;73(16):3097-114.

224. Kalb R, Neveling K, Nanda I, Schindler D, Hoehn H. Fanconi anemia: causes and consequences of genetic instability. Genome Dyn. 2006;1:218-42.

225. McCabe KM, Olson SB, Moses RE. DNA interstrand crosslink repair in mammalian cells. J Cell Physiol. 2009;220(3):569-73.

226. Sasaki MS, Tonomura A. A high susceptibility of Fanconi's anemia to chromosome breakage by DNA cross-linking agents. Cancer Res. 1973;33(8):1829-36.

227. Cervenka J, Arthur D, Yasis C. Mitomycin C test for diagnostic differentiation of idiopathic aplastic anemia and Fanconi anemia. Pediatrics. 1981;67(1):119-27.

228. Auerbach AD. Fanconi anemia diagnosis and the diepoxybutane (DEB) test. Exp Hematol. 1993;21(6):731-3.

229. Deviren A, Yalman N, Hacihanefioglu S. Differential diagnosis of Fanconi anemia by nitrogen mustard and diepoxybutane. Ann Hematol. 2003;82(4):223-7.

230. Chen CC, Taniguchi T, D'Andrea A. The Fanconi anemia (FA) pathway confers glioma resistance to DNA alkylating agents. J Mol Med (Berl). 2007;85(5):497-509.

231. Langevin F, Crossan GP, Rosado IV, Arends MJ, Patel KJ. Fancd2 counteracts the toxic effects of naturally produced aldehydes in mice. Nature. 2011;475(7354):53-8.

232. Kondo N, Takahashi A, Mori E, Noda T, Zdzienicka MZ, Thompson LH, et al. FANCD1/BRCA2 plays predominant role in the repair of DNA damage induced by ACNU or TMZ. PLoS One. 2011;6(5):e19659.

233. Kaiser TN, Lojewski A, Dougherty C, Juergens L, Sahar E, Latt SA. Flow cytometric characterization of the response of Fanconi's anemia cells to mitomycin C treatment. Cytometry. 1982;2(5):291-7.

234. Kubbies M, Schindler D, Hoehn H, Schinzel A, Rabinovitch PS. Endogenous blockage and delay of the chromosome cycle despite normal recruitment and growth phase explain poor proliferation and frequent edomitosis in Fanconi anemia cells. Am J Hum Genet. 1985;37(5):1022-30.

235. Miglierina R, Le Coniat M, Berger R. A simple diagnostic test for Fanconi anemia by flow cytometry. Anal Cell Pathol. 1991;3(2):111-8.

236. Chan KL, Palmai-Pallag T, Ying S, Hickson ID. Replication stress induces sister-chromatid bridging at fragile site loci in mitosis. Nat Cell Biol. 2009;11(6):753-60.

237. Naim V, Rosselli F. The FANC pathway and BLM collaborate during mitosis to prevent micro-nucleation and chromosome abnormalities. Nat Cell Biol. 2009;11(6):761-8.

238. Federico MB, Vallerga MB, Radl A, Paviolo NS, Bocco JL, Di Giorgio M, et al. Chromosomal Integrity after UV Irradiation Requires FANCD2-Mediated Repair of Double Strand Breaks. PLoS Genet. 2016;12(1):e1005792.

239. Lachaud C, Moreno A, Marchesi F, Toth R, Blow JJ, Rouse J. Ubiquitinated Fancd2 recruits Fan1 to stalled replication forks to prevent genome instability. Science. 2016;351(6275):846-9.

240. Vinciguerra P, Godinho SA, Parmar K, Pellman D, D'Andrea AD. Cytokinesis failure occurs in Fanconi anemia pathway-deficient murine and human bone marrow hematopoietic cells. J Clin Invest. 2010;120(11):3834-42.

241. Waisfisz Q, Morgan NV, Savino M, de Winter JP, van Berkel CG, Hoatlin ME, et al. Spontaneous functional correction of homozygous fanconi anaemia alleles reveals novel mechanistic basis for reverse mosaicism. Nat Genet. 1999;22(4):379-83.

242. Gross M, Hanenberg H, Lobitz S, Friedl R, Herterich S, Dietrich R, et al. Reverse mosaicism in Fanconi anemia: natural gene therapy via molecular self-correction. Cytogenet Genome Res. 2002;98(2-3):126-35.

243. Mankad A, Taniguchi T, Cox B, Akkari Y, Rathbun RK, Lucas L, et al. Natural gene therapy in monozygotic twins with Fanconi anemia. Blood. 2006;107(8):3084-90.

244. Rosenberg PS, Socie G, Alter BP, Gluckman E. Risk of head and neck squamous cell cancer and death in patients with Fanconi anemia who did and did not receive transplants. Blood. 2005;105(1):67-73.

245. Anur P, Friedman DN, Sklar C, Oeffinger K, Castiel M, Kearney J, et al. Late effects in patients with Fanconi anemia following allogeneic hematopoietic stem cell transplantation from alternative donors. Bone Marrow Transplant. 2016;51(7):938-44.

246. Auerbach AD, Liu Q, Ghosh R, Pollack MS, Douglas GW, Broxmeyer HE. Prenatal identification of potential donors for umbilical cord blood transplantation for Fanconi anemia. Transfusion. 1990;30(8):682-7.

247. Daneshbod-Skibba G, Martin J, Shahidi NT. Myeloid and erythroid colony growth in non-anaemic patients with Fanconi's anaemia. Br J Haematol. 1980;44(1):33-8.

248. Rathbun RK, Faulkner GR, Ostroski MH, Christianson TA, Hughes G, Jones G, et al. Inactivation of the Fanconi anemia group C gene augments interferon-gamma-induced apoptotic responses in hematopoietic cells. Blood. 1997;90(3):974-85.

249. Haneline LS, Broxmeyer HE, Cooper S, Hangoc G, Carreau M, Buchwald M, et al. Multiple inhibitory cytokines induce deregulated progenitor growth and apoptosis in hematopoietic cells from Fac-/- mice. Blood. 1998;91(11):4092-8.

250. Epperly MW, Rhieu BH, Franicola D, Dixon T, Cao S, Zhang X, et al. Induction of TGF-beta by Irradiation or Chemotherapy in Fanconi Anemia (FA) Mouse Bone Marrow Is Modulated by Small Molecule Radiation Mitigators JP4-039 and MMS350. In Vivo. 2017;31(2):159-68.

251. Rosselli F, Sanceau J, Gluckman E, Wietzerbin J, Moustacchi E. Abnormal lymphokine production: a novel feature of the genetic disease Fanconi anemia. II. In vitro and in vivo spontaneous overproduction of tumor necrosis factor alpha. Blood. 1994;83(5):1216-25.

252. Dufour C, Corcione A, Svahn J, Haupt R, Poggi V, Beka'ssy AN, et al. TNF-alpha and IFN-gamma are overexpressed in the bone marrow of Fanconi anemia patients and TNF-alpha suppresses erythropoiesis in vitro. Blood. 2003;102(6):2053-9.

253. Li J, Sejas DP, Zhang X, Qiu Y, Nattamai KJ, Rani R, et al. TNF-alpha induces leukemic clonal evolution ex vivo in Fanconi anemia group C murine stem cells. J Clin Invest. 2007;117(11):3283-95.

254. Joenje H, Oostra AB. Effect of oxygen tension on chromosomal aberrations in Fanconi anaemia. Hum Genet. 1983;65(2):99-101.

255. Schindler D, Hoehn H. Fanconi anemia mutation causes cellular susceptibility to ambient oxygen. Am J Hum Genet. 1988;43(4):429-35.

256. Park SJ, Ciccone SL, Beck BD, Hwang B, Freie B, Clapp DW, et al. Oxidative stress/damage induces multimerization and interaction of Fanconi anemia proteins. J Biol Chem. 2004;279(29):30053-9.

257. Saadatzadeh MR, Bijangi-Vishehsaraei K, Hong P, Bergmann H, Haneline LS. Oxidant hypersensitivity of Fanconi anemia type C-deficient cells is dependent on a redox-regulated apoptotic pathway. J Biol Chem. 2004;279(16):16805-12.

258. Pagano G, Degan P, d'Ischia M, Kelly FJ, Nobili B, Pallardo FV, et al. Oxidative stress as a multiple effector in Fanconi anaemia clinical phenotype. Eur J Haematol. 2005;75(2):93-100.

259. Cohen-Haguenauer O, Peault B, Bauche C, Daniel MT, Casal I, Levy V, et al. In vivo repopulation ability of genetically corrected bone marrow cells from Fanconi anemia patients. Proc Natl Acad Sci U S A. 2006;103(7):2340-5.

260. Hadjur S, Ung K, Wadsworth L, Dimmick J, Rajcan-Separovic E, Scott RW, et al. Defective hematopoiesis and hepatic steatosis in mice with combined deficiencies of the genes encoding Fancc and Cu/Zn superoxide dismutase. Blood. 2001;98(4):1003-11.

261. Li J, Du W, Maynard S, Andreassen PR, Pang Q. Oxidative stress-specific interaction between FANCD2 and FOXO3a. Blood. 2010;115(8):1545-8.

262. Ito K, Hirao A, Arai F, Takubo K, Matsuoka S, Miyamoto K, et al. Reactive oxygen species act through p38 MAPK to limit the lifespan of hematopoietic stem cells. Nat Med. 2006;12(4):446-51.

263. Jang YY, Sharkis SJ. A low level of reactive oxygen species selects for primitive hematopoietic stem cells that may reside in the low-oxygenic niche. Blood. 2007;110(8):3056-63.

264. Miyamoto K, Araki KY, Naka K, Arai F, Takubo K, Yamazaki S, et al. Foxo3a is essential for maintenance of the hematopoietic stem cell pool. Cell Stem Cell. 2007;1(1):101-12.

265. Tothova Z, Kollipara R, Huntly BJ, Lee BH, Castrillon DH, Cullen DE, et al. FoxOs are critical mediators of hematopoietic stem cell resistance to physiologic oxidative stress. Cell. 2007;128(2):325-39.

266. Chen C, Liu Y, Liu R, Ikenoue T, Guan KL, Liu Y, et al. TSC-mTOR maintains quiescence and function of hematopoietic stem cells by repressing mitochondrial biogenesis and reactive oxygen species. J Exp Med. 2008;205(10):2397-408.

267. Yahata T, Takanashi T, Muguruma Y, Ibrahim AA, Matsuzawa H, Uno T, et al. Accumulation of oxidative DNA damage restricts the self-renewal capacity of human hematopoietic stem cells. Blood. 2011;118(11):2941-50.

268. Ruscetti FW, Akel S, Bartelmez SH. Autocrine transforming growth factor-beta regulation of hematopoiesis: many outcomes that depend on the context. Oncogene. 2005;24(37):5751-63.

269. MacMillan ML, Wagner JE. Haematopoeitic cell transplantation for Fanconi anaemia - when and how? Br J Haematol. 2010;149(1):14-21.

270. Raaijmakers MH, Mukherjee S, Guo S, Zhang S, Kobayashi T, Schoonmaker JA, et al. Bone progenitor dysfunction induces myelodysplasia and secondary leukaemia. Nature. 2010;464(7290):852-7.

271. Beerman I, Luis TC, Singbrant S, Lo Celso C, Mendez-Ferrer S. The evolving view of the hematopoietic stem cell niche. Exp Hematol. 2017;50:22-6.

272. Aizawa S, Nakano M, Iwase O, Yaguchi M, Hiramoto M, Hoshi H, et al. Bone marrow stroma from refractory anemia of myelodysplastic syndrome is defective in its ability to support normal CD34-positive cell proliferation and differentiation in vitro. Leuk Res. 1999;23(3):239-46.

273. Tauro S, Hepburn MD, Peddie CM, Bowen DT, Pippard MJ. Functional disturbance of marrow stromal microenvironment in the myelodysplastic syndromes. Leukemia. 2002;16(5):785-90.

274. Flores-Figueroa E, Arana-Trejo RM, Gutierrez-Espindola G, Perez-Cabrera A, Mayani H. Mesenchymal stem cells in myelodysplastic syndromes: phenotypic and cytogenetic characterization. Leuk Res. 2005;29(2):215-24.

275. Flores-Figueroa E, Montesinos JJ, Flores-Guzman P, Gutierrez-Espindola G, Arana-Trejo RM, Castillo-Medina S, et al. Functional analysis of myelodysplastic syndromes-derived mesenchymal stem cells. Leuk Res. 2008;32(9):1407-16.

276. Klaus M, Stavroulaki E, Kastrinaki MC, Fragioudaki P, Giannikou K, Psyllaki M, et al. Reserves, functional, immunoregulatory, and cytogenetic properties of bone marrow mesenchymal stem cells in patients with myelodysplastic syndromes. Stem Cells Dev. 2010;19(7):1043-54.

277. Kurt Yuksel M, Topcuoglu P, Kurdal M, Ilhan O. The clonogenic potential of hematopoietic stem cells and mesenchymal stromal cells in various hematologic diseases: a pilot study. Cytotherapy. 2010;12(1):38-44.

278. Zhao ZG, Xu W, Yu HP, Fang BL, Wu SH, Li F, et al. Functional characteristics of mesenchymal stem cells derived from bone marrow of patients with myelodysplastic syndromes. Cancer Lett. 2012;317(2):136-43.

279. Geyh S, Oz S, Cadeddu RP, Frobel J, Bruckner B, Kundgen A, et al. Insufficient stromal support in MDS results from molecular and functional deficits of mesenchymal stromal cells. Leukemia. 2013;27(9):1841-51.

280. Varga G, Kiss J, Varkonyi J, Vas V, Farkas P, Paloczi K, et al. Inappropriate Notch activity and limited mesenchymal stem cell plasticity in the bone marrow of patients with myelodysplastic syndromes. Pathol Oncol Res. 2007;13(4):311-9.

281. Campioni D, Moretti S, Ferrari L, Punturieri M, Castoldi GL, Lanza F. Immunophenotypic heterogeneity of bone marrow-derived mesenchymal stromal cells from patients with hematologic disorders: correlation with bone marrow microenvironment. Haematologica. 2006;91(3):364-8.

282. Campioni D, Rizzo R, Stignani M, Melchiorri L, Ferrari L, Moretti S, et al. A decreased positivity for CD90 on human mesenchymal stromal cells (MSCs) is associated with a loss of immunosuppressive activity by MSCs. Cytometry B Clin Cytom. 2009;76(3):225-30.

283. Lopez-Villar O, Garcia JL, Sanchez-Guijo FM, Robledo C, Villaron EM, Hernandez-Campo P, et al. Both expanded and uncultured mesenchymal stem

cells from MDS patients are genomically abnormal, showing a specific genetic profile for the 5q- syndrome. Leukemia. 2009;23(4):664-72.

284. Zhao Z, Wang Z, Li Q, Li W, You Y, Zou P. The different immunoregulatory functions of mesenchymal stem cells in patients with low-risk or high-risk myelodysplastic syndromes. PLoS One. 2012;7(9):e45675.

285. Aanei CM, Flandrin P, Eloae FZ, Carasevici E, Guyotat D, Wattel E, et al. Intrinsic growth deficiencies of mesenchymal stromal cells in myelodysplastic syndromes. Stem Cells Dev. 2012;21(10):1604-15.

286. Blau O, Hofmann WK, Baldus CD, Thiel G, Serbent V, Schumann E, et al. Chromosomal aberrations in bone marrow mesenchymal stroma cells from patients with myelodysplastic syndrome and acute myeloblastic leukemia. Exp Hematol. 2007;35(2):221-9.

287. Blau O, Baldus CD, Hofmann WK, Thiel G, Nolte F, Burmeister T, et al. Mesenchymal stromal cells of myelodysplastic syndrome and acute myeloid leukemia patients have distinct genetic abnormalities compared with leukemic blasts. Blood. 2011;118(20):5583-92.

288. Flores-Figueroa E, Varma S, Montgomery K, Greenberg PL, Gratzinger D. Distinctive contact between CD34+ hematopoietic progenitors and CXCL12+ CD271+ mesenchymal stromal cells in benign and myelodysplastic bone marrow. Lab Invest. 2012;92(9):1330-41.

289. Shipounova IN, Petrova TV, Svinareva DA, Momotuk KS, Mikhailova EA, Drize NI. Alterations in hematopoietic microenvironment in patients with aplastic anemia. Clin Transl Sci. 2009;2(1):67-74.

290. Chao YH, Peng CT, Harn HJ, Chan CK, Wu KH. Poor potential of proliferation and differentiation in bone marrow mesenchymal stem cells derived from children with severe aplastic anemia. Ann Hematol. 2010;89(7):715-23.

291. Li J, Yang S, Lu S, Zhao H, Feng J, Li W, et al. Differential gene expression profile associated with the abnormality of bone marrow mesenchymal stem cells in aplastic anemia. PLoS One. 2012;7(11):e47764.

292. Xu Y, Takahashi Y, Wang Y, Hama A, Nishio N, Muramatsu H, et al. Downregulation of GATA-2 and overexpression of adipogenic gene-PPARgamma in mesenchymal stem cells from patients with aplastic anemia. Exp Hematol. 2009;37(12):1393-9.

293. Cheng NC, van de Vrugt HJ, van der Valk MA, Oostra AB, Krimpenfort P, de Vries Y, et al. Mice with a targeted disruption of the Fanconi anemia homolog Fanca. Hum Mol Genet. 2000;9(12):1805-11.

294. Ara T, Song L, Shimada H, Keshelava N, Russell HV, Metelitsa LS, et al. Interleukin-6 in the bone marrow microenvironment promotes the growth and survival of neuroblastoma cells. Cancer Res. 2009;69(1):329-37.

295. Alberts B, Johnson A, Lewis J, Raff M, Roberts K, Walter P. Molecular Biology of the Cell. 4th ed. New York: Garland Science; 2002.

296. Reik W, Dean W, Walter J. Epigenetic reprogramming in mammalian development. Science. 2001;293(5532):1089-93.

297. Albert M, Peters AH. Genetic and epigenetic control of early mouse development. Curr Opin Genet Dev. 2009;19(2):113-21.

298. Hemberger M, Dean W, Reik W. Epigenetic dynamics of stem cells and cell lineage commitment: digging Waddington's canal. Nat Rev Mol Cell Biol. 2009;10(8):526-37.

299. Niwa H, Miyazaki J, Smith AG. Quantitative expression of Oct-3/4 defines differentiation, dedifferentiation or self-renewal of ES cells. Nat Genet. 2000;24(4):372-6.

300. Mitsui K, Tokuzawa Y, Itoh H, Segawa K, Murakami M, Takahashi K, et al. The homeoprotein Nanog is required for maintenance of pluripotency in mouse epiblast and ES cells. Cell. 2003;113(5):631-42.

301. Loh YH, Wu Q, Chew JL, Vega VB, Zhang W, Chen X, et al. The Oct4 and Nanog transcription network regulates pluripotency in mouse embryonic stem cells. Nat Genet. 2006;38(4):431-40.

302. Wu Q, Chen X, Zhang J, Loh YH, Low TY, Zhang W, et al. Sall4 interacts with Nanog and co-occupies Nanog genomic sites in embryonic stem cells. J Biol Chem. 2006;281(34):24090-4.

303. Yagi R, Kohn MJ, Karavanova I, Kaneko KJ, Vullhorst D, DePamphilis ML, et al. Transcription factor TEAD4 specifies the trophectoderm lineage at the beginning of mammalian development. Development. 2007;134(21):3827-36.

304. Farthing CR, Ficz G, Ng RK, Chan CF, Andrews S, Dean W, et al. Global mapping of DNA methylation in mouse promoters reveals epigenetic reprogramming of pluripotency genes. PLoS Genet. 2008;4(6):e1000116.

305. Senner CE, Krueger F, Oxley D, Andrews S, Hemberger M. DNA methylation profiles define stem cell identity and reveal a tight embryonic-extraembryonic lineage boundary. Stem Cells. 2012;30(12):2732-45.

306. Tsumura A, Hayakawa T, Kumaki Y, Takebayashi S, Sakaue M, Matsuoka C, et al. Maintenance of self-renewal ability of mouse embryonic stem cells in the absence of DNA methyltransferases Dnmt1, Dnmt3a and Dnmt3b. Genes Cells. 2006;11(7):805-14.

307. Santos-Rosa H, Schneider R, Bannister AJ, Sherriff J, Bernstein BE, Emre NC, et al. Active genes are tri-methylated at K4 of histone H3. Nature. 2002;419(6905):407-11.

308. Azuara V, Perry P, Sauer S, Spivakov M, Jorgensen HF, John RM, et al. Chromatin signatures of pluripotent cell lines. Nat Cell Biol. 2006;8(5):532-8.

309. Barski A, Cuddapah S, Cui K, Roh TY, Schones DE, Wang Z, et al. High-resolution profiling of histone methylations in the human genome. Cell. 2007;129(4):823-37.

310. Bernstein BE, Mikkelsen TS, Xie X, Kamal M, Huebert DJ, Cuff J, et al. A bivalent chromatin structure marks key developmental genes in embryonic stem cells. Cell. 2006;125(2):315-26.

311. Pan G, Tian S, Nie J, Yang C, Ruotti V, Wei H, et al. Whole-genome analysis of histone H3 lysine 4 and lysine 27 methylation in human embryonic stem cells. Cell Stem Cell. 2007;1(3):299-312.

312. Zhao XD, Han X, Chew JL, Liu J, Chiu KP, Choo A, et al. Whole-genome mapping of histone H3 Lys4 and 27 trimethylations reveals distinct genomic compartments in human embryonic stem cells. Cell Stem Cell. 2007;1(3):286-98.

313. Vastenhouw NL, Zhang Y, Woods IG, Imam F, Regev A, Liu XS, et al. Chromatin signature of embryonic pluripotency is established during genome activation. Nature. 2010;464(7290):922-6.

314. Means AL, Gudas LJ. The roles of retinoids in vertebrate development. Annu Rev Biochem. 1995;64:201-33.

315. Bastien J, Rochette-Egly C. Nuclear retinoid receptors and the transcription of retinoid-target genes. Gene. 2004;328:1-16.

316. Mark M, Ghyselinck NB, Chambon P. Function of retinoid nuclear receptors: lessons from genetic and pharmacological dissections of the retinoic acid signaling pathway during mouse embryogenesis. Annu Rev Pharmacol Toxicol. 2006;46:451-80.

317. Langston AW, Gudas LJ. Identification of a retinoic acid responsive enhancer 3' of the murine homeobox gene Hox-1.6. Mech Dev. 1992;38(3):217-27.

318. Langston AW, Thompson JR, Gudas LJ. Retinoic acid-responsive enhancers located 3' of the Hox A and Hox B homeobox gene clusters. Functional analysis. J Biol Chem. 1997;272(4):2167-75.

319. Mainguy G, In der Rieden PM, Berezikov E, Woltering JM, Plasterk RH, Durston AJ. A position-dependent organisation of retinoid response elements is conserved in the vertebrate Hox clusters. Trends Genet. 2003;19(9):476-9.

320. Glass CK, Rosenfeld MG. The coregulator exchange in transcriptional functions of nuclear receptors. Genes Dev. 2000;14(2):121-41.

321. Li J, Wang J, Wang J, Nawaz Z, Liu JM, Qin J, et al. Both corepressor proteins SMRT and N-CoR exist in large protein complexes containing HDAC3. EMBO J. 2000;19(16):4342-50.

322. Rochette-Egly C. Dynamic combinatorial networks in nuclear receptor-mediated transcription. J Biol Chem. 2005;280(38):32565-8.

323. Kouzarides T. Acetylation: a regulatory modification to rival phosphorylation? EMBO J. 2000;19(6):1176-9.

324. Grozinger CM, Schreiber SL. Deacetylase enzymes: biological functions and the use of small-molecule inhibitors. Chem Biol. 2002;9(1):3-16.

325. Agger K, Cloos PA, Christensen J, Pasini D, Rose S, Rappsilber J, et al. UTX and JMJD3 are histone H3K27 demethylases involved in HOX gene regulation and development. Nature. 2007;449(7163):731-4.

326. Gillespie RF, Gudas LJ. Retinoic acid receptor isotype specificity in F9 teratocarcinoma stem cells results from the differential recruitment of coregulators to retinoic response elements. J Biol Chem. 2007;282(46):33421-34.

327. Boyer LA, Plath K, Zeitlinger J, Brambrink T, Medeiros LA, Lee TI, et al. Polycomb complexes repress developmental regulators in murine embryonic stem cells. Nature. 2006;441(7091):349-53.

328. Lee TI, Jenner RG, Boyer LA, Guenther MG, Levine SS, Kumar RM, et al. Control of developmental regulators by Polycomb in human embryonic stem cells. Cell. 2006;125(2):301-13.

329. Simon JA, Kingston RE. Occupying chromatin: Polycomb mechanisms for getting to genomic targets, stopping transcriptional traffic, and staying put. Mol Cell. 2013;49(5):808-24.

330. Negre N, Hennetin J, Sun LV, Lavrov S, Bellis M, White KP, et al. Chromosomal distribution of PcG proteins during Drosophila development. PLoS Biol. 2006;4(6):e170.

331. Woo CJ, Kharchenko PV, Daheron L, Park PJ, Kingston RE. A region of the human HOXD cluster that confers polycomb-group responsiveness. Cell. 2010;140(1):99-110.

332. McGinnis W, Levine MS, Hafen E, Kuroiwa A, Gehring WJ. A conserved DNA sequence in homoeotic genes of the Drosophila Antennapedia and bithorax complexes. Nature. 1984;308(5958):428-33.

333. Scott MP, Weiner AJ. Structural relationships among genes that control development: sequence homology between the Antennapedia, Ultrabithorax, and fushi tarazu loci of Drosophila. Proc Natl Acad Sci U S A. 1984;81(13):4115-9.

334. Gehring WJ, Qian YQ, Billeter M, Furukubo-Tokunaga K, Schier AF, Resendez-Perez D, et al. Homeodomain-DNA recognition. Cell. 1994;78(2):211-23.

335. Burglin T. Comprehensive classification of homeobox genes. In: Duboule D, editor. Guidebook to the Homeobox Genes. Oxford, UK.: Oxford University Press; 1994.

336. Banerjee-Basu S, Baxevanis AD. Molecular evolution of the homeodomain family of transcription factors. Nucleic Acids Res. 2001;29(15):3258-69.

337. Pearson JC, Lemons D, McGinnis W. Modulating Hox gene functions during animal body patterning. Nat Rev Genet. 2005;6(12):893-904.

338. Holland PW, Booth HA, Bruford EA. Classification and nomenclature of all human homeobox genes. BMC Biol. 2007;5:47.

339. Garcia-Fernandez J. The genesis and evolution of homeobox gene clusters. Nat Rev Genet. 2005;6(12):881-92.

340. Gaunt SJ. The significance of Hox gene collinearity. Int J Dev Biol. 2015;59(4-6):159-70.

341. Dressler GR, Gruss P. Anterior boundaries of Hox gene expression in mesoderm-derived structures correlate with the linear gene order along the chromosome. Differentiation. 1989;41(3):193-201.

342. Duboule D, Dolle P. The structural and functional organization of the murine HOX gene family resembles that of Drosophila homeotic genes. EMBO J. 1989;8(5):1497-505.

343. Graham A, Papalopulu N, Krumlauf R. The murine and Drosophila homeobox gene complexes have common features of organization and expression. Cell. 1989;57(3):367-78.

344. Gaunt SJ. Expression patterns of mouse Hox genes: clues to an understanding of developmental and evolutionary strategies. Bioessays. 1991;13(10):505-13.

345. Izpisua-Belmonte JC, Falkenstein H, Dolle P, Renucci A, Duboule D. Murine genes related to the Drosophila AbdB homeotic genes are sequentially expressed during development of the posterior part of the body. EMBO J. 1991;10(8):2279-89.

346. Gaunt SJ, Strachan L. Temporal colinearity in expression of anterior Hox genes in developing chick embryos. Dev Dyn. 1996;207(3):270-80.

347. Deschamps J, van Nes J. Developmental regulation of the Hox genes during axial morphogenesis in the mouse. Development. 2005;132(13):2931-42.

348. Iimura T, Pourquie O. Collinear activation of Hoxb genes during gastrulation is linked to mesoderm cell ingression. Nature. 2006;442(7102):568-71.

349. Hombria JC, Lovegrove B. Beyond homeosis--HOX function in morphogenesis and organogenesis. Differentiation. 2003;71(8):461-76.

350. Condie BG, Capecchi MR. Mice with targeted disruptions in the paralogous genes hoxa-3 and hoxd-3 reveal synergistic interactions. Nature. 1994;370(6487):304-7.

351. Kostic D, Capecchi MR. Targeted disruptions of the murine Hoxa-4 and Hoxa-6 genes result in homeotic transformations of components of the vertebral column. Mech Dev. 1994;46(3):231-47.

352. Horan GS, Ramirez-Solis R, Featherstone MS, Wolgemuth DJ, Bradley A, Behringer RR. Compound mutants for the paralogous hoxa-4, hoxb-4, and hoxd-4 genes show more complete homeotic transformations and a dose-dependent increase in the number of vertebrae transformed. Genes Dev. 1995;9(13):1667-77.

353. Fromental-Ramain C, Warot X, Lakkaraju S, Favier B, Haack H, Birling C, et al. Specific and redundant functions of the paralogous Hoxa-9 and Hoxd-9 genes in forelimb and axial skeleton patterning. Development. 1996;122(2):461-72.

354. McIntyre DC, Rakshit S, Yallowitz AR, Loken L, Jeannotte L, Capecchi MR, et al. Hox patterning of the vertebrate rib cage. Development. 2007;134(16):2981-9.

355. van den Akker E, Fromental-Ramain C, de Graaff W, Le Mouellic H, Brulet P, Chambon P, et al. Axial skeletal patterning in mice lacking all paralogous group 8 Hox genes. Development. 2001;128(10):1911-21.

356. Wellik DM, Capecchi MR. Hox10 and Hox11 genes are required to globally pattern the mammalian skeleton. Science. 2003;301(5631):363-7.

357. Mallo M, Wellik DM, Deschamps J. Hox genes and regional patterning of the vertebrate body plan. Dev Biol. 2010;344(1):7-15.

358. Moens CB, Selleri L. Hox cofactors in vertebrate development. Dev Biol. 2006;291(2):193-206.

359. Seifert A, Werheid DF, Knapp SM, Tobiasch E. Role of Hox genes in stem cell differentiation. World J Stem Cells. 2015;7(3):583-95.

360. Fromental-Ramain C, Warot X, Messadecq N, LeMeur M, Dolle P, Chambon P. Hoxa-13 and Hoxd-13 play a crucial role in the patterning of the limb autopod. Development. 1996;122(10):2997-3011.

361. Raines AM, Magella B, Adam M, Potter SS. Key pathways regulated by HoxA9,10,11/HoxD9,10,11 during limb development. BMC Dev Biol. 2015;15:28.

362. Merabet S, Galliot B. The TALE face of Hox proteins in animal evolution. Front Genet. 2015;6:267.

363. Mukherjee K, Burglin TR. Comprehensive analysis of animal TALE homeobox genes: new conserved motifs and cases of accelerated evolution. J Mol Evol. 2007;65(2):137-53.

364. Burglin TR. Analysis of TALE superclass homeobox genes (MEIS, PBC, KNOX, Iroquois, TGIF) reveals a novel domain conserved between plants and animals. Nucleic Acids Res. 1997;25(21):4173-80.

365. Burglin TR. The PBC domain contains a MEINOX domain: coevolution of Hox and TALE homeobox genes? Dev Genes Evol. 1998;208(2):113-6.

366. Bürglin TR. Homeodomain proteins. In: Meyers RA, editor. Encyclopedia of Molecular Cell Biology and Molecular Medicine. 6. 2nd ed. Weinheim: Wiley-VCH Verlag GmbH & Co.; 2005. p. 179-222.

367. Berthelsen J, Zappavigna V, Ferretti E, Mavilio F, Blasi F. The novel homeoprotein Prep1 modulates Pbx-Hox protein cooperativity. EMBO J. 1998;17(5):1434-45.

368. Berthelsen J, Zappavigna V, Mavilio F, Blasi F. Prep1, a novel functional partner of Pbx proteins. EMBO J. 1998;17(5):1423-33.

369. Williams TM, Williams ME, Innis JW. Range of HOX/TALE superclass associations and protein domain requirements for HOXA13:MEIS interaction. Dev Biol. 2005;277(2):457-71.

370. Fognani C, Kilstrup-Nielsen C, Berthelsen J, Ferretti E, Zappavigna V, Blasi F. Characterization of PREP2, a paralog of PREP1, which defines a novel sub-family of the MEINOX TALE homeodomain transcription factors. Nucleic Acids Res. 2002;30(9):2043-51.

371. Noyes MB, Christensen RG, Wakabayashi A, Stormo GD, Brodsky MH, Wolfe SA. Analysis of homeodomain specificities allows the family-wide prediction of preferred recognition sites. Cell. 2008;133(7):1277-89.

372. Knoepfler PS, Calvo KR, Chen H, Antonarakis SE, Kamps MP. Meis1 and pKnox1 bind DNA cooperatively with Pbx1 utilizing an interaction surface disrupted in oncoprotein E2a-Pbx1. Proc Natl Acad Sci U S A. 1997;94(26):14553-8.

373. Penkov D, Mateos San Martin D, Fernandez-Diaz LC, Rossello CA, Torroja C, Sanchez-Cabo F, et al. Analysis of the DNA-binding profile and function of TALE homeoproteins reveals their specialization and specific interactions with Hox genes/proteins. Cell Rep. 2013;3(4):1321-33.

374. Piper DE, Batchelor AH, Chang CP, Cleary ML, Wolberger C. Structure of a HoxB1-Pbx1 heterodimer bound to DNA: role of the hexapeptide and a fourth homeodomain helix in complex formation. Cell. 1999;96(4):587-97.

375. Takahashi Y, Hamada J, Murakawa K, Takada M, Tada M, Nogami I, et al. Expression profiles of 39 HOX genes in normal human adult organs and anaplastic thyroid cancer cell lines by quantitative real-time RT-PCR system. Exp Cell Res. 2004;293(1):144-53.

376. Bosch J, Houben AP, Radke TF, Stapelkamp D, Bunemann E, Balan P, et al. Distinct differentiation potential of "MSC" derived from cord blood and umbilical cord: are cord-derived cells true mesenchymal stromal cells? Stem Cells Dev. 2012;21(11):1977-88.

377. Sagi B, Maraghechi P, Urban VS, Hegyi B, Szigeti A, Fajka-Boja R, et al. Positional identity of murine mesenchymal stem cells resident in different organs is determined in the postsegmentation mesoderm. Stem Cells Dev. 2012;21(5):814-28.

378. Chae SW, Jee BK, Lee JY, Han CW, Jeon YW, Lim Y, et al. HOX gene analysis in the osteogenic differentiation of human mesenchymal stem cells. Genetics and Molecular Biology. 2008;31(4):815-23.

379. Rux DR, Song JY, Swinehart IT, Pineault KM, Schlientz AJ, Trulik KG, et al. Regionally Restricted Hox Function in Adult Bone Marrow Multipotent Mesenchymal Stem/Stromal Cells. Dev Cell. 2016;39(6):653-66.

380. Chung N, Jee BK, Chae SW, Jeon YW, Lee KH, Rha HK. HOX gene analysis of endothelial cell differentiation in human bone marrow-derived mesenchymal stem cells. Mol Biol Rep. 2009;36(2):227-35.

381. Man YG, Fu SW, Schwartz A, Pinzone JJ, Simmens SJ, Berg PE. Expression of BP1, a novel homeobox gene, correlates with breast cancer progression and invasion. Breast Cancer Res Treat. 2005;90(3):241-7.

382. Samuel S, Naora H. Homeobox gene expression in cancer: insights from developmental regulation and deregulation. Eur J Cancer. 2005;41(16):2428-37.

383. Wu X, Chen H, Parker B, Rubin E, Zhu T, Lee JS, et al. HOXB7, a homeodomain protein, is overexpressed in breast cancer and confers epithelial-mesenchymal transition. Cancer Res. 2006;66(19):9527-34.

384. Argiropoulos B, Humphries RK. Hox genes in hematopoiesis and leukemogenesis. Oncogene. 2007;26(47):6766-76.

385. Rauch T, Wang Z, Zhang X, Zhong X, Wu X, Lau SK, et al. Homeobox gene methylation in lung cancer studied by genome-wide analysis with a microarray-based methylated CpG island recovery assay. Proc Natl Acad Sci U S A. 2007;104(13):5527-32.

386. Ma L, Teruya-Feldstein J, Weinberg RA. Tumour invasion and metastasis initiated by microRNA-10b in breast cancer. Nature. 2007;449(7163):682-8.

387. Rinn JL, Kertesz M, Wang JK, Squazzo SL, Xu X, Brugmann SA, et al. Functional demarcation of active and silent chromatin domains in human HOX loci by noncoding RNAs. Cell. 2007;129(7):1311-23.

388. Care A, Silvani A, Meccia E, Mattia G, Peschle C, Colombo MP. Transduction of the SkBr3 breast carcinoma cell line with the HOXB7 gene induces bFGF expression, increases cell proliferation and reduces growth factor dependence. Oncogene. 1998;16(25):3285-9.

389. Care A, Felicetti F, Meccia E, Bottero L, Parenza M, Stoppacciaro A, et al. HOXB7: a key factor for tumor-associated angiogenic switch. Cancer Res. 2001;61(17):6532-9.

390. Naora H, Yang YQ, Montz FJ, Seidman JD, Kurman RJ, Roden RB. A serologically identified tumor antigen encoded by a homeobox gene promotes growth of ovarian epithelial cells. Proc Natl Acad Sci U S A. 2001;98(7):4060-5.

391. Yoshida H, Broaddus R, Cheng W, Xie S, Naora H. Deregulation of the HOXA10 homeobox gene in endometrial carcinoma: role in epithelial-mesenchymal transition. Cancer Res. 2006;66(2):889-97.

392. Storti P, Donofrio G, Colla S, Airoldi I, Bolzoni M, Agnelli L, et al. HOXB7 expression by myeloma cells regulates their pro-angiogenic properties in multiple myeloma patients. Leukemia. 2011;25(3):527-37.

393. Jin K, Kong X, Shah T, Penet MF, Wildes F, Sgroi DC, et al. The HOXB7 protein renders breast cancer cells resistant to tamoxifen through activation of the EGFR pathway. Proc Natl Acad Sci U S A. 2012;109(8):2736-41.

394. Ko SY, Barengo N, Ladanyi A, Lee JS, Marini F, Lengyel E, et al. HOXA9 promotes ovarian cancer growth by stimulating cancer-associated fibroblasts. J Clin Invest. 2012;122(10):3603-17.

395. Rubin E, Wu X, Zhu T, Cheung JC, Chen H, Lorincz A, et al. A role for the HOXB7 homeodomain protein in DNA repair. Cancer Res. 2007;67(4):1527-35.

396. Gille JJ, Floor K, Kerkhoven L, Ameziane N, Joenje H, de Winter JP. Diagnosis of Fanconi Anemia: Mutation Analysis by Multiplex Ligation-Dependent Probe Amplification and PCR-Based Sanger Sequencing. Anemia. 2012;2012:603253.

397. Schouten JP, McElgunn CJ, Waaijer R, Zwijnenburg D, Diepvens F, Pals G. Relative quantification of 40 nucleic acid sequences by multiplex ligation-dependent probe amplification. Nucleic Acids Res. 2002;30(12):e57.

398. Naipal KA, Verkaik NS, Ameziane N, van Deurzen CH, Ter Brugge P, Meijers M, et al. Functional ex vivo assay to select homologous recombination-deficient breast tumors for PARP inhibitor treatment. Clin Cancer Res. 2014;20(18):4816-26.

399. Livak KJ, Schmittgen TD. Analysis of relative gene expression data using real-time quantitative PCR and the 2(-Delta Delta C(T)) Method. Methods. 2001;25(4):402-8.

400. Auerbach AD. Diagnosis of fanconi anemia by diepoxybutane analysis. Curr Protoc Hum Genet. 2003;Chapter 8:Unit 8 7.

401. Auerbach AD. Diagnosis of Fanconi anemia by diepoxybutane analysis. Curr Protoc Hum Genet. 2015;85:8 7 1-17.

402. Zuk PA, Zhu M, Mizuno H, Huang J, Futrell JW, Katz AJ, et al. Multilineage cells from human adipose tissue: implications for cell-based therapies. Tissue Eng. 2001;7(2):211-28.

403. Dimri GP, Lee X, Basile G, Acosta M, Scott G, Roskelley C, et al. A biomarker that identifies senescent human cells in culture and in aging skin in vivo. Proc Natl Acad Sci U S A. 1995;92(20):9363-7.

404. Lee BY, Han JA, Im JS, Morrone A, Johung K, Goodwin EC, et al. Senescence-associated beta-galactosidase is lysosomal beta-galactosidase. Aging Cell. 2006;5(2):187-95.

405. Davarinejad H. Quantifications of Western Blots with ImageJ [Internet]. [Accessed on 01 October 2017]. Available from: http://www.yorku.ca/yisheng/Internal/Protocols/ImageJ.pdf

406. Vincze T, Posfai J, Roberts RJ. NEBcutter: A program to cleave DNA with restriction enzymes. Nucleic Acids Res. 2003;31(13):3688-91.

407. Fraser SP, Salvador V, Manning EA, Mizal J, Altun S, Raza M, et al. Contribution of functional voltage-gated Na+ channel expression to cell behaviors involved in the metastatic cascade in rat prostate cancer: I. Lateral motility. J Cell Physiol. 2003;195(3):479-87.

408. Gregory CA, Gunn WG, Peister A, Prockop DJ. An Alizarin red-based assay of mineralization by adherent cells in culture: comparison with cetylpyridinium chloride extraction. Anal Biochem. 2004;329(1):77-84.

409. van Buuren S, Groothuis-Oudshoorn K. mice: Multivariate Imputation by Chained Equations in R. Journal of Statistical Sotware. 2011;45:1-67.

410. Azur MJ, Stuart EA, Frangakis C, Leaf PJ. Multiple imputation by chained equations: what is it and how does it work? Int J Methods Psychiatr Res. 2011;20(1):40-9.

411. Waljee AK, Mukherjee A, Singal AG, Zhang Y, Warren J, Balis U, et al. Comparison of imputation methods for missing laboratory data in medicine. BMJ Open. 2013;3(8).

412. Oliveros JC. Venny. An interactive tool for comparing lists with Venn's diagrams [Internet]. 2007-2015 [Accessed on 01 October 2017]. Available from: http://bioinfogp.cnb.csic.es/tools/venny/index.html

413. Ashburner M, Ball CA, Blake JA, Botstein D, Butler H, Cherry JM, et al. Gene ontology: tool for the unification of biology. The Gene Ontology Consortium. Nat Genet. 2000;25(1):25-9.

414. The Gene Ontology Consortium. Expansion of the Gene Ontology knowledgebase and resources. Nucleic Acids Res. 2017;45(D1):D331-8.

415. Mi H, Huang X, Muruganujan A, Tang H, Mills C, Kang D, et al. PANTHER version 11: expanded annotation data from Gene Ontology and Reactome pathways, and data analysis tool enhancements. Nucleic Acids Res. 2017;45(D1):D183-9.

416. Patil A, Nakai K, Nakamura. HitPredict: a database of quality assessed protein-protein interactions in nine species. Nucleic Acids Res. 2011;39:D744-9.

417. Patil A, Nakamura H. Filtering high-throughput protein-protein interaction data using a combination of genomic features. BMC Bioinformatics. 2005;6:100.

418. Lopez Y, Nakai K, Patil A. HitPredict version 4: comprehensive reliability scoring of physical protein-protein interactions from more than 100 species. Database. 2015;bav117.

419. Mindaye ST, Ra M, Lo Surdo JL, Bauer SR, Alterman MA. Global proteomic signature of undifferentiated human bone marrow stromal cells: evidence for donor-to-donor proteome heterogeneity. Stem Cell Res. 2013;11(2):793-805.

420. Castella M, Pujol R, Callen E, Trujillo JP, Casado JA, Gille H, et al. Origin, functional role, and clinical impact of Fanconi anemia FANCA mutations. Blood. 2011;117(14):3759-69.

421. Liu TX, Howlett NG, Deng M, Langenau DM, Hsu K, Rhodes J, et al. Knockdown of zebrafish Fancd2 causes developmental abnormalities via p53-dependent apoptosis. Dev Cell. 2003;5(6):903-14.

422. Taniguchi T, Garcia-Higuera I, Andreassen PR, Gregory RC, Grompe M, D'Andrea AD. S-phase-specific interaction of the Fanconi anemia protein, FANCD2, with BRCA1 and RAD51. Blood. 2002;100(7):2414-20.

423. Kalb R, Neveling K, Hoehn H, Schneider H, Linka Y, Batish SD, et al. Hypomorphic mutations in the gene encoding a key Fanconi anemia protein, FANCD2, sustain a significant group of FA-D2 patients with severe phenotype. Am J Hum Genet. 2007;80(5):895-910.

424. Guo Z, Yang J, Liu X, Li X, Hou C, Tang PH, et al. Biological features of mesenchymal stem cells from human bone marrow. Chin Med J (Engl). 2001;114(9):950-3.

425. Fa X, Lixia W, Hou J, Zhang R, Wang H, Yang C. Biological characteristics of human bone marrow mesenchymal stem cell cultured in vitro. J Huazhong Univ Sci Technolog Med Sci. 2005;25(3):307-9.

426. Maijenburg MW, Kleijer M, Vermeul K, Mul EP, van Alphen FP, van der Schoot CE, et al. The composition of the mesenchymal stromal cell compartment in human bone marrow changes during development and aging. Haematologica. 2012;97(2):179-83.

427. Espagnolle N, Guilloton F, Deschaseaux F, Gadelorge M, Sensebe L, Bourin P. CD146 expression on mesenchymal stem cells is associated with their vascular smooth muscle commitment. J Cell Mol Med. 2014;18(1):104-14.

428. Halfon S, Abramov N, Grinblat B, Ginis I. Markers distinguishing mesenchymal stem cells from fibroblasts are downregulated with passaging. Stem Cells Dev. 2011;20(1):53-66.

429. Levesque JP, Takamatsu Y, Nilsson SK, Haylock DN, Simmons PJ. Vascular cell adhesion molecule-1 (CD106) is cleaved by neutrophil proteases in the bone marrow following hematopoietic progenitor cell mobilization by granulocyte colony-stimulating factor. Blood. 2001;98(5):1289-97.

430. Baddoo M, Hill K, Wilkinson R, Gaupp D, Hughes C, Kopen GC, et al. Characterization of mesenchymal stem cells isolated from murine bone marrow by negative selection. J Cell Biochem. 2003;89(6):1235-49.

431. Puissant B, Barreau C, Bourin P, Clavel C, Corre J, Bousquet C, et al. Immunomodulatory effect of human adipose tissue-derived adult stem cells: comparison with bone marrow mesenchymal stem cells. Br J Haematol. 2005;129(1):118-29.

432. Delorme B, Charbord P. Culture and characterization of human bone marrow mesenchymal stem cells. Methods Mol Med. 2007;140:67-81.

433. Lee TC, Lee TH, Huang YH, Chang NK, Lin YJ, Chien PW, et al. Comparison of surface markers between human and rabbit mesenchymal stem cells. PLoS One. 2014;9(11):e111390.

434. Ip JE, Wu Y, Huang J, Zhang L, Pratt RE, Dzau VJ. Mesenchymal stem cells use integrin beta1 not CXC chemokine receptor 4 for myocardial migration and engraftment. Mol Biol Cell. 2007;18(8):2873-82.

435. Ode A, Kopf J, Kurtz A, Schmidt-Bleek K, Schrade P, Kolar P, et al. CD73 and CD29 concurrently mediate the mechanically induced decrease of migratory capacity of mesenchymal stromal cells. Eur Cell Mater. 2011;22:26-42.

436. Pietila M, Lehtonen S, Tuovinen E, Lahteenmaki K, Laitinen S, Leskela HV, et al. CD200 positive human mesenchymal stem cells suppress TNF-alpha secretion from CD200 receptor positive macrophage-like cells. PLoS One. 2012;7(2):e31671.

437. Muruganandan S, Roman AA, Sinal CJ. Adipocyte differentiation of bone marrow-derived mesenchymal stem cells: cross talk with the osteoblastogenic program. Cell Mol Life Sci. 2009;66(2):236-53.

438. Graneli C, Thorfve A, Ruetschi U, Brisby H, Thomsen P, Lindahl A, et al. Novel markers of osteogenic and adipogenic differentiation of human bone marrow stromal cells identified using a quantitative proteomics approach. Stem Cell Res. 2014;12(1):153-65.

439. Guillot PV, De Bari C, Dell'Accio F, Kurata H, Polak J, Fisk NM. Comparative osteogenic transcription profiling of various fetal and adult mesenchymal stem cell sources. Differentiation. 2008;76(9):946-57.

440. Miron RJ, Zhang YF. Osteoinduction: a review of old concepts with new standards. J Dent Res. 2012;91(8):736-44.

441. Zhou Y, He Y, Xing W, Zhang P, Shi H, Chen S, et al. An abnormal bone marrow microenvironment contributes to hematopoietic dysfunction in Fanconi anemia. Haematologica. 2017;102(6):1017-27.

442. Yun J, Zhong Q, Kwak JY, Lee WH. Hypersensitivity of Brca1-deficient MEF to the DNA interstrand crosslinking agent mitomycin C is associated with defect in homologous recombination repair and aberrant S-phase arrest. Oncogene. 2005;24(25):4009-16.

443. Bellagamba BC, Abreu BR, Grivicich I, Markarian CF, Chem E, Camassola M, et al. Human mesenchymal stem cells are resistant to cytotoxic and genotoxic effects of cisplatin in vitro. Genet Mol Biol. 2016;39(1):129-34.

444. Fujita T, Epperly MW, Zou H, Greenberger JS, Wan Y. Regulation of the anaphase-promoting complex-separase cascade by transforming growth factor-beta modulates mitotic progression in bone marrow stromal cells. Mol Biol Cell. 2008;19(12):5446-55.

445. Blank U, Karlsson G, Karlsson S. Signaling pathways governing stem-cell fate. Blood. 2008;111(2):492-503.

446. Chagraoui H, Komura E, Tulliez M, Giraudier S, Vainchenker W, Wendling F. Prominent role of TGF-beta 1 in thrombopoietin-induced myelofibrosis in mice. Blood. 2002;100(10):3495-503.

447. Li J, Tripathi BJ, Chalam KV, Tripathi RC. Transforming growth factor-beta 1 and -beta 2 positively regulate TGF-beta 1 mRNA expression in trabecular cells. Invest Ophthalmol Vis Sci. 1996;37(13):2778-82.

448. Letterio JJ, Geiser AG, Kulkarni AB, Dang H, Kong L, Nakabayashi T, et al. Autoimmunity associated with TGF-beta1-deficiency in mice is dependent on MHC class II antigen expression. J Clin Invest. 1996;98(9):2109-19.

449. Babushok DV, Duke JL, Xie HM, Stanley N, Atienza J, Perdigones N, et al. Somatic HLA Mutations Expose the Role of Class I-Mediated Autoimmunity in Aplastic Anemia and its Clonal Complications. Blood Adv. 2017;1(22):1900-10.

450. Wimmel A, Wiedenmann B, Rosewicz S. Autocrine growth inhibition by transforming growth factor beta-1 (TGFbeta-1) in human neuroendocrine tumour cells. Gut. 2003;52(9):1308-16.

451. Ikushima H, Todo T, Ino Y, Takahashi M, Miyazawa K, Miyazono K. Autocrine TGF-beta signaling maintains tumorigenicity of glioma-initiating cells through Sry-related HMG-box factors. Cell Stem Cell. 2009;5(5):504-14.

452. Perrot CY, Javelaud D, Mauviel A. Insights into the Transforming Growth Factor-beta Signaling Pathway in Cutaneous Melanoma. Ann Dermatol. 2013;25(2):135-44.

453. Rizzo S, Killick SB, Patel S, Ball SE, Wadhwa M, Dilger P, et al. Reduced TGF-beta1 in patients with aplastic anaemia in vivo and in vitro. Br J Haematol. 1999;107(4):797-803.

454. Wu J, Niu J, Li X, Wang X, Guo Z, Zhang F. TGF-beta1 induces senescence of bone marrow mesenchymal stem cells via increase of mitochondrial ROS production. BMC Dev Biol. 2014;14:21.

455. Kumari U, Ya Jun W, Huat Bay B, Lyakhovich A. Evidence of mitochondrial dysfunction and impaired ROS detoxifying machinery in Fanconi anemia cells. Oncogene. 2014;33(2):165-72.

456. He T, Quan T, Shao Y, Voorhees JJ, Fisher GJ. Oxidative exposure impairs TGF-beta pathway via reduction of type II receptor and SMAD3 in human skin fibroblasts. Age (Dordr). 2014;36(3):9623.

457. Bhatlekar S, Fields JZ, Boman BM. HOX genes and their role in the development of human cancers. J Mol Med (Berl). 2014;92(8):811-23.

458. Platais C, Hakami F, Darda L, Lambert DW, Morgan R, Hunter KD. The role of HOX genes in head and neck squamous cell carcinoma. J Oral Pathol Med. 2016;45(4):239-47.

459. Cao H, Shockey JM. Comparison of TaqMan and SYBR Green qPCR methods for quantitative gene expression in tung tree tissues. J Agric Food Chem. 2012;60(50):12296-303.

460. Greenbaum D, Colangelo C, Williams K, Gerstein M. Comparing protein abundance and mRNA expression levels on a genomic scale. Genome Biol. 2003;4(9):117.

461. Imoto I, Sonoda I, Yuki Y, Inazawa J. Identification and characterization of human PKNOX2, a novel homeobox-containing gene. Biochem Biophys Res Commun. 2001;287(1):270-6.

462. Haller K, Rambaldi I, Kovacs EN, Daniels E, Featherstone M. Prep2: cloning and expression of a new prep family member. Dev Dyn. 2002;225(3):358-64.

463. Chang I, Parrilla M. Expression patterns of homeobox genes in the mouse vomeronasal organ at postnatal stages. Gene Expr Patterns. 2016;21(2):69-80.

464. Haller K, Rambaldi I, Daniels E, Featherstone M. Subcellular localization of multiple PREP2 isoforms is regulated by actin, tubulin, and nuclear export. J Biol Chem. 2004;279(47):49384-94.

465. Hurov KE, Cotta-Ramusino C, Elledge SJ. A genetic screen identifies the Triple T complex required for DNA damage signaling and ATM and ATR stability. Genes Dev. 2010;24(17):1939-50.

466. Wang KS, Zhang Q, Liu X, Wu L, Zeng M. PKNOX2 is associated with formal thought disorder in schizophrenia: a meta-analysis of two genome-wide association studies. J Mol Neurosci. 2012;48(1):265-72.

467. Zuo L, Lu L, Tan Y, Pan X, Cai Y, Wang X, et al. Genome-wide association discoveries of alcohol dependence. Am J Addict. 2014;23(6):526-39.

468. NCBI Conserved Domains [Internet]. [Accessed on 01 October 2017]. Available from: https://www.ncbi.nlm.nih.gov/Structure/cdd/wrpsb.cgi

469. Zhou W, Zhu H, Zhao J, Li H, Wan Y, Cao J, et al. Misexpression of Pknox2 in mouse limb bud mesenchyme perturbs zeugopod development and deltoid crest formation. PLoS One. 2013;8(5):e64237.

470. Walenda G, Abnaof K, Joussen S, Meurer S, Smeets H, Rath B, et al. TGF-beta1 does not induce senescence of multipotent mesenchymal stromal cells and has similar effects in early and late passages. PLoS One. 2013;8(10):e77656.

471. Haley JA, Haughney E, Ullman E, Bean J, Haley JD, Fink MY. Altered Transcriptional Control Networks with Trans-Differentiation of Isogenic Mutant-KRas NSCLC Models. Front Oncol. 2014;4:344.

472. Valluru M, Staton CA, Reed MWR, Brown NJ. Transforming growth factor-β and endoglin signalling orchestrate wound healing. Frontiers in Physiology. 2011;2:89.

473. Seita J, Weissman IL. Hematopoietic stem cell: self-renewal versus differentiation. Wiley Interdiscip Rev Syst Biol Med. 2010;2(6):640-53.

474. Baum CM, Weissman IL, Tsukamoto AS, Buckle AM, Peault B. Isolation of a candidate human hematopoietic stem-cell population. Proc Natl Acad Sci U S A. 1992;89(7):2804-8.

475. Huang S, Terstappen LW. Lymphoid and myeloid differentiation of single human CD34+, HLA-DR+, CD38- hematopoietic stem cells. Blood. 1994;83(6):1515-26.

476. Petzer AL, Hogge DE, Landsdorp PM, Reid DS, Eaves CJ. Self-renewal of primitive human hematopoietic cells (long-term-culture-initiating cells) in vitro and their expansion in defined medium. Proc Natl Acad Sci U S A. 1996;93(4):1470-4.

477. Hao QL, Thiemann FT, Petersen D, Smogorzewska EM, Crooks GM. Extended long-term culture reveals a highly quiescent and primitive human hematopoietic progenitor population. Blood. 1996;88(9):3306-13.

478. Miller JS, McCullar V, Punzel M, Lemischka IR, Moore KA. Single adult human CD34(+)/Lin-/CD38(-) progenitors give rise to natural killer cells, B-lineage cells, dendritic cells, and myeloid cells. Blood. 1999;93(1):96-106.

479. McKenzie JL, Gan OI, Doedens M, Dick JE. Reversible cell surface expression of CD38 on CD34-positive human hematopoietic repopulating cells. Exp Hematol. 2007;35(9):1429-36.

480. Hanna J, Hubel A. Preservation of stem cells. Organogenesis. 2009;5(3):134-7.

481. Ikeda H, Toyama D, Matsuno R, Fujmoto Y, Isoyama K. Aldehyde dehydrogenase activity as a marker of quality in cryopreserved cord blood. The Showa University Journal of Medical Sciences. 2013;25(4):297-306.

482. Perez-Oteyza J, Bornstein R, Corral M, Hermosa V, Alegre A, Torrabadella M, et al. Controlled-rate versus uncontrolled-rate cryopreservation of peripheral blood progenitor cells: a prospective multicenter study. Group for Cryobiology and Biology of Bone Marrow Transplantation (CBTMO), Spain. Haematologica. 1998;83(11):1001-5.

483. Balint B, Ivanovic Z, Petakov M, Taseski J, Jovcic G, Stojanovic N, et al. The cryopreservation protocol optimal for progenitor recovery is not optimal for preservation of marrow repopulating ability. Bone Marrow Transplant. 1999;23(6):613-9.

484. Baust JM, Van B, Baust JG. Cell viability improves following inhibition of cryopreservation-induced apoptosis. In Vitro Cell Dev Biol Anim. 2000;36(4):262-70.

485. Baust JM, Vogel MJ, Van Buskirk R, Baust JG. A molecular basis of cryopreservation failure and its modulation to improve cell survival. Cell Transplant. 2001;10(7):561-71.

486. Baust JM, Van Buskirk R, Baust JG. Modulation of the cryopreservation cap: elevated survival with reduced dimethyl sulfoxide concentration. Cryobiology. 2002;45(2):97-108.

487. Wingert S, Rieger MA. Terminal differentiation induction as DNA damage response in hematopoietic stem cells by GADD45A. Exp Hematol. 2016;44(7):561-6.

488. Sugrue T, Brown JA, Lowndes NF, Ceredig R. Multiple facets of the DNA damage response contribute to the radioresistance of mouse mesenchymal stromal cell lines. Stem Cells. 2013;31(1):137-45.

489. Cagnan I, Gunel-Ozcan A, Aerts-Kaya F, Ameziane A, Kuskonmaz B, Dorsman J, et al. Bone marrow mesenchymal stem cells carrying FANCD2 mutation differ from the other Fanconi anemia complementation groups in terms of TGF-β1 production. Stem Cell Rev. (in press). 2017. 10.1007/s12015-017-9794-5

8. APPENDICES

Appendix-1: Ethics Committee Permits Related to the Thesis

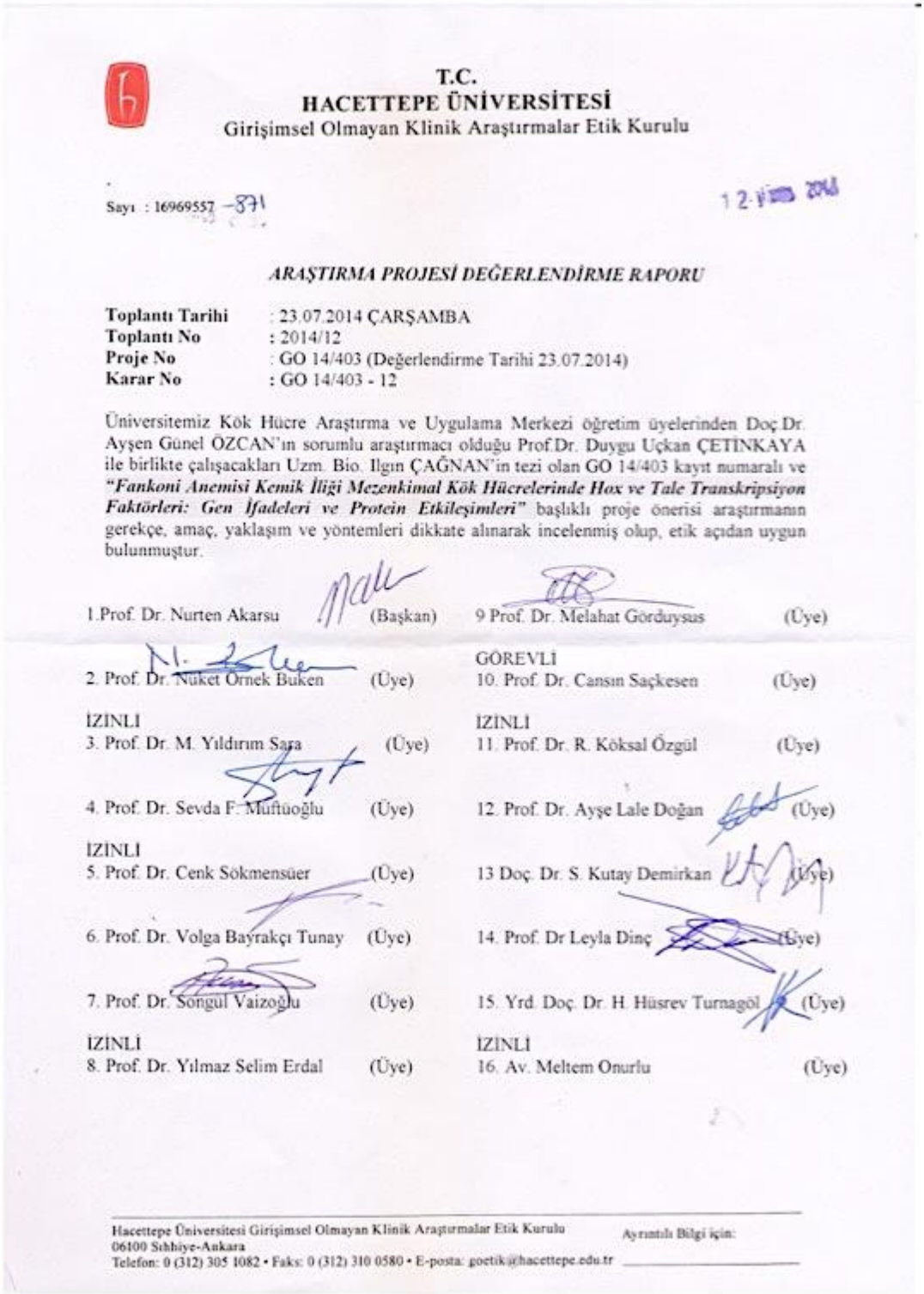

T.C.
HACETTEPE ÜNİVERSİTESİ
Girişimsel Olmayan Klinik Araştırmalar Etik Kurulu

Sayı : 16969557 -871

12 [illegible] 2014

ARAŞTIRMA PROJESİ DEĞERLENDİRME RAPORU

Toplantı Tarihi : 23.07.2014 ÇARŞAMBA
Toplantı No : 2014/12
Proje No : GO 14/403 (Değerlendirme Tarihi 23.07.2014)
Karar No : GO 14/403 - 12

Üniversitemiz Kök Hücre Araştırma ve Uygulama Merkezi öğretim üyelerinden Doç.Dr. Ayşen Günel ÖZCAN'ın sorumlu araştırmacı olduğu Prof.Dr. Duygu Uçkan ÇETİNKAYA ile birlikte çalışacakları Uzm. Bio. Ilgın ÇAĞNAN'in tezi olan GO 14/403 kayıt numaralı ve ***"Fankoni Anemisi Kemik İliği Mezenkimal Kök Hücrelerinde Hox ve Tale Transkripsiyon Faktörleri: Gen İfadeleri ve Protein Etkileşimleri"*** başlıklı proje önerisi araştırmanın gerekçe, amaç, yaklaşım ve yöntemleri dikkate alınarak incelenmiş olup, etik açıdan uygun bulunmuştur.

1.Prof. Dr. Nurten Akarsu (Başkan)
2. Prof. Dr. Nüket Örnek Büken (Üye)
İZİNLİ
3. Prof. Dr. M. Yıldırım Sara (Üye)
4. Prof. Dr. Sevda F. Müftüoğlu (Üye)
İZİNLİ
5. Prof. Dr. Cenk Sökmensüer (Üye)
6. Prof. Dr. Volga Bayrakçı Tunay (Üye)
7. Prof. Dr. Songül Vaizoğlu (Üye)
İZİNLİ
8. Prof. Dr. Yılmaz Selim Erdal (Üye)
9 Prof. Dr. Melahat Görduysus (Üye)
GÖREVLİ
10. Prof. Dr. Cansın Saçkesen (Üye)
İZİNLİ
11. Prof. Dr. R. Köksal Özgül (Üye)
12. Prof. Dr. Ayşe Lale Doğan (Üye)
13 Doç. Dr. S. Kutay Demirkan (Üye)
14. Prof. Dr Leyla Dinç (Üye)
15. Yrd. Doç. Dr. H. Hüsrev Turnagöl (Üye)
İZİNLİ
16. Av. Meltem Onurlu (Üye)

Hacettepe Üniversitesi Girişimsel Olmayan Klinik Araştırmalar Etik Kurulu
06100 Sıhhiye-Ankara
Telefon: 0 (312) 305 1082 • Faks: 0 (312) 310 0580 • E-posta: goetik@hacettepe.edu.tr
Ayrıntılı Bilgi için:

Appendix-2: Funding of the Thesis

Studies funded by #110S021 TUBİTAK 1001 project;

- Characterization of BM-MSCs derived from FA patients and donors
- HOX and TALE gene expression profile of BM-MSCs derived from FA patients and donors

Studies funded by #214Z033 TUBİTAK 1001 project;

- Evaluating PKNOX2 protein levels in BM-MSCs derived from FA patients and donors
- Levels of TGF-β1, TGF-β2, TGF-β3 secretion by BM-MSCs derived from FA patients and donors
- Inducing FA and donor BM-MSCs with rTGF-β1 protein
- PKNOX2 overexpression in BM-MSCs
- Characterization of PKNOX2 overexpressing BM-MSCs
- Following Co-IP, identifying proteins interacting with PKNOX2 using western-blotting
- Following Co-IP, identifying proteins interacting with PKNOX2 using mass spectrometry analysis

Appendix-2: (Continued) Funding of the Thesis

EK-1

PROJE ÖNERİSİ ÜZERİNDEKİ *ORTAK HAK* SAHİPLİĞİ BEYANI

(Bu form, hak sahipliği belirlenmeyen/bölünemeyen tüm hak sahipleri ile proje önerisinde adı geçen ve hak sahibi olmayan tüm proje ekibi - Proje yürütücüsü, Araştırmacı, Danışman ve Danışan - tarafından imzalanmalıdır.)

'HOX/TALE genlerinin Kemik İliği Nakli yapılan FANCONI anemisi hastalarının kemik iliği mezenkimal kök hücrelerindeki ekspresyon profillerinin saptanması ve HOX/TALE gen regulasyonunda rol oynayan tüm genom miRNA ve ekspresyon mikroarray korelasyonlarının araştırılması' başlıklı proje ile ilgili aşağıda imzaları bulunan biz, proje öneri formunda sunulan tüm veri ve bilgilerin kendimize ait ve 5846 sayılı Fikir ve Sanat Eserleri Kanunu anlamında özgün bir eser niteliğinde olduğunu kabul ve taahhüt ederiz.

Ayrıca, proje önerisini hazırlayan ve sunan kişilerin proje önerisi üzerindeki payları belirlenemiyorsa,

- Proje önerisi üzerindeki hak sahibinin, 5846 sayılı Fikir ve Sanat Eserlerinin 10. maddesi uyarınca proje başvurusunda adı geçen kişilerin tamamı olduğunu ve bunun aksinin iddiasının mümkün olmadığını,
- Hak sahipleri tamamı rıza göstermedikçe proje önerisi üzerinde herhangi bir taahhüt veya tasarruf işleminde bulunmayacaklarını,
- Hak sahipleri tamamı rıza göstermedikçe aynı veya benzeri proje önerisini TÜBİTAK veya diğer kurumlar nezdinde bir başvuru konusu yapmayacaklarını,
- Yukarıda belirtilen kurallara aykırı davranışın TÜBİTAK Araştırma ve Yayın Etiği Kurulu Esaslarının 8. maddesine aykırılık teşkil edeceği ve aynı esasların 9. maddesine göre projenin iptali ve diğer yaptırımların herhangi bir ihtara veya ihbara gerek kalmadan kendisine uygulanabileceğini,
- Burada belirtilen hususlardan hiçbirinin TÜBİTAK ilgili mevzuatı ve 5846 sayılı Fikir ve Sanat Eserleri Kanununa aykırılık teşkil edebilecek bir işlem yapılmasına cevaz vermeyeceğini

kabul, beyan ve taahhüt ederiz.

Hak Sahiplerinin		
Adı Soyadı	**Tarih**	**İmza**
Öğr. Görev. Dr. Ayşen Günel-Özcan	30/07/2009	
Prof. Dr. Duygu Uçkan Çetinkaya	30/07/2009	

Kişi sayısının fazla olması halinde ilave yapılabilir.

x☐ Projede adım geçmekle birlikte proje önerisi üzerinde hiçbir fikri katkım yoktur.

Adı Soyadı	Tarih	İmza
Uzm. Dr. Bülent Barış Kuşkonmaz	30/07/2009	
Uzm. Biy. Özlem Küçükbayrak	30/07/2009	

2008 / 2. Dönem

Appendix-2: (Continued) Funding of the Thesis

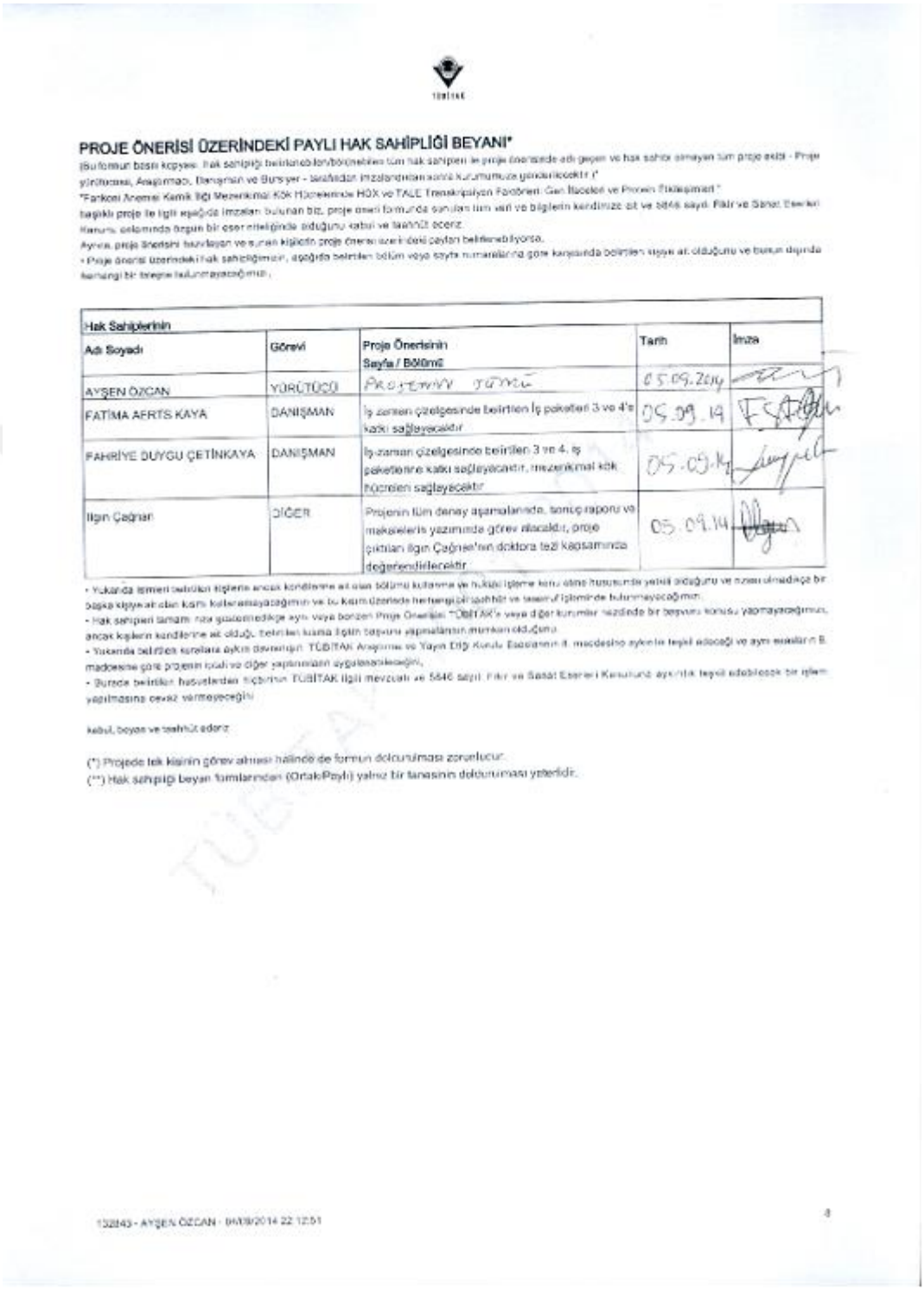

TÜBİTAK

PROJE ÖNERİSİ ÜZERİNDEKİ PAYLI HAK SAHİPLİĞİ BEYANI*

(Bu formun basılı kopyası, hak sahipliği belirlenebilen/belirlenebilen tüm hak sahipleri ile proje önerisinde adı geçen ve hak sahibi olmayan tüm proje ekibi - Proje yürütücüsü, Araştırmacı, Danışman ve Burs'yer - tarafından imzalandıktan sonra kurumumuza gönderilecektir.)*

"Farklılaşmış Anemisi Kemik İliği Mezenkimal Kök Hücrelerinde HOX ve TALE Transkripsiyon Faktörleri Gen İfadeleri ve Protein Fosforilasyonları"

başlıklı proje ile ilgili eşliğinde imzaları bulunan bu proje öneri formunda sunulan tüm veri ve bilgilerin kendimize ait ve bilimsel sayılı. Fikir ve Sanat Eserleri Kanunu çerçevesinde özgün bir eser niteliğinde olduğunu kabul ve taahhüt ederiz.

Ayrıca, proje önerisini hazırlayan ve eserden kişilerin proje önerisi üzerindeki payları belirlenebiliyorsa,

• Proje önerisi üzerindeki hak sahipliğimizin, aşağıda belirtilen bölüm veya sayfa numaralarına göre karşısında belirtilen oranda ait olduğunu ve bunun dışında herhangi bir talepte bulunmayacağımızı,

Hak Sahiplerinin				
Adı Soyadı	**Görevi**	**Proje Önerisinin Sayfa / Bölümü**	**Tarih**	**İmza**
AYŞEN ÖZCAN	YÜRÜTÜCÜ	PROJENİN TAMAMI	05.09.2014	
FATİMA AFRİTS KAYA	DANIŞMAN	İş zamanı çizelgesinde belirtilen İş paketleri 3 ve 4'e katkı sağlayacaktır	05.09.14	
FAHRİYE DUYGU ÇETİNKAYA	DANIŞMAN	İş zamanı çizelgesinde belirtilen 3 ve 4. iş paketlerine katkı sağlayacaktır, mezenkimal kök hücreleri sağlayacaktır	05.09.14	
Ilgın Çağnan	DİĞER	Projenin tüm deney aşamalarında, sonuç raporu ve makalelerin yazımında görev alacaktır, proje çıktıları Ilgın Çağnan'ın doktora tezi kapsamında değerlendirilecektir	05.09.14	

• Yukarıda isimleri belirtilen kişilerle ancak kendilerine ait olan bölümü kullanma ve hukuki işleme konu olma hususunda yetkili olduğunu ve aynen olmadığı bir başka kişiyle ait olan kısmı kullanmayacağımızı ve bu kısım üzerinde herhangi bir tasarruf ve tasarruf işleminde bulunmayacağımızı,

• Hak sahipleri tamamı rıza gösterilmedikçe aynı veya benzeri Proje Önerisini "TÜBİTAK'a veya diğer kurumlar nezdinde bir başvuru konusu yapmayacağımızı, ancak kişilerin kendilerine ait olduğu belirtilen kısma ilgili başvuru yapılmasının mümkün olduğunu,

• Yukarıda belirtilen kurallara aykırı davranılması TÜBİTAK Araştırma ve Yayın Etiği Kurulu Esaslarının 8. maddesine aykırılık teşkil edeceği ve aynı esasların 8. maddesine göre projenin iptali ve diğer yaptırımların uygulanabileceğini,

• Burada belirtilen hususlardan hiçbirinin TÜBİTAK ilgili mevzuatı ve 5846 sayılı Fikir ve Sanat Eserleri Kanunu'na aykırılık teşkil edebilecek bir işlem yapılmasına cevaz vermeyeceğini

kabul, beyan ve taahhüt ederiz.

(*) Projede tek kişinin görev alması halinde de formun doldurulması zorunludur.
(**) Hak sahipliği beyan formlarından (Ortak/Paylı) yalnız bir tanesinin doldurulması yeterlidir.

132843 - AYŞEN ÖZCAN - 04/09/2014 22:12:51

4

Appendix-2: (Continued) Funding of the Thesis

PROJE NO : 2147033

VÜCUDA GETİRİLECEK FİKRİ VE SINAİ ÜRÜNLER ÜZERİNDEKİ HAKLARIN DEVRİNE İLİŞKİN TAAHHÜT SÖZLEŞMESİ

1. TARAFLAR

1.1. İşbu sözleşme bir yanda Atatürk Bulvarı No:221 06100 Kavaklıdere/Ankara adresinde mukim Türkiye Bilimsel ve Teknolojik Araştırma Kurumu (TÜBİTAK) ile diğer yanda sözleşmenin sonunda isimleri ve adresleri bulunan kişiler (fikri ürün sahipleri) arasında imzalanmıştır.

2. TANIMLAR

Fikri ürün : Fikri ürün sahiplerinin, burada sayılanlarla sınırlı olmamak üzere bu sözleşme kapsamında geliştirecekleri ve vücuda getirecekleri proje esnasında veya sonucunda ortaya çıkacak olan 5846 sayılı Fikir ve Sanat Fikri ürünleri Kanunu kapsamındaki bilgisayar programları ve bunların kaynak kodları hariç her türlü fikri yaratımı,

Sınai ürün : Burada sayılanlarla sınırlı olmamak üzere; projenin yürütülmesi esnasında veya sonucunda ortaya çıkan patent, faydalı model, endüstriyel tasarım, entegre devre topografyası, yeni bitki ve hayvan türleri ve bunların ıslah yöntemleri, bilgisayar programları ve bunların kaynak kodları ile fikri mülkiyet haklarının konusunu oluşturabilecek nitelikteki her türlü fikri yaratımı,

Hak Sahipler : Yönetmelik uyarınca desteklenen projeler esnasında veya sonucunda ortaya çıkan fikri ürün üzerinde hak sahibi olan ve Fikri Haklar Esasları uyarınca sınai ürünü ortaya çıkararak hak talebinde bulunacak proje personeli ve/veya bursiyerleri,

Proje Personeli : Proje yürütücüsü ile araştırmacı, yardımcı personel ve danışmanlardan oluşan proje çalışanlarını,

Bursiyer : Tarihkat amacıyla projede yer alan, Türkiye'de kurulu yükseköğretim kurumlarında lisans ve lisansüstü eğitimlerini yapan öğrenciler ile doktora sonrası araştırmacıları,

Yönetmelik : 12/7/2005 tarihli ve 25873 sayılı Resmi Gazete'de yayımlanarak yürürlüğe giren TÜBİTAK Proje ve Destekleme Esaslarına İlişkin Yönetmeliği,

Esaslar : Proje Teşvik ve Destekleme Esaslarına İlişkin Yönetmelik Uyarınca Desteklenen Projelerde Uygulanacak Fikri Haklar Esasları'nı

ifade eder.

3. SÖZLEŞMENİN KONUSU

İşbu sözleşme, yönetmelik uyarınca yürütülen proje esnasında veya sonucunda ortaya çıkacak olan hak sahiplerinin üzerinde münhasıran hak sahibi oldukları fikri ürünlere ilişkin, mevzuattan ve hususiyetle 5846 sayılı kanundan doğan hakları üzerinde TÜBİTAK'a basit ruhsat sağlanması; sınai ürünlere ilişkin, mevzuattan doğan hakları üzerinde TÜBİTAK'a devredilemez, geri alınamaz ve inhisarı olmayan lisans hakkının sağlanmasına veya esaslarda belirtilen durumların söz konusu olduğu hallerde bütün hakların TÜBİTAK'a devredilmesi taahhüdünü konu alır.

Sayfa 1/4

Appendix-2: (Continued) Funding of the Thesis

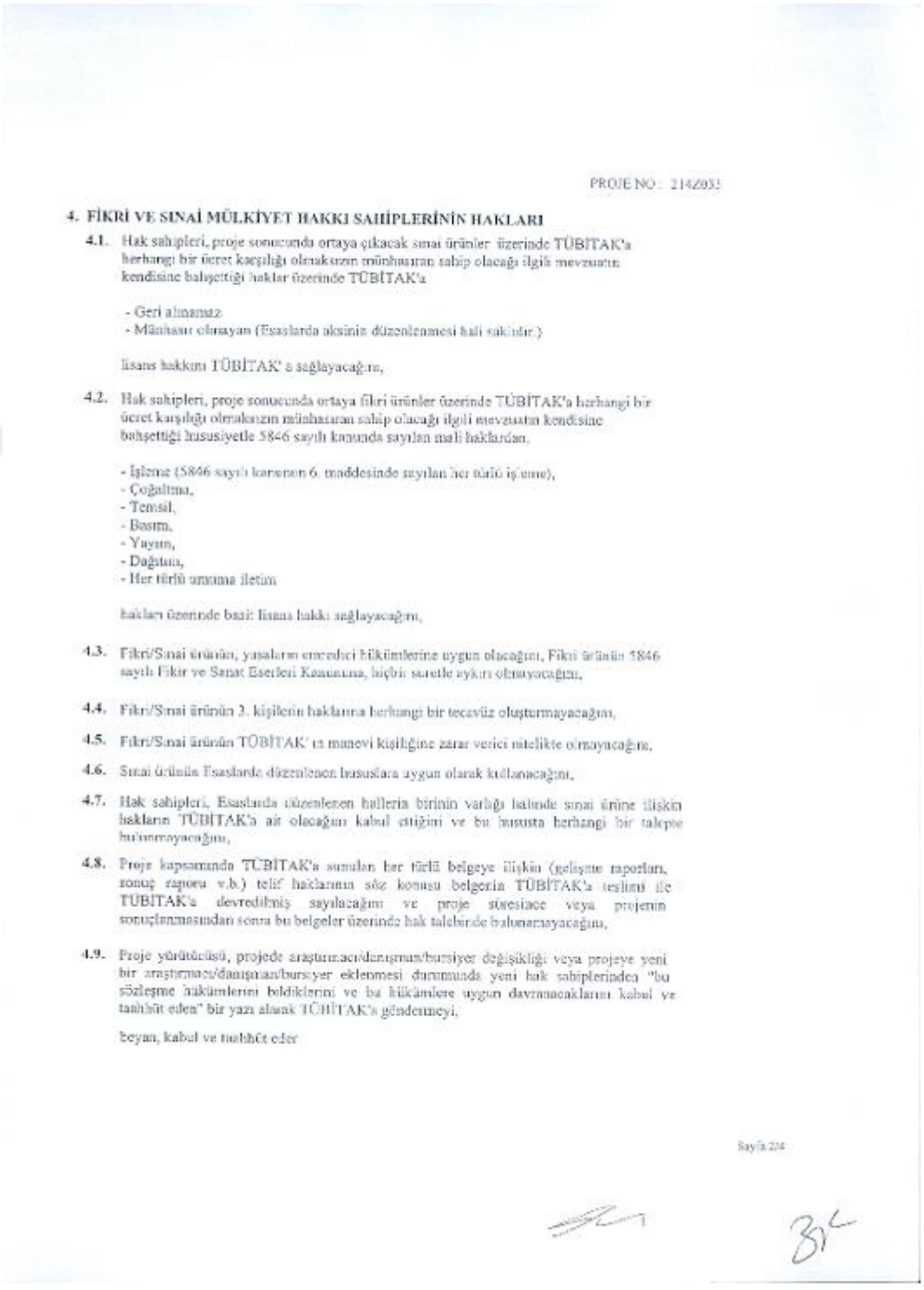

PROJE NO : 214Z033

4. FİKRİ VE SINAİ MÜLKİYET HAKKI SAHİPLERİNİN HAKLARI

4.1. Hak sahipleri, proje sonucunda ortaya çıkacak sınai ürünler üzerinde TÜBİTAK'a herhangi bir ücret karşılığı olmaksızın münhasıran sahip olacağı ilgili mevzuatın kendisine bahşettiği haklar üzerinde TÜBİTAK'a

- Geri alınamaz
- Münhasır olmayan (Esaslarda aksinin düzenlenmesi hali saklıdır.)

lisans hakkını TÜBİTAK' a sağlayacağını,

4.2. Hak sahipleri, proje sonucunda ortaya fikri ürünler üzerinde TÜBİTAK'a herhangi bir ücret karşılığı olmaksızın münhasıran sahip olacağı ilgili mevzuatın kendisine bahşettiği hususiyetle 5846 sayılı kanunda sayılan mali haklardan,

- İşleme (5846 sayılı kanunun 6. maddesinde sayılan her türlü işleme),
- Çoğaltma,
- Temsil,
- Basım,
- Yayım,
- Dağıtma,
- Her türlü umuma iletim

hakları üzerinde basit lisans hakkı sağlayacağını,

4.3. Fikri/Sınai ürünün, yasaların emredici hükümlerine uygun olacağını, Fikri ürünün 5846 sayılı Fikir ve Sanat Eserleri Kanununa, hiçbir suretle aykırı olmayacağını,

4.4. Fikri/Sınai ürünün 3. kişilerin haklarına herhangi bir tecavüz oluşturmayacağını,

4.5. Fikri/Sınai ürünün TÜBİTAK' ın manevi kişiliğine zarar verici nitelikte olmayacağını,

4.6. Sınai ürünün Esaslarda düzenlenen hususlara uygun olarak kullanacağını,

4.7. Hak sahipleri, Esaslarda düzenlenen hallerin birinin varlığı halinde sınai ürüne ilişkin hakların TÜBİTAK'a ait olacağını kabul ettiğini ve bu hususta herhangi bir talepte bulunmayacağını,

4.8. Proje kapsamında TÜBİTAK'a sunulan her türlü belgeye ilişkin (gelişme raporları, sonuç raporu v.b.) telif haklarının söz konusu belgelerin TÜBİTAK'a teslimi ile TÜBİTAK'a devredilmiş sayılacağını ve proje süresince veya projenin sonuçlanmasından sonra bu belgeler üzerinde hak talebinde bulunamayacağını,

4.9. Proje yürütücüsü, projede araştırmacı/danışman/bursiyer değişikliği veya projeye yeni bir araştırmacı/danışman/bursiyer eklenmesi durumunda yeni hak sahiplerinden "bu sözleşme hükümlerini bildiklerini ve bu hükümlere uygun davranacaklarını kabul ve taahhüt eden" bir yazı alarak TÜBİTAK'a göndermeyi,

beyan, kabul ve taahhüt eder

Sayfa 2/4

Appendix-2: (Continued) Funding of the Thesis

5. TÜBİTAK' IN YÜKÜMLÜLÜKLERİ

5.1. Fikri ürünü 5846 sayılı kanunda düzenlenen manevi hakları ihlal etmeyecek şekilde kullanacağını

5.2. Hakları hak sahiplerinin izni olmaksızın 3. kişilere devretmeyeceğini,

kabul ve taahhüt eder.

6. BİLDİRİMLER

6.1. Taraflar, işbu sözleşmenin başındaki adreslerin yasal tebligat adresleri olduğunu; tebligat adreslerinde değişiklik olması halinde yeni adreslerini 15 gün içinde yazılı olarak karşı tarafa bildirmedikçe bu adreslere yapılacak tebligatın hüküm ve sonuçlarını doğuracağını,

6.2. Yapılacak tüm bildirimlerin yazılı olacağını kabul ve taahhüt ederler.

7. DELİLLER

7.1. Taraflar tüm TÜBİTAK kayıtlarının delil olduğunu ve yazılı belge haricindeki işbu belgenin delil olarak kabul edilmeyeceğini kabul, beyan ve taahhüt ederler.

8. UYUŞMAZLIKLARIN ÇÖZÜMÜ

8.1. Taraflar, işbu sözleşmenin tatbik ve tefsirinden doğacak uyuşmazlıkları karşılıklı görüşmelerle halletmeye gayret edeceklerdir.

8.2. Sulhen halledilemeyen uyuşmazlıkların ortaya çıkması durumunda bunların çözümünde Ankara Mahkemeleri ile İcra Daireleri'nin yetkili olduğunu kabul ederler.

8.3. İşbu sözleşmeye uygulanacak hukuk "Türk Hukuku"dur.

İşbu sözleşme (8) madde ve (4) sayfadan ibaret olup, aşağıdaki imza sahiplerince tam olarak okunup anlaşıldıktan sonra (1) asıl nüsha olmak üzere imzalanmış ve asıl nüsha TÜBİTAK tarafından alıkonulmuştur. Diğer imza sahiplerinin talebi halinde sözleşmenin 'aslına uygun olduğu TÜBİTAK tarafından onaylı suretleri' TÜBİTAK tarafından düzenlenip talep sahibine verilecektir.

Appendix-2: (Continued) Funding of the Thesis

PROJE NO : 2142333

TÜBİTAK ADINA	HAK SAHİPLERİ	PROJE ÖNERİSİNDE FİKRİ HAKKI
Adı Soyadı: Prof. Dr. Erol ARCAKLIOĞLU TÜBİTAK Başkan Yardımcısı V. İmza :	Adı Soyadı : Doç. Dr. AYŞEN ÖZCAN TC Kimlik No : 48067336748 İmza :	VAR
	Adı Soyadı : Prof. Dr. FAHRİYE DUYGU ÇETİNKAYA TC Kimlik No : 20509950756 İmza :	VAR
	Adı Soyadı : Dr. FATİMA AERTS KAYA TC Kimlik No : 99553108752 İmza :	VAR

Tarih : 10/04/2015

Sayfa 4/4

Appendix-3: Published Articles Related to This Thesis

- Cagnan I, Cosgun E, Aerts-Kaya F, Konu O, Uckan D, Gunel-Ozcan A. *PKNOX2* is dysregulated in Fanconi anemia bone-marrow mesencyhmal stem cells as a possible target of TGF-β1 signaling pathway. *Manuscript in preparation.*
- Cagnan I, Gunel-Ozcan A, Aerts-Kaya F, Ameziane A, Kuskonmaz B, Dorsman J, Gumruk F, Uckan D. (2017). Bone marrow mesenchymal stem cells carrying FANCD2 mutation differ from the other Fanconi anemia complementation groups in terms of TGF-β1 production. Stem Cell Reviews and Reports, doi: 10.1007/s12015-017-9794-5.
- Cagnan I, Aerts-Kaya F, Uckan D, Gunel-Ozcan A. (2017). Stably expressed reference genes during differentiation of bone marrow derived mesenchymal stem cells. *Turkish Journal of Biology*, 41:88-97.

Appendix-4: Published Abstracts in Conference Proceedings Related to This Thesis

- Cagnan I, Gunel-Ozcan A, Aerts-Kaya F, Ameziane N, Kuskonmaz B, Dorsman J, Gumruk F, Cetinkaya D. Poster number: 2464. TGF-β1 production by bone marrow mesenchymal stem cells of FANCD2 differs from other Fanconi anemia complementation groups. Blood, 130, Supplement 1: 2464. 59th ASH Annual Meeting and Exposition, Atlanta, USA, 9-12 December 2017.
- Cagnan I, Aerts Kaya F, Cosgun E, Konu O, Uckan-Cetinkaya D, Gunel-Ozcan A. (2017). Poster number: 3261. PKNOX2 regulated by TGFbeta is a new candidate to explain bone marrow failure in Fanconi anemia. Experimental Hematology, 53: S136. 46th Annual Scientific Meeting International Scoiety for Experimental Hematology, Frankfurt, Germany, 24-27 August 2017.
- Cagnan I, Aerts Kaya F, Uckan-Cetinkaya D, Gunel-Ozcan A. Poster number: P11. High PKNOX2 level of mesenchymal stem cells prompts hematopoietic stem cell differentiation towards myeloid lineages in coculture experiments. 2nd International Conference on Stem Cells and Cancer, Lyon, France, 15-16 November 2016.
- Cagnan I, Uckan D, Gunel-Ozcan A. (2016). Abstract number: ST-05.03.3-006. PBX/Knotted 1 Homeobox 2 is an activator and a downstream target of transforming growth factor beta-1. The FEBS Journal, 283, Supplement 1: 59-60. 41st FEBS Congress, Kuşadası, Turkey, 3-8 September 2016.
- Cagnan I, Cosgun E, Konu O, Aerts Kaya FS, Kuskonmaz B, Uckan D, Gunel-Ozcan A. HOX and TALE gene expression profile of bone marrow derived mesenchymal stem/stromal cells from Fanconi anaemia patients and donors. 3rd International Molecular Biology Congress, İzmir, Turkey, 10-12 September 2014. *Abstract selected as oral presentation, Session: Cell Biology/ Developmetal Biology/ Stem Cell Research.*
- Cagnan I, Cosgun E, Konu O, Aerts Kaya FS, Kuskonmaz B, Uckan D, Gunel-Ozcan. Poster number: P-17. Fankoni anemili hastaların kemik iliği mezenkimal kök hücrelerinde PREP2 gen ifadesi donörlere oranla düşüş

göstermektedir. 1st Congress on Stem Cell and Cell Therapies, Kocaeli, Turkey, 20-23 March 2014.

- Cagnan I, Ameziane N, Floor K, Kuskonmaz B, Uckan D, Gunel-Ozcan A. Poster no: P-13. Fankoni anemili hastalardan elde edilen mezenkimal kök hücrelerin proliferasyon ve yaşlanma özellikleri. 4. Ulusal Hücresel Tedavi ve Rejeneratif Tıp Kongresi, Kapadokya, Turkey, 28 February-2 March 2014.
- Cagnan I, Konu O, Cosgun E, Aerts-Kaya F, Kuskonmaz B, Uckan D, Gunel-Ozcan A. HOX-TALE expression patterns in Fanconi anaemia. HOX and TALE Transcription Factors in Development and Disease programme and abstract book, pg. 51. EU COST Action BM0805 Annual Meeting, Egmond aan Zee, the Netherlands, 2-4 October 2013.
- Cagnan I, Cosgun E, Konu O, Kuskonmaz B, Uckan D, Gunel-Ozcan A. Poster no: 48. Random forest and support vector machines analyses of HOX-TALE gene expressions of Fanconi anaemia patient's bone marrow mesenchymal stem cells. HIBIT 2013: The 8th International Symposium on Health Informatics and Bioinformatics, Ankara, Turkey, 25-27 September 2013.
- Cagnan I, Konu O, Aerts-Kaya S F F, Kuskonmaz B, Uckan-Cetinkaya D, Gunel-Ozcan A. Poster number: 4. Hox-TALE genes show highly conserved yet heterogeneous expression profiles among Fanconi anaemia patients and healthy donors. COST Action-BM0805: Symposium on HOX and TALE Transcription Factors in Development and Disease, Madrid, Spain, 28 November-01 December 2012.
- Gunel-Ozcan A, Cagnan I, Kuskonmaz B, Aerts-Kaya F, Uckan-Cetinkaya D. Poster number: T-2180. Expression of Hox genes in the bone marrow derived mesenchymal stromal/stem cells from Fanconi anaemia patients changes following bone marrow transplantation. ISSCR 10th Annual Meeting, Pacifico Yokohama, Yokohama-Japan, 13-16 June 2012.
- Gunel-Ozcan A, Cagnan I, Kuskonmaz B and Uckan-Cetinkaya D. HOX-TALE expression in bone marrow derived mesenchymal stromal cells of Fanconi anaemia patients. HOX and TALE Transcription Factors in Development and Disease programme and abstract book, pg. 42. EU COST

Action BM0805 Annual Meeting, Carry-Le-Rouet, France, 28 September-01 October 2011.

Appendix-5: Collaborators' Contributions

- Patient materials were provided by Prof. Dr. Duygu Uçkan-Çetinkaya at Department of Pediatrics, Division of Bone Marrow Transplantation Unit, Faculty of Medicine, Hacettepe University, Ankara, Turkey.
- Clinical information of Fanconi anemia patients and donors were provided by Assoc. Prof. Dr. Barış Kuşkonmaz at Department of Pediatrics, Division of Bone Marrow Transplantation Unit, Faculty of Medicine, Hacettepe University, Ankara, Turkey.
- Flow cytometry analyses and co-culture experiments were performed by the help of Assist. Prof. Dr. Fatima Aerts-Kaya, Hacettepe University Center for Stem Cell Research and Development, Ankara, Turkey.
- Mutation analyses of Fanconi anemia patients was performed together with Dr. Najim Ameziane in Prof. Johan de Winters' (deceased) laboratory at Department of Clinical Genetics, VU University Medical Center, Amsterdam, The Netherlands.
- Imputation of HOX and TALE profile was performed using Multivariate Imputation by Chained Equations (MICE) in R Statistical software by Dr. Erdal Coşgun at Department of Biostatistics, Faculty of Medicine, Hacettepe University, Ankara, Turkey (current address: Microsoft Genomics, Redmond, Washington, USA).
- Mass spectrometry analyses were performed at Assoc. Prof. Dr. Nurhan Özlüs' laboratory, Koç University Cell Biology and Proteomics Laboratory, İstanbul, Turkey.

9. CURRICULUM VITAE

I- Personal Information

Name-Surname: Ilgın ÇAĞNAN
Place and date of birth: Nicosia, 12/12/1987
Nationality: T.R.N.C.
Contact Adress: Gültekin Şengör Sok., AK3 Apt. no: 5, Kumsal/Lefkoşa, T.R.N.C.
Telephone: 03922277831

II- Education

- PhD, Stem Cell Sciences, Hacettepe University Center for Stem Cell Research and Development, Ankara, Turkey
- MSc by Research in Life Sciences, College of Medicine and Veterinary Medicine, University of Edinburgh, U.K.
- BSc Honours in Biological Sciences (Genetics), College of Science and Engineering, University of Edinburgh, Edinburgh, U.K.
- High School Diploma, Eastern Mediterranean College, Famagusta, Cyprus

III- Professional Experience

- Pharma Research Discovery Basel, Vascular & Metabolic, F. Hoffmann-La Roche, Switzerland

IV- Academic Activities

Published Articles

- Cagnan I, Gunel-Ozcan A, Aerts-Kaya F, Ameziane A, Kuskonmaz B, Dorsman J, Gumruk F, Uckan D. (2017). Bone marrow mesenchymal stem cells carrying FANCD2 mutation differ from the other Fanconi anemia complementation groups in terms of TGF-β1 production. Stem Cell Reviews and Reports, doi: 10.1007/s12015-017-9794-5.

- Cagnan I, Aerts-Kaya F, Uckan D, Gunel-Ozcan A. (2017). Stably expressed reference genes during differentiation of bone marrow derived mesenchymal stem cells. Turkish Journal of Biology, 41:88-97.
- Morgan K, Meyer C, Miller N, Sims A H, Cagnan I, Faratian D, Langdon S P, Harrison D J, Millar R P. (2011). GnRH receptor activation competes at a low level with growth signaling in stably transfected human breast cell lines, BMC Cancer, 11 (476): 1-13.

Published Abstracts

- Cagnan I, Gunel-Ozcan A, Aerts-Kaya F, Ameziane N, Kuskonmaz B, Dorsman J, Gumruk F, Cetinkaya D. TGF-β1 production by bone marrow mesenchymal stem cells of FANCD2 differs from other Fanconi anemia complementation groups. Blood, 130, Supplement 1: 2464.
- Cagnan I, Aerts Kaya F, Cosgun E, Konu O, Uckan-Cetinkaya D, Gunel-Ozcan A. (2017). PKNOX2 regulated by TGFbeta is a new candidate to explain bone marrow failure in Fanconi anemia. Experimental Hematology, 53: S136.
- Cagnan I, Uckan D, Gunel-Ozcan A. (2016). PBX/Knotted 1 Homeobox 2 is an activator and a downstream target of transforming growth factor beta-1. The FEBS Journal, 283, Supplement 1: 59-60.
- Gunel-Ozcan A, Cagnan I, Kansu E, Uckan D. (2014). miRNA expression profiling in mesenchymal stromal/stem cells derived from G-CSF primed bone marrows. Blood, 124: 5140.
- Cagnan I, Uckan D, Gunel-Ozcan A. (2015). Genome-wide non-coding RNA expression profile indicates upregulation of hsa-miR-761 in the bone marrow mesenchymal stromal cells of Fanconi Anemia patients. Human Gene Therapy, 26(10):A86-A87, doi: 10.1089/hum.2015.29008.abstracts.
- Kopru C Z, Cagnan I, Akar Soycan I, Esendagli G, Korkusuz P, Gunel-Ozcan A. (2015). Mesenchymal stem cells induce proliferation of NCI-H82 small cell lung cancer. Human Gene Therapy, 26(10): A49-A50, doi: 10.1089/hum.2015.29008.abstracts.

- Kopru C Z, Korkusuz P, Cagnan I, Akar Soycan I, Esendagli Gunel-Ozcan A. (2015). PCR3::GITRL Transfected MSCs Induce Apoptotic Cell Death and SIVA1 expression in SCLC-21H lung cancer cell line. Human Gene Therapy, 26(10):A49, doi: 10.1089/hum.2015.29008.abstracts.
- Aydin G, Aerts-Kaya F, Cagnan I, Gunel-Ozcan A, Uckan-Cetinkaya D. (2014). Gene expression of Notch receptors and ligands by plastic adherent and prospectively isolated MSCs. Human Gene Therapy, 25:A2–A121, doi: 10.1089/hum.2014.2536.abstracts.
- Aerts-Kaya F, Cagnan I, Aydin G, Kose S, Semerci A, Kuskonmaz B, Uckan D. (2013). Assessment of human bone marrow plasma samples suggests a different role for mesenchymal stromal cells in distinct areas mediated by PDGF-BB/PDGF-R. Experimental Hematology, 41(8):S61.
- Gunel-Ozcan A, Cagnan I, Konu O, Aerts-Kaya F, Kuskonmaz B, Uckan D. (2013). Differential miRNA expression profile of bone marrow derived mesenchymal stem cells in Fanconi anaemia patients and healthy donors. Experimental Hematology, 41(8):S61.
- Aerts-Kaya F, Kilic E, Aydin G, Kose S, Cagnan I, Gultekin O, Kuskonmaz B, Uckan D. (2013). Differential expression profile of healthy human bone marrow plasma samples from the endosteal and vascular region. Experimental Hematology, 41(8):S61.
- Aerts-Kaya F, Kose S, Aydin G, Cagnan I, Bocutcu S, Kuskonmaz B, Uckan D. (2013). Effects of in-vivo G-CSF stimulation on cytokine levels in bone marrow plasma samples from healthy donors. Experimental Hematology, 41(8):S61.
- Gunel-Ozcan A, Cagnan I, Kuskonmaz B, Uckan-Cetinkaya D. (2011). Relative gene expression analysis shows increased mRNA levels of HoxB7 and HoxA10 and decreased mRNA levels of Pbx1 in the bone marrow derived mesenchymal progenitors from Fanconi anaemia patients. Current Opinion in Biotechnology, 22, Supplement 1:S151.

Poster Presentations

- Cagnan I, Aerts Kaya F, Uckan-Cetinkaya D, Gunel-Ozcan A. High PKNOX2 level of mesenchymal stem cells prompts hematopoietic stem cell differentiation towards myeloid lineages in coculture experiments. 2nd International Conference on Stem Cells and Cancer, Lyon, France, 15-16 November 2016.
- Cagnan I, Cosgun E, Konu O, Aerts Kaya FS, Kuskonmaz B, Uckan D, Gunel-Ozcan. Fankoni anemili hastaların kemik iliği mezenkimal kök hücrelerinde PREP2 gen ifadesi donörlere oranla düşüş göstermektedir. 1st Congress on Stem Cell and Cell Therapies, Kocaeli, Turkey, 20-23 March 2014.
- Cagnan I, Dardaei L, Uckan D, Blasi F, Gunel-Ozcan A. PREP1 overeksprese eden kemik iliği kaynaklı mezenkimal kök hücrelerinde TALE homeodomain protein düzeyleri. 1st Congress on Stem Cell and Cell Therapies, Kocaeli, Turkey, 20-23 March 2014.
- Cagnan I, Ameziane N, Floor K, Kuskonmaz B, Uckan D, Gunel-Ozcan A. Fankoni anemili hastalardan elde edilen mezenkimal kök hücrelerin proliferasyon ve yaşlanma özellikleri. 4. Ulusal Hücresel Tedavi ve Rejeneratif Tıp Kongresi, Kapadokya, Turkey, 28 February-2 March 2014.
- Cagnan I, Konu O, Aerts-Kaya F S, Kuskonmaz B, Uckan-Cetinkaya D, Gunel-Ozcan A. Expression of hsa-miR-3065-3p was significantly downregulated in Fanconi anaemia patient bone marrow derived mesenchymal stem cells following bone marrow transplantation. ISSCR Regional Forum Series 2013: Stem Cells in Translation, Florence, Italy, 15-18 September 2013.
- Cagnan I, Konu O, Aerts-Kaya S F F, Kuskonmaz B, Uckan-Cetinkaya D, Gunel-Ozcan A. Hox-TALE genes show highly conserved yet heterogeneous expression profiles among Fanconi anaemia patients and healthy donors. COST Action-BM0805: Symposium on HOX and TALE Transcription Factors in Development and Disease, Madrid, Spain, 28 November-01 December 2012.

Oral Short Talk Presentations

- Cagnan I, Uckan D, Gunel-Ozcan A. Fankoni anemisi mezenkimal kök hücrelerinde miRNA profili. Hacettepe Üniversitesi Kök Hücre Günü, Ankara, Turkey, 19 November 2014.
- Cagnan I, Cosgun E, Konu O, Aerts Kaya FS, Kuskonmaz B, Uckan D, Gunel-Ozcan A. HOX and TALE gene expression profile of bone marrow derived mesenchymal stem/stromal cells from Fanconi anaemia patients and donors. 3rd International Molecular Biology Congress, İzmir, Turkey, 10-12 September 2014.
- Cagnan I, Cosgun E, Konu O, Aerts Kaya F, Kuskonmaz B, Uckan D, Gunel-Ozcan A. Fankoni anemisi kemik iliği mezenkimal kök hücrelerinde HOX/Tale gen ekspresyonları. Hacettepe Üniversitesi Kök Hücre Günü, Ankara, Turkey, 8 November 2013.
- Cagnan I, Cosgun E, Konu O, Kuskonmaz B, Uckan D, Gunel-Ozcan A. Random forest and support vector machines analyses of HOX-TALE gene expressions of Fanconi anaemia patient's bone marrow mesenchymal stem cells. HIBIT 2013: The 8th International Symposium on Health Informatics and Bioinformatics, Ankara, Turkey, 25-27 September 2013.

Conference Proceedings

- Gunel-Ozcan A, Cagnan I, Aerts-Kaya F, Kuskonmaz B, Uckan D. HOXA1, HOXA7 and HOXB7 gene expression are deregulated in mesenchymal stromal/stem cells derived from G-CSF primed bone marrows. ISSCR 12th Annual Meeting, Vancouver, Canada, 18-21 June 2014.
- Aerts-Kaya F, Cagnan I, Kose S, Aydın G, Kuskonmaz B, Uckan D. Sağlıklı insan kemik iliği endosteal ve santral bölgelerinde sitokin ekspresyonları ve G-CSF etkisi. 39th National Hematology Congress, Antalya, Turkey, 23-26 October 2013.
- Cagnan I, Konu O, Cosgun E, Aerts-Kaya F, Kuskonmaz B, Uckan D, Gunel-Ozcan A. HOX-TALE expression patterns in Fanconi anaemia. EU COST Action BM0805 Annual Meeting, Egmond aan Zee, the Netherlands, 2-4

October 2013. (‘HOX and TALE Transcription Factors in Development and Disease’ programme and abstract book pg. 51)

- Kopru C Z, Korkusuz P, Cagnan I, Akar-Soycan I, Esendagli G, Uckan-Cetinkaya D, Gunel-Ozcan A. Human bone marrow derived mesenchymal stem cells show heterogenous mRNA levels of glucocorticoid induced tumor necrosis factor receptor (GITR) and its ligand (GITRL). ISSCR 11th Annual Meeting, Boston, MA, USA, 12-15 June 2013.
- Gunel-Ozcan A, Cagnan I, Kuskonmaz B, Aerts-Kaya F, Uckan-Cetinkaya D. Expression of Hox genes in the bone marrow derived mesenchymal stromal/stem cells from Fanconi anaemia patients changes following bone marrow transplantation. ISSCR 10th Annual Meeting, Pacifico Yokohama, Yokohama-Japan, 13-16 June 2012.
- Gunel-Ozcan A, Cagnan I, Kuskonmaz B and Uckan-Cetinkaya D. HOX-TALE expression in bone marrow derived mesenchymal stromal cells of Fanconi anaemia patients. EU COST Action BM0805 Annual Meeting, Carry-Le-Rouet, France, 28 September-01 October 2011. (‘HOX and TALE Transcription Factors in Development and Disease’ programme and abstract book pg. 42)
- Keupp K, Li Y, Alanay Y, Thiele H, Uz E, Frommolt P, Utine E, Cagnan I, Boduroglu K, Nürnberg P, Akarsu N, Wollnik B. Whole-exome sequencing in combination with simultaneous analysis of homozygous stretches of exome variants identified causative mutations in two genes in Malpuech syndrome. 22nd Meeting of German Human Genetics Society, Regensburg, Germany, 16-18 March 2011.
- Mihci E, Uz E, Akman S, Yücel S, Cagnan I, Akarsu N A. Homozygosity mapping and mutation analysis of the HPSE2 gene support genetic homogeneity in Urofacial Syndrome. 9th National Medical Genetics Congress, Istanbul, Turkey, 01-05 December 2010.

Awards and Funding

- Funding for Ph.D. studies provided by two TUBİTAK 1001 projects (#110S021 and #214Z033)

- Funding for registration to FEBS Congress 2016 provided by Turkish Biochemical Society
- 2nd Prize for poster presentation at 1st Congress on Stem Cell and Cell Therapies, Kocaeli, Turkey
- Short Term Scientific Missions provided by COST Action-BM0805 for the experiments carried out at FIRC Institute of Molecular Oncology (IFOM), Milan, Italy